Universidade do Minho
Escola de Engenharia

Ana Rita da Costa Pinto

Potential of human bone marrow derived stem cells combined with chitosan based biodegradable scaffolds for bone tissue engineering

Outubro de 2010

Potential of human bone marrow derived stem cells combined with chitosan based biodegradable scaffolds for bone tissue engineering
Ana Rita da Costa Pinto
UMinho | 2010

Universidade do Minho
Escola de Engenharia

Ana Rita da Costa Pinto

Potential of human bone marrow derived stem cells combined with chitosan based biodegradable scaffolds for bone tissue engineering

Tese de Doutoramento em Engenharia de Tecidos, Medicina Regenerativa e Células Estaminais

Trabalho efectuado sob a orientação do
Professor Nuno João Meleiro Alves das Neves
e do
Professor Rui Luís Gonçalves dos Reis

Outubro de 2010

É AUTORIZADA A REPRODUÇÃO PARCIAL DESTA TESE APENAS PARA EFEITOS
DE INVESTIGAÇÃO, MEDIANTE DECLARAÇÃO ESCRITA DO INTERESSADO, QUE A TAL SE
COMPROMETE;

Universidade do Minho, ___/___/_____

Assinatura: _____

To my parents

“The only true wisdom is in knowing you know nothing.”

Socrates

ACKNOWLEDGEMENTS

Five years have passed from the moment I started this PhD and now that I am finishing, it is time to express my gratitude to the persons involved in this long journey. Unfortunately, I cannot acknowledge to each one of you, otherwise all the pages included in this thesis would not be enough. So many things happened during this period both professional as personal, but above all, I am pleased that this moment has come.

I want to acknowledge my supervisor, Professor Nuno Neves for all the dedication to my work and for all the scientific discussions that we had. The discussions were never easy and I know that I am difficult to convince, sometimes. This thesis is the result of 5 years of mutual work. Thank you for believing in me and always trying to pursuit to what were the best interests for me.

I would like to acknowledge my co-supervisor, Professor Rui Reis, director of 3B's research group, for given me the opportunity to join the group. Professor Rui is a remarkable example of a leading researcher in international scientific community, being recognized for his great work. I thank the important lessons I have learned through these years, in order to grow as a scientist and as human being.

I would also to acknowledge to all my co-authors for the contribution to the papers included in this thesis.

I also acknowledge the Portuguese Foundation for Science and Technology (FCT) for my scholarship SFRH/BD/24735/2005.

I also would like to acknowledge to Hospital of São Marcos in Braga, for kindly providing the human samples.

The work developed in this thesis was partially supported by the EU Integrated Project GENOSTEM (Adult Mesenchymal Stem Cells Engineering for connective tissue disorders: from the bench to the bedside, LSHB-CT-2003-5033161), and the

European Network of Excellence EXPERTISSUES (NMP3-CT-2004-500283).

I also would like to express my gratitude to the School of Health Sciences of the University of Minho for the opportunity of using its facilities.

I want to thank Professor Paolo Bianco for receiving me in his lab and for teaching me some of his brilliant scientific knowledge, as well as to Mara, Alessia, Benedetto, Stefania, Federico, Stefano, Cristina and Antonella. Grazie per tutti.

I also want to acknowledge Professor Erhan Piskin, Kadrus and Dr. Ibrahim for receiving me in Turkey with their hospitality and good humour.

I would like to acknowledge my colleagues of the 3B's group that somehow contributed for this thesis. Your scientific skills, support and friendship were very important to me.

Obrigada à MT por ajudarem sempre, com aquelas questões burocráticas que eu "gosto" tanto.

Adriano e Liliana, obrigado por me terem aturado tantas vezes, quer seja pelo lado da informática, quer seja pelo lado do laboratório. Obrigada por estarem presentes, nos momentos mais importantes.

Ruizinho, tenho saudades dos nossos momentos de gargalhadas desesperadas às tantas da noite quando o trabalho já não rendia nada.

Analuce, minha querida, foste uma revelação. Mais que minha aluna, tornaste-te uma amiga sincera, com um coração do tamanho do mundo. Obrigada por tudo.

Minha amiga Marta, obrigada por aturares tantas vezes o meu mau humor. Por nunca me teres falhado, por teres sido a mão amiga quando tanto precisei. Por teres ido comigo a hospitais, por te teres preocupado sempre, mesmo quando estava longe. Nunca esqueço quem me faz bem e tu sabes que me tens aqui sempre que precisares.

Ana Martins, não tenho palavras para expressar o quanto te sou grata. Desde aquela noite em que senti que estavas tão desesperada, a nossa amizade foi crescendo e hoje posso dizer que és muito especial para mim. Por tudo e para tudo! Obrigado por fazeres parte da minha vida.

E finalmente um agradecimento muito especial aos meus pais que sem eles, não estaria neste momento a escrever estes agradecimentos. Por tudo o que fizeram por mim, pelo que fazem e pelo que eu sei que farão no futuro, sempre que eu precisar. O meu muito obrigado por terem acreditado em mim, me terem dado forças quando estas faltaram.

Um obrigada enorme aos meus irmãos, principalmente à minha irmã Magui, com quem partilhei todas as alegrias e tristezas, dia após dia. Por me ter dado força, chorado, sorrido, gritado… Obrigada pela tua amizade. E muito obrigada por me teres dado um afilhado lindo, que amo muito. Meu querido Gui, amorzinho do meu coração.

E por último, quero agradecer à pessoa com quem partilho a minha vida, Vasco. Obrigada por me ouvires, pelos sábios conselhos que tens partilhado comigo, por me fazeres sentir uma mulher especial e amada. É muito bom sentir que finalmente encontrei a pessoa que ouve a mesma canção…

Potential of human bone marrow derived stem cells combined with chitosan based biodegradable scaffolds for bone tissue engineering

ABSTRACT

Bone tissue engineering has emerged as a promising alternative in cases of bone loss, overcoming problems of rejection and donor scarcity associated to the clinical used bone grafts (autografts, allografts and xenografts). By combining three-dimensional structures (3D) – scaffolds, autologous cells and growth factors, bone tissue engineering seeks to achieve a long lasting and fully functional regeneration of bone. The selected scaffold should be biodegradable, allowing cells to adhere, proliferate and differentiate into the osteogenic phenotype, producing a mineralized extracellular matrix (ECM), to be later implanted into the bone defect. The rate of degradation of the scaffold should, therefore, be compatible to the rate of neo-tissue ingrowth.

The rationale of the experimental work of this thesis was designed to study a bone tissue engineering strategy by combining chitosan based scaffolds and human bone marrow mesenchymal stem cells (hBMSCs), aiming bone tissue regeneration.

Blends of chitosan with different types aliphatic polyesters were produced by extrusion. Afterwards, scaffolds were produced by compression molding followed by salt leaching. Several scaffolds formulations were produced and subjected to cytotoxicity and cytocompatibility tests, allowing selecting the most suitable formulation in terms of biological response. From the results obtained, the chitosan-poly(butylene succinate) (PBS) formulation presented the most promising results in *in vitro* cell studies with relevant cell lines. To understand why this formulation has enhanced cell performance, several formulations using different percentages of chitosan (0, 25 and 50%) and PBS (100, 75 and 50%) were used to produce scaffolds. The influence of chitosan content was evaluated with hBMSCs *in vitro.* All *in vitro* results evidenced a better performance for the highest chitosan containing scaffolds, as for cell adhesion and proliferation, as for osteogenic differentiation. Scaffolds containing chitosan (50% chitosan-50% PBS) and without chitosan (100% PBS) were implanted in different anatomic regions (cranial defect, auricular pocket and submuscular) of rats. The tissue response was evaluated by studying the inflammatory response to the implanted scaffolds. Again, scaffolds with higher chitosan amounts evidenced superior results, with a mild inflammatory response

without cell necrosis, *in vivo*, as compared to PBS scaffolds, that evidenced tissue necrosis in all implantation regions.

A different morphology of chitosan-PBS scaffolds was developed by fiber bonding to improve the porous structure. These scaffolds were clearly non-cytotoxic and cytocompatible. Furthermore, chitosan-PBS scaffolds seeded and cultured with hBMSCs in osteogenic conditions, showed an excellent cell performance.

The biodegradation of chitosan-PBS scaffolds was assessed *in vitro* using enzymes responsible for the degradation of chitosan (lysozyme) and PBS (lipase), in similar concentrations to the ones found in human body. The cocktail of both enzymes induced a superior effect on the scaffolds biodegradation. The *in vivo* biodegradation and biocompatibility of the scaffolds were evaluated. The *in vivo* model applied to this study was the rat subcutaneous model. Results showed that the *in vivo* degradation was much slower than *in vitro*. The host tissue response was the typically associated with biomaterials' implantation, with the presence of foreign body giant cells and an inflammatory response that progressed over time. The *in vivo* response was similar to those observed for biodegradable fixation devices or bioresorbable sutures.

The final study included in this thesis was performed to confirm the tissue engineering strategy followed in this work. The potential of chitosan-PBS scaffolds combined with hBMSCs, as previously demonstrated, was studied in a relevant animal model. A critical size cranial defect in nude mice was used. This model allowed evaluating the *in vivo* matured construct using human cells. The results showed that constructs were able to promote bone regeneration in a superior level than scaffolds without cells. The strategy followed under the scope of this PhD thesis was successfully validated in this small animal model, using a combination of chitosan-poly(butylene succinate) scaffolds with hBMSCs.

Potencial de células estaminais de medula óssea associadas a scaffolds biodegradáveis à base de quitosano para engenharia de tecido ósseo.

RESUMO

A área de engenharia de tecidos ósseos surgiu como uma alternativa de tratamento em casos clínicos de perdas ósseas, evitando problemas de rejeição e morbidez associada a enxertos ósseos obtidos do próprio paciente. Combinando estruturas tridimensionais (3D) porosas, células autólogas e factores de crescimento, a engenharia de tecidos ósseos visa encontrar soluções para a regeneração de osso neste tipo de pacientes. O suporte 3D seleccionado deverá ser biodegradável, permitindo a adesão, proliferação e diferenciação osteogénica das células, de forma a produzir uma matriz extracelular mineralizada, sendo posteriormente implantada no defeito ósseo. A taxa de degradação do suporte 3D poroso deverá ser compatível com a taxa de regeneração do tecido ósseo.

O objectivo do trabalho experimental desenvolvido nesta tese foi planeado de forma validar uma estratégia de engenharia de tecidos ósseos, através da combinação de suportes 3D porosos biodegradáveis à base de quitosano e células estaminais adultas de origem humana obtidas a partir de medula óssea.

Neste trabalho foram produzidas várias misturas de quitosano com diferentes tipos de poliésteres alifáticos usando a técnica de extrusão. Usando estas misturas desenvolveram-se suportes tridimensionais que foram processados por moldação por compressão com partículas de sacrifício de sal. As misturas produzidas foram avaliadas em termos de citotoxicidade e citocompatibilidade. Desta forma, foi possível seleccionar a formulação mais adequada em termos de resposta biológica. A formulação de quitosano e polibutileno succinato (PBS) foi a formulação seleccionada para posterior desenvolvimento da estratégia de engenharia de tecidos. Por ter tido consistentemente os melhores resultados biológicos *in vitro*, a mistura seleccionada foi usada para produzir suportes porosos contendo diferentes percentagens de quitosano (0, 25 and 50%) e PBS, de forma a estudar a importância do quitosano nas formulações. A influência da percentagem de quitosano nos suportes porosos foi avaliada através de estudos *in vitro* com culturas primárias de

células estaminais mesenquimais de origem humana. Os resultados celulares obtidos mostraram um melhor desempenho em termos de adesão e proliferação, assim como na diferenciação osteogénica das células nos suportes 3D com maior percentagem de quitosano. Tendo-se observado uma maior eficácia no desempenho biológico dos suportes porosos contendo quitosano, interessava confirmar estes resultados *in vivo*, tendo como controlo suportes sem quitosano, só com PBS. Suportes porosos sem quitosano e com quitosano (50%), uma vez que foram aqueles para os quais se obteve o pior e o melhor comportamento celular *in vivo* respectivamente, foram implantados em diferentes regiões anatómicas (defeito craniano, implantação auricular e submuscular) em ratos. A resposta inflamatória foi avaliada, tendo os suportes porosos com quitosano evidenciado uma resposta inflamatória moderada, não se observando necrose celular. Suportes porosos com apenas PBS na sua constituição, mostraram necrose celular em todos os locais anatómicos implantados.

O passo seguinte passou por optimizar a morfologia dos suportes, tendo sido neste caso desenvolvida uma estrutura porosa de malha de fibras de quitosano e PBS, por compressão a quente. Estes suportes porosos foram avaliados e confirmou-se também que não eram citotóxicos e que eram citocompatíveis. Adicionalmente, foram cultivadas células primárias humanas de medula óssea nestas estruturas tridimensionais, em condições de diferenciação osteogénica, mostrando um excelente desempenho *in vitro*. A biodegradação destes suportes porosos de quitosano-PBS foi estudada usando enzimas responsáveis pela degradação do quitosano (lisozima) e PBS (lipase) em concentrações idênticas às encontradas no corpo humano. Os resultados obtidos mostraram que um cocktail das duas enzimas teve um efeito pronunciado no que respeita à taxa de degradação dos suportes porosos. O estudo foi complementado pela análise da biodegradação e biocompatibilidade dos suportes tridimensionais *in vivo*. O modelo *in vivo* escolhido para este estudo foi o implante subcutâneo em ratos. Os resultados obtidos mostraram que a taxa de degradação *in vivo* foi consideravelmente menor comparativamente com os estudos efectuados *in vitro*. A resposta *in vivo* foi semelhante à observada em implantes de placas de fixação óssea biodegradáveis ou em suturas bioabsorvíveis.

O último estudo incluído nesta tese foi realizado para confirmar a estratégia de engenharia de tecidos proposta neste trabalho: a associação de suportes porosos biodegradáveis de quitosano e PBS e células estaminais humanas de medula óssea

diferenciadas para a linhagem osteogénica. O potencial desta estratégia foi estudado num modelo animal relevante: um defeito craniano de tamanho crítico em ratinhos imunocomprometidos. Este modelo permitiu avaliar o efeito da implantação dos suportes porosos cultivados com células humanas naqueles defeitos ósseos. Os resultados obtidos mostraram que esta associação de suportes porosos de quitosano-PBS com células humanas pré-cultivados *in vitro* em condições osteogénicas, promoveram regeneração óssea de uma forma mais significativa quando comparados com suportes porosos implantados sem células. A estratégia de engenharia de tecidos seguida no âmbito desta tese de doutoramento, através da combinação de suportes porosos de quitosano-PBS e células estaminais humanas de medula óssea foi validada com sucesso neste modelo animal de pequeno porte.

TABLE OF CONTENTS

SECTION 2

CHAPTER II
MATERIALS AND METHODS

SECTION 3

CHAPTER III

Adhesion, proliferation and osteogenic differentiation of a mouse mesenchymal stem cell line (BMC9) seeded on novel melt based chitosan/polyester 3D porous scaffolds

LIST OF ABBREVIATIONS

A

ALP	Alkaline phosphatise
ATTC	American type culture collection
α-MEM	Alfa-Minimum essential medium
α-SMA	Alfa-smooth muscle actin
ASCs	Adult stem cells
ADAS	Adipose derived stem cells

B

BCP	Biphasic calcium phosphate
BMPs	Bone morphogenetic proteins
BMP-2	Bone morphogenetic protein-two
BMSC	Bone marrow stromal cell
BMC-9	Mouse mesenchymal stem cell line-nine
BSP	Bone sialoprotein

C

Ca	Calcium
CA	Cartilage
$CaCl_2$	Calcium chloride
CAD	Computer aided design
CaP	Calcium phosphate
CB	Compact bone
CD	Cluster of differentiation
cDNA	Complementary deoxyribonucleic acid
CFU	Colony forming unit
Ch	Chitosan
CH3	Acetyl group

Ch-PBS	Chitosan-poly(butylene succinate)
CO_2	Carbon dioxide
CO_3^{2-}	Carbonate
Coll I	Type I collagen
CPC	Calcium phosphate cement
CT	Connective tissue

D

DD	Degree of deacetylation
ddH2O	Double distilled water
De	Dermis
DNA	Deoxyribonucleic acid
dsDNA	Double strand deoxyribonucleic acid
DMEM	Dulbecco's modified Eagle medium
dsDNA	Double strand DNA

E

E	Empty
ECM	Extracellular matrix
EDTA	Ethylenediamine tetraacetic acid
EDS	Energy dispersive spectroscopy
e.g.	*Exempli gratia*
Ep	Epidermis
ESCs	Embryonic stem cells

F

FBS	Foetal bovine serum
FGF	Fibroblast growth factor
FGFs	Fibroblast growth factors
FTIR	Fourier transform infrared spectroscopy

G

G	Giant cells
GAPDH	Glyceraldehyde-3-phosphate dehydrogenase
GAGs	Glycosaminoglycans

H

H	Hour
HA	Hydroxyapatite
H&E	Hematoxylin and eosin
hBMSC	Human bone marrow stromal cells
HCL	Hydrochloric acid
HDMS	Hexamethyldisilazane
HRP	Horseradish peroxidase

I

i.e.	*Id est*
IGF-2	Insulin-like growth factor-two
ISO	International Organization for Standardization
IP	Intraperitoneal

K

KBr	Potassium bromide

L

L929	Mouse lung fibroblast cell line

M

MSCs	Mesenchymal stem cells
MC3T3-E1	Osteoblast cell line
µCT	Micro computed tomography

Mw	Molecular weight
MTS	3-(4,5-dimethylthiazol-2-yl)-5-(3-carboxymethoxyphenyl)-2-(4 sulfofenyl)-2H tetrazolium, inner salt

N

NaCl	Sodium chloride
NADH	Nicotinamide adenine dinucleotide
NADPH	Nicotinamide adenine dinucleotide phosphate
Na_2SO_4	Sodium sulphate
NaOH	Sodium hydroxide
NH	Amine group
pNP	Nitrophenyl phosphate
pNPP	Nitrophenyl phosphate disodium salt

O

O.D.	Optical density
OCN	Osteocalcin

P

PBS	Poly(butylene succinate)
PBS 100	Poly(butylene succinate) 100%(wt)
PBSA	Poly(butylene succinate adipate)
PBTA	Poly(butylene teraphtalate adipate)
PCL	Poly(ε-caprolactone)
PDLLA	Poly(D,L-lactic acid)
PDGF	Platelet derived growth factor
PEO	Poly(ethylene oxide)
PLAGA	Poly(lactide-co-glicolic acid)
PLLA	Poly-L-lactide acid
PVA	Poly(vinyl alcohol)

R

rhBMP-2	Recombinant human bone morphogenetic protein-2
RNA	Ribonucleic acid
RP	Rapid prototyping
Rpm	Rotations per minute
RT	Room temperature
RT-PCR	Reverse transcriptase polymerase chain reaction
Runx2	Runt related transcription factor-two

S

SaOS-2	Human osteosarcoma cells
SC	Subcutaneous
Sc	Scaffold
Sc+MSCs	Scaffolds with hBMSCs pre-cultured *in vitro* in osteogenic medium
SD	Standard deviation
SEM	Scanning electron microscopy
SPCL	Blend of starch and poly(ε-caprolactone)
ssDNA	Single strand deoxyribonucleic acid

T

T	Temperature
TCP	Tricalcium phosphate
TF-XRD	Thin-film X-ray diffraction
TGF-β	Transforming growth factor-beta
3D	Three-dimensional
Tm	Temperature of melting
Tris-HCl	Trisaminomethane hydrochloride
TN	Tissue necrosis
2D	Two-dimensional

U

U	Units
UV	Ultraviolet light

V

VEGF	Vascular endothelial growth factor
VOI	Volume of interest
V_m	Volume of scaffold material
V_{sw}	Volume after three-dimensional shrink-wrap processing
V_t	Total volume

W

W_i	Initial weight
W_f	Final weight

LIST OF FIGURES

SECTION 1

CHAPTER I

INTRODUCTION

Chitosan based scaffolds for bone tissue engineering applications

SECTION 2

CHAPTER II

MATERIALS AND METHODS

SECTION 3

CHAPTER III

Adhesion, proliferation and osteogenic differentiation of a mouse mesenchymal stem cell line (BMC9) seeded on novel melt based chitosan/polyester 3d porous scaffolds

CHAPTER IV

Influence of chitosan content in the scaffold composition over the *in vitro* osteogenic differentiation of hBMSCs and *in vivo* tissue response

CHAPTER VI

***In vitro* degradation and biocompatibility assessment of chitosan-poly(butylene succinate) fiber mesh scaffolds**

SECTION V

CHAPTER VII

Chitosan-poly(butylene succinate) scaffolds and human bone marrow stromal cells induce bone repair in a mouse calvaria model

LIST OF TABLES

SECTION 1

CHAPTER I
INTRODUCTION
Chitosan based scaffolds for bone tissue engineering applications

SECTION 3

CHAPTER III
Adhesion, proliferation and osteogenic differentiation of a mouse mesenchymal stem cell line (BMC9) seeded on novel melt based chitosan/polyester 3D porous scaffolds

CHAPTER IV
Influence of chitosan content in the scaffold composition over the *in vitro* osteogenic differentiation of hBMSCs and *in vivo* tissue response

SECTION 5

CHAPTER VII

Chitosan-poly(butylene succinate) scaffolds and human bone marrow stromal cells induce bone repair in a mouse calvaria model

SHORT *CURRICULUM VITAE*

Ana Rita da Costa Pinto was born on December 22nd of December of 1980, in Felgueiras, Portugal. She is currently a PhD candidate at the 3B's Research Group (Biomaterials, Biodegradables and Biomimetics), University of Minho, Portugal. Her doctoral work has been supervised by Professors Nuno Neves and Rui L. Reis (Director of 3B's Research Group). She has just submitted her PhD thesis on Biomedical Engineering to the University of Minho.

She obtained her Bachelor of Science in Applied Biology from the University of Minho in 2003, with a final grade of 15 (0-20 scale). As her senior research project she spent one year at the Instituto de Genética Médica Jacinto de Magalhães, under the supervision of Professor Laura Vilarinho, with her research project graded with 18 (0-20 scale).

In October 2005, she formally started her PhD at the 3B's Research Group where she has been working on the development of a bone tissue engineering strategy, using human bone marrow stem cells and chitosan-based scaffolds. During this time she has been abroad, under european projects collaborations, in Rome, Italy, under the supervision of Professor Paolo Bianco and in Ankara, Turkey, under the supervision of Professor Erhan Piskin. She was also mentor of several undergraduate students, with different projects. During her PhD work, she has acquired a firm foundation of knowledge and experience with cell isolation, culture and characterization of stem cells from different sources, such as bone marrow and umbilical cord. She has also received training with *in vivo* animal models, related with tissue engineering strategies.

She also has been also involved in the writing and preparation of several grants proposals, both at National (Portuguese Foundation for Science and Technology) and European levels (Framework Programme VI).

As a result of her research she attended the most important international conferences in the field of Biomaterials, Tissue Engineering and Regenerative Medicine. She was awarded with two awards for the best communication in two meetings. Presently, she is the first author of 5 papers in international journals (2 published and 4 submitted).

LIST OF PUBLICATIONS

The work performed during this PhD work resulted in the following publications:

INTERNATIONAL JOURNALS WITH REFEREE

A.R. Costa-Pinto, V.M. Correlo, P. Sol, M. Bhattacharya, P. Charbord, B. Delorme, R.L. Reis, N.M. Neves. "Adhesion, proliferation and osteogenic differentiation of a mouse mesenchymal stem cell line (BMC9) seeded on novel melt based chitosan/polyester 3d porous scaffolds". Tissue Engineering Part A 2008;14(6): 1049-1057.

A.R. Costa-Pinto, V. M. Correlo, P. C. Sol, M. Bhattacharya, P. Charbord, B. Delorme, R. L. Reis, N. M. Neves. "Osteogenic Differentiation of Human Bone Marrow Mesenchymal Stem Cells Seeded on Melt based Chitosan scaffolds for Bone Tissue Engineering Applications". Biomacromolecules 2009;10(8): 2067-2073.

A.R. Costa-Pinto, V. M. Correlo, P. C. Sol, M. Bhattacharya, S. Srouji, E. Livne, R. L. Reis, N. M. Neves. "Chitosan-PBS scaffolds and human bone marrow stromal cells induce bone repair in a mouse calvaria model". Submitted..

A.R. Costa-Pinto, I. Vargel, S. Faria, K. Tuzlakoglu, V. M. Correlo, P. C. Sol, M. Bhattacharya, E. Piskin, R. L. Reis, N. M. Neves. "Influence of chitosan content in the scaffold composition over the *in vitro* osteogenic differentiation of hBMSCs and *in vivo* tissue response". Submitted.

A. R. Costa-Pinto, Ana M. Martins, Magda C. Carlos, V. M. Correlo, P. C. Sol, M. Bhattacharya, P. Charbord, B. Delorme, R. L. Reis, N. M. Neves. "*In vitro* degradation and biocompatibility assessment of chitosan-poly(butylene succinate) fiber mesh scaffolds". Submitted.

A. R. Costa-Pinto, R. L. Reis, N. M. Neves. "Chitosan based scaffolds for Bone Tissue Engineering applications". Submitted.

INTERNATIONAL CONFERENCES

A. R. Pinto, A.J. Salgado, J.T. Oliveira V.M. Correlo, M. Bhattacharya, P. Charbord, R.L. Reis, N.M. Neves (2005). "Evaluation of the adhesion, proliferation and differentiation of a mouse mesenchymal stem cell line on novel chitosan/polyester based scaffolds". ESB 2005 - 19th European Conference on Biomaterials, September 11-15, Sorrento, Italy, oral presentation.

A. R. Pinto, V.M. Correlo, M. Bhattacharya, P. Charbord, R.L. Reis, N.M. Neves (2005). "Behaviour of Human Bone Marrow Mesenchymal Stem Cells Seeded on Fiber Bonding Chitosan Polyester based for Bone Tissue Engineering Scaffolds". 8th TESI Annual Meeting, Shanghai, October 22-25, oral presentation.

A. R. Costa-Pinto, V. M. Correlo, M. Bhattacharya, P. Charbord, R. L. Reis, N. M. Neves (2006). "Study of the Osteogenic Behaviour of Primary Cultures of Human Bone Marrow MSCs seeded onto Chitosan-Polyester based Scaffolds". Genostem 2nd Workshop on Mesenchymal Stem Cells Engineering for Connective Tissue Disorders, Porto, Portugal, January 18-21, poster presentation.

A. R. Costa-Pinto, V. M. Correlo, P. Sol, A. Salgado, M. Bhattacharya, P. Charbord, R. L. Reis, N. M. Neves (2006). "Study of the osteogenic behaviour of adult stem cells and novel melt-processable chitosan-polyester based scaffolds for bone tissue engineering". Regenerate World Congress on Tissue Engineering and Regenerative Medicine - TERMIS, Pittsburgh, Pennsylvania, USA, April 24-27, oral presentation.

A. R. Costa-Pinto, V. M. Correlo, P. Sol, M. Bhattacharya, P. Charbord, R. L. Reis, N. M. Neves (2006). "Human bone marrow mesenchymal stem cells differentiation when seeded onto novel chitosan-polyesters fiber mesh scaffolds: a bone tissue engineering approach". 1st Annual Meeting of Portuguese Society for Stem Cells and Cell Therapy (SPCE-TC), Madeira, Portugal, May 30-31, poster presentation.

A. R. Costa-Pinto, V.M. Correlo, P. Sol, M. Bhattacharya, P. Charbord, R. L. Reis, N. M. Neves (2006). "Human bone marrow mesenchymal stem cells

differentiation when seeded onto novel chitosan-polyesters fiber mesh scaffolds: a bone tissue engineering approach". ESF-EMBO Symposium Conference on Stem Cells in Tissue Engineering, Sant Feliu de Guixols, Spain, October 28 - November 2, oral presentation.

A.R. Costa-Pinto, V.M. Correlo, P. Sol, M. Bhattacharya, P. Charbord, R. L. Reis, N. M. Neves (2007). "Engineering three-dimensional bone tissue *in vitro* using chitosan melt based biodegradable scaffolds and hBMSCs". Genostem 3rd Workshop on Mesenchymal Stem Cells Engineering for Connective Tissue Disorders, Barcelona, Spain, February 7-9, poster presentation.

A. R. Costa-Pinto, V. M. Correlo, P. Sol, M. Bhattacharya, P. Charbord, B. Delorme, R. L. Reis, N. M. Neves (2007). "*In vivo* testing of chitosan based scaffolds for bone tissue engineering". Week of School of Engineering of University of Minho, Guimarães, Portugal, October 23, poster presentation.

A. R. Costa-Pinto, V.M. Correlo, P. Sol, M. Bhattacharya, P. Charbord, B. Delorme, R.L. Reis, N.M. Neves (2007). "*In vivo* testing of chitosan based scaffolds for bone tissue engineering". Genostem 4th Workshop on Mesenchymal Stem Cells Enginnering for Connective Tissue Disorders, Montpellier, France, November 14-17, poster presentation.

A. R. Costa-Pinto, V.M. Correlo, P. Sol, M. Bhattacharya, P. Charbord, B. Delorme, R.L. Reis, N.M. Neves (2007). "Biological performance of human bone marrow mesenchymal stem cells cultured onto novel chitosan polyester scaffolds". Termis-AP, Tokyo, Japan 3-5 December, oral presentation.

A. R. Costa-Pinto, A. M. Frias, M. Alves da Silva, S. Fernandes, A. Barros, R. L. Reis, N. M. Neves (2008). "Comparative study of the multidifferentiation potential of Human Wharton's Jelly and Amniotic Fluid derived Stem Cells". Termis-EU, Porto 22-26 June, oral presentation.

A. R. Costa-Pinto, R. L. Reis, N. M. Neves (2008). "Potential of human adult stem cells and natural-based biodegradable scaffolds for bone tissue engineering".

6th Marie Curie Cutting-Edge Conference, entitled “Stem cells: from the petri dish to the clinical application”, Algarve October 27-31, oral presentation.

A. R. Costa-Pinto, V.M. Correlo, P.C. Sol, M. Battacharya, A. Martins, P.F. Costa, R.L. Reis, N.M. Neves (2009). “Scaffold composition conditions the osteogenic differentiation in flow perfusion culture of human mesenchymal stem cells”. 2nd TERMIS World Congress in conjunction with 2009 Seoul Stem Cell Symposium, Seoul, Korea (south), August 31 – September 3, oral presentation.

A. R. Costa-Pinto, V.M. Correlo, P.C. Sol, M. Battacharya, A. Martins, P.F. Costa, R.L. Reis, N.M. Neves (2009). “The culture of human mesenchymal stem cells on chitosan based scaffolds in a multi-chamber flow perfusion bioreactor for bone tissue engineering”. 2nd TERMIS World Congress, Seoul, Korea (south), August 31 – September 3, poster presentation.

A. R. Costa-Pinto, R. L. Reis, N. M. Neves (2009). “Culture of hBMSCS on chitosan based scaffolds in a multi-chamber flow perfusion bioreactor for bone tissue engineering”. Week of School of Engineering of University of Minho, Guimarães, Portugal, October 23-24, poster presentation.

A. R. Costa-Pinto, A. M. Martins, M. J. Castelhano-Carlos, V. M. Correlo, P. C. Sol, R. L. Reis, N. M. Neves (2010). “Tissue response and *in vitro* degradation of chitosan-PBS based scaffolds”. TERMIS AP 2010 Meeting, Sydney, NSW, Australia, oral presentation.

A. R. Costa-Pinto, A. M. Martins, M. J. Castelhano-Carlos, V. M. Correlo, P. C. Sol, R. L. Reis, N. M. Neves (2010). “*In vitro* degradation and biocompatibility of chitosan-PBS based scaffolds”. Week of School of Engineering of University of Minho, Guimarães, Portugal, October 18, oral presentation.

A. R. Costa-Pinto, A. M. Martins, M. J. Castelhano-Carlos, V. M. Correlo, P. C. Sol, R. L. Reis, N. M. Neves (2010). “Degradation kinetics and host response of chitosan based scaffolds”. IBB 2nd Annual Scientific Meeting, October 23-24, accepted as oral presentation

STRUCTURE OF THE THESIS

This thesis is divided in six sections containing eight chapters, being five of them experimental work. The structure of the thesis was adopted having in mind the final objective of this PhD research, leading to a successful bone tissue engineering strategy. The experimental part was divided in 3 sections, 3, 4 and 5. In each of these sections it is described each one of the phases of the work developed in this thesis. The contents of each section are summarized below.

SECTION 1 (Chapter I)

Chapter I is based on a review paper, presenting an overview on bone tissue engineering using chitosan based scaffolds. Bone biology is briefly analyzed to clarify the role of the various components required to achieve a successful bone tissue engineering strategy. These components are discussed in detail, covering from the type of scaffold to the *in vivo* proof of concept. The choice of cells, type of biomaterial used to produce the scaffold and its *in vivo* validation, as well as the type of animal models are also presented. In all these aspects, a special attention was given to chitosan as a suitable biomaterial to produce scaffolds for bone tissue engineering. It is also included a review of the literature on the different types of chitosan processing methodologies. The review also discusses the reports *in vitro* and *in vivo* on bone tissue engineering strategies using chitosan.

SECTION 2 (Chapter II)

Chapter II presents the materials and experimental procedures used in the present thesis. This chapter contains additional information about the experimental methods used in the various chapters of the thesis. Furthermore, it aims also at providing a general framework for the testing of new tissue engineering strategies in a comprehensive and structured way.

SECTION 3 (Chapters III and IV)

Chapter III describes the *in vitro* testing of scaffolds produced with various chitosan-polyester formulations (PBS, PCL and PBTA) using in all cases the same

percentage of chitosan (50% wt). The scaffolds were processed by compression molding and particulate leaching. The eventual cytotoxicity of extracts from the scaffolds is evaluated with a L929 cell line. This chapter also presents the results of the first biological evaluation of these scaffolds, by using a mouse MSC cell line (BMC9) to select the most adequate scaffold formulation for bone tissue engineered applications. These *in vitro* results evidenced a superior performance for chitosan-poly(butylene succinate) scaffolds. The next step aimed at clarifying why this specific scaffold formulation evidenced a superior cell performance.

Chapter IV presents further *in vitro* studies using primary cultures of human MSCs differentiated into the osteogenic lineage on scaffolds produced with different chitosan percentages (0, 25 and 50%). The *in vitro* results allowed concluding that chitosan containing scaffolds have stronger biological performance than 100% PBS scaffolds. This work also reports an experimental design to assess the *in vivo* effect of the chitosan, by implanting the scaffolds without and with 50% chitosan. The trend already observed *in vitro* was further confirmed *in vivo*, showing that the chitosan containing scaffolds elicit a milder inflammatory response and no signs of tissue necrosis when compared with scaffolds of PBS (without chitosan).

SECTION 4 (Chapters V and VI)

Chapter V reports the results of the *in vitro* testing of scaffolds produced by fiber bonding, with an optimized porous morphology and with the formulation having the strongest performance in previous experiments (chitosan-PBS 50% wt). These scaffolds have enhanced porosity and interconnectivity, facilitating the cell ingrowth. In fact, the previous *in vitro* results obtained in chapter IV evidenced some difficulty of the cells to penetrate the porous structure of the scaffolds produced by compression molding/salt leaching. The results obtained *in vitro* using human MSCs differentiated into the osteogenic lineage evidenced a superior cell ingrowth throughout the entire scaffolds structure. This evidence showed that the optimized morphology indeed was able to facilitate the cell migration into the porous structure of the scaffold.

Chapter VI reports the results of the study of the biodegradation of the scaffolds previously tested in chapter V, both *in vitro* and *in vivo*. The *in vitro* studies were intended to model the degradation *in vivo*, using specific enzymes. The

selected enzymes (lysozyme and lipase) are known to degrade the two polymers used to produce the scaffolds. The concentrations of enzymes used *in vitro* were similar to those found in the human serum, to predict the degradation of the developed scaffolds. The *in vivo* analysis was performed to assess the biodegradation of the scaffolds and to compare its kinetics with the one obtained in the *in vitro* results. Furthermore, it was also evaluated the tissue response to the implantation of the new scaffold morphology, comparing the inflammatory response with the one previously obtained for the scaffolds with similar composition but with different porous morphology.

SECTION 5 (Chapter VII)

Chapter VII describes the *in vivo* validation of the tissue engineering strategy proposed in this thesis. After studying the *in vitro* performance and the *in vivo* tissue response of the developed scaffolds, in the context of bone tissue engineering, it was necessary to demonstrate if the strategy would be effective in a relevant *in vivo* model. For that, it was used an orthotopic model in the calvaria of nude mice to verify if pre-cultured human bone MSCs on chitosan-PBS scaffolds were able to stimulate bone regeneration *in vivo*. The scaffolds used in this model were produced by compression molding and salt leaching, being the preferred morphology enabling producing a scaffold with the geometry required to fit into the bone defect used.

SECTION 6 (Chapter VIII)

Chapter VIII contains the general conclusions and final remarks regarding the series of studies performed under the scope of this thesis. It is intended to provide a general summing up of the conclusions extracted in the various sections and allowing a complete analysis of the progress obtained in the framework of this thesis.

SECTION 1

CHAPTER I

INTRODUCTION

Chitosan based scaffolds for bone tissue engineering applications

This chapter is based on the following publication: Costa-Pinto AR, Reis RL, Neves NM. "Chitosan based scaffolds for bone tissue engineering applications" 2010; Submitted.

CHAPTER I
INTRODUCTION

ABSTRACT

As life expectancy increases, malfunction or loss of tissue caused by injury or disease leads to reduced quality of life in many patients at significant socio-economic cost. Even though major progresses have been made in the field of bone tissue engineering during the last few years, current therapies such as bone grafts still have limitations. Current research on biodegradable polymers is emerging, combining these structures with osteogenic cells, as an alternative to autologous bone grafts.

Different types of biodegradable materials have been proposed to be used as three-dimensional (3D) porous scaffolds for bone tissue engineering. Among them, natural polymers are one of the most attractive options, mainly due to their similarities with extracellular matrix (ECM), chemical versatility, good biological performance and inherent cellular interactions. In this review, special attention is given to chitosan as a biomaterial for bone tissue engineering. An extensive literature survey was performed about the processing of chitosan scaffolds and its biological performance *in vitro* as well as its *in vivo* bone regeneration potential.

The present review also aims to offer the reader a general overview on all components needed to engineer new bone tissue, giving a brief background on bone biology, followed by an explanation of all components in bone tissue engineering, as well as describing different tissue engineering strategies. Moreover, it will be exploited the typical model to evaluate the *in vitro* functionality of a tissue engineered construct and the *in vivo* models to assess the potential to regenerate bone tissue.

1. INTRODUCTION

Bone tissue, when injured, leads to dramatic changes in the quality of life of patients. It can limit the ability to perform basic tasks, such as walking and frequently causes social and psychological problems. The current clinical available solutions for these problems rely on bone graft transplants (autologous, allogenous and xenogenic), bone transport methods (Ilizarov technique) and implants based on different types of materials. More than 2.2 million bone graft procedures (autologous bone graft and banked bone) take place annually

worldwide (1, 2). Those procedures ensure adequate bone healing in many skeletal problems, such as non-union fractures, cervical and lumbar spine fusion, joint arthrodesis or revision arthroplasty. Bone grafting is a strong and mature business generating sales of more than $2.5 billion a year (3). Autografts are considered the gold standard for bone repair. However, some complications may occur, such as bone non-unions and blood loss, which increases the need for blood transfusions (4-7). Moreover, besides being an expensive procedure, there is a limited supply of tissue and it causes significant donor site morbidity (6, 8). Allografts are typically non-vital (dead) bone harvested from a cadaver and then processed using a freeze-drying method that extracts all the water via a vacuum drying process. These type of grafts avoid donor site morbidity, but present a potential risk for disease transmission and severe immune response by the patient (9). Similar to allogeneic bone, xenogenic bone is non-vital bone derived from other species, mainly from bovine origin. Because the potential for immune rejection and contamination by viral proteins is higher in bovine bone than in human cadaver bone, xenograft material is processed at very high temperatures. The Ilizarov methodology consists of an osteotomy followed by bone distraction by extendable fixation devices. This technique avoids problems related with the osteointegration of bone grafts, but requires longer periods of treatment (12-18 months) and can be quite painful for the patient (10). The aforementioned limitations justify the need to develop new therapies using alternative concepts that are currently the focus of intense research efforts.

Bone has a notable regenerative ability but a considerable amount of bone loss or the development of an adverse microenvironment can hinder this capacity, such in cases of severe trauma, developmental deformities, revision surgeries and tumor resection (11, 12). In these cases, bone tissue engineering holds the promise of great therapeutic potential (13). Bone tissue engineering may constitute the needed breakthrough technology to solve the problem of bone shortage in various destructive clinical conditions and deformities, by providing functional tissue engineered biological substitutes (14). The most promising strategy used in this field is based on the seeding and *in vitro* culture of primary osteoblasts or adult stem cells, differentiated into the osteogenic phenotype on three-dimensional (3D) scaffolds (synthetic, natural or ceramics). These constructs will be further implanted into a bone defect. The cells will synthesize the ECM of the new bone tissue, while the scaffold will provide the adequate 3D environment for the cells to adhere, proliferate and differentiate. The scaffolds will be not only temporary 3D supports for the cells to create new bone, but also space filling and local controlled release devices of signaling molecules. To accomplish all these goals, the scaffold should meet stringent requirements, such as biodegradability at

such rate that is compatible to the rate of new tissue formation. Other important properties include the biocompatibility with host tissues, non-toxicity and non-immunogenicity, appropriate mechanical properties, adequate porosity and morphology (15-17). All these properties are essential to facilitate and guide cell ingrowth, transport of gases, metabolites, nutrients and signaling molecules, both within the scaffold and between the scaffold and the native local environment.

The selection of the most suitable material to produce a scaffold to be used in bone tissue engineering applications is a determinant step, since its properties will determine its final characteristics. Biodegradable polymers, either synthetic or natural, are the most appropriate substrates for the cells to attach, grow and maintain a differentiated phenotype. In the last years, natural origin polymers have been increasingly proposed for the referred application. In our group, we have been working with natural based polymers, such as starch (18-22), chitosan (23-27), gellan gum (28-31), soy (32) or silk (33, 34). Our strategy is to mimic nature and, for that, we have been using those polymers to design functional microenvironments stimulating tissue morphogenesis. In particular, chitosan has shown an excellent combination of properties and it has been demonstrated that it is a suitable biomaterial to develop scaffolds for bone tissue engineering. Chitosan can be used either alone (23, 35-41) or in combination with other biodegradable polymers, such as aliphatic polyesters (25, 42-47), other natural polymers such as starch (26, 48, 49) or silk (50, 51), or with ceramics, such as hydroxyapatite (HA) (24, 52-60).

This manuscript aims to provide an overview of the most important concepts in bone tissue engineering and a review on chitosan based scaffolds proposed in the literature to regenerate bone tissue. The potential of this biomaterial as a suitable substrate to support osteogenic differentiation of mesenchymal stem cells (MSCs) will also be explored.

2. BRIEF OVERVIEW OF BONE BIOLOGY

Bone is a dynamic and complex tissue evolving and adapting to various stimuli throughout the entire lifetime (61). It plays crucial roles in both mechanical support and mineral homeostasis (62). Within a skeletal element, there are different morphologies of bone, such as cortical and trabecular bone. Cortical bone is a compact structural tissue, with only 10% porosity, being 80% of the mass of an adult human skeleton. Trabecular bone is a spongy structure with 50-90% porosity, filled with bone marrow. The majority of bones are covered by a highly vascularized fibrous connective tissue, the periosteum (63). Five different

cell types are involved in bone maintenance and remodeling: MSCs, bone-lining cells, osteoblasts, osteocytes and osteoclasts. Within the bone structure, MSCs are found in the bone marrow (64-67) and also in the periosteum (68). The bone marrow is composed of hematopoietic tissue and the supporting stroma (69). Marrow stromal cells, originally thought to only contribute to the hematopoietic microenvironment, later came to the center stage with the recognition of being the stem/progenitor cells of skeletal tissues (65). Human autologous bone marrow associated with macroporous hydroxyapatite scaffolds were implanted in large bone segmental defects and shown to promote bone regeneration (70). After a 7 years follow up (71), the patients presented a complete healing of the defects. Bone-lining cells are flat cells that cover all bone surfaces and are believed to have origin from osteoblasts that become inactive (72, 73). These cells form an important cellular barrier that divides the canalicular network (where osteocytes are present) from other fluids (63). Osteoblasts are cells derived from MSCs that synthesize the osteoid (non-mineralized organic matrix of the bone, *i.e.* type I collagen, osteocalcin, osteopontin, bone sialoproteins and bone morphogenetic proteins) (74). Osteoblasts also have an active role in the vascularization process by secreting morphogens that activate angiogenesis by signaling endothelial cells (75-77). Osteocytes are terminally differentiated osteoblasts entrapped within the bone ECM, that are involved in the maintenance of ECM and calcium homeostasis (63). Osteocytes are also the cells sensing mechanical stress and communicating signals for bone remodeling and tissue maintenance (78). The fifth cell type is the osteoclast, responsible for bone resorption that is the first stage of the bone remodeling process, followed by bone homeostasis. These cells are large multinucleated cells differentiated from a fraction of monocytes found in the peripheral blood (63).

As many other connective tissues, one of the main components of bone is its ECM, that in this case is mineralized. Bone ECM is composed of 35% of organic matrix and 65% of mineral matrix. The most abundant mineral in bone ECM is HA, a calcium phosphate crystallized at the surface of collagen fibrils, required to resist to bending and compression stresses (61). The organic matrix is mainly proteic composed of type I collagen (90%) and the remaining fraction includes up to 200 other non-collagenous proteins, such as glycoproteins, proteoglycans, integrin-binding proteins and growth factors (61).

Bones are developed by two main processes: intramembranous and endochondral ossification (79, 80). Intramembranous ossification is a process that generates flat bones and the skull structure. In this pathway, the embryonic mesenchyme condenses and develops in primary ossification centers, which will eventually fuse to form a network of anastomosing

interconnected trabeculae made of woven bone (79). After that, periosteum is formed at the surface of trabeculae, further mineralized and part of the intertrabecular connective tissue is transformed in hematopoietic tissue (80). Finally, the woven bone is remodeled into a lamellar type of bone (81). Endochondral ossification is an osteogenic process through which long bones, vertebrae and pelvis are generated from their precursor cartilaginous tissue. (82). This process starts in the fetus stage where MSCs differentiate into chondrocytes, converting the condensed mesenchyme into a cartilaginous model of bone that will expand in its extremities, while becoming hypertrophic in the center. These hypertrophic chondrocytes will promote primary ossification by secreting molecules (such as alkaline phosphatase, type X collagen or vascular endothelial growth factor - VEGF) that will induce calcification of cartilage. This tissue will be resorbed, becoming a structure onto which progenitor cells differentiate into osteoblasts that start to deposit osteoids. After birth, the secondary ossification centers are developed at the extremity of long bones allowing the development and growth of bone structure (81).

3. BONE TISSUE ENGINEERING STRATEGIES

Bone has an intrinsic self-ability to regenerate, but over a large defect, inherent osseous processes are not able to repair the defect during the patient´s lifetime (83). Furthermore, diseased bones do not heal properly, and under certain pathological conditions start damaging themselves (83-85). Tissue engineering has emerged as a possible solution for these clinical conditions. Several strategies can be employed to develop new bone tissue. Those strategies may involve the use of an ECM-like structure (scaffold), cells, and/or growth factors. These three basic components need to be well synchronized in order to achieve a successful tissue engineering therapy. The strategy used for a specific bone defect must be adapted to the clinical state of the patient. There are three main approaches originally described for tissue engineering: 1) to use engineered matrices alone, in order to guide tissue regeneration; 2) to inject autologous, allogeneic, or xenogeneic cells alone; 3) to develop constructs of cells seeded on those matrices (14). The first method involves implanting the scaffold at the site of interest, allowing host cells to migrate from the surrounding tissues to colonize the scaffold. The second strategy has the advantage of involving minimal surgical invasion and cells can be manipulated by recombinant gene technology or clonal expansion prior to injection or infusion. However, this methodology has limitations for bone critical size defects, due to the absence of the supporting matrix to keep cells at the defect site. In the last approach, cells are seeded onto scaffolds (construct) and

later implanted into the bone defect. Usually constructs are produced *ex vivo* prior to transplantation to a bone defect and over time cells will synthesize a new ECM, as the scaffold degrades, creating a new functional tissue. This review will focus on the third tissue engineering strategy, exploring the potential use of autologous stem cells cultured onto biodegradable scaffolds that will act as extracellular matrices, supporting cell growth and tissue development.

4. NATURAL BASED POLYMERS FOR SCAFFOLD DESIGN

Nature offers a remarkable set of materials with great potential to be used in different fields. The study and use of natural materials comes from ancient times, such as cellulose, that is used to produce paper or silk to produce clothes. In medicine for example, chitosan is used as wound dressing material and collagen as a substitute in reconstructive surgery. Today, powerful tools are available and the micro and nanostructures of these materials were already clarified. The new level of knowledge brought new opportunities to develop materials for other applications, such as scaffolds for tissue engineering. Great efforts have been made to recapitulate the key features of bone ECM by developing structures that mimic this naturally occurring matrix. ECM plays an important role over cell activities, modulating their behavior (86). One difficulty in developing such scaffolds is the complexity to recreate a similar microenvironment to the tissue of interest. A simple approach to mimic nature is to use naturally occurring materials. Moreover, natural polymers have different functions, such as the role of polysaccharides in the cell membranes, intracellular communication and storage, or proteins that are structural materials and catalysts (enzymes) (87). Natural polymers such as starch (18-20, 22, 88-90) or chitosan (91-94) have been described as biocompatible, biodegradable and having tailored degradation rate (88, 92). Some drawbacks of these biomaterials are the limited mechanical properties and processability or variability between different batches (15). Examples of natural polymers commonly used to produce scaffolds are collagen (95-99), hyaluronan (100, 101), alginate (102), silk (50, 103, 104) and chitosan (23, 37, 41). These polymers can be combined with other synthetic materials, to improve their processability and mechanical properties. Combinations with HA (105), aliphatic polyesters (25, 27, 106, 107) or composites of different natural polymers (26, 48) have also been described. Herein a special focus will be given to the natural polysaccharide chitosan, the deacetylated product of chitin obtained from the exoskeleton of crustaceans.

5. CHITOSAN AS A NATURAL ORIGIN BIOPOLYMER

The history of chitosan dates back from the 19th century when Rouget discussed its deacetylated form (108). Chitosan is a linear polysaccharide, obtained from the deacetylation of chitin, the primary structural polymer of the exoskeleton of crustaceans, cuticles of insects and cell wall of fungi (109, 110). Chitosan is composed of glucosamine and *N*-acetyl glucosamine with β (1-4) link (111). Chitosan is the common name for the family of deacetylated chitins, with different degrees of deacetylation. By definition, when the number of N-acetyl glucosamine units is higher than 50%, the polymer is considered chitin. On the other hand, when the number of N-glucosamine units is superior, its name is chitosan (112). The molecular weight of chitosan may range from 300 to more than 1,000 kDa, depending on its origin and on the preparation method (35). The solubility of chitosan depends on the free amino and N-acetyl groups, being soluble in acidic pH (35). The cationic nature of chitosan allows electrostatic interactions with anionic glycosaminoglycans (GAGs) and proteoglycans. Natural polymers are known to influence cell morphology, modulation and differentiation (113, 114), as referred previously. This property is of crucial importance in tissue engineering field, because GAGs molecules modulate the action of several cytokines and growth factors (115).

Chitosan presents a wide range of properties that makes it suitable for tissue engineering applications, namely its biodegradability (91, 116, 117), biocompatibility (93, 94, 118-120), antibacterial activity (121-123), wound healing properties (124-130) and easy accessibility.

Chitosan can be hydrolyzed by chitosanases (131), which are absent in mammals. It is well documented that lysozyme is responsible for the biodegradation of chitosan *in vitro* (91, 92, 132, 133). The degradation rate of chitosan is inversely related to the degree of deacetylation (132), which represents the proportion of N-acetyl-D-glucosamine units to the total number of units (131). Lysozyme is ubiquitous in the human body (134). It is found in lacrimal gland, middle ear, nose, bronchus, bronchiole, bone marrow and digestive tract (135). Lysozyme has an important role in inflammatory response, being secreted by macrophages, monocytes, and granulocytes (136, 137). Monocytes and macrophages are the main contributors to the presence of lysozyme in human serum in concentrations between 7 and 13 mg/L (134).

Chitosan has intrinsic anti-microbial properties against several microorganisms, namely fungi and bacteria (138). The accurate mechanism is still unknown, although its

cationic nature associates with anions in bacteria cell wall, suppressing biosynthesis and also disrupting the mass transport across the cell wall, leading to the death of bacteria (138).

Chitosan has been described as a potent wound healing accelerator (139), and to possess immunological activity, by activating macrophages (140), to produce cytokines (141) and to inhibit infection (142).

One of the most important characteristics of chitosan, for tissue engineering applications, is its ability to be shaped into various structures, such as microspheres (143), paste (144), membranes (113), sponges (37, 145-148), fibers (27, 38, 149) and porous scaffolds (25, 27, 56, 150, 151). Several processing methodologies have been used to produce chitosan porous scaffolds and will be herein further discussed in detail. Nevertheless, before describing the scaffolds processing techniques, it is important to underline the properties that a scaffold must possess to be successfully applied in bone tissue engineering applications.

6. SCAFFOLD REQUIREMENTS FOR BONE TISSUE ENGINEERING

Bone is a 3D tissue and cells alone do not grow in a 3D manner *in vitro*. For that reason, a tridimensional structure is required to support the formation of new functional bone tissue. This structure should provide a suitable environment for cell attachment, proliferation, differentiation and ECM deposition. The *in vitro* cultured constructs, when implanted into the defect must be vascularized and osteointegrated into the host bone (152). The 3D structures should be biocompatible, *i.e.,* not evoking an immune response when implanted in the host tissue. When a scaffold is implanted into the defect to restore bone functionality, it should activate the healing mechanisms (inflammatory response). The time course of healing is influenced by interactions between blood, scaffold surface and degradation products, which are released from the scaffold and therefore, influencing biocompatibility. The ideal scaffold should degrade in a rate compatible with the rate of bone growth, physically creating open space for the new bone formation, until full regeneration is achieved. The process of polymer degradation follows the mechanisms through which polymer chains are cleaved into oligomers and finally to monomers, that can be metabolized by natural mechanisms (153). If a biological process mediates the degradation process, it is designated by biodegradation (153). Several factors influence the kinetics of degradation: type of chemical bonds, pH, polymer composition, crystallinity, molecular weight, porosity, water uptake and anatomical location of the implant (153). Ideally, natural pathways of the animal body should eliminate

the degradation products.

As previously discussed, bone is a highly vascularized tissue, relying on the interactions between bone cells and blood vessels. In this way, angiogenesis and neovascularization play a crucial role in bone repair, and should be taken into account when designing a scaffold. Angiogenesis is mainly characterized by the protrusion and outgrowth of capillary buds and sprouts from pre-existing blood vessels, while neovascularization comprises the formation of functional microvascular networks with red blood cell perfusion (154). Both processes are required to ensure successful engraftment of the construct into the surrounding host tissue. A vascular network can be included in a biodegradable and biocompatible scaffold by microfabrication techniques (155). The main property of the scaffold that is directly related to vascularization is its porosity (156). Scaffolds should have highly interconnected porosity to promote cell ingrowth and distribution throughout the matrix, as well as facilitating the development of neovascularization. The minimum pore size is considered to be approximately 100-150 μm (157), due to cell size, migration requirements and fluid transport. However, due to vascularization requirement, pore sizes were shown to affect the course of osteogenesis (156). Large pores rapidly become well-vascularized leading to direct osteogenesis (158, 159). In contrast, small pores lead to hypoxic conditions, which tend to induce the development of osteochondral process, before osteogenesis occurs. The porosity strongly influences scaffold mechanical properties. High porosity and pore size facilitates tissue ingrowth, but the consequence is a drastic reduction of mechanical properties, compromising the structural integrity of the scaffold (160). The mechanical properties of a scaffold should be compatible with those of the native tissue, maintaining its structural integrity after implantation (161). In general, the scaffold should be strong enough to not only resist to stresses that may cause important dimensional changes, but also to overcome the contraction that will exist during the *in vivo* tissue healing. Scaffold integrity is critical, since cells and tissue remodeling are important to achieve stable biomechanical environment and vascularization at the host site. The topography and surface chemistry of the scaffold play a crucial role in its performance, since those are the first elements that cells recognize when in contact with the scaffold surface. The type of proteins that will adsorb to the surface of the material, hydrophilicity or hydrophobicity will modulate to a great extent the protein adsorption, which will influence cell activity upon seeding (162).

The methodology used to produce scaffolds for bone tissue engineering must not adversely affect biocompatibility or physical and chemical properties of the biomaterials used. Different scaffold batches should exhibit minor variations in their properties, when processed

with similar processing parameters and conditions (163). Different processing methodologies for chitosan based scaffolds were already reported in the literature and will be further discussed in detail.

7. CHITOSAN SCAFFOLDING METHODOLOGIES

The most common processing methodology described for chitosan scaffolds is freeze-drying. This process consists in the lyophilization of a frozen chitosan solution, where the chitosan acetate salt is induced by the freezing conditions to phase-separate from the ice crystal phase. The ice phase is further sublimated, producing a porous structure (24, 35, 37, 51, 56, 148, 151, 160, 164-175). In most cases, the scaffolds can still have chitosan acetate that will cause fast swelling and subsequently dissolution in a neutral aqueous medium. This can be overcomed by crosslinking upon immersion in sodium hydroxide (35, 169), sodium sulfate (38), tripolyphosphate (37, 148), ethanol series (35), or with a combination of crosslinking with rehydration (164). The freeze-drying technique requires a very tight control of the temperature. If the temperature is not sufficiently low, the matrix will not become rigid enough to support the interfacial tension caused by the evaporation of the solvent without collapsing, creating a surface skin. Another limitation of the structures produced by this technique is that the size of the pores is not very large. Also the mechanical properties of the porous structures are very limited, even after cross-linking. Due to the susceptibility of freeze-drying methodology, solvent exchange phase separation has been proposed as an alternative methodology. This technique is based in the gelation of a solution of chitosan using an alkaline solution below its gelation point (26, 36, 53, 176). In freeze-drying process, the choice of the solvent is limited, since the solvent vapor pressure at the drying temperature (usually low) must be high enough to allow its removal (36). With this alternative method, less time consuming and more economic, the choice of the solvent is wider (36).

Another processing methodology of chitosan is wet spinning, allowing producing fibers. Due to the strong inter-chain forces derived from the hydroxyl and amino groups, chitosan tends to degrade at temperatures below its melting temperature, limiting its processability by melt or dry spinning methods (38, 41, 149, 177-179). Basically, chitosan is dissolved in a solution of diluted acetic acid. This solution is spun through a spinneret into a coagulation bath, in this way producing fibers. Chitosan can also be processed by electrospinning into a nanofiber mesh scaffold. This method uses an electrical field created between a collector and a capillary connected to a reservoir with the polymer solution. The

elongation of the drop of solution caused by the electrical field leads to the formation of very thin fibers with nanometer scale diameters. Electrospinning of pure chitosan (39, 180-183) is considered to be quite difficult, since the resulting chitosan salt is soluble in water. Its stability in solution requires neutralization or crosslinking in a post-processing stage that frequently has an impact in the morphology of the mesh. Several studies report the blending of chitosan with other polymers, being easier to process by electrospinning, namely silk fibroin (184), poly(ethylene oxide) (PEO) (185, 186), poly(vinyl alcohol) (PVA) (187), collagen (188) or polycaprolactone (189).

Less conventional is the particle aggregation method (Figure 1) proposed by Malafaya *et al*. (23). This process relies on the bioadhesive character of chitosan that confers a strong bonding between individual particles. The scaffolds produced by this method have shown very interesting mechanical properties. In another study, chitosan-poly(lactic-co-glycolic acid) (PLAGA) microspheres were molded by mixing them with acetic acid solution, in a stainless steel mold (190).

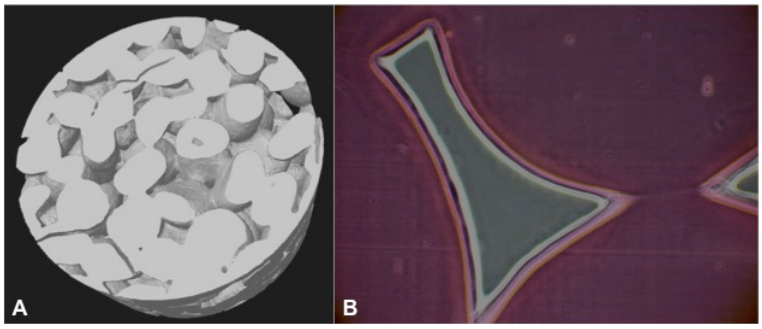

Figure 1. Micro computed tomography image of a cross-section of chitosan scaffolds obtained by particle aggregation method (A) and interface between particles stained with eosin (B).

Rapid prototyping is a processing route enabling also to develop chitosan porous scaffolds. This methodology is based on the production of a 3D physical model from computer aided design data (CAD software), which is generated in a layer-by-layer deposition process (150, 191). Theoretically, a great variety of morphologies and shapes can be created by different variants of these techniques, and the scaffolds will be highly reproducible.

Our group developed different chitosan based scaffolds by melt based routes (42, 44). The vast majority of the processing methods used to produce chitosan scaffolds involve the use of solvents. Those solvents are frequently harmful for cells, because residual solvent may be entrapped in the scaffold and these are toxic for the cells. We developed various blends of chitosan with different aliphatic polyesters. Those blends can be processed by compression molding followed by salt leaching (42) and by melt spinning and fiber bonding (27, 44) into porous scaffolds with different morphologies and mechanical properties (Figure 2).

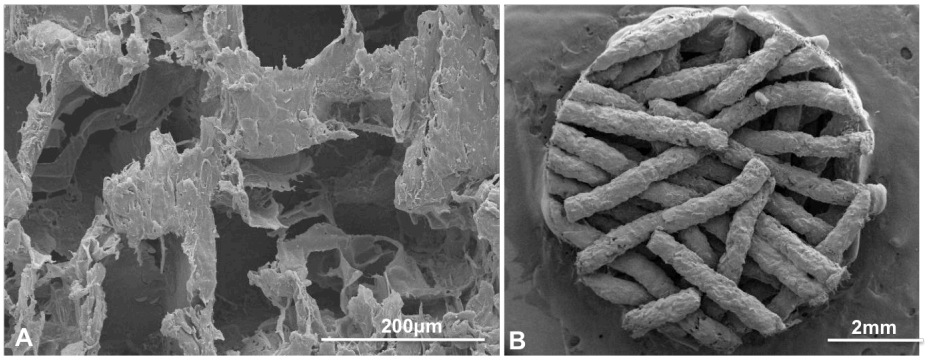

Figure 2. Chitosan based scaffolds produced by compression molding followed by particle leaching (A) and fiber bonding (B) methodologies.

A systematic list of various porous scaffold compositions using chitosan, the processing methods used to obtain the scaffolds and the *in vitro* evaluation with different cell types is provided in Table I. It is clear from the table that the most used processing method to obtain chitosan-based porous scaffolds is freeze drying or freeze related processes. The main reason is probably the simplicity of the process.

Table I. Survey of *in vitro* studies with chitosan based scaffolds proposed in the literature for bone tissue engineering applications.

Scaffold structure	Processing method	Cell type (source)	References
Chitosan scaffolds	Freeze drying	-	(35)
Chitosan-TCP sponges	Freeze drying	Fetal rat calvaria cells	(148)
Chitosan-gelatin scaffolds	Freeze drying	-	(164)
Chitosan-TCP sponges	Freeze drying	MG63 human cell line	(192)
Chitosan-HA scaffolds	RP and Freeze drying	-	(150)
Chitosan-calcium phosphate scaffolds	Freeze drying	MG63 human cell line	(56)
Chitosan scaffolds	Freeze gelation	ROS 17/2.8 cells	(36)
Chitosan sponges	Freeze drying	Rat calvaria cells	(37)
Chitosan fiber mesh scaffolds	Wet spinning	Human SAOS-2 cell line	(38)
Chitosan scaffolds	Freeze drying	MG63 human cell line	(165)
Chitosan-silk scaffold	Freeze drying	-	(51)
Chitosan scaffolds	RP	Porcine BMSCs	(191)
Chitosan scaffolds	Electrospinning	-	(39)
Chitosan-gelatin scaffolds	Freeze drying	HUVECs	(193)
Chitosan scaffolds	Precipitation/Particle aggregation	ADAS	(23)
Chitosan sponges	Freeze drying	MG63 human cell line	(167)
CPC-Chitosan scaffold	Cement/Particle leaching	MG63 human cell line	(194)
Chitosan-starch scaffolds	Solvent-exchange phase separation	-	(48)
Chitosan scaffolds with HA formation	Freeze drying	Human SAOS-2 cell line	(169)
Chitosan-nanoHA scaffolds	Freeze drying	MC3T3-E1 cell line	(168)
Chitosan-coralline scaffolds	Freeze drying	CRL-12424 cell line	(170)
HA-chitosan scaffold	Freeze drying	Goat bone marrow cells	(24)
Chitosan-gelatin scaffolds	Freeze gelation	hBMSCs	(53)
BCP-chitosan scaffolds	Freeze drying	MC3T3-E1 cell line	(171)
Chitosan-PLAGA scaffolds	Particle aggregation	MC3T3-E1 cell line	(195)
Chitosan gelatin/montmorillonite scaffolds	Freeze drying	Rat stromal cells TC1	(172)
Chitosan scaffolds	Freeze gelation	-	(40)
Chitosan and chitosan-starch scaffolds	Freeze gelation	Human SAOS-2 cell line	(26)
Chitosan-collagen sponges	Freeze drying	Rat BMSCs	(173)
Chitosan-PBS/PBTA/PCL	Compression molding/salt leaching	Mouse BMC-9 cell line	(25)
Chitosan scaffolds	Wet spinning	Mouse osteoblast 7F2 cell line	(41)
Chitosan-PBS scaffolds	Melt spinning/fiber bonding	Human BMSCs	(27)
Chitosan-PBS/PCL/PBTA/PBSA	Compression molding/salt leaching	-	(42)
Chitosan-PCL scaffolds	Electrospinning	MC3T3-E1 cell line	(189)
Chitosan scaffolds	Freeze drying	MC3T3-E1 cell line	(175)
PLGA-chitosan scaffolds	Freeze drying	Human BMSCs	(174)
Chitosan sponges	Freeze drying	Chicken embryo chondrocytes	(196)
Chitosan and chitosan-starch + lysozyme scaffolds	Freeze gelation	Rat BMSCs	(197)
PCL-chitosan	Solvent casting/salt leaching/ freeze-drying	Rat osteoblasts	(46)

HA-Hydroxyapatite; TCP-Tricalcium phosphate; RP-Rapid prototyping; PLLA-Poly(L-lactic acid); ROS-Rat ostosarcoma cells; HUVECs- Human Umbilical Vein Endothelial Cells; ADAS-Adipose derived stem cells; CPC-Calcium phosphate cement; BCP- biphasic calcium phosphate; PLAGA-Poly(lactic acid-glycolic acid); PBS-Poly(butylene succinate); PCL-Polycaprolactone; PBTA-Poly (butylene terephtalate adipate); PBSA-Poly(butylene succinate adipate); PLGA-Poly(L-glycolic acid.

8. *IN VITRO* CELLULAR APPROACH IN BONE TISSUE ENGINEERING

The development of new scaffolds follows a typical evaluation routine. The first step is the assessment of the eventual cytotoxicity. This initial screening is based on the use of extracted leachables from the scaffold, *i.e.*, substances that leach out of the biomaterials. These leachables are added in defined concentrations to standard culture medium and placed in contact with a cell line for a determined period of time. After this, cell viability and cell morphology are evaluated to determine the eventual toxicity to the cells. The use of cell lines is recommended in a first stage, given that these cells are reproducible and can be expanded into large numbers. Cell lines, such as mouse fibroblast cells (L929) or human osteosarcoma cells (SAOS-2), are frequently used. If the scaffolds show no signs of cell cytotoxicity or morphology changes, the next step involves direct contact assays with an appropriate cell type to evaluate the cytocompatibility and phenotype functionality. A valid 3D construct for bone tissue engineering applications should have a positive outcome from this sequence of initial in-vitro tests.

8.1. SELECTION OF CELLS

The cell source should be ideally non-immunogenic, easily available, non-tumorogenic and with defined and adequate characteristics. It should be expandable into large numbers and have demonstrated osteogenic potential. Autologous cells, from each patient, are the most preferred (198-202). These cells may be isolated from a biopsy of tissue (*e.g.* cartilage, bone, skin) from the patient. The tissue obtained is dissociated and the isolated cells are expanded in culture for later implantation into the same patient (29, 70, 198). The use of autologous cells eliminates the risk of immune rejection, avoiding the need of using immunosuppressive drugs. For bone tissue engineering applications, osteoblasts are the most obvious selection, since those cells are responsible for the bone formation (74). However, these cells have limited availability since the number of cells that are obtained after the isolation procedure is low and the expansion rate is slow (203). In the last years, stem cells appeared as a valid alternative (203). The term stem cell is used to describe undifferentiated cells with ability to self-renew and maintain itself for long periods of time keeping its multilineage differentiation capacity (65). Stem cells can be classified as embryonic or adult. Embryonic stem cells (ESCs) are pluripotent cells derived from the inner cell mass of the blastocyst stage of an embryo (204). These cells possess long-term proliferation potential and are able to differentiate into all the types of somatic cells in the

organism. Nevertheless, ethical issues regarding its source restrain its use in regenerative medicine. Adult stem cells (ASCs) are a valid and alternative option to ESCs. These cells can be isolated from different adult tissue sources such as bone marrow (65), peripheral blood (205), adipose tissue (206), or fetal tissues such as umbilical cord (207), amniotic fluid (208) or placenta (209). ASCs are multipotential cells, capable of differentiating into several cell lineages such as osteoblasts, chondrocytes and adipocytes (210). Recent reports sustain the plasticity of these cells, *i.e.* the ability of differentiate into other cell types rather than the ones they are committed (211).

The process of osteogenic differentiation of stem cells may be achieved by expanding the cells in standard culture medium, supplemented with β-glycerophosphate (212), ascorbic acid (213), and dexamethasone (67, 213). These agents activate the osteogenic commitment of stem cells. Culture of osteogenic cells depends on the adequate supplementation of their growth medium with a source of inorganic phosphate (214), β-glycerophosphate, a non physiological organic substrate of alkaline phosphatase (ALP) (215), in order to produce mineralized ECM. Ascorbic acid is essential for the survival of human osteoblasts *in vitro* (216). This osteogenic inducing agent is required for collagen synthesis and alkaline phosphatase activity (213). Dexamethasone is a glucocorticoid that increases the expression of several genes associated with osteogenic differentiation (217). Moreover, the timing, size and number of bone like nodules is affected by the dose of dexamethasone used (218). Osteogenic medium can also be supplemented with growth factors, naturally existent in the bone structure, such as bone morphogenic proteins (BMPs) fibroblast growth factors (FGFs), platelet derived growth factor (PDGF), transforming growth factor beta (TGF-β) and insulin growth factors (IGFs) (219-226). The process of osteogenic differentiation is coordinated and involves three main stages: i) cell proliferation; ii) ECM deposition and maturation; and iii) mineralization (227). During cell proliferation, growth genes are expressed (228). Immediately following the down-regulation of the proliferation, the expression of ALP increases (227). During this period, the ECM undergoes a series of events that renders it competent for mineralization (ECM maturation and hydroxyapatite formation) (228). After this stage ECM becomes mineralized (227, 228). With the onset of mineralization, the ECM protein genes become up-regulated, like osteopontin and osteocalcin that are increasingly expressed with the accumulation of mineral (227). ALP activity prior to the onset of the mineralization suggests that this enzyme is involved in the preparation of the ECM for mineral deposition (227). This enzyme is considered to be an early marker of osteogenic differentiation and used to assess *in vitro* the osteogenic differentiation (20, 229, 230). The mineral content of the bone ECM can be qualitatively assessed by alizarin red or von Kossa

staining and the calcium content can be quantitatively assessed. This information can be complemented by the analysis of the mineral fraction by energy dispersive spectroscopy to detect the presence of calcium and phosphorous elements, thin-film X-ray diffraction to analyze the crystallinity of the ECM and Fourier-transformed spectroscopy to detect the carbonate and phosphate groups (27, 231).

8.2. *In vitro* studies with chitosan as a biomaterial

It is well accepted that the cells strongly interact with their environment, namely with neighboring cells, ECM and the surface to which they adhere (232). Chitosan as a biomaterial, like previously mentioned, has an analogous structure to the GAGs present in the ECM of connective tissues. Several studies describe the positive influence of chitosan over cell attachment, proliferation and over the osteogenic differentiation of MSCs (Table I). Mouse MSCs in contact with a chitosan suspension were shown to facilitate its osteogenic differentiation, when compared to cells seeded onto polystyrene culture wells (233). Lahiji *et al*. reported that chitosan, coated in coverslips, is an appropriate substrate for the growth of human osteoblasts and chondrocytes (110). Poly(D,L-lactic acid) (PDLLA) films modified with chitosan solution evidenced improved cell adhesion, proliferation, and biosynthetic activity, using human osteoblasts (234). Moreover, neonatal rat calvaria osteoblasts proliferate at superior rates on titanium surfaces coated with chitosan compared with titanium alone (235). In fact, coating of titanium pins with chitosan, induced minimal inflammatory response and a positive healing of a rabbit tibia bone defect (236). MC3T3-E1 osteoblast-like cells proliferated and evidenced increased ALP activity, as well as up-regulation of osteogenic genes expression in composite chitosan/poly(lactide-co-glicolic acid) (PLAGA) scaffolds as compared to PLAGA scaffolds (190). Chitosan–collagen sponges with higher concentration of chitosan positively promoted osteoblastic differentiation of BMSCs and improved the mechanical and physical properties of the matrices (173). Previous studies from our group, using flat discs obtained by injection molding composed of chitosan-PBS and PBS blends, showed that chitosan had a positive effect on osteoblast like cells (237). Furthermore, in literature, PCL nanofibrous scaffolds containing chitosan, revealed that stem cells adhered, proliferated and expressed phenotypic markers of osteogenic differentiation in a superior way when compared to nanofibrous scaffolds alone (189, 238). The ability of chitosan to support cell adhesion and influence osteogenic differentiation of cells can be attributed to its chemical properties.

The *in vitro* testing systems are inevitably limited in their capacity to recreate the complex *in vivo* environment. Therefore, these tests are unable to predict accurately the *in vivo* performance, particularly in the context of tissue engineering and regeneration of functional tissues. Thus, in a later stage of development it is critical to test the developed strategies *in vivo*.

9. *IN VIVO* ANIMAL MODELS

The general trend in bone tissue engineering after successful *in vitro* testing of the constructs is to implant the tissue-engineered construct into a relevant animal model. First, it is necessary to obtain a proof of concept of the tissue engineering strategy, *in vivo*. For this, an ectopic model in a small animal (mouse or rat) is commonly used. The constructs are implanted into a non-bone related anatomic location of the animal body (90, 239-241). These areas can be intraperitoneal, intramuscular, mesenteric or subcutaneous. This model is also interesting to determine if a scaffold has adequate properties namely porosity and interconnectivity, to allow tissue ingrowth and neovascularization. It is important to conclude about the biodegradation of the implanted material, in terms of degradation products and also the host immune response. If the aim is to use human cells, nude mouse/rat models are the most commonly used, because these animals do not have thymus, being unable to produce mature T lymphocytes, compromising the immune system. Therefore, its immune system is not able to react against xenogeneic cells (89, 220, 242). The purpose of using such model is to conclude about the ability of the tissue-engineered constructs to form ectopic bone and also to verify about osteoinductivity, *i.e.* the ability of the scaffold to induce proliferation of undifferentiated stem cells, as well as their differentiation into the osteogenic lineage (243-245).

The *in vivo* approach should mimic as close as possible the real clinical situation. Frequently, it is created an intraosseous wound that will not heal spontaneously during the lifetime of the animal (critical size defect) (83). The minimum size considered being a critical size defect is not absolute clear. The defect cannot be defined only by size, it is dependent on various variables, such as type of specie, anatomic location, among many others (246). Guidelines are available for the dimensions of implants based on the size of the animal, type of bone chosen and on the implant design to avoid pathological fracture of the test location (247). It is important to include controls in the experimental design. These controls should be of a material already in clinical use and also a control consisting of an empty defect, to prove

that the bone defect is not able to regenerate by itself (247). There are several types of bone defects that can be used, such as cranial, segmental, partially cortical and cancellous bone. These locations can be subjected to load or non-load bearing (*e.g.* femur or calvarial, respectively). The type of animal can be small (mouse or rat) (90, 104, 226, 248, 249) or large (rabbit, sheep, goat, dogs or primates) (146, 198, 250-255). Typically, researchers start with a smaller model mainly with less costs involved but also because it is easier to compare results between a wealth of experiments reported in the literature. One of the most accepted non-loading bearing models is the calvaria bone defect. This bone is a flat bone, allowing the creation of a uniform circular defect, and has an adequate size for easy surgical procedure and specimen handling. The dura mater and the overlying skin provide fixation of the scaffold. The model has been systematically studied and is very well established (83, 84, 256, 257). This model can be performed in small animals using rat (258, 259) or mouse (226, 248). It can be also applied to large animals, like rabbit (260-262) or sheep (202).

The last stage of preclinical trials of a bone tissue engineering strategy should be performed in animals that are believed to be more similar to humans, in terms of metabolism, physiology, anatomy, etc. Bones of small animals are more reactive to specific stimuli and are not subjected to comparable stresses. For example, a femur defect in rats (263-265) is believed to heal faster that in larger animals (256). However, in a study where the authors compared the bone ingrowth using the same chamber, in rats and in goats, no significant differences were observed between the two animals (266). *In vivo* experimentation design is therefore not an easy task, it is necessary to balance all the variables and decide which animal models suits better the specific goals of the experiment. Surgeries involving load-bearing conditions, involving stabilization with internal or external fixation devices, require the presence of experts to perform the surgery. The maintenance of the animals is expensive and variations within the same group may be larger as compared to those that are found in small laboratory animals. A countless number of variables need to be addressed to assure that the chosen model is the most appropriate for testing a specific situation. Consequently, variables should be minimized and very well controlled to reduce the random effects and to ensure as much as possible statistical significance. It is also very important to moderate the number of variables, such as physical condition of the animal (nutritional status, diet, age, sex), anesthesics and analgesics, type of bone defect (location, use of fixation) and, finally, the methodologies used to assess the sample collection and characterization. Despite the issues aforementioned, the final pre-clinical tests should be performed in large animals, subjected to load bearing comparable to the human case. For this proposes, the sheep or goat may be a good option. Both have a similar metabolism and bone remodeling rate to

humans, as well as a comparable weight (12, 18, 199, 202, 252).

9.1. *In vivo* bone regeneration studies with chitosan material

As described before, chitosan is already used in medicine, as a biomaterial for wound dressings. However, there are several reports in the literature showing the ability of chitosan to be used as material to regenerate bone (Table II). The first report describing the attempt to *in vivo* regenerate bone using chitosan structures dates back from 1988 (113), when Muzzarelli and colleagues implanted chitosan membranes and chitosan ascorbate gel into cranial defects in cats. Their findings suggested that chitosan seems to induce some type of stimulatory and/or attractive effect over the stromal cells of the surrounding tissues.

Table II. Survey of *in vivo* studies with chitosan based scaffolds proposed in the literature for bone tissue engineering applications.

Scaffold structure	Processing method	Cell type (source)	Animal model	References
Methylpyrrolidinone chitosan sponges	Freeze drying	-	Human, dental application	(145)
Methylpyrrolidinone chitosan sponges	Freeze drying	-	Rabbit, tibia defect	(146)
Modifyed chitosan with imidazole groups sponges	Freeze drying	-	Sheep, femur defect	(147)
Chitosan-HA membranes	Paste	-	Rat, implanted over calvaria	(267)
Chitosan-PLLA scaffolds	Freeze drying	Rat calvaria cells	Rat, Calvaria defect	(268)
Chitosan-gelatin-TCP scaffolds	Freeze drying	-	Subcutaneous implantation	(151)
Chitosan membrane	Wet spinning	-	Dog, dental application	(149)
Chitosan nanofiber membrane	Electrospinning	MG63 human cell line	Rabbit, calvaria defect	(182)
Chitosan-alginate scaffold	Freeze drying	MG63 human cell line	Rat, intramuscular	(166)
Chitosan scaffolds	Particle agregation	-	Rat, intramuscular	(269)
Chtosan-nanoHA	Particle agregation	Human fetal osteoblasts	Rat, Calvaria defect	(54)
Chitosan-silk scaffolds	Freeze gelation	-	Sheep, rib defect	(50)
Chitosan gel	Freeze drying-dilution in acetic acid	-	Rat, Calvaria defect	(270)
Chitosan-PLAGA scaffolds	Particle agregation	-	Rabbit, ulna segmental defect	(271)

HA-Hydroxyapatite; TCP-Tricalcium phosphate; PLLA-Poly(L-lactic acid);

The subsequent studies from the same authors describe the use of methylpirrolidone

chitosan in defects created in the tibia of rabbits (146) and in the femoral head of sheep (147). These studies confirmed the previous results (113) about the possible stimulatory and/or attractive effect of chitosan over cells. Chitosan has been also used as carrier for growth factors, such as platelet-derived growth factor-BB (PDGF-BB) to promote bone formation in a calvaria critical sized defect in rats (221, 268). Osteoconductive chitosan/tricalcium phosphate (TCP) sponges promoted osseous healing of the rat calvarial defects as compared to controls (without scaffolds) and the addition of PDGF-BB to the carrier further enhanced bone regeneration, favoring its osteoinductivity (268). These authors observed that chitosan/TCP sponge with PDGF-BB promoted more bone formation of the defects as compared to chitosan-TCP without the bioactive agents (221). PDGF growth factor is produced by platelets, osteoblasts and monocytes/macrophages and it is believed to have a role in the migration of MSCs to the wounding sites (272). Electrospun chitosan nanofiber membranes evidenced new bone formation at four weeks in calvaria defects of rabbits when compared to the controls (empty bone defects), where only soft tissue formation was observed (182). Chitosan combined with nano-hydroxyapatite in the form of microspheres were implanted in rat calvaria defects for twelve weeks, being able to promote bone regeneration (54). Moreover, chitosan-PLAGA microspheres conjugated in a scaffold by particle aggregation, with or without heparin and recombinant human bone morphogenetic protein 2 (rhBMP-2) showed to promote bone regeneration *in vivo* (271). More pronounced results were obtained for the scaffolds with the incorporated growth factor (271). A study by Ríos and co-workers (50) used a model mimicking the clinical bone free flaps, by flap prefabrication technique, which involves the design of the desired tissue at an ectopic site in the patient own body. This study used chambers containing silk fibroin-chitosan scaffolds implanted on top of the grafted periosteum over the *latissimus dorsi* muscle of sheeps (50). Bone grafts were used as positive controls and empty defects as negative controls. The authors found that the same amount of bone was regenerated in the defects with the tested scaffolds, as for the defects with the bone grafts (50).

10. CONCLUSIONS AND FINAL REMARKS

The developments in bone tissue engineering were considerable but there is not yet a tissue-engineered product that has reached clinical application. Both cells and biomaterial components need to be optimized to produce a functional bone tissue engineered therapy.

New stem cell sources are being explored, such as the extra-embryonic tissues,

placenta, amniotic fluid or umbilical cord. These stem cells have been shown to express pluripotent markers and low immunogenicity, evidencing a more primitive state. These cells are usually discarded, which make these sources attractive candidates for tissue engineering applications. Moreover, the low immunogenic potential could enable the use of these cells as an allogenic cell source for successful bone repair.

A new generation of biodegradable natural biomaterials is emerging, being chitosan one of the most interesting. Chitosan has been extensively studied as a biomaterial for bone tissue engineering scaffolding, but in practice it is still and only used as a wound dressing and hemostatic agent in medicine. Several morphologies can be successfully obtained by different processing techniques, which turn this material attractive for this end. Although several studies reporting the biological enhancement by chitosan and its influence over osteogenic differentiation and bone regeneration, still remains unclear the mechanism of action. It is worthwhile to continue to pursuit research over this interesting natural polymer in order to clarify its function over cell performance, as well as, to improve the scaffold processing methodologies, that will lead to the clinical use in the bone regeneration field.

ACKNOWLEDGEMENTS

This review was supported by the FCT grant (SFRH/24735/2005) attributed to Ana Costa-Pinto. The authors will also want to acknowledge the precious help of Ana M. Martins in the revision of the manuscript.

REFERENCES

1. Muschler GF, Negami S, Hyodo A, Gaisser D, Easley K, Kambic H. Evaluation of Collagen Ceramic Composite Graft Materials in a Spinal Fusion Model. Clinical Orthopaedics and Related Research. 1996;328:250-60.
2. Lewandrowski K-U, Gresser J, Wise DL, Trantolo DJ. Bioresorbable bone graft substitutes of different osteoconductivities: a histologic evaluation of osteointegration of poly(propylene glycol-co-fumaric acid)-based cement implants in rats. Biomaterials. 2000;21(8):757-64.
3. Desai B. Osteobiologics. Am J Orthop. 2007;36:8-11.
4. Muramatsu K, Doi K, Ihara K, Shigetomi M, Kawai S. Recalcitrant posttraumatic nonunion of the humerus: 23 patients reconstructed with vascularized bone graft: 23 patients reconstructed with vascularized bone graft. Acta Orthopaedica Scandinavica. 2003;74(1):95 - 7.
5. Al-Sayyad M, Abdulmajeed T. Fracture of the anterior iliac crest following autogenous bone grafting. Saudi Med J. 2006;27(2):254-8.
6. Chou L, Mann R, Coughlin M, Mcpeake W, Mizel M. Stress fracture as a complication of autogenous bone graft harvest from the distal tibia. Baltimore: Williams & Wilkins; 2007.
7. Pritsch T, Bickels J, Wu C-C, Squires H, Malawer M. The Risk for Fractures after Curettage and Cryosurgery Around the Knee. Clinical Orthopaedics and Related Research. 2007;458:159-67
8. Chen Y-C, Chen C-H, Chen P-L, Huang I-Y, Shen Y-S, Chen C-M. Donor site morbidity after harvesting of proximal tibia bone. Head & Neck. 2006;28(6):496-500.
9. Laurencin C, Khan Y, El-Amin SF. Bone graft substitutes. Expert Review of Medical Devices. 2005;3(1):49-57.
10. Ilizarov G. The Tension-Stress Effect on the Genesis and Growth of Tissues: Part I. The Influence of Stability of Fixation and Soft-Tissue Preservation. Clinical Orthopaedics and Related Research. 1989;238:249-81.
11. Perka C, Schultz O, Spitzer R-S, Lindenhayn K, Burmester G-R, Sittinger M. Segmental bone repair by tissue-engineered periosteal cell transplants with bioresorbable fleece and fibrin scaffolds in rabbits. Biomaterials. 2000;21(11):1145-53.
12. Gugala Z, Gogolewski S. Healing of critical-size segmental bone defects in the sheep tibiae using bioresorbable polylactide membranes. Injury. 2002;33(Supplement 2):71-6.
13. Cook D, Salkeld S, Rueger D. Comparison of osteoinductive and osteoconductive biomaterials in healing large segmental bone defects. American Academy of Orthopaedic Surgeons1995.
14. Langer R, Vacanti J. Tissue engineering. Science. 1993;260(5110):920-6.
15. Hutmacher DW. Scaffolds in tissue engineering bone and cartilage. Biomaterials. 2000;21(24):2529-43.
16. Hutmacher DW, Schantz JT, Lam CXF, Tan KC, Lim TC. State of the art and future directions of scaffold-based bone engineering from a biomaterials perspective. JTERM. 2007;1(4):245-60.
17. Bonfield W. Designing porous scaffolds for tissue engineering. Phil Trans R Soc 2006;364:227-32.
18. Mendes S, Reis R, Bovell Y, Cunha A, Van Blitterswijk CA, de Bruijn J. Biocompatibility testing of novel starch-based materials with potential application in orthopaedic surgery: a preliminary study. Biomaterials. 2001;22:2057-64.
19. Salgado A, Gomes M, Chou A, Coutinho O, Reis R, Hutmacher D. Preliminary study on the adhesion and proliferation of human osteoblasts on starch-based scaffolds. Materials Science and Engineering C. 2002;20(2002):27-33.

20. Gomes M, Sikavitsas V, Behravesh E, Reis R, Mikos A. Effect of flow perfusion on the osteogenic differentiation of bone marrow stromal cells cultured on starch-based three-dimensional scaffolds. J Biomed Mater Res. 2003;67A:87-95.
21. Salgado A, Coutinho O, Reis R. Novel Starch-Based Scaffolds for Bone Tissue Engineering: Cytotoxicity, Cell Culture, and Protein Expression. Tissue Engineering. 2004;10(3/4):465-74.
22. Gomes ME, Godinho JS, Tchalamov D, Cunha AM, Reis RL. Alternative tissue engineering scaffolds based on starch: processing methodologies, morphology, degradation and mechanical properties. Materials Science and Engineering C. 2002;20:19-26.
23. Malafaya P, Pedro A, Peterbauer A, Gabriel C, Redl H, Reis RL. Chitosan particles agglomerated scaffolds for cartilage and osteochondral tissue engineering approaches with adipose tissue derived stem cells. Journal of Materials Science: Materials in Medicine. 2005;16:1077-85.
24. Oliveira J, Rodrigues M, Silva S, Malafaya P, Gomes M, Viegas C, et al. Novel hydroxyapatite/chitosan bilayered scaffold for osteochondral tissue-engineering applications: Scaffold design and its performance when seeded with goat bone marrow stromal cells. Biomaterials. 2006;27(36):6123-37.
25. Costa-Pinto A, Correlo V, Sol P, Bhattacharya M, Charbord P, Delorme B, et al. Adhesion, Proliferation, and Osteogenic Differentiation of a Mouse Mesenchymal Stem Cell Line (BMC9) Seeded on Novel Melt-Based Chitosan/Polyester 3D Porous Scaffolds. Tissue Engineering. 2008;14(6):1049-52.
26. Martins A, Santos M, Azevedo H, Malafaya P, Reis R. Natural origin scaffolds with in situ pore forming capability for bone tissue engineering applications. Acta Biomaterialia. 2008;4:1637-45.
27. Costa-Pinto A, Correlo V, Sol P, Bhattacharya M, Charbord P, Delorme B, et al. Osteogenic Differentiation of Human Bone Marrow Mesenchymal Stem Cells Seeded on Melt Based Chitosan Scaffolds for Bone Tissue Engineering Applications. Biomacromolecules. 2009.
28. Oliveira J, Santos T, Martins L, Picciochi R, Marques A, Castro A, et al. Gellan Gum Injectable Hydrogels for Cartilage Tissue Engineering Applications: *In vitro* Studies and Preliminary *In vivo* Evaluation. Tissue Engineering Part A. 2010;16(1):343-53.
29. Oliveira J, Gardel L, Rada T, Martins L, Gomes M, Reis R. Injectable gellan gum hydrogels with autologous cells for the treatment of rabbit articular cartilage defects. Journal of Orthopaedic Research. 2010;28(9):1193-9.
30. Oliveira JT, Martins L, Picciochi R, Malafaya PB, Sousa RA, Neves NM, et al. Gellan gum: A new biomaterial for cartilage tissue engineering applications. Journal of Biomedical Materials Research Part A. 2010;93A(3):852-63.
31. Silva NA, Salgado AJ, Sousa RA, Oliveira JT, Pedro AJ, Leite-Almeida H, et al. Development and Characterization of a Novel Hybrid Tissue Engineering Based Scaffold for Spinal Cord Injury Repair. Tissue Engineering Part A. 2010;16(1):45-54.
32. Silva SS, Santos MI, Coutinho OP, Mano JF, Reis RL. Physical properties and biocompatibility of chitosan/soy blended membranes. Journal of Materials Science: Materials in Medicine. 2005;16(6):575-9.
33. Silva SS, Maniglio D, Motta A, Mano JF, Reis RL, Migliaresi C. Genipin-Modified Silk-Fibroin Nanometric Nets. Macromolecular Bioscience. 2008;8(8):766-74.
34. Silva SS, Motta A, Rodrigues MT, Pinheiro AFM, Gomes ME, Mano JF, et al. Novel Genipin-Cross-Linked Chitosan/Silk Fibroin Sponges for Cartilage Engineering Strategies. Biomacromolecules. 2008;9(10):2764-74.
35. Madihally S. Porous chitosan scaffolds for tissue engineering. Biomaterials. 1999;20 1133-42.
36. Ho MH, Kuo PY, Hsieh HJ, Hsien TY, Hou LT, Lai JY, et al. Preparation of porous scaffolds by using freeze-extraction and freeze-gelation methods. Biomaterials. 2004 Jan;25(1):129-38.

37. Seol YJ, Lee JY, Park YJ, Lee YM, Young K, Rhyu IC, et al. Chitosan sponges as tissue engineering scaffolds for bone formation. Biotechnology letters. 2004 Jul;26(13):1037-41.
38. Tuzlakoglu K, Alves CM, Mano JF, Reis RL. Production and characterization of chitosan fibers and 3-D fiber mesh scaffolds for tissue engineering applications. Macromol Biosci. 2004 Aug 9;4(8):811-9.
39. Geng X, Kwon O-H, Jang J. Electrospinning of chitosan dissolved in concentrated acetic acid solution. Biomaterials. 2005;26(27):5427-32.
40. Hsieh C-Y, Tsai S-P, Ho M-H, Wang D-M, Liu C-E, Hsieh C-H, et al. Analysis of freeze-gelation and cross-linking processes for preparing porous chitosan scaffolds. Carbohydrate Polymers. 2007;67(1):124-32.
41. Heinemann C, Heinemann S, Bernhardt A, Worch H, Hanke T. Novel Textile Chitosan Scaffolds Promote Spreading, Proliferation, and Differentiation of Osteoblasts. Biomacromolecules. 2008;9(10):2913-20.
42. Correlo V, Boesel L, Pinho E, Costa-Pinto A, Alves da Silva M, Bhattacharya M, et al. Melt-based compression-molded scaffolds from chitosan–polyester blends and composites: Morphology and mechanical properties. J Biomed Mater Res A. 2009;91A(2):498-504.
43. Costa-Pinto AR, Correlo VM, Sol PC, Bhattacharya M, Charbord P, Delorme B, et al. Osteogenic Differentiation of Human Bone Marrow Mesenchymal Stem Cells Seeded on Melt Based Chitosan Scaffolds for Bone Tissue Engineering Applications. Biomacromolecules. 2009;10(8):2067-73.
44. Correlo VM, Costa-Pinto AR, Sol P, Covas JA, Bhattacharya M, Neves NM, et al. Melt Processing of Chitosan-Based Fibers and Fiber-Mesh Scaffolds for the Engineering of Connective Tissues. Macromolecular Bioscience. 2010.
45. Cao W, Wang A, Jing D, Gong Y, Zhao N, Zhang X. Novel biodegradable films and scaffolds of chitosan blended with poly(3-hydroxybutyrate). Journal of biomaterials science. 2005;16(11):1379-94.
46. Wu H, Wan Y, Dalai S, Zhang R. Response of rat osteoblasts to polycaprolactone/chitosan blend porous scaffolds. Journal of Biomedical Materials Research Part A. 2009;92A(1):238-45.
47. Sarasam A, Madihally SV. Characterization of chitosan-polycaprolactone blends for tissue engineering applications. Biomaterials. 2005 Sep;26(27):5500-8.
48. Nakamatsu J, Torres FG, Troncoso OP, Min-Lin Y, Boccaccini AR. Processing and Characterization of Porous Structures from Chitosan and Starch for Tissue Engineering Scaffolds. Biomacromolecules. 2006;7(12):3345-55.
49. Baran ET, Mano JF, Reis RL. Starch-chitosan hydrogels prepared by reductive alkylation cross-linking. J Mater Sci Mater Med. 2004 Jul;15(7):759-65.
50. Ríos CN, Skoracki RJ, Miller MJ, Satterfield WC, Mathur AB. *In vivo* Bone Formation in Silk Fibroin and Chitosan Blend Scaffolds via Ectopically Grafted Periosteum as a Cell Source: A Pilot Study. Tissue Engineering Part A. 2009;15(9):2717-25.
51. Gobin AS, Froude VE, Mathur AB. Structural and mechanical characteristics of silk fibroin and chitosan blend scaffolds for tissue regeneration. J Biomed Mater Res A. 2005 Sep 1;74(3):465-73.
52. Manjubala I, Woesz A, Pilz C, Rumpler M, Fratzl-Zelman N, Roschger P, et al. Biomimetic mineral-organic composite scaffolds with controlled internal architecture. Journal of Materials Science: Materials in Medicine. 2005;16(12):1111-9.
53. Zhao F, Grayson WL, Ma T, Bunnell B, Lu WW. Effects of hydroxyapatite in 3-D chitosan-gelatin polymer network on human mesenchymal stem cell construct development. Biomaterials. 2006 Mar;27(9):1859-67.
54. Chesnutt BM, Yuan Y, Buddington K, Haggard WO, Bumgardner JD. Composite Chitosan/Nano-Hydroxyapatite Scaffolds Induce Osteocalcin Production by Osteoblasts *In vitro* and Support Bone Formation *In vivo*. Tissue Engineering Part A. 2009;15(9):2571-9.

55. Finisie MR, Josue A, Favere VT, Laranjeira MC. Synthesis of calcium-phosphate and chitosan bioceramics for bone regeneration. Anais da Academia Brasileira de Ciencias. 2001 Dec;73(4):525-32.
56. Zhang Y, Ni M, Zhang M, Ratner B. Calcium phosphate-chitosan composite scaffolds for bone tissue engineering. Tissue Eng. 2003 Apr;9(2):337-45.
57. Xu HH, Takagi S, Quinn JB, Chow LC. Fast-setting calcium phosphate scaffolds with tailored macropore formation rates for bone regeneration. J Biomed Mater Res A. 2004 Mar 15;68(4):725-34.
58. Correlo VM, Boesel LF, Bhattacharya M, Mano JF, Neves NM, Reis RL. Hydroxyapatite reinforced chitosan and polyester blends for biomedical applications. Macromolecular Materials and Engineering 2005;290(12):1157-65.
59. Zhang Y, Xu HH, Takagi S, Chow LC. In-situ hardening hydroxyapatite-based scaffold for bone repair. J Mater Sci Mater Med. 2006;17(5):437-45.
60. Mukherjee DP, Tunkle AS, Roberts RA, Clavenna A, Rogers S, Smith D. An animal evaluation of a paste of chitosan glutamate and hydroxyapatite as a synthetic bone graft material. J Biomed Mater Res B Appl Biomater. 2003;67(1):603-9.
61. Rodan GA. Introduction to bone biology. Bone. 1992;13(Supplement 1):S3-S6.
62. Weiner S, Wagner H. The material bone: structure mechanical function relations. Annu Rev Mater Sci 1998;28:271-98.
63. Jee W. Integrated bone tissue physiology: anatomy and physiology. In: Cowin SC, editor. Bone mechanics handbook. 4th ed. Boca Raton: CRC press; 2001.
64. Friedenstein A, Deriglasova U, Kulagina N, Panasuk A, Rudakowa S, Luriá E, et al. Precursors for fibroblasts in different populations of hematopoietic cells as detected by the *in vitro* colony assay method. Exp Hematol. 1974;2(2):83-92.
65. Owen M. Marrow Stromal Stem Cells. J Cell Sci Suppl. 1988;10:63-76.
66. Simmons P, Torok-Storb B. CD34 Expression by Stromal Precursors in Normal Human Adult Bone Marrow Blood. 1991;11:2848-53.
67. Haynesworth SE, Goshima J, Goldberg VM, Caplan AI. Characterization of cells with osteogenic potential from human marrow. Bone. 1992;13(1):81-8.
68. Nakahara H, Goldberg VM, Caplan AI. Culture-expanded human periosteal-derived cells exhibit osteochondral potential *in vivo*. Journal of Orthopaedic Research. 1991;9(4):465-76.
69. Bianco P, Riminucci M, Gronthos S, Robey PG. Bone Marrow Stromal Stem Cells: Nature, Biology, and Potential Applications. Stem cells. 2001;19:180-92.
70. Quarto R, Mastrogiacomo M, Cancedda R, Kutepov S, Mukhaev V, Lakroukov A, et al. Repair of large bone defects with the use of autologous bone marrow stromal cells. New England Journal of Medicine. 2001;344(5):385-6.
71. Marcacci M, Kon E, Moukhachev V, Lavroukov A, Kutepov S, Quarto R, et al. Stem Cells Associated with Macroporous Bioceramics for Long Bone Repair: 6- to 7-Year Outcome of a Pilot Clinical Study. Tissue Engineering. 2007;13(5):947-55.
72. Calvi LM, Adams GB, Weibrecht KW, Weber JM, Olson DP, Knight MC, et al. Osteoblastic cells regulate the haematopoietic stem cell niche. Nature. 2003;425(6960):841-6.
73. Zhang J, Niu C, Ye L, Huang H, He X, Tong W-G, et al. Identification of the haematopoietic stem cell niche and control of the niche size. Nature. 2003;425(6960):836-41.
74. Robey P, Termine J. Human bone cells *in vitro*. Calcified Tissue International. 1985;37(5):453-60.
75. Fuchs S, Hofmann A, Kirkpatrick CJ. Microvessel-Like Structures from Outgrowth Endothelial Cells from Human Peripheral Blood in 2-Dimensional and 3-Dimensional Co-Cultures with Osteoblastic Lineage Cells. Tissue Engineering. 2007;13(10):2577-88.
76. Unger RE, Sartoris A, Peters K, Motta A, Migliaresi C, Kunkel M, et al. Tissue-like self-assembly in cocultures of endothelial cells and osteoblasts and the formation of

microcapillary-like structures on three-dimensional porous biomaterials. Biomaterials. 2007;28(27):3965-76.
77. Santos MI, Unger RE, Sousa RA, Reis RL, Kirkpatrick CJ. Crosstalk between osteoblasts and endothelial cells co-cultured on a polycaprolactone-starch scaffold and the *in vitro* development of vascularization. Biomaterials. 2009;30(26):4407-15.
78. Nomura S, Takano-Yamamoto T. Molecular events caused by mechanical stress in bone. Matrix Biology. 2000;19(2):91-6.
79. Kronenberg HM. Developmental regulation of the growth plate. Nature. 2003;423(6937):332-6.
80. Horton W. The biology of bone growth. Growth Genet Horm. 1990;6(2):1-3.
81. Bruder S, Caplan A. Cellular and molecular events during embryonic bone development. Cellular and molecular events during embryonic bone development. 1989;20(1-4):65-71.
82. Bianco P, Cancedda F, Riminucci M, Cancedda R. Bone Formation via Cartilage Models: The "Borderline" Chondrocyte. Matrix Biology. 1998;17:185-92.
83. Schmitz J, Hollinger J. The Critical Size Defect as an Experimental Model for Craniomandibulofacial Nonunions. Clinical Orthopaedics and Related Research. 1986;205:299-308.
84. Hollinger JO, Kleinschmidt JC. The Critical Size Defect as an Experimental Model To Test Bone Repair Materials. Journal of Craniofacial Surgery. 1990;1(1):60-8.
85. Aaboe M, Pinholt E, Hjorting-Hansen E. Healing of experimentally created defects: a review. Br J Oral Maxillofac Surg. 1995;33(5):312-8.
86. Pham QP, Kurtis Kasper F, Scott Baggett L, Raphael RM, Jansen JA, Mikos AG. The influence of an *in vitro* generated bone-like extracellular matrix on osteoblastic gene expression of marrow stromal cells. Biomaterials. 2008;29(18):2729-39.
87. Kaplan D. Biopolymers from renewable resources. New York: Springer; 1998.
88. Azevedo HS, Gama FM, Reis RL. *In vitro* Assessment of the Enzymatic Degradation of Several Starch Based Biomaterials. Biomacromolecules. 2003;4(6):1703-12.
89. Mendes SC, Bezemer J, Claase MB, Grijpma DW, Bellia G, Degli-Innocenti F, et al. Evaluation of two biodegradable polymeric systems as substrates for bone tissue engineering. Tissue Engineering. 2003;9:S91-S101.
90. Salgado A, Coutinho O, Reis R, Davies J. *In vivo* response to starch-based scaffolds designed for bone tissue engineering applications. J Biomed Mater Res A. 2006;80:983-9.
91. Tomihata K, Ikada Y. *In vitro* and in tivo degradation of films of chitin and its deacetylated derivatives. Biomaterials. 1997;18:261-8.
92. Varum K, Myhr M, Hjerde R, Smidsrod O. *In vitro* degradation rates of partially N-acetylated chitosans in human serum. Carbohydrate res. 1997;299:99-101.
93. Molinaro G, Leroux JC, Damas J, Adam A. Biocompatibility of thermosensitive chitosan-based hydrogels: an *in vivo* experimental approach to injectable biomaterials. Biomaterials. 2002;23(13):2717-22.
94. Rucker M, Laschke MW, Junker D, Carvalho C, Schramm A, Mulhaupt R, et al. Angiogenic and inflammatory response to biodegradable scaffolds in dorsal skinfold chambers of mice. Biomaterials. 2006;27(29):5027-38.
95. Xiao Y, Young WG, Bartold PM. Tissue engineering for bone regeneration using osteoblasts in collagen scaffolds. J Dent Res. 2002 Mar;81:0851.
96. Sachlos E, Reis N, Ainsley C, Derby B, Czernuszka JT. Novel collagen scaffolds with predefined internal morphology made by solid freeform fabrication. Biomaterials. 2003;24(8):1487-97.
97. Xiao Y, Qian H, Young WG, Bartold PM. Tissue engineering for bone regeneration using differentiated alveolar bone cells in collagen scaffolds. Tissue Engineering. 2003;9(6):1167-77.

98. George J, Kuboki Y, Miyata T. Differentiation of mesenchymal stem cells into osteoblasts on honeycomb collagen scaffolds. Biotechnol Bioeng. [Article]. 2006;95(3):404-11.
99. Schneider RK, Puellen A, Kramann R, Raupach K, Bornemann J, Knuechel R, et al. The osteogenic differentiation of adult bone marrow and perinatal umbilical mesenchymal stem cells and matrix remodelling in three-dimensional collagen scaffolds. Biomaterials. 2010 Jan;31(3):467-80.
100. Lisignoli G, Fini M, Giavaresi G, Nicoli Aldini N, Toneguzzi S, Facchini A. Osteogenesis of large segmental radius defects enhanced by basic fibroblast growth factor activated bone marrow stromal cells grown on non-woven hyaluronic acid-based polymer scaffold. Biomaterials. 2002;23(4):1043-51.
101. Kim J, Kim IS, Cho TH, Lee KB, Hwang SJ, Tae G, et al. Bone regeneration using hyaluronic acid-based hydrogel with bone morphogenic protein-2 and human mesenchymal stem cells. Biomaterials. 2007;28(10):1830-7.
102. Abbah S, Lu W, Chan D, Cheung K, Liu W, Zhao F, et al. Osteogenic behavior of alginate encapsulated bone marrow stromal cells: An *in vitro* study. Journal of Materials Science: Materials in Medicine. 2008;19(5):2113-9.
103. Li C, Vepari C, Jin H-J, Kim HJ, Kaplan DL. Electrospun silk-BMP-2 scaffolds for bone tissue engineering. Biomaterials. 2006;27(16):3115-24.
104. Meinel L, Betz O, Fajardo R, Hofmann S, Nazarian A, Cory E, et al. Silk based biomaterials to heal critical sized femur defects. Bone. 2006;39(4):922-31.
105. Bakos D, Soldan M, Hernandez-Fuentes I. Hydroxyapatite-collagen-hyaluronic acid composite. Biomaterials. 1999;20(2):191-5.
106. Solchaga LA, Temenoff JS, Gao JZ, Mikos AG, Caplan AI, Goldberg VM. Repair of osteochondral defects with hyaluronan- and polyester-based scaffolds. Osteoarthritis Cartilage. 2005;13(4):297-309.
107. Schumann D, Ekaputra AK, Lam CXF, Hutmacher DW. Biomaterials/scaffolds. Design of bioactive, multiphasic PCL/collagen type I and type II-PCL-TCP/collagen composite scaffolds for functional tissue engineering of osteochondral repair tissue by using electrospinning and FDM techniques. Methods Mol Med. 2007;140:101-24.
108. Rouget C. Des substances amylacées dans les tissus des animaux, spécialement des Articulés (chitine). CR Acad Sci Ser III. 1859;48:792-5.
109. Suh. Application of chitosan-based polysaccharide biomaterials in cartilage tissue engineering: a review. Biomaterials. 2000;21:2589-98.
110. Lahiji A, Sohrabi A, Hungerford DS, Frondoza CG. Chitosan supports the expression of extracellular matrix proteins in human osteoblasts and chondrocytes. J Biomed Mater Res. 2000;51(4):586-95.
111. Kurita K. Chemistry and application of chitin and chitosan. Polymer Degradation and Stability. 1997;59(1-3):117-20.
112. Shi C, Zhu Y, Ran X, Wang M, Su Y, Cheng T. Therapeutic Potential of Chitosan and Its Derivatives in Regenerative Medicine. Journal of Surgical Research. 2006;133(2):185-92.
113. Muzzarelli R, Baldassarre V, Conto F, Ferrara P, Biagini G, Gazzanelli G, et al. Biological activity of chitosan: ultrastructural study. Biomaterials. 1988;9(3):247-52.
114. Denuziere A, Ferrier D, Damour O, Domard A. Chitosan-chondroitin sulfate and chitosan-hyaluronate polyelectrolyte complexes: biological properties. Biomaterials. 1998;19(14):1275-85.
115. Di Martino A, Sittinger M, Risbud MV. Chitosan: a versatile biopolymer for orthopaedic tissue-engineering. Biomaterials. 2005;26(30):5983-90.
116. Nordtveit RJ, VArum KM, Smidsrd O. Degradation of partially N-acetylated chitosans with hen egg white and human lysozyme. Carbohydrate Polymers. 1996;29(2):163-7.
117. Kjell M. Varum, Mildrid M. Myhr, Ragnhild J.N. Hjerde, Smidsrod O. *In vitro* degradation rates of partially N-acetylated chitosans in human serum. Carbohydrate res. 1997;299:99-101.

118. Lu F, Cao Z, Zhuang Z, Mou ZX, Feng X. [Biodegradation and biocompatibility of a chitosan film]. Sheng wu yi xue gong cheng xue za zhi = Journal of biomedical engineering = Shengwu yixue gongchengxue zazhi. 1998 Jun;15(2):183-5.
119. Laschke MW, Strohe A, Scheuer C, Eglin D, Verrier S, Alini M, et al. *In vivo* biocompatibility and vascularization of biodegradable porous polyurethane scaffolds for tissue engineering. Acta Biomaterialia. 2009;5(6):1991-2001.
120. Spin-Neto R, de Freitas RM, Pavone C, Cardoso MB, Campana-Filho SP, Marcantonio RA, et al. Histological evaluation of chitosan-based biomaterials used for the correction of critical size defects in rat's calvaria. J Biomed Mater Res A. 2010;93(1):107-14.
121. Muzzarelli R., Tarsi R, Filippini O, Giovanetti E, Biagini G, Varaldo PE. Antimicrobial properties of N-carboxybutyl chitosan. Antimicrobial agents and chemotherapy. 1990;34(10):2019-23.
122. Loke WK, Lau SK, Yong LL, Khor E, Sum CK. Wound dressing with sustained anti-microbial capability. J Biomed Mater Res. 2000;53(1):8-17.
123. No HK, Park NY, Lee SH, Meyers SP. Antibacterial activity of chitosans and chitosan oligomers with different molecular weights. International journal of food microbiology. 2002;74(1-2):65-72.
124. Sall KN, Kreter JK, Keates RH. The effect of chitosan on corneal wound healing. Annals of ophthalmology. 1987;19(1):31-3.
125. Biagini G, Bertani A, Muzzarelli R, Damadei A, DiBenedetto G, Belligolli A, et al. Wound management with N-carboxybutyl chitosan. Biomaterials. 1991 Apr;12(3):281-6.
126. Okamoto Y, Shibazaki K, Minami S, Matsuhashi A, Tanioka S, Shigemasa Y. Evaluation of chitin and chitosan on open would healing in dogs. J Vet Med Sci. 1995;57(5):851-4.
127. Ueno H, Yamada H, Tanaka I, Kaba N, Matsuura M, Okumura M, et al. Accelerating effects of chitosan for healing at early phase of experimental open wound in dogs. Biomaterials. 1999;20(15):1407-14.
128. Peh K, Khan T, Ch'ng H. Mechanical, bioadhesive strength and biological evaluations of chitosan films for wound dressing. J Pharm Pharm Sci. 2000;3(3):303-11.
129. Mi FL, Shyu SS, Wu YB, Lee ST, Shyong JY, Huang RN. Fabrication and characterization of a sponge-like asymmetric chitosan membrane as a wound dressing. Biomaterials. 2000;22(2):165-73.
130. Azad AK, Sermsintham N, Chandrkrachang S, Stevens WF. Chitosan membrane as a wound-healing dressing: characterization and clinical application. J Biomed Mater Res B Appl Biomater. 2004;69(2):216-22.
131. Chatelet C, Damour O, Domard A. Influence of the degree of acetylation on some biological properties of chitosan films. Biomaterials. 2001;22(3):261-8.
132. Pangburn SH, Trescony PV, Heller J. Lysozyme degradation of partially deacetylated chitin, its films and hydrogels. Biomaterials. 1982;3(2):105-8.
133. Sashiwa H, Saimoto H, Shigemasa Y, Ogawa R, Tokura S. Lysozyme susceptibility of partially deacetylated chitin. International Journal of Biological Macromolecules. 1990;12(5):295-6.
134. Hankiewicz J, Swierczek E. Lysozyme in human body fluids. Clinica Chimica Acta. 1974;57(3):205-9.
135. Muzzarelli RAA. Biochemical significance of exogenous chitins and chitosans in animals and patients. Carbohydrate Polymers. 1993;20(1):7-16.
136. Torsteinsdottir I, Hakansson L, Hallgren R, Gudbjornsson B, Arvidson N-G, Venge P. Serum lysozyme: a potential marker of monocyte/macrophage activity in rheumatoid arthritis. Rheumatology. 1999 December 1, 1999;38(12):1249-54.
137. TeijÛn C, Olmo R, Dolores Blanco M, Romero A, MarÌa TeijÛn J. Effects of lead administration at low doses by different routes on rat spleens. Study of response of splenic lymphocytes and tissue lysozyme. Toxicology. 2003;191(2-3):245-58.

138. Rabea EI, Badawy MET, Stevens CV, Smagghe G, Steurbaut W. Chitosan as Antimicrobial Agent: Applications and Mode of Action. Biomacromolecules. 2003;4(6):1457-65.
139. Prudden JF, Migel P, Hanson P, Friedrich L, Balassa L. The discovery of a potent pure chemical wound-healing accelerator. The American Journal of Surgery. 1970;119(5):560-4.
140. Peluso. Chitosan-mediated stimulation of macrophage function. Biomaterials. 1994;15:1215-20.
141. Mori. Effects of chitin and its derivatives on the proliferation and cytokine production of fibroblasts *in vitro*. Biomaterials. 1997;18:947-51.
142. Nishimura K, Nishimura S, Nishi N, Saiki I, Tokura S, Azuma I. Immunological activity of chitin and its derivatives. Vaccine. 1984 Mar;2(1):93-9.
143. Jameela SR, Misra A, Jayakrishnan A. Cross-linked chitosan microspheres as carriers for prolonged delivery of macromolecular drugs. Journal of biomaterials science. 1994;6(7):621-32.
144. Maruyama M, Ito M. *In vitro* properties of a chitosan-bonded self-hardening paste with hydroxyapatite granules. J Biomed Mater Res. 1996;32(4):527-32.
145. Muzzarelli RA, Biagini G, Bellardini M, Simonelli L, Castaldini C, Fratto G. Osteoconduction exerted by methylpyrrolidinone chitosan used in dental surgery. Biomaterials. 1993;14(1):39-43.
146. Muzzarelli RA, Zucchini C, Ilari P, Pugnaloni A, Mattioli Belmonte M, Biagini G, et al. Osteoconductive properties of methylpyrrolidinone chitosan in an animal model. Biomaterials. 1993;14(12):925-9.
147. Muzzarelli RA. Stimulatory effect on bone formation exerted by a modified chitosan. Biomaterials. 1994;15(13):1075-81.
148. Lee YM, Park YJ, Lee SJ, Ku Y, Han SB, Choi SM, et al. Tissue engineered bone formation using chitosan/tricalcium phosphate sponges. Journal of periodontology. 2000;71(3):410-7.
149. Yeo Y-J, Jeon D-W, Kim C-S, Choi S-H, Cho K-S, Lee Y-K, et al. Effects of chitosan nonwoven membrane on periodontal healing of surgically created one-wall intrabony defects in beagle dogs. Journal of Biomedical Materials Research. 2004;72B(1):86-93.
150. Ang TH, Sultana FSA, Hutmacher DW, Wong YS, Fuh JYH, Mo XM, et al. Fabrication of 3D chitosan-hydroxyapatite scaffolds using a robotic dispensing system. Materials Science and Engineering: C. 2002;20(1-2):35-42.
151. Yin Y, Ye F, Cui J, Zhang F, Li X, Yao K. Preparation and characterization of macroporous chitosan-gelatin/beta-tricalcium phosphate composite scaffolds for bone tissue engineering. J Biomed Mater Res A. 2003 ;67(3):844-55.
152. Burg KJL, Porter S, Kellam JF. Biomaterial developments for bone tissue engineering. Biomaterials. 2000;21(23):2347-59.
153. Gopferich A. Mechanisms of polymer degradation and erosion. Biomaterials. 1996;17(2):103-14.
154. Carmeliet P. Mechanisms of angiogenesis and arteriogenesis. Nat Med. 2000;6(4):389-95.
155. Borenstein JT, Weinberg EJ, Orrick BK, Sundback C, Kaazempur-Mofrad MR, Vacanti JP. Microfabrication of Three-Dimensional Engineered Scaffolds. Tissue Engineering. 2007;13(8):1837-44.
156. Mastrogiacomo M, Scaglione S, Martinetti R, Dolcini L, Beltrame F, Cancedda R, et al. Role of scaffold internal structure on *in vivo* bone formation in macroporous calcium phosphate bioceramics. Biomaterials. 2006;27(17):3230-7.
157. Klawitter J, Hulbert S. Application of porous ceramics for the attachment of load bearing internal orthopedic applications. Journal of Biomedical Materials Research. 1971;5(6):161-229.

158. Lewandrowski K-U, Gresser JD, P.Bondre S, Silva AE, Wise DL, Trantolo DJ. Developing porosity of poly(propylene glycol-co-fumaric acid) bone graft substitutes and the effect on osteointegration: A preliminary histology study in rats. Journal of Biomaterials Science, Polymer Edition. 2000;11:879-89.
159. Gomes M, Holtorf H, Reis R, Mikos AG. Influence of the Porosity of Starch-Based Fiber Mesh Scaffolds on the Proliferation and Osteogenic Differentiation of Bone Marrow Stromal Cells Cultured in a Flow Perfusion Bioreactor. Tissue Engineering. 2006;12(4):801-9.
160. Zhang Y, Zhang M. Three-dimensional macroporous calcium phosphate bioceramics with nested chitosan sponges for load-bearing bone implants. J Biomed Mater Res. 2002;61(1):1-8.
161. Yang S, Leong K-F, Du Z, Chua C-K. The Design of Scaffolds for Use in Tissue Engineering. Part I. Traditional Factors. Tissue Engineering. 2004;7(6):679-89.
162. Boyan BD, Hummert TW, Dean DD, Schwartz Z. Role of material surfaces in regulating bone and cartilage cell response. Biomaterials. 1996;17(2):137-46.
163. Leong KF, Cheah CM, Chua CK. Solid freeform fabrication of three-dimensional scaffolds for engineering replacement tissues and organs. Biomaterials. 2003;24(13):2363-78.
164. Shen F, Cui YL, Yang LF, Yao KD, Dong XH, Jia WY, et al. A study on the fabrication of porous chitosan/gelatin network scaffold for tissue engineering. Polymer International. 2000;49(12):1596-9.
165. Zhang Y, Zhang M. Cell growth and function on calcium phosphate reinforced chitosan scaffolds. Journal of materials Science: materials in medicine. 2004;15:255-60.
166. Li Z, Ramay HR, Hauch KD, Xiao D, Zhang M. Chitosan-alginate hybrid scaffolds for bone tissue engineering. Biomaterials. 2005;26(18):3919-28.
167. Amaral IF, Sampaio P, Barbosa MA. Three-dimensional culture of human osteoblastic cells in chitosan sponges: the effect of the degree of acetylation. J Biomed Mater Res A. 2006;76(2):335-46.
168. Kong L, Gao Y, Lu G, Gong Y, Zhao N, Zhang X. A study on the bioactivity of chitosan/nano-hydroxyapatite composite scaffolds for bone tissue engineering European Polymer Journal. 2006;42(12):3171-9.
169. Manjubala I, Scheler S, Bˆssert J, Jandt KD. Mineralisation of chitosan scaffolds with nano-apatite formation by double diffusion technique. Acta Biomaterialia. 2006;2(1):75-84.
170. Gravel M, Gross T, Vago R, Tabrizian M. Responses of mesenchymal stem cell to chitosan–coralline composites microstructured using coralline as gas forming agent Biomaterials. 2006;27:1899-906.
171. Sendemir-Urkmez A, Jamison RD. The addition of biphasic calcium phosphate to porous chitosan scaffolds enhances bone tissue development *in vitro*. Journal of Biomedical Materials Research Part A. 2007;81A(3):624-33.
172. Zheng JP, Wang CZ, Wang XX, Wang HY, Zhuang H, Yao KD. Preparation of biomimetic three-dimensional gelatin/montmorillonite-chitosan scaffold for tissue engineering. Reactive and Functional Polymers. 2007;67(9):780-8.
173. Arpornmaeklong P, Pripatnanont P, Suwatwirote N. Properties of chitosan-collagen sponges and osteogenic differentiation of rat-bone-marrow stromal cells. International Journal of Oral and Maxillofacial Surgery. 2008;37(4):357-66.
174. Kuo Y-C, Yeh C-F, Yang J-T. Differentiation of bone marrow stromal cells in poly(lactide-co-glycolide)/chitosan scaffolds. Biomaterials. 2009;30(34):6604-13.
175. Akman AC, Tigli RS, Gumusderelioglu M, Nohutcu RM. Bone morphogenetic protein-6-loaded chitosan scaffolds enhance the osteoblastic characteristics of MC3T3-E1 cells. Artif Organs. 2010;34(1):65-74.
176. Hsieh Chien-Yang, Tsai Sung-Pei, Ho Ming-Hwa, Wang Da-Ming, Liu Chung-En, Cheng-Hsuan, et al. Analysis of freeze-gelation and cross-linking processes for preparing porous chitosan scaffolds. 2007;67:9.

177. Knaul JZ, Hudson SM, Creber KAM. Improved mechanical properties of chitosan fibers. Journal of Applied Polymer Science. 1999;72(13):1721-32.
178. Hirano S. Wet-spinning and applications of functional fibers based on chitin and chitosan. Macromolecular Symposia. 2001;168(1):21-30.
179. Tuzlakoglu K, Reis R. Formation of bone-like apatite layer on chitosan fiber mesh scaffolds by a biomimetic spraying process. Journal of Materials Science: Materials in Medicine. 2007;18(7):1279-86.
180. Duan B, Dong C, Yuan X, Yao K. Electrospinning of chitosan solutions in acetic acid with poly(ethylene oxide). Journal of Biomaterials Science, Polymer Edition. 2004;15:797-811.
181. Ohkawa K, Cha D, Kim H, Nishida A, Yamamoto H. Electrospinning of Chitosan. Macromolecular Rapid Communications. 2004;25(18):1600-5.
182. Shin SY, Park HN, Kim KH, Lee MH, Choi YS, Park YJ, et al. Biological evaluation of chitosan nanofiber membrane for guided bone regeneration. Journal of periodontology. 2005;76(10):1778-84.
183. De Vrieze S, Westbroek P, Van Camp T, Van Langenhove L. Electrospinning of chitosan nanofibrous structures: feasibility study. Journal of Materials Science. 2007;42(19):8029-34.
184. Park WH, Jeong L, Yoo DI, Hudson S. Effect of chitosan on morphology and conformation of electrospun silk fibroin nanofibers. Polymer. 2004;45(21):7151-7.
185. Subramanian A, Lin HY, Vu D, Larsen G. Synthesis and evaluation of scaffolds prepared from chitosan fibers for potential use in cartilage tissue engineering. Biomedical sciences instrumentation. 2004;40:117-22.
186. Bhattarai N, Edmondson D, Veiseh O, Matsen FA, Zhang M. Electrospun chitosan-based nanofibers and their cellular compatibility. Biomaterials. 2005;26(31):6176-84.
187. Li L, Hsieh Y-L. Chitosan bicomponent nanofibers and nanoporous fibers. Carbohydrate Research. 2006;341(3):374-81.
188. Chen Z, Mo X, Qing F. Electrospinning of collagen-chitosan complex. Materials Letters. 2007;61(16):3490-4.
189. Yang X, Chen X, Wang H. Acceleration of Osteogenic Differentiation of Preosteoblastic Cells by Chitosan Containing Nanofibrous Scaffolds. Biomacromolecules. 2009;10(10):2772-8.
190. Jiang T, Abdel-Fattah WI, Laurencin CT. *In vitro* evaluation of chitosan/poly(lactic acid-glycolic acid) sintered microsphere scaffolds for bone tissue engineering. Biomaterials. 2006;27(28):4894.
191. Geng L, Feng W, Hutmacher D, Wong Y, Loh H, Fuh J. Direct writing of chitosan scaffolds using a robotic system Rapid Prototyping Journal 2005;11(2):90-7.
192. Zhang Y, Zhang M. Synthesis and characterization of macroporous chitosan/calcium phosphate composite scaffolds for tissue engineering. J Biomed Mater Res. 2001;55(3):304-12.
193. Huang Y, Onyeri S, Siewe M, Moshfeghian A, Madihally SV. *In vitro* characterization of chitosan-gelatin scaffolds for tissue engineering. Biomaterials. 2005;26(36):7616-27.
194. Xu HH, Simon CG, Jr. Fast setting calcium phosphate-chitosan scaffold: mechanical properties and biocompatibility. Biomaterials. 2005;26(12):1337-48.
195. Abdel-Fattah WI, Jiang T, El-Bassyouni GE-T, Laurencin CT. Synthesis, characterization of chitosans and fabrication of sintered chitosan microsphere matrices for bone tissue engineering. acta biomaterialia. 2007;3(4):503-14.
196. Oliveira JT, Santos TC, Martins L, Silva MA, Marques AP, Castro AG, et al. Performance of new gellan gum hydrogels combined with human articular chondrocytes for cartilage regeneration when subcutaneously implanted in nude mice. Joirnal of Tissue Engineering and Regenerative Medicine 2009;3(7):493-500.
197. Martins A, Pereira R, Leonor I, Azevedo H, RL R. Chitosan scaffolds incorporating lysozyme into CaP coatings produced by a biomimetic route: A novel concept for tissue

engineering combining a self-regulated degradation system with in situ pore formation. Acta Biomaterialia. 2009;5:3328–3336
198. Kon E, Muraglia A, Corsi A, Bianco P, Marcacci M, Martin I, et al. Autologous bone marrow stromal cells loaded onto porous hydroxyapatite ceramic accelerate bone repair in critical-size defects of sheep long bones. Journal of Biomedical Materials Research. 2000;49(3):328-37.
199. Kruyt M, Dhert W, Yuan H, Wilson C, van Blitterswijk C, Verbout A, et al. Bone tissue engineering in a critical size defect compared to ectopic implantations in the goat. J Orthop Res. 2004;22(3):544-51.
200. Lucarelli E, Donati D, Cenacchi A, Fornasari PM. Bone reconstruction of large defects using bone marrow derived autologous stem cells. Transfusion and Apheresis Science. 2004;30:169-74.
201. Willers C, Chen J, Wood D, Xu J, Zheng MH. Autologous Chondrocyte Implantation with Collagen Bioscaffold for the Treatment of Osteochondral Defects in Rabbits. Tissue Engineering. 2005;11(7-8):1065-76.
202. Giannoni P, Mastrogiacomo M, Alini M, Pearce SG, Corsi A, Santolini F, et al. Regeneration of large bone defects in sheep using bone marrow stromal cells. J Tissue Eng Regen Med. 2008;2(5):253-62.
203. Heath CA. Cells for tissue engineering. Trends in Biotechnology. 2000;18(1):17-9.
204. Evans M, Kaufman M. Establishment in culture of pluripotential cells from mouse embryos. Nature. 1981;292:154-6.
205. Huss R, Lange C, Weissinger E, Kolb H-J, Thalmeier K. Evidence of Peripheral Blood-Derived, Plastic-Adherent CD34–/low Hematopoietic Stem Cell Clones with Mesenchymal Stem Cell Characteristics. Stem cells. 2000;18:252-60.
206. Gimble JM, Guilak F. Adipose-derived adult stem cells: isolation, characterization, and differentiation potential. Cytotherapy. 2003;5(5):362-9.
207. Sarugaser R, Lickorish D, Baksh D, Hosseini M, Davies J. Human Umbilical Cord Perivascular (HUCPV) Cells: A Source of Mesenchymal Progenitors. Stem cells. 2005;23:220-9.
208. De Coppi P, Bartsch G, Siddiqui M, Xu T, Santos C, Perin L, et al. Isolation of amniotic stem cell lines with potential for therapy. Nature. 2007;25:100-6.
209. Fukuchi Y, Nakajima H, Sugiyama D, Hirose I, Kitamura T, Tsuji K. Human Placenta-Derived Cells Have Mesenchymal Stem/Progenitor Cell Potential. Stem cells. 2004;22(5):649-58.
210. Pittenger M, Mackay AM, Beck S, Jaiswal R, Douglas R, Mosca JD, et al. Multilineage Potential of Adult Human Mesenchymal Stem Cells. Science. 1999;284:143-7.
211. Jiang Y, Jahagirdar B, Reinhardt R, Schwartz R, Keene C, Ortiz-Gonzalez X, et al. Pluripotency of mesenchymal stem cells derived from adult marrow. Nature. 2002;418(6893):41-9.
212. Jaiswal N, Haynesworth SE, Caplan AI, Bruder SP. Osteogenic differentiation of purified, culture-expanded human mesenchymal stem cells *in vitro*. Journal of Cellular Biochemistry. 1997;64(2):295-312.
213. Takamizawa S, Maehata Y, Imai K, Senoo H, Sato S, Hata R-I. Effects of ascorbic acid and ascorbic acid 2-phosphate, a long-acting vitamin C derivative, on the proliferation and differentiation of human osteoblast-like cells. Cell Biology International. 2004;28(4):255-65.
214. Bellows CG, Heersche JNM, Aubin JE. Inorganic phosphate added exogenously or released from [beta]-glycerophosphate initiates mineralization of osteoid nodules *in vitro*. Bone and Mineral. 1992;17(1):15-29.
215. Gerstenfeld LC, Chipman SD, Glowacki J, Lian JB. Expression of differentiated function by mineralizing cultures of chicken osteoblasts. Developmental Biology. 1987;122(1):49-60.

216. Koshihara Y, Kawamura M, Oda H, Higaki S. calcification in human osteoblastic cell line derived from periosteum. Biochemical and Biophysical Research Communications. 1987;145(2):651-7.
217. Subramaniam M, Colvard D, Keeting PE, Rasmussen K, Riggs BL, Spelsberg TC. Glucocorticoid regulation of alkaline phosphatase, osteocalcin, and proto-oncogenes in normal human osteoblast-like cells. Journal of Cellular Biochemistry. 1992;50(4):411-24.
218. Maniatopoulos C, Sodek J, Melcher A. Bone formation *in vitro* by stromal cells obtained from bone marrow of young adult rats. cell Tissue Res. 1988;254(2):317-30.
219. Canalis E, Agnusdei D. Insulin-like growth factors and their role in osteoporosis. Calcified Tissue International. 1996;58(3):133-4.
220. Mendes SC, Van den Brink I, De Bruijn JD, Van Blitterswijk CA. *In vivo* bone formation by human bone marrow cells: effect of osteogenic culture supplements and cell densities. J Mater Sci-Mater Med. 1999;9(12):855-8.
221. Lee YM, Park YJ, Lee SJ, Ku Y, Han SB, Klokkevold PR, et al. The bone regenerative effect of platelet-derived growth factor-BB delivered with a chitosan/tricalcium phosphate sponge carrier. Journal of periodontology. 2000;71(3):418-24.
222. Boyan B, Bonewald L, Paschalis E, Lohmann C, Rosser J, Cochran D, et al. Osteoblast-mediated mineral deposition in culture is dependent on surface microtopography. Calcif Tissue Int. 2002;71(6):519-29.
223. Govinden R, Bhoola KD. Genealogy, expression, and cellular function of transforming growth factor-[beta]. Pharmacology & Therapeutics. 2003;98(2):257-65.
224. Dean D. Effect of Transforming Growth Factor 2 on Marrow-Infused Foam Poly(Propylene Fumarate) Tissue-Engineered Constructs for the Repair of Critical-Size Cranial Defects in Rabbits. Tissue Engineering. 2005;11(5-6): 923-939
225. Gomez G, Korkiakoski S, Gonzalez M-M, Lansman S, Ella V, Salo T, et al. Effect of FGF and Polylactide Scaffolds on Calvarial Bone Healing With Growth Factor on Biodegradable Polymer Scaffolds. The Journal of Craniofacial Surgery 2006;17(5):935-42.
226. Osathanon T, Linnes ML, Rajachar RM, Ratner BD, Somerman MJ, Giachelli CM. Microporous nanofibrous fibrin-based scaffolds for bone tissue engineering. Biomaterials. 2008;29(30):4091-9.
227. Lian JB, Stein GS. Concepts of Osteoblast Growth and Differentiation: Basis for Modulation of Bone Cell Development and Tissue Formation. Critical Reviews in Oral Biology & Medicine. 1992;3(3):269-305.
228. Owen TA, Aronow M, Shalhoub V, Barone LM, Wilming L, Tassinari MS, et al. Progressive development of the rat osteoblast phenotype *in vitro*: Reciprocal relationships in expression of genes associated with osteoblast proliferation and differentiation during formation of the bone extracellular matrix. Journal of Cellular Physiology. 1990;143(3):420-30.
229. Sabokbar A, Millett P, Myer B, Rushton N. A rapid, quantitative assay for measuring alkaline phosphatase activity in osteoblastic cells *in vitro*. 1994;27:57-67.
230. Toquet J, Rohanizadeh R, Guicheux J, Couillaud S, Passuti N, Daculsi G, et al. Osteogenic potential *in vitro* of human bone marrow cells cultured on macroporous biphasic calcium phosphate ceramic. Journal of Biomedical Materials Research. 1999;44(1):98-108.
231. Weiner S. Biomineralization: A structural perspective. Journal of Structural Biology. 2008;163(3):229-34.
232. Werb Z. Ecm and cell surface proteolysis: Regulating cellular ecology. Cell 1997;91(4):439-42.
233. Klokkevold PR. Osteogenesis enhanced by chitosan (poly-N-acetyl glucosaminoglycan) *in vitro*. J Periodontol 1996;67(11):1170-5.
234. Cai K, Yao K, Cui Y, Lin S, Yang Z, Li X, et al. Surface modification of poly (D,L-lactic acid) with chitosan and its effects on the culture of osteoblasts *in vitro*. J Biomed Mater Res. 2002 Jun 5;60(3):398-404.

235. Cai K, Hu Y, Jandt K, Wang Y. Surface modification of titanium thin film with chitosan via electrostatic self-assembly technique and its influence on osteoblast growth behavior. Journal of Materials Science: Materials in Medicine. 2008;19(2):499-506.
236. Bumgardner JD, Chesnutt BM, Yuan Y, Yang Y, Appleford M, Oh S, et al. The Integration of Chitosan-Coated Titanium in Bone: An *In vivo* Study in Rabbits. Implant Dentistry. 2007;16(1):66-79
237. Coutinho D, Pashkuleva I, Alves C, Marques A, Neves N, Reis R. The Effect of Chitosan on the *In vitro* Biological Performance of Chitosan-Poly(butylene succinate) Blends. Biomacromolecules. 2008;9(4):1139-45.
238. Mohammadi Y, Soleimani M, Fallahi-Sichani M, Gazme A, Haddadi-Asl V, Arefian E, et al. Nanofibrous poly(epsilon-caprolactone)/poly(vinyl alcohol)/chitosan hybrid scaffolds for bone tissue engineering using mesenchymal stem cells. Int J Artif Organs. 2007;30(3):204-11.
239. Holtorf H, Jansen J, Mikos A. Ectopic bone formation in rat marrow stromal cell/titanium fiber mesh scaffold constructs:Effect of initial cell phenotype. Biomaterials. 2005;26:6208-16.
240. Kasten P, Vogel J, Luginbu R, Niemeyer P, Tonak M, Lorenz H, et al. Ectopic bone formation associated with mesenchymal stem cells in a resorbable calcium deficient hydroxyapatite carrier. Biomaterials. 2005;26:5879-89.
241. Trojani T, Boukhechba F, Scimeca J-C, Vandenbos F, Michiels J-F, Daculsi G, et al. Ectopic bone formation using an injectable biphasic calcium phosphate/Si-HPMC hydrogel composite loaded with undifferentiated bone marrow stromal cells. Biomaterials. 2006;27:3256–64.
242. Rentsch C, Rentsch B, Breier A, Hofmann A, Manthey S, Scharnweber D, et al. Evaluation of the osteogenic potential and vascularization of 3D poly(3)hydroxybutyrate scaffolds subcutaneously implanted in nude rats. Journal of Biomedical Materials Research Part A. 2010;92A(1):185-95.
243. Schantz JT, Hutmacher DW, Chim H, Ng KW, Lim TC, Teoh SH. Induction of ectopic bone formation by using human periosteal cells in combination with a novel scaffold technology. Cell Transplant. 2002;11(2):125-38.
244. Cai XX, Lin YF, Ou GM, Luo E, Man Y, Yuan QA, et al. Ectopic osteogenesis and chondrogenesis of bone marrow stromal stem cells in alginate system. Cell Biology International. 2007;31(8):776-83.
245. Claase MB, de Bruijn JD, Grijpma DW, Feijen J. Ectopic bone formation in cell-seeded poly(ethylene oxide)/poly(butylene terephthalate) copolymer scaffolds of varying porosity. J Mater Sci-Mater Med. 2007;18(7):1299-307.
246. Lindsey RW, Gugala Z, Milne E, Sun M, Gannon FH, Latta LL. The efficacy of cylindrical titanium mesh cage for the reconstruction of a critical-size canine segmental femoral diaphyseal defect. Journal of Orthopaedic Research. 2006;24(7):1438-53.
247. Pearce A, Richards R, Milz S, Schneider E, Pearce S. Animal models for implant biomaterial research in bone: a review. Eur Cell Mater. 2007;2(13):1-10.
248. Fuji T, Anada T, Honda Y, Shiwaku Y, Koike H, Kamakura S, et al. Octacalcium phosphate-precipitated alginate scaffold for bone regeneration. Tissue Eng Part A. 2009;15(11):3525-35.
249. Zhang Z-Y, Teoh S-H, Chong MSK, Lee ESM, Tan L-G, Mattar CN, et al. Neo-vascularization and bone formation mediated by fetal mesenchymal stem cell tissue-engineered bone grafts in critical-size femoral defects. Biomaterials. 2010;31(4):608-20.
250. Fialkov JA, Holy CE, Shoichet MS, Davies JE. *In vivo* bone engineering in a rabbit femur. Journal of Craniofacial Surgery. 2003;14(3):324-32.
251. Nasser NJ, Friedman A, Friedman M, Moor E, Mosheiff R. Guided bone regeneration in the treatment of segmental diaphyseal defects: a comparison between resorbable and non-resorbable membranes. Injury. 2005;36(12):1460-6.

252. Mastrogiacomo M, Corsi A, E F, Di Comite M, Monetti F, Scaglione FA, et al. Reconstruction of Extensive Long Bone Defects in Sheep Using Resorbable Bioceramics Based on Silicon Stabilized Tricalcium Phosphate. Tissue Engineering. 2006;12(5):1261-73.
253. Zhu L, Liu W, Cui L, Cao YL. Tissue-engineered bone repair of goat femur defects with osteogenically induced bone marrow stromal cells. Tissue Engineering. 2006 Mar;12(3):423-33.
254. Takahashi Y, Yamamoto M, Yamada K, Kawakami O, Tabata Y. Skull Bone Regeneration in Nonhuman Primates by Controlled Release of Bone Morphogenetic Protein-2 from a Biodegradable Hydrogel. Tissue Engineering. 2007;13(2):293-300.
255. Umeda H, Kanemaru Si, Yamashita M, Kishimoto M, Tamura Y, Nakamura T, et al. Bone Regeneration of Canine Skull Using Bone Marrow-Derived Stromal Cells and β-Tricalcium Phosphate. The Laryngoscope. 2007;117(6):997-1003.
256. Yuehuei H, Freidman R. Animal Models in Orthopaedic Research. 1st ed. Boca Raton: CRC press; 1999.
257. Montjovent MO, Mathieu L, Schmoekel H, Mark S, Bourban PE, Zambelli PY, et al. Repair of critical size defects in the rat cranium using ceramic-reinforced PLA scaffolds obtained by supercritical gas foaming. Journal of Biomedical Materials Research Part A. 2007;83A(1):41-51.
258. Whang K, Healy KE, Elenz DR, Nam EK, Tsai DC, Thomas CH, et al. Engineering bone regeneration with bioabsorbable scaffolds with novel microarchitecture. Tissue Engineering. 1999;5(1):35-51.
259. Stephan SJ, Tholpady SS, Gross B, Petrie-Aronin CE, Botchway EA, Nair LS, et al. Injectable tissue-engineered bone repair of a rat calvarial defect. The Laryngoscope. 2010;120(5):895-901.
260. Kim HW, Shin SY, Kim HE, Lee YM, Chung CP, Lee HH, et al. Bone formation on the apatite-coated zirconia porous scaffolds within a rabbit calvarial defect. J Biomater Appl. 2008;22(6):485-504.
261. Kim SJ, Lim JW, Ryu JJ, Ahn JS, Han IH, Shin SW. Effects of 4 Different Alloplastic Materials on Bone Regeneration in Rabbit Calvarial Defects. Tissue Eng Regen Med. 2009;6(1-3):63-8.
262. Yeo A, Wong WJ, Teoh SH. Surface modification of PCL-TCP scaffolds in rabbit calvaria defects: Evaluation of scaffold degradation profile, biomechanical properties and bone healing patterns. Journal of Biomedical Materials Research Part A. 2010;93A(4):1358-67.
263. Holmbom J, Sodergard A, Ekholm E, Martson M, Kuusilehto A, Saukko P, et al. Long-term evaluation of porous poly(epsilon-caprolactone-co-L-lactide) as a bone-filling material. Journal of Biomedical Materials Research Part A. 2005;75A(2):308-15.
264. Yokoyama A, Gelinsky M, Kawasaki T, Kohgo T, Konig U, Pompe W, et al. Biomimetic porous scaffolds with high elasticity made from mineralized collagen - An animal study. J Biomed Mater Res Part B. 2005;75B(2):464-72.
265. Chu TMG, Warden SJ, Turner CH, Stewart RL. Segmental bone regeneration using a load-bearing biodegradable carrier of bone morphogenetic protein-2. Biomaterials. 2007;28(3):459-67.
266. van der Donk S, Buma P, Aspenberg P, Schreurs B. Similarity of bone ingrowth in rats and goats: a bone chamber study. Comp Med. 2001;51(4):336-40.
267. Hidaka Y, Ito M, Mori K, Yagasaki H, Kafrawy AH. Histopathological and immunohistochemical studies of membranes of deacetylated chitin derivatives implanted over rat calvaria. Journal of Biomedical Materials Research. 1999;46(3):418-23.
268. Lee JY, Nam SH, Im SY, Park YJ, Lee YM, Seol YJ, et al. Enhanced bone formation by controlled growth factor delivery from chitosan-based biomaterials. J Control Release. 2002;78(1-3):187-97.

269. Malafaya PB, Santos TC, van Griensven M, Reis RL. Morphology, mechanical characterization and *in vivo* neo-vascularization of chitosan particle aggregated scaffolds architectures. Biomaterials. 2008;29(29):3914-26.
270. Spin-Neto R, Freitas RMd, Pavone C, Cardoso MrB, Campana-Filho SP, Marcantonio RAC, et al. Histological evaluation of chitosan-based biomaterials used for the correction of critical size defects in rats calvaria. Journal of Biomedical Materials Research Part A. 2009;93A(1):107-14.
271. Jiang T, Nukavarapu SP, Deng M, Jabbarzadeh E, Kofron MD, Doty SB, et al. Chitosan-poly(lactide-co-glycolide) microsphere-based scaffolds for bone tissue engineering: *In vitro* degradation and *in vivo* bone regeneration studies. Acta Biomaterialia. 2010;9: 3457-3470
272. Chang S-N, Chuang H, Chen Y, Chen J, Chung Y, Lu Y-L, et al. Gene expression profiling reveals PDGF recepor alpha as a target of cell contact dependent gene regulation in an endothelial cell-osteoblast co-culture model. Tissue Engineering. 2003;12(10):2889-903.

SECTION 2

CHAPTER II

MATERIALS AND METHODS

Chapter II

MATERIALS AND METHODS

The main aim of this chapter is to describe in more detail the experimental work and protocols related to the experiments performed and the obtained results. Together with chapter I, it will establish the rationale of the research reported in this thesis, which was the biological evaluation of chitosan based scaffolds, *in vitro* and *in vivo*, envisioning bone tissue engineering applications. For that, it will be briefly described the materials used and the scaffolds processing methodologies. It will be explained in more detail the *in vitro* biological characterization techniques and the *in vivo* animal models used and respective characterization methodologies.

1. Materials

1.1. Chitosan

Chitosan (Ch) is a linear polysaccharide, obtained from the alkaline deacetylation of chitin, composed of glucosamine and N-acetyl glucosamine linked in a β (1-4) link (1). Important parameters affecting the characteristics of chitosan are its molecular weight (M_w) and its degree of deacetylation (DD) (2). The degree of deacetylation of chitosan refers to the ratio between the deacetylated and acetylated units. The solubility of chitosan depends on the free amino and N-acetyl groups being soluble in acidic pH (3). Chitosan is a semi-crystalline polymer and the degree of crystallinity depends on the degree of deacetylation. Chitosan is a biodegradable polymer being degraded by lysozyme (4). The degradation rate of chitosan is inversely related to the degree of deacetylation (5).

Chitosan presents a wide range of biological properties, which makes it one of the most promising materials for tissue engineering applications. Important characteristics to be highlighted are its biodegradability, biocompatibility, antibacterial activity, wound healing properties and easy accessibility (low cost). Moreover, the chemical structure of chitosan (Figure 1) resembles the structure of glycosaminoglycans (GAGs) and these molecules play an important role in the modulation of various cell functions, morphology and differentiation (6).

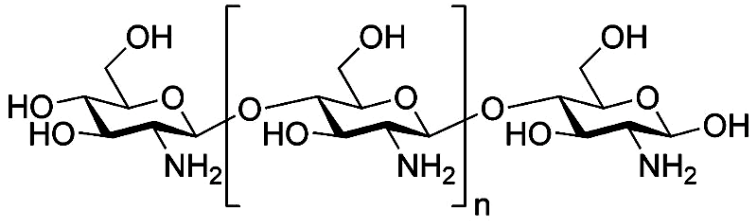

Figure 1. Chemical structure of chitosan

The chitosan herein used was purchased from France Chitine (Orange, France). Firstly, chitin was isolated from shrimp shells and squid bones by deproteinization and/or demineralization, respectively. The chitosan was further obtained by the removal of enough acetyl groups (CH_3-CO) from the chitin molecule (deacetylation process), releasing the amine groups (NH) and giving to chitosan a cationic characteristic.

1.2. Aliphatic polyesters

Synthetic polymers have been extensively studied in tissue engineering field, such as poly(lactic acid), poly(glycolic acid), poly(ε-caprolactone) (PCL) and their copolymers. These polymers are biodegradable, because the ester bonds present in its structure are hydrolyzed into non-toxic natural metabolites and are eliminated from the body via respiration. In the present thesis the synthetic materials used were PCL, poly(butylene succinate) (PBS) and poly(butylene terephthalate adipate) (PBTA). More detail and special emphasis will be given to PBS, since it was the material used in the majority of the studies due to its biological performance.

1.2.1. Poly(butylene succinate)

Poly(butylene succinate) (PBS) is an aliphatic polyester (Figure 2), commercially available under the trademark Bionolle®. It was obtained from Showa Highpolymer Co. Ltd. (Tokyo, Japan), with the reference 1050, a polybutylene succinate copolymer. Bionolle® has been shown to be biodegradable in a variety of natural environments, decomposing into water and carbon dioxide. It has been processed into films, sheets, filaments, nonwoven fabrics, laminates, molded foams and injection-molded products for diverse applications, namely in agriculture, fishery, forestry, civil engineering and for common household goods.

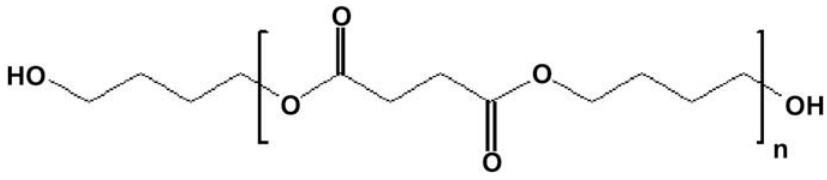

Figure 2. Chemical structure of poly(butylene succinate).

Pure PBS presents a hydrophobic behavior with low water uptake (~ 1.5%) and after 60 days of immersion in the isotonic saline solution it displays a decrease in the mechanical properties without any appreciable weight loss (~ 0.5%). This polymer presents a melting temperature (T_m) of 104.3ºC.

2. Processing methods

The materials used in this thesis were, always composed by chitosan and a synthetic polymer. The compositions were prepared by extrusion prior to be processed into a three dimensional (3D) structure. For the scaffolds production two different methodologies were used: compression molding followed by salt leaching and fiber bonding. Chitosan and polyester blends used for the production of the scaffolds are described in chapters III, IV, V, VI and VII. Those materials were compounded in a twin-screw extruder. Blends of chitosan with poly(butylene succinate) (Ch-PBS) were mixed at two different ratios - 25/75 wt% and 50/50wt%, blends of chitosan with poly(caprolactone) (Ch-PCL) and poly(butylene terephthalate adipate) (Ch-PBTA) were mixed at 50/50 wt%. In chapter IV, it was used poly(butylene succinate) to produce scaffolds to be used as controls in an experiment designed to test the relevance of chitosan in biological terms.

2.1. Compression molding/particulate leaching

The scaffolds described in chapters III, IV and VII were prepared after grinding the compounded blends by solid mixing with NaCl particles, loaded into a mold that was further heated, and molded into large discs by compression. The salt content was 60% by weight and the size range of NaCl particles was 250–500 μm for all the blends. These compression-molded discs were further sliced to obtain different types of geometrical structures used in different chapters, because of the size required to *in vivo* models employed. In chapter III, cubes of 5 mm^3 were used, in chapter IV were used discs of 8 mm of diameter and 1 mm thick and in chapter VII were used small discs with 5 mm of diameter and 1mm thick were

used (Figure 3). These structures were then immersed in distilled water to leach out the porogen particles. The cubes were dried to constant weight and used for further tests.

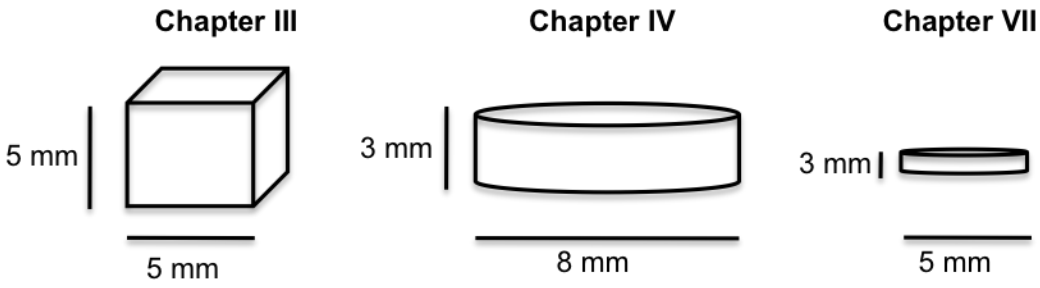

Figure 3. Scheme of the scaffolds produced by compression molding followed by salt leaching used in different chapters.

2.2. Fiber Bonding

The chitosan/polyester blends used to process the scaffolds presented in chapters V and VI were compounded as previously described. The mixture of chitosan with poly(butylene succinate) (Ch-PBS) (50-50% wt) was extruded into fibers, by using a single screw micro-extruder. The obtained fibers were cut into 1 cm long and loaded into a Teflon mold. This mold was heated at 150ºC during a previously optimized time period. After that, pressure was applied to allow fibers to weld at the junctions, forming a stable fiber mesh structure. The porous mesh was further cut into discs with diameter of 6.5 mm and 1.5 mm thick.

3. Scaffolds Characterization

When new polymeric scaffolds are developed, it is imperative to characterize these novel structures. Physical and chemical characterization is performed to determine the surface topography, morphological properties, 3D architecture, porosity and pore size, interconnectivity and mechanical properties. The following techniques were used to characterize the developed scaffolds used in this work.

3.1. Scanning Electron Microscopy

All the developed chitosan based scaffolds were evaluated by scanning electron microscopy (SEM). This methodology is extremely important to study the morphology of polymeric materials and structures. This technique allows to analyze the morphology of the specimen, at large magnifications and also the details of the structure up to the sub-micron level. Polymeric structures are non-conductive, being generally coated with conductive materials, such as gold or carbon. This fact is due to the fact that the intensity of the electron beam can damage the thin polymeric samples, which can lead to the deformation and even melting of the polymer. Furthermore, the accumulation of electrons at the surface of the specimen causes the loss of image formed at the detector.
The developed scaffolds were sputter-coated with gold (Fisons Instruments, model SC502; England) for 2 minutes at 15 mA. The samples were further analyzed by scanning electron microscopy (Leica Cambridge, model S360; England). Micrographs were recorded at 15 kV with magnifications ranging from 100 to 5000 times.

3.2. Micro computed tomography

Micro computed tomography (μCT) technique was used to recreate 3D images of the scaffolds. This methodology is based on the use of a X-ray source to create shadow images/projections of a 3D object that later can be used with an appropriate software to recreate a virtual model. It is named micro because pixel sizes of the cross-sections are in the micrometer range. The X-ray source and detector are typically stationary during the scan, while the sample rotates, to allow obtaining the slices of the object morphology.

The scaffolds used in chapter III, V and VI were evaluated by μ-CT, carried out by scanning in high-resolution mode of 8.7 μm x/y/z and an exposure time of 1792 ms. The energy parameters defined in the scanner were 63 keV with a current of 157 μA. Data were obtained by the system and reconstructed in 2D images. These slice images were further compiled and analyzed to render 3D images and obtain quantitative architecture parameters. A μCT analyzer and a μCT Volume Realistic 3D Visualization, both from SkyScan, were used as image processing tools for both μCT reconstruction and to create/visualize the 3D representation. Regions of interest (square of 4.5x4.5 mm^2) were selected in each slice image and thresholded to eliminate background noise. This threshold (to distinguish polymer material from pore voids) was selected and maintained constant for all the scanned

specimens and samples. The threshold was also inverted to obtain pore volume and to analyze both the pore morphology and its interconnectivity.

Chitosan-based fiber mesh scaffolds, exploited in chapter IV and VII, were scanned in high resolution mode using a pixel size of 8.24 µm and integration time of 2.0 ms. The X-ray source was set at 80 keV of energy and 124 µA of current. For all the scanned specimens representative data sets of 150 slices were transformed into binary using a dynamic threshold of 60-255 (grey values) to distinguish polymer material from pore voids. This data was used for morphometric analysis (CT Analyzer v1.5.1.5, SkyScan). 3D virtual models of representative regions in the bulk of the scaffolds were also created, visualized and registered using both image processing softwares (ANT 3D creator v2.4, SkyScan). Five scaffolds were examined for each type of scaffolds.

3.3. Mechanical properties

The mechanical testing of the scaffolds was performed under compression loading using a crosshead speed of 2 mm/min and the results presented are the average of at least five specimens. Samples were conditioned at room temperature for at least 48 h before testing. The values reported are the average of at least five specimens per condition. The compressive modulus was determined in the most linear region of the stress–strain graph using the secant method. In the cases that the yield stress was not clearly defined, it was calculated as the stress at the intersection of a line drawn parallel to the linear region and intercepting the *x*-axis at 1% strain.

3.4. *In vitro* degradation studies

The biomaterials used in this PhD thesis were biodegradable polymers. These materials degrade over time in a way that the neo-tissue can develop, without long-term presence of foreign components and finally cleared from the organism. Biodegradation of polymeric biomaterials requires cleavage of hydrolytically or enzymatically sensitive bonds in the polymer, leading to polymer erosion (7). Degradation products should be non-toxic and non-immunogenic, therefore not inducing strong inflammatory reaction. These products should be small enough to dissolve in the body fluids and, after transportation via lymphatic system into kidneys, these should be able to excrete them from the body (8). Polymers that

are known to degrade in the body, either by hydrolysis and/or enzymatic degradation can be modeled *in vitro*, in order to predict their behavior when implanted *in vivo*.

The degradation studies described in chapter VII were performed by incubating the scaffolds in phosphate buffered saline solution (pH 7.4) (control), with lipase from *Aspergillus oryzal* (Fluka) and/or lysozyme from chicken egg white (Sigma, St. Louis), at concentrations similar to the ones found in human blood serum (110 U/L for lipase and 13 mg/L for lysozyme), at 37ºC in dynamic conditions (60 rpm) for 1, 3, 6 and 12 weeks. In one experiment the solutions were changed every 7 days, while in the other the solutions were not changed throughout the experiment. At the end of each degradation period, the samples were removed, gently blotted to eliminate the water excess and immediately weighed for determination of water uptake and dried for later calculation of weight loss.

3.4.1. Water uptake and weight loss measurements

At the end of each degradation period, the samples were removed and immediately weighed for determination of water uptake (Equation 1) (Chapter V), washed thoroughly with distilled water and dried for later calculation of weight loss (Equation 2) (Chapters III, V, VI, and VII):

$$\text{Water uptake (\%)} = [(w_w - w_i)/ w_i] \times 100 \qquad \text{(Equation 1)}$$

$$\text{Weight loss (\%)} = [w_i - w_f)/ w_i] \times 100 \qquad \text{(Equation 2)}$$

where w_i is the initial weight, w_w is the wet weight and w_f is the final weight of the sample.

4. *In vitro* biological characterization

All the scaffolds used in the next sections of this thesis were sterilized by ethylene oxide. The routine followed in biological assessment of the developed scaffolds included cytotoxicity evaluation, direct contact tests with cell lines and in a later stage with human primary cells.

4.1. Cytotoxicity assessment

After the development of the scaffolds, the next step is the assessment of the eventual cytotoxicity. This initial screening is based on the use of the scaffold leachables*, i.e.*, substances that leach out of the biomaterials. These leachables are placed in contact with a cell line, for a determined period of time. After that time, cell viability and morphology are evaluated, to determine the eventual toxicity to the cells. In this first stage it is recommended the use of cell lines, because these cells are reproducible, well characterized in the literature and large amounts of cells can be obtained with cell expansion.

In the work developed in this thesis it was used a rat lung fibroblast cell line -L929, acquired from the European Collection of Cell Cultures, to perform the initial cytotoxicity evaluation of the developed scaffolds. Cells were grown as monolayers in Dulbecco's modified eagle's medium (DMEM) (Sigma, St. Louis, MO) supplemented with 1% fetal bovine serum (FBS) (Biochrom, Berlin, Germany) and 1% of antibiotic/antimycotic mixture (10,000 U/mL penicillin G sodium; 10,000 U/mL streptomycin sulphate; 25 μg/mL amphotericin B) (Gibco, Invitrogen, USA). Trypsin/EDTA (0.25% w/v trypsin/0.02% EDTA, Sigma) was used to detach the cells from the culture flasks before the experiments were conducted.

Cells were seeded in 96-well plates (n=6) at a density of 1.8 x 10^4 cells/well and incubated for 24 h at 37ºC, in a humidified atmosphere with 5% CO_2. The ratio of material weight to extract fluid was constant and equal to 0.25 g/mL. Latex rubber was used as a positive control of cell death, because it has a strong cytotoxic effect leading to extensive cell death. The ratio of latex material outer surface to extraction fluid was 2.5 cm^2/mL. Culture medium was used as negative control of cytotoxicity, considered to be the ideal condition for cell growth. Test scaffolds (n=6) and positive control were extracted for 24 h at 37ºC, using complete culture medium as the extraction fluid. Before the tests, culture medium was removed from wells with cells adhered, and an identical volume (200 μL) of extraction fluid was added. The cells were left to proliferate in the extract fluid for 72 h. After this period, the extraction fluid was removed, and the metabolic activity and, consequently, cell viability was determined by a colorimetric assay named CellTiter 96® AQueous One Solution Cell Proliferation Assay (Promega, USA). Briefly, this assay is based on the bioreduction of a tetrazolium compound (3-(4,5-dimethylthiazol-2-yl)-5-(3-carboxymethoxyphenyl)-2-(4-sulfofenyl)-2H tetrazolium, inner salt (MTS)) into a brown formazan product that is soluble in culture medium. This conversion is accomplished by the production of nicotinamide adenine dinucleotide phosphate (NADPH) or nicotinamide adenine dinucleotide (NADH) by the dehydrogenase enzymes existing in the metabolically active cells. The quantity of formazan

product bioreduced is directly proportional to the number of living cells in culture, as measured by the amount of 490 nm absorbance in a microplate reader (Bio-Tek, model Synergie HT, USA), after 3 h of incubation at 37ºC. Triplicates were made for each sample and per culture time.

4.2. Direct cell contact tests

4.2.1. Mouse bone marrow mesenchymal stem cell line - BMC9

If the scaffolds show no signs of cell cytotoxicity or morphological changes, the next step will be to proceed for direct contact assays with an appropriate cell source to develop a valid 3D construct for bone tissue engineering applications.

The developed scaffolds were composed of several aliphatic polyesters and chitosan. First all of these scaffolds were evaluated in terms of cell adhesion, proliferation and osteogenic potential. For this initial screening, described in chapter III, it was used a mouse mesenchymal stem cell line – BMC9. These cells were previously shown to be able to differentiate into several phenotypes, including the osteogenic lineage (9).

Cells were grown in DMEM, supplemented with 10% of FBS and 1% of antibiotic–antimycotic mixture. When the adequate number of cells was obtained, they were detached with trypsin, and seeded at a density of $5x10^5$ cells per scaffold. The seeding methodology consisted in dropping an aliquot of 10 μL on top of the scaffolds. After 2 h, 1 mL of osteogenic inducing culture medium was added to each well. The cell-seeded scaffolds were maintained at 37ºC, and 5% CO_2. The osteogenic medium consisted in the same medium described before, but supplemented with osteogenic agents, dexamethasone 10^{-8} M, ascorbic acid 50 μg/mL and β-glycerophosphate 10 mM. These supplements are required for a successful osteogenic differentiation of stem cells. Dexamethasone is a glucocorticoid that increases the expression of several different genes associated with osteogenic differentiation (10). Ascorbic acid is essential for collagen synthesis and alkaline phosphatase activity (11). Culture of osteogenic cells depends on supplementation of their growth medium with a source of inorganic phosphate (12) - β-glycerophosphate, a non-physiological organic substrate of alkaline phosphatase, allowing to produce mineralized ECM. To simplify the nomenclature of the cell seeded and cultured scaffolds *in vitro*, these will be identified as “constructs” in the next chapters.

4.2.2. Primary cultures of human bone marrow mesenchymal stem cells

The subsequent work developed after the screening of the best scaffold formulation for bone tissue engineering, was performed with primary cultures of human bone marrow mesenchymal stem cells (hBMSCs). These cells were isolated from human bone marrow aspirates obtained during routine surgical procedures involving knee arthroplasties. The collection of samples was approved by the ethical committee of the São Marcos hospital in Braga, under the cooperation agreement established between the 3B´s research group-UM and that hospital. A detailed informed consent was signed by each donor. The isolation procedure relies on the principle that from the several cell populations existent in bone marrow, only the adherent fraction will be isolated, being considered marrow stromal cells (13). Briefly, the bone marrow aspirate was centrifuged and all the fat tissue fraction, as well as cartilage and bone remnants were discarded. The cell suspension was incubated with eritrocytes lysis buffer to lyse these cells. The resultant cell suspension was plated and cultured. The cell population characterized by flow cytometry for stemness markers (clusters of differentiation-CD) CD29, 44, 73, 90, 105 and 106 and as well for the hematopoietic exclusion markers CD34 and 45. These adherent cells showed spindle-shape morphology and colony-forming unit (CFU) capacity. The isolated cells were also characterized for its multipotential ability, being differentiated for osteogenic, chondrogenic and adipogenic lineages.

4.3. hBMSCs culture, seeding into the scaffolds and differentiation into the osteogenic lineage

High numbers of hBMSCs are required to perform cell seeding into the developed scaffolds, for all quantitative and qualitative analysis. The isolated cells were expanded in basal medium consisting of alfa Eagle's medium (α-MEM; Sigma-Aldrich, Germany) supplemented with 10% FBS and 1 % antibiotic/antimyotic solution. Cells were cultured at 37°C in an atmosphere of 5% CO_2.

When cells reached confluency, at passages 4-5 they were harvested for static seeding onto the scaffolds, at a density of $2.5x10^5$ cells/scaffold. The constructs were cultured under static conditions, in standard osteogenic differentiation medium, described in subsection 4.2.1. The constructs were collected at different culture times: 7, 14 and 21 days, because it is expected that by the end of the experiment, the cells already show a definied osteogenic phenotype (14).

4.3.1. Evaluation of cell morphology and distribution

SEM was used to analyze the level of cell attachment and its morphology, as well as distribution on the surface of the scaffolds. To achieve those goals it is required the use of methods of fixation or stabilization of the cells on the scaffolds to obtain biological samples in their natural state. Coating of the mples with gold was performed as described in subsection 3.1. Additionally, due to the non-electric conductivity of those samples it is also needed to coat the samples with a conductive material such as gold or carbon. The constructs were fixed with 2.5% glutaraldehyde (Sigma, USA) in phosphate buffered saline (Sigma, USA) solution, during 15 min at RT. Then, they were dehydrated through graded series of ethanol and let to dry overnight. Finally, they were gold or carbon sputter coated (Fisons Instruments, model SC502; England) during 2 min at 15 mA, and analyzed by SEM (Leica Cambridge, model S360; England) equipped with an energy dispersive spectrometer (EDS; link-eXL-II).

The constructs were also analyzed by confocal laser scanning microscopy (FluoView1000, Olympus, Germany) in chapters III and IV. Cells were stained with calcein AM (Molecular Probes, Invitrogen, USA). This molecule is hydrolyzed by endogenous esterases into the highly negatively charged calcein, which is retained inside the cells. In this way, it is possible to observe the distribution of viable cells throughout the scaffold structure.

Histological analysis of the scaffolds was reported in chapter III. Hematoxylin-Eosin (H&E) staining was performed to observe the cell morphology and its distribution into the developed scaffolds. Basically, constructs were stained with Harris hematoxylin (Merck, Germany) during 1 to 3 minutes, until reaching the desired staining intensity. They were further washed in running tap water and afterwards a blue stain enhancement was performed by an immersion in 0.5% ammonia (Aldrich, Germany) for 5–10 seconds. The constructs were washed again in running tap water, followed by an immersion in alcohol 96 %, and stained in Shandon Eosin-Y (Thermo Scientific, UK) for 30 seconds. The samples were again washed in alcohol 96% and dehydrated through two immersions in alcohol 100 %. Before permanent mounting in Histomount™ (National Diagnostics, UK), the stained constructs were immersed in xylene for 1-2 min. Stained sections were observed under an optical microscope (BX61, Olympus Corporation, Germany) and images captured with a digital camera (DP70, Olympus Corporation, Germany).

4.3.2. Cell viability assay

Cell viability was assessed by indirect measurements based on its metabolic activity, at each time period by CellTiter 96® AQueous One Solution Cell Proliferation Assay (Promega; USA), as described in subsection 4.1.

4.3.3. Cell proliferation assay – DNA quantification

Measurements of DNA synthesis are frequently taken to be representative of the amount of cell proliferation (15). Cell proliferation rate determination is often used to determine the response of cells to a particular stimulus, *i.e.*, physical (*e.g.* topography of a substrate) or chemical (toxin or growth/differentiation factor).

In the present work, cell proliferation was quantified by the total amount of double-stranded DNA (dsDNA) using an ultrasensitive fluorescent nucleic acid stain. Quant-iT™ PicoGreen® dsDNA reagent was selected since it enables to quantify as little as 25 pg/mL of dsDNA (50 pg dsDNA in a 2 mL assay volume) with a standard spectrofluorometer and specific fluorescein excitation and emission wavelengths. Additionally, dsDNA can be quantified in the presence of equimolar concentrations of ssDNA and RNA with minimal effect on the quantitative results obtained. The Quant-iT™ PicoGreen dsDNA Assay Kit (Invitrogen™, Molecular Probes™; Oregon, USA) was used according to the manufacturer's instructions. Briefly, cells in the construct were lysed by osmotic and thermal shock and the supernatant used for the DNA quantification assay. A fluorescent dye, PicoGreen, was used because of its high sensitivity and specificity to double-stranded DNA. The fluorescence of the dye was measured at an excitation wavelength of 485/20 nm and at an emission wavelength of 528/20 nm, in a microplate reader (Synergie HT, Bio-Tek, USA). The DNA concentration for each sample was calculated using a standard curve (DNA concentration ranging from 0.0 to 1.5 µg/ml) relating quantity of DNA and fluorescence intensity. Triplicates were made for each sample and per culturing time

4.3.4. Alkaline phosphatase (ALP) quantification

A detailed analysis of the mineralization and of the progression of differentiation can be obtained by biochemical assays. Routine assessments involve the quantification of total calcium content and the activity of alkaline phosphatase (ALP), a cell surface protein bound

to the plasma membrane though phosphatidylinositol phospholipid complexes (16). High ALP activity is associated with the active formation of mineralized matrix and highest levels are found in the mineralization front of the bone healing process.

The concentration of ALP was determined for all time culture periods, using the same samples used for DNA quantification. Briefly, the activity of ALP was assessed using the *p*-nitrophenol assay. Nitrophenyl phosphate disodium salt (pnPP; Fluka BioChemika, Austria) is colourless, is hydrolyzed by alkaline phosphatase, produced by cells, at pH 10.5 and temperature of 37ºC, to form free *p*-nitrophenol, which is yellow. The reaction was stopped by the addition of 2 M NaOH (Panreac Quimica, Spain) and the absorbance read at 405 nm in a microplate reader (Bio-Tek, Synergie HT; USA). Standards were prepared with 10 µmol/ml *p*-nytrophenol (pNP; Sigma, USA) solution, to obtain a standard curve ranging from 0 to 0.25 µmol/ml). Triplicates of each sample and standard were made, and the ALP concentrations read off directly from the standard curve.

4.3.5. Extracellular matrix mineralization content by energy dispersive spectroscopy (EDS)

Energy dispersive spectroscopy (EDS) methodology was used to detect the presence of calcium (Ca) and phosphorous (P) elements by analyzing the surface of the constructs. These two chemical elements are constituents of the mineral phase (hydroxyapatite) of bone ECM. Their presence positively indicates the formation of mineralized ECM at the surface of the constructs. As controls, it was analyzed the surface of unseeded scaffolds immersed in osteogenic medium for the same time periods, showing that the presence of P and Ca were the result of cellular activity.

The constructs were processed as described previously for SEM in subsection 3.1. The samples were sputter coated with carbon (JEOL JFC-1100) with the purpose of analyzing the presence of Ca and P elements at the surface by EDS with a Leica Cambridge S360 scanning electron microscope. Sputter coating with carbon avoids overlapping of signals of the coating with the elements being analyzed.

4.3.6. Extracellular matrix mineralization crystallinity by fourier transform infra-red spectroscopy (FTIR)

Fourier transform infrared spectroscopy (FTIR) method is used to study the chemical structure of a polymer, but it can also be used to analyze the chemical composition of the surface of a scaffold. In the present thesis it was used to confirm the results obtained from EDS analyses, indicating the presence of phosphate and carbonate groups, which are typical for carbonated apatite (17). Briefly, constructs were washed in phosphate buffered saline and fixed in 2.5% glutaraldehyde. The samples were pressed into pellets with potassium bromide (KBr; Riedel-de Haen, Germany) and further analysed by FTIR. The infrared spectrum was measured using a FTIR Spectrometer (model IRPrestige-21, Shimadzu; Germany) in the wavelength range of 4000–400 cm^{-1}. The same controls (acellular scaffolds) used for the EDS analysis were used in tests.

4.3.7. Gene expression analysis of specific osteogenic genes

The constructs cultured *in vitro* in osteogenic inducing medium were evaluated by analyzing the expression of genes encoding specific proteins during osteogenic differentiation of hBMSCs. This process is characterized by three sequential periods: proliferation, ECM maturation and mineralization (18). The osteogenic phenotype is recognized by cell maturation coordinated with the secretion of specific proteins, in a process that is asynchronously acquired as the progenitor cells successfully differentiate and the matrix matures and mineralizes (19). To evaluate the transient state of the stem cells during the differentiation process polymerase chain reaction (PCR) was performed, by amplifying specific sequences of a target osteogenic specific gene.

4.3.7.1. RNA isolation

Total ribonucleic acid (RNA) from the constructs was extracted using the Trizol® (Invitrogen, Life Technologies Inc., UK) method according to the manufacturer's protocol. At each time point, the constructs were washed with phospate buffered saline, immersed in Trizol and stored at -80ºC until further use. Proteins were removed with chloroform extraction and the RNA pellets were washed once with isopropyl alcohol and once with 70 % ethanol. The total RNA pellets were reconstituted in RNAase free water (Gibco, Invitrogen, UK). Determination of the RNA concentration for each scaffold replica (triplicates of each scaffold

per time point) was performed by spectrophotometry (NanoDrop ND-1000, USA). The integrity of the RNA samples was checked using agarose 1.2% gel electrophoresis.

4.3.7.2. Reverse-transcriptase and real-time quantitative polymerase chain reaction

In chapter V, it was used non-quantitative reverse-transcriptase polymerase chain reaction (PCR). Briefly, aliquots of the total RNA (100 ng/µl) were used to synthesize complementary deoxyribonucleic acid (cDNA) and amplified by PCR, in one step RT-PCR beads (Amersham Biosciences, USA). The cDNA synthesis was executed by incubating the reaction mixture 5 min at 25ºC, followed by 30 min at 42ºC and terminated by an incubation at 85ºC for 5 min, using a termocycler (MyCycler™, Thermal Cycler, Biorad).

Specific osteogenic gene sequences (primers) were used in PCR reaction. Human specific primers used were: for runt related transcription factor 2 (Runx2), osteocalcin, type I collagen, bone sialoprotein (BSP) and for the house keeping gene glyceraldehyde-3-phosphate dehydrogenase (GAPDH). Each cDNA sample was run in triplicate for every PCR. Amplification was performed using a termocycler (MyCycler™, Thermal Cycler, Biorad). The first reverse transcription step at 42ºC for 30 min was followed by a step of denaturation at 95ºC during 5 min. After this, 35 cycles of PCR were performed, each consisting of a denaturation stage at 95ºC for 1 min, annealing at a given temperature accordingly with the specific primer used and then an extension stage at 72ºC for 2 min. In all cases, a final extension at 72ºC for 5 min was performed before storing the samples at 4ºC.

PCR products were separated by 1% agarose (Biorad, USA) at least twice. The separated DNA fragments were visualized by ethidium bromide staining (Sigma, St Louis, MO) and observed with Eagleye software (Alpha Innotech, USA) using excitation at 514 nm and emission at 610 nm.

In chapter IV, it was used quantitative real-time PCR. This technology presents several advantages over traditional PCR (reverse-transcriptase PCR). The measurement of the amount of amplified product is carried out with a quantitative laser-based method, and data collection is performed in the early exponential phase of the reaction, when none of the reagents is rate-limiting. The genes analyzed were Runx2, osterix (OSX), osteocalcin, type I collagen, BSP, osteopontin (OPN) and for the house keeping gene glyceraldehyde-3-phosphate dehydrogenase (GAPDH). Real time PCR was performed accordingly to the protocol from iScript™ cDNA synthesis kit (BioRad, Hercules, CA, USA). Succinctly, a reaction mixture consisting of 1X iScript Reaction Mix, 1 μl iScript Reverse Transcriptase,

RNA template (1 μg total RNA) and nuclease-free water was prepared, in 40 μl of total volume. The single-strand cDNA synthesis occurred as described for conventional PCR.

Amplification of the target cDNA for real-time PCR quantification was performed according to manufacturer protocol, using 2 μl RT cDNA products, 1 μM each primer, 1X iQ SYBR Green Supermix (BioRad, Hercules, CA, USA) and nuclease-free water, in a final volume of 25 μL. Forty-four cycles of denaturation (95ºC, 10 s), annealing (temperature dependent on the gene, 30 s) and extension (72ºC, 30 s) were carried out in the gradient thermocycler MiniOpticon real-time PCR detection system (BioRad, Hercules, CA, USA) for all genes. The transcripts expression data were normalized to the housekeeping gene glyceraldehyde-3-phosphate-dehygrogenase (GAPDH) for each time point and relative quantification calculated by the ΔC_T method.

5. *In vivo* studies

In vitro experimentation is limited in recreating the complex *in vivo* environment, being most of the times incapable of predicting *in vivo* performance in many settings, particularly in tissue engineering and regeneration of functional tissues.

All procedures were conducted in accordance with European regulations for animal testing (European Union Directive 86/609/EEC).

5.1. *In vivo* tissue response in different locations

This work was developed in chapter IV. Twelve Wistar rats were used. This study was conducted after receiving approval from the Animal Ethical Committee of the Kırıkkale University, Ankara, Turkey. The scaffolds (8 mm in diameter and 1 mm thick) were sterilized by ethylene oxide. Animals were anaesthetized by intraperitoneal (IP) injection with a mixture of ketamine HCl (Parke Davis, 50 mg/ml, Taiwan) and Rompun (2%, Bayer, Germany). The scaffolds were implanted in 3 different regions per animal:

(i) single critical size defect with 8 mm diameter in crania;

(ii) pocket incision between perichondrium and ear cartilage, the scaffold being placed on the 1/3 proximal cartilage of the pocket;

(iii) incision of 10 mm close to iliac bone, the scaffolds being placed between periosteum and iliac bone (onlay model) (21).

A total of 3 scaffolds per animal were implanted (one in each location). In all cases, the incisions were closed using 5.0 silk sutures. After one month of implantation, the animals were sacrificed and implants were collected with the surrounding tissue and processed for histological processing.

5.2. *In vivo* degradation studies and evaluation of the host response

In vivo implantation of developed scaffolds was performed in parallel with *in vitro* degradation studies. Biocompatibility is directly related with degradation process of the scaffolds. This is due to the fact that degradation of a biomaterial implanted in a host is influenced by the presence and recruitment of inflammatory cells and consequently by the production of inflammatory mediators. One of the most important requisites for clinical application of a biomaterial is its biocompatibility, that is defined as the ability of a material to perform with an appropriate host response in a specific application (22). The local reaction of an implant is studied histologically after a 3 months implantation period, as described in ISO standard 10993-6 (23).

For this study, described in chapter VII, Wistar rats were used. Scaffolds were implanted subcutaneously and at 1, 3, 6 and 12 weeks, samples were retrieved for further analysis. Animals were anesthetized by an IP injection of a solution of 75//0.5 mg/kg body weight ketamine:metedomidine (Imalgene®:Dorbenvet®). Subcutaneous (SC) pockets were created and 4 scaffolds were placed in each animal, away from the sutures site (incision) to avoid inflammation of the wound. The anaesthesia was then reverted with a SC injection of 0.25 mg/kg Atipamezol (Antisedan®). After recovering from anaesthesia, animals were placed in their home cages and water and food were supplied *ad libitum*. Each animal received an SC injection of 1mg/kg analgesic Butorphanol (Torbugesic®) administered immediately after surgery and 24 h later, to avoid post-operative pain. At each time point, 3 animals were euthanized by intraperitoneal injection of sodium penthobarbital, at a lethal dose and the respective implants were retrieved.

5.3. *In vivo* cranial defect in nude mice

The *in vivo* approach should mimic the future clinical application envisaged and the bone defect must not heal spontaneously, *i.e.*, a critical size defect (CSD) should be created (20). The work developed was described in detail in chapter VII.

Athymic nude mice were used to examine the healing of cranial critical size bone defects filled with transplants of pre-cultured constructs. All procedures involving the use of animals were conducted in accordance with the guidelines of the Institutional Animal Care and Use Committee of the Technion, Haifa in Israel. In brief, the *in vitro* constructs (with $1x10^6$ cells) were cultured in osteogenic inducing medium for 2 weeks prior to implantation. The surgery consisted on drilling 2 bilateral critical size circular defects (5 mm diameter and 1mm thick) in the parietal bones of the skull on either side of the sagittal suture line, with a hand drill and trephine bit. Extremely care was taken to not damage the sagittal suture or to interrupt the dura matter beneath the bone. During procedure, sterile saline was dripped over the drilling site, in order to avoid extensive heating and to protect brain tissue. Surgeries were performed under general anesthesia (xylazine: ketamine 1:1 solution in saline) by IP injection. Scaffolds (scaffolds seeded and cultured for 2 weeks with $1x10^6$ hBMSC and scaffold without cells) were implanted into the defects. A total of 6 nude mice were used and 12 cranial defects were created. Animals were kept under aseptic conditions. After 8 weeks post-surgery, animals were euthanized and crania were removed, cleaned and fixed immediately in formalin to be further analyzed by micro computed tomography analysis.

5.4. *In vivo* results analysis

5.4.1. Histological evaluation

Histological sections show the tissue inside of implant as well as the tissue surrounding it. To further identify the resident cells of those tissues, sections must be stained with specific staining. Retrieved samples at each time point were fixed in 10% neutral buffered formalin. The fixed samples were dehydrated and further embedded in paraffin, as described in subsection 4.3.1. The specimens were sectioned to obtain 3 μm thick longitudinal and transverse sections.

5.4.1.1. Haematoxylin and Eosin (H&E) staining

H&E staining is a standard protocol to identify microscopically the morphology of the cells in tissues. Haematoxylin stains the nucleus with a dark blue color. Eosin stains the cytoplasm of the cell with a pink colour. Thus, the main cell structures are easily indentified. A standard protocol for H&E staining was used. Stained sections were observed by light microscopy.

5.4.1.2. Masson´s trichrome staining

Masson´s trichrome stain was performed to analyze the amount and distribution of mature collagen, differentiating the collagen fibers from smooth muscle and elastin fibers. Sections were stained with Weigert's haematoxilin at RT, for 5 min and washed with water. After that, slides were stained with ponceau-fucsin solution and washed. Then, slides were immersed in phosphomolibdic acid to remove the previous stain. Finally, sections were stained with light green, washed and immediately placed in ethanol 95% and then in xylene. Finally, they were mounted with Histofluid (Marienfeld GmbH & Co. KG, Germany) and observed by light microscopy (BX61, Olympus Corporation, Germany) and images captured with a digital camera (DP70, Olympus Corporation, Germany).

5.4.1.3. Immunohistochemistry

Immunohistochemistry principle is based on a highly specific reaction antigen-antibody, which implies that a determined antibody only reacts with a specific antigen. For formalin fixed and paraffin embedded sections, the most used protocol involves the use of an enzyme conjugated with a secondary antibody with specificity to the primary antibody used. This enzyme reacts with a specific protein (avidin or streptavidin), which will be revealed by a dye, such as horseradish peroxidase (HRP). Immunolocalization of a specific antibody is detected by a brown staining visible at light microscopy.

Immunostaining for alpha-smooth muscle actin (α-SMA) antibody was performed to evaluate the new vascularization (24). In order to perform immunohistochemistry, paraffin was removed. The antigen retrieval was heat induced in a water bath at 96ºC for 20 min, with incubation of the slides in citrate buffer (pH=6). The slides were washed with phosphate buffer saline and endogenous peroxidase was blocked with 0.6% hydrogen peroxide (H_2O_2) in methanol, at room temperature (RT) for 30 min. R.T.U. Vectastain® Universal Elite ABC Kit (Vector, VCPK-7200, USA) was used for antibody incubation, according to the instructions of the manufacturer. Briefly, sections were incubated with α-SMA primary antibody (Abcam, ab5694, UK) overnight at 4ºC, in a humidified atmosphere. After washing with phosphate buffered saline, antibody detection was revealed by using the Peroxidase Substrate Kit DAB (Vector, VCSK-4100). Slides were washed in water for 5 minutes and then counterstained with Harris' haematoxylin for nuclear contrast, at RT for 2 min. After this, samples were washed with water, dehydrated in graded ethanol (50, 70, 95 and 100%), cleared with xylene, and mounted with Histofluid (Marienfeld GmbH & Co. KG, Germany).

Slides were observed by light microscopy (BX61, Olympus Corporation, Germany) and images captured with a digital camera (DP70, Olympus Corporation, Germany).

5.4.2. Bone regeneration analysis by micro computed tomography

Entire crania were analyzed using a high-resolution µCT 1072 scanner (Skyscan, Kontich, Belgium). Specimens were scanned in high-resolution mode using a pixel size of 19.13 µm and integration time of 1.7 ms. The X-ray source was set at 91 keV of energy and 110 µA of current. For all the scanned specimens representative data sets of 1023 slices were transformed into binary using a dynamic threshold of 255-120, to distinguish bone from polymeric material. This data was used for morphometric analysis (CT Analyzer v1.5.1.5, SkyScan). 3D virtual models of the mice crania were created, visualized and registered using image processing software (ANT 3D creator v2.4, SkyScan).

References

1. Kurita K. Chemistry and application of chitin and chitosan. Polymer Degradation and Stability. 1997;59(1-3):117-20.
2. Rinaudo M. Chitin and chitosan: Properties and applications. Progress in Polymer Science. 2006;31(7):603-32.
3. Madihally SV, Matthew HWT. Porous chitosan scaffolds for tissue engineering. Biomaterials. 1999;20(12):1133-42.
4. Tomihata K, Ikada Y. *In vitro* and in tivo degradation of films of chitin and its deacetylated derivatives. Biomaterials. 1997;18:261-8.
5. Kjell M. Varum, Mildrid M. Myhr, Ragnhild J.N. Hjerde, Smidsrod O. *In vitro* degradation rates of partially N-acetylated chitosans in human serum. Carbohydrate res. 1997;299:99-101.
6. Nishikawa H, Ueno A, Nishikawa S, Kido J-i, Ohishi M, Inoue H, et al. Sulfated Glycosaminoglycan Synthesis and Its Regulation by Transforming Growth Factor-[beta] in Rat Clonal Dental Pulp Cells. Journal of Endodontics. 2000;26(3):169-71.
7. Katti DS, Lakshmi S, Langer R, Laurencin CT. Toxicity, biodegradation and elimination of polyanhydrides. Advanced Drug Delivery Reviews. 2002;54(7):933-61.
8. van Dijkhuizen-Radersma R, Moroni L, Apeldoorn Av, Zhang Z, Grijpma D, Clemens van B, et al. Degradable polymers for tissue engineering. Tissue Engineering. Burlington: Academic Press; 2008. p. 193-221.
9. Dennis J, Merriam A, Awadallah A, Yoo J, Johnstone B, Caplan A. A quadripotential mesenchymal progenitor cell isolated from the marrow of an adult mouse. J Bone Miner Res. 1999;14(5):700-9.
10. Takamizawa S, Maehata Y, Imai K, Senoo H, Sato S, Hata R-I. Effects of ascorbic acid and ascorbic acid 2-phosphate, a long-acting vitamin C derivative, on the proliferation and differentiation of human osteoblast-like cells. Cell Biology International. 2004;28(4):255-65.
11. Koshihara Y, Kawamura M, Oda H, Higaki S. Calcification in human osteoblastic cell line derived from periosteum. Biochemical and Biophysical Research Communications. 1987;145(2):651-7.
12. Cheng S, Yang J, Rifas L, Zhang S, Avioli L. Differentiation of human bone marrow osteogenic stromal cells *in vitro*: induction of the osteoblast phenotype by dexamethasone. Endocrinology. 1994;134(1):277-86.
13. Owen M. Marrow Stromal Stem Cells. J Cell Sci Suppl. 1988;10:63-76.
14. Jaiswal N, Haynesworth SE, Caplan AI, Bruder SP. Osteogenic Differentiation of Purified, Culture-Expanded Human Mesenchymal Stem Cells *In vitro*. Journal of Cellular Biochemistry. 1997;64:295-312.
15. Freshney R. Cytotoxicity. In: Freshney R, editor. Culture of Animal Cells: A Manual of Basic Technique. Fifth ed: John Wiley & Sons, Inc.; 2005. p. 359-73.
16. Hofmann S, Kaplan D, Vunjak-Novakovic G. Tissue Engineering of Bone. In: Vunjak-Novakovic G, Freshney RI, editors. Culture of Cells for Tissue Engineering. New Jersey: John Wiley & Sons, Inc.,; 2006. p. 323-73.
17. Rehman I, Bonfield W. Characterization of hydroxyapatite and carbonated apatite by photo acoustic FTIR spectroscopy. Journal of Materials Science: Materials in Medicine. 1997;8(1):1-4.
18. Lian JB, Stein GS. Concepts of Osteoblast Growth and Differentiation: Basis for Modulation of Bone Cell Development and Tissue Formation. Critical Reviews in Oral Biology & Medicine. 1992 January 1, 1992;3(3):269-305.
19. Madras N, Gibbs AL, Zhou Y, Zandstra PW, Aubin JE. Modeling Stem Cell Development by Retrospective Analysis of Gene Expression Profiles in Single Progenitor-Derived Colonies. Stem cells. 2002;20(3):230-40.

20. Salgado A J. Bone tissue engineering: state of the art and future trends. Macromolecular Bioscience. 2004;4:743-5.
21. Bölgen N, Vargel I, Korkusuz P, Güzel E, Plieva F, Galaev I, et al. Tissue responses to novel tissue engineering biodegradable cryogel scaffolds: an animal model. J Biomed Mater Res A 2008;91(1):60-8.
22. Williams DF, Remes A. Immune response in biocompatibility. Biomaterials. 1992;13(11):731-41.
23. ISO. Biological evaluation of medical devices. Part 6: tests for local efects after implantation. Geneva: International Organization for Standardization; 1994.
24. Malafaya PB, Santos TC, van Griensven M, Reis RL. Morphology, mechanical characterization and *in vivo* neo-vascularization of chitosan particle aggregated scaffolds architectures. Biomaterials. 2008 29(29):3914-26.

SECTION 3

CHAPTER III

Adhesion, proliferation and osteogenic differentiation of a mouse mesenchymal stem cell line (BMC9) seeded on novel melt based chitosan/polyester 3D porous scaffolds

This chapter is based on the following publication: Costa-Pinto AR, Correlo VM, Sol PC, Bhattacharya M, Charbord P, Delorme B, Reis RL, Neves NM. "Adhesion, proliferation and osteogenic differentiation of a mouse mesenchymal stem cell line (BMC9) seeded on novel melt based chitosan/polyester 3D porous scaffolds". Tissue Engineering Part A 2008; 14(6): 1049-105

CHAPTER III

Adhesion, proliferation and osteogenic differentiation of a mouse mesenchymal stem cell line (BMC9) seeded on novel melt based chitosan/polyester 3D porous scaffolds

ABSTRACT

The aim of the present work is to study the biological behavior of a mouse mesenchymal stem cell line when seeded and cultured under osteogenic conditions onto novel processed melt based chitosan scaffolds.

Scaffolds were produced by compression molding, followed by salt leaching. Scanning electron microscopy (SEM) observations and μCT analysis showed the pore sizes ranging between 250 to 500 μm and the interconnectivity of the porous structure. The chitosan-PBS scaffolds presented the high mechanical properties, similar to the ones of trabecular bone (E1% ~ 87.4MPa). Cytotoxicity assays were carried out using standard tests (accordingly to ISO/EN 10993 part 5 guidelines), namely MTS test with a 24 h extraction period, revealing that L929 cells had similar metabolic activities to that obtained for the negative control.

Cell culture studies were conducted using a mouse mesenchymal stem cell line (BMC9). Cells were seeded onto the scaffold and allowed to proliferate for 3 weeks, under osteogenic conditions. SEM observations demonstrated that cells were able to proliferate and massively colonize the scaffolds structure. The cell viability assay MTS demonstrated that BMC9 cells were viable after 3 weeks in culture. The cells clearly evidenced a positive differentiation towards the osteogenic lineage, as confirmed by the high ALP activity levels. Moreover, energy dispersive spectroscopy (EDS) analysis revealed the presence of Ca and P in the elaborated extracellular matrix (ECM).

These combined results indicate that the novel melt based chitosan/polyester scaffolds support the adhesion, proliferation and osteogenic differentiation of the mouse MSCs and shows adequate physicochemical and biological properties for being used as scaffolds in bone tissue engineering related strategies.

1. INTRODUCTION

The last 15 years have witnessed the emergence of a novel multidisciplinary field of science called Tissue Engineering that has been in the forefront of a new wave of therapeutic/regenerative approaches for a variety of tissues, including bone. Its main purposes are the production of tissues and organs substitutes/equivalents that can replace or restore the natural features and physiological functions of natural tissues *in vivo* (1, 2).

The most common approach used in the bone tissue engineering field is based on the seeding of cells with osteogenic potential, commonly mesenchymal stem cells, on three dimensional (3D) scaffolds followed either by direct implantation on the injury site or by an *in vitro* culturing period upon which the construct is implanted (3). Ultimately, these so-called bone tissue engineering constructs should have two main functions when implanted *in vivo* (4-6): 1) provide structural support until the neotissue can assure it by itself and 2) promote osteoinduction, meaning in a simplistic way, the promotion of migration and differentiation of mesenchymal stem and osteoprogenitor cells, which later will lead to new bone formation. From the lines above it can be clearly concluded that 3D scaffolds play a major role within any bone tissue engineering concept. Ideally these temporary scaffolds should be porous in order to accommodate cell growth and facilitate both tissue regeneration and vascularization (1, 2, 7). Furthermore, they should also be biocompatible, mechanically stable under loads and have a physiologic biodegradation rate similar to the cell/tissue growth rates (1, 2, 7, 8).

Up to now, several materials, such as titanium alloys (9-11), ceramics (12-14) and biodegradable polymers (15-18) have been used to obtain these 3D structures. Among those materials, and due to their intrinsic characteristics, biodegradable polymers are those that have been used more frequently. The most widely used are poly(α-hydroxy acids), such as poly(lactic acid), poly(glycolic acid), and their copolymers because they have been already accepted by regulatory agencies. In spite of the fact that these materials have been thoroughly studied and extensively used in the clinical practice, it is also true that upon degradation they release acidic by-products, which may trigger inflammatory responses and compromise the needed integration by the host tissue (19, 20).

Therefore, there is an urgent need for the development of new biomaterials with scaffolding potential for bone tissue engineering. It is in this context that natural based polymers have been put forward in the last few years. Within this group, the polysaccharides, like starch (19, 21, 22) and chitosan (23-29) have been highlighted as the most promising, as they may act as analogs of polyssacharides present *in vivo* and adopt their roles (24). An

example of such affinity is the structural similarity observed between chitosan and glycosaminoglycans (GAGs) (29). Several reports about chitosan (23-29), the alkaline deacetylated product of chitin, have shown that this polymer might have a range of interesting properties, from biodegradability to biocompatibility, considered to be suitable for bone tissue engineering scaffolding. Nevertheless, chitosan still presents a challenge when compared to other materials, that is, the inability of being processed by means other than by solvent based technology, which frequently leads to the development of scaffolds with poor mechanical properties and insufficient control of its morphology.

Since 2005, we have developed a new concept based on the development of thermoplastic chitosan polymers (30-33). This was achieved by melt-blending chitosan with different aliphatic polyesters, poly(caprolactone) (PCL), poly(butylene succinate) (PBS), poly(butylene terephthalate adipate) (PBTA), and poly(butylene succinate adipate) (PBSA). By doing this, we conjugated the favourable biological properties of chitosan with the predictable degradative behavior of the aliphatic polyesters. Further information on the physical and chemical properties of these materials can be found in the reports of Correlo *et al.* (30-33).

The present study reports on the morphology, mechanical properties, cytocompatibility, cell proliferation and osteogenic differentiation of a mesenchymal stem cell line - BMC9 - on novel compression molding/salt leaching scaffolds based on blends of chitosan with PCL, PBS, PBTA and PBSA. Results have showed that the developed scaffolds had the adequate mechanical properties. Furthermore, they disclosed a non-cytotoxic behavior and simultaneously supported the growth and osteogenic differentiation of mouse mesenchymal stem cells within its structure.

2. MATERIALS AND METHODS

2.1. Scaffolds production and processing

Chitosan was melt blended with several biodegradable polyesters for the first time by our group (31) a twin screw extruder with the purpose of producing scaffolds for tissue engineering applications. For the development of this work, the polyesters compounded with chitosan (ch) were PBS, PCL and PBTA. In all of these blends there was a rate of 50% (wt%) chitosan with 50% (wt%) polyester.

The methodology used for the scaffolds production was melt based compression molding followed by salt leaching. The details of the processing conditions are described elsewhere (32). Briefly, the developed blends were grained and the powder mixed with salt particles with sizes between 250 and 500 μm. The chitosan based blends mixed with salt were loaded into a mold that was further heated and compression molded into discs. The salt content was 60% by weight. The discs were cut into 5x5x5 mm^3 cubes. These cubes were then immersed in distilled water to leach out the salt, dried, sterilized by ethylene oxide and used for cell culture studies.

2.2. Scaffolds characterization

The cross-section of all the developed scaffolds was analyzed using a Leica-Cambridge S-360 Scanning Electron Microscope (SEM) for preliminary assessment on the scaffolds morphology. All the samples were sputter-coated with gold prior to SEM observations.

To investigate the internal 3D structure of the scaffolds, Micro-Computed Tomography equipment (SkyScan, Belgium) was used as a non-destructive technique. Four scaffolds of each condition were scanned in high resolution mode of 8.7 μm x/y/z and an exposure time of 1792 ms. The energy of the scanner used was 63 keV with 157 μA current. μCT scans followed by 3D reconstruction of serial image sections allowed to analyze 3D microarchitecture of the scaffolds, pore morphology as well as the determination of the porosity.

Uniaxial compression tests were performed on a square cross-section specimen of scaffolds using a Universal tensile testing machine (Instron 4505 Universal Machine). A crosshead speed of 2 mm/min was used. The values reported were the average of at least five specimens. The compressive modulus was determined by selecting the linear region of the stress-strain graph.

2.3. Cell culture

A fibroblast cell line of rat lung - L929 -, acquired from the european collection of cell cultures (ECACC), was used for cytotoxicity tests. The cells were grown as monolayers in Dulbecco's modified Eagle's medium (DMEM; Sigma, St. Louis, MO) supplemented with 10% foetal bovine serum (FBS; Biochrom, Berlin, Germany) and 1% of antibiotic-antimycotic

mixture (10000 U/ml penicillin G sodium; 10000 U/ml streptomycin sulphate; 25 µg/ml amphotericin B) (Gibco, Invitrogen, USA). Trypsin/EDTA (0.25% w/v trypsin/0.02% EDTA, Sigma) was used to detach the cells from the culture flasks before the experiments were conducted.

2.3.1. Cell viability assay - MTS test

The ratio of material weight to extract fluid was constant and equal to 0.25 g/ml. Latex rubber and standard culture medium were used as positive and negative controls, respectively. Latex rubber is known to have a strong cytotoxic effect leading to extensive cell death. For the positive control the ratio of material outer surface to extraction fluid was 2.5 cm^2/ml. Test material (*n*=6) and positive control were extracted for 24 h at 37ºC, using complete culture medium as extraction fluid. Before the tests, culture medium was removed and an identical volume (200 µl) of extraction fluid was added to each well.

Cells were seeded in 96 well plates (*n*=6) at a density of $1.8x10^4$ cells/well and incubated for 24 h at 37ºC, in a humidified atmosphere with 5% CO_2. A kit (CellTiter 96 One solution Cell Proliferation Assay kit - Promega, Madison, WI) was used and it is based on the reduction of the substrate, 3-(4,5-dimethylthiazol-2-yl)-5(3-carboxymethoxyphenyl)-2(4-sulfofenyl)-2H-tetrazolium (MTS), into a brown formazan product by dehydrogenase enzymes active in the viable cells. After 72 h, the extraction fluid was removed and 200 µl of a serum-free culture medium without phenol red and MTS, in a proportion of 5:1, was added to each well. Cells were then incubated for 3 h at 37ºC in a humidified atmosphere containing 5% CO_2. After this time, optical density (O.D.) was measured with a plate reader (Bio-tek, model Synergy HTi, USA) at 490 nm. The O.D. values obtained were standardized taking into account the values for the negative control.

2.4. Cell culture studies

2.4.1. Cell seeding and culture

A mouse mesenchymal stem cell line (BMC9) was used. This conditionally immortalized clone was shown to exhibit four mesenchymal cell phenotypes: chondrocyte, adipocyte, stromal (support osteoclast formation), and osteoblast (34). The cells were grown as monolayer cultures in a culture medium consisting of DMEM medium, 10% FBS and 1% antibiotic/antimycotic mixture. When the adequate cell number was obtained, cells at

passage 10 were trypsinized, centrifuged and ressuspended in cell culture medium. Cells were seeded at a density of $5x10^5$cells/scaffold under static conditions, using for this purpose aliquots of 10 µL loaded on the top of scaffolds. Two hours after seeding, 1 ml of culture medium was added to each well. The cell-seeded scaffolds were maintained in a humidified atmosphere at 37ºC, containing 5% CO_2, under osteogenic differentiation inducing medium, during 21 days. The culture medium consisted of DMEM without phenol red, dexamethasone 10^{-8} M (Sigma), ascorbic acid 50 µg/ml (Sigma) and ß-glycerophosphate 10 mM (Sigma), and was changed every 3 to 4 days until the end of the experiment.

2.4.2. Cellular viability assay - MTS test

Cell viability was assessed after 3 h, 7, 14 and 21 days, by using the MTS test. The cell-seeded scaffolds (*n*=6) were rinsed in 0.15M phosphate buffered saline (Sigma) and immersed in a mixture consisting of serum-free cell culture medium and MTS reagent at 5:1 ratio and incubated for 3 h at 37ºC in a humidified atmosphere containing 5% CO_2. After this, 200 Ml (*n*=6) were transferred to 96 well plates and the optical density (O.D.) determined at 490 nm.

2.4.3. Cell adhesion and morphology by SEM

Cell adhesion, morphology and average distribution were observed by SEM. The cell-seeded scaffolds were washed in 0.15 M phosphate buffered saline and fixed in 2.5% glutaraldehyde in phosphate buffered saline.

After rinsing 3 times in phosphate buffered saline, the constructs were dehydrated using a series of graded ethyl alcohols (30, 50, 70, 90, 100% ethanol) for 15 minutes each, twice. Then, the samples were subjected to 2 changes for 15 minutes each with 100% hexamethyldisilazane (HDMS; Electron Microscopy Sciences, Washington, USA). Finally HDMS was removed and let to air dry for 2h. Afterwards, the constructs were sputter coated with gold (JEOL JFC-1100) and analyzed with a Leica Cambridge S360 scanning electron microscope.

2.4.4. Cell adhesion and cell viability by calcein AM staining through confocal laser microscopy

Cells were incubated with calcein AM (Molecular Probes, Oregan, USA). Once inside the cells, this compound is hydrolyzed by endogenous esterase into the highly negatively charged green fluorescent calcein, which is retained in the cytoplasm. The cell-seeded scaffolds were sectioned and cell adhesion and viability was observed in the inner regions of the scaffolds using an Olympus FluoView FV1000 confocal laser microscope.

2.4.5. Histology

Eight-micron-thick sections from the 3 weeks culture of the constructs were cut with a cryomicrotome (CM 1900; Leica, Bensheim, Germany) and mounted on poly-L-lysine (Sigma) coated slides. Slides were stained with H&E and observed under optical microscope.

2.4.6. Alkaline phosphatase quantification

A description of the assay can be found elsewhere (35). Briefly, the level of alkaline phosphatase (ALP) activity from the constructs (n=3) was quantified by the specific conversion of p-nitrophenyl phosphate (pNPP) (Sigma) into p-nitrophenol (pNP). The cell-seeded scaffolds were allowed to thaw at room temperature and then were sonicated for roughly 15 min. The enzyme reaction was set up by mixing 100 ml of the sample with 300 ml of substrate buffer containing 1 M diethanolamine HCl (pH 9.8) and 2 mg/ml of pNPP. The solution was incubated at 37ºC for 1 h and the reaction was then stopped by a solution containing 2 M NaOH and 0.2 mM EDTA in distilled water. The optical density was determined at 405 nm. A standard curve was made using pNP values ranging from 0 to 20 µmol/ml. The results are expressed in µmol of pNP produced/ml/h.

2.4.7. Mineralization content by EDS

The constructs were processed as described previously for SEM. The samples were sputter coated with carbon (JEOL JFC-1100), in order to verify the presence of calcium and phosphate elements with a Leica Cambridge S360 electronic microscope.

2.5. Statistical analysis

Statistical evaluation was performed using 2 tailed paired t-student tests, to assess the statistical differences between each two groups of different time points. Statistical significance was defined as $p<0.05$ for a 95% confidence interval.

3. RESULTS

3.1. Scaffolds characterization

The mechanical properties (compressive modulus) of the developed scaffolds are presented in table I. The compressive modulus of the thermally produced scaffolds is in the range of the trabecular bone modulus (36).

Table I. Compressive modulus and porosity of the 50% (wt) chitosan based scaffolds produced by melt based compression molding with salt leaching (60% salt and granulometry of 250-500 µm).

Composition	Compressive Modulus (MPa)	Porosity (%)
50Ch-50PBS	87.4±21.6	59.9 ± 6.5
50Ch-50PCL	53.1±23.7	63.9 ± 0.7
50C/50PBTA	21.8±7.8	59.4 ± 3.8

Scaffolds with higher and lower compressive modulus are the ones obtained using the blends Ch-PBS and Ch-PBTA, respectively. These results are in accordance with previous results obtained with compact injection molded samples (31).

Representative µCT images of the entire scaffolds (300 slices) are shown in figure 1. Three dimensional reconstructions of the bulk of the scaffolds were also performed. No considerable differences in terms of morphology were observed between the more interior parts (bulk) of the scaffolds and the most exterior ones. Two dimensional X-ray µCT images, with a region of interest of 4.5x4.5 mm, were also analyzed (figure not shown).

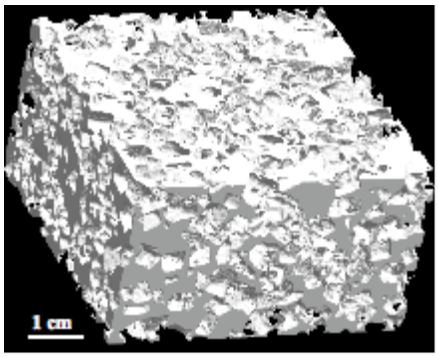

Figure 1. Representative 3D μCT image of the scaffolds obtained using chitosan based blends and NaCl particles with size 250-500 μm.

No significant morphological differences were observed between scaffolds produced using different chitosan based blends. Pores resulting from the leaching of the NaCl particles mimic the cubic shape of the porogen used. The scaffolds have a very narrow distribution of pores dimensions coincident with the NaCl particles size. Two dimensional binary images were analyzed for total porosity calculations. The porosity values presented in table I are the average of the individual porosity of 300 slices per scaffold. For each processing condition, 4 scaffolds were analyzed. As expected, porosity depended on the amount of porogen used. In all the cases the porosity was very similar to the amount of salt used.

3.2. Mechanical properties

The nominal stress – nominal strain curves for the developed chitosan-polyester scaffolds are shown in figure 2. The compressive modulus was calculated as the slope of the linear most region of the stress-strain curve prior to the yield point and their value is shown in table I. As expected, the shape of the stress-strain curve, and consequently the modulus, varies with the type of polyester. Scaffolds with higher and lower compressive modulus are the ones obtained using the blends Ch-PBS and Ch-PBTA, respectively. These results are in accordance with previous results obtained with compact injection molded samples (31). Nevertheless, the compressive modulus of the thermally produced scaffolds is in the range of the trabecular bone modulus (36).

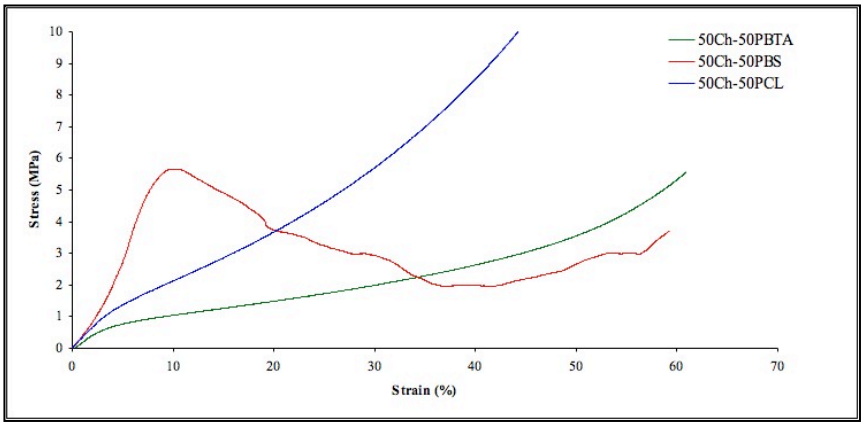

Figure 2. Stress-strain plot of the chitosan-polyester scaffolds.

3.3. *In vitro* cytotoxicity tests

In the MTS test (Figure 3), L929 cells produced large amounts of the brown formazan product after incubation with the tested extract. This fact shows that cells had similar metabolic activities (about 80%) to those obtained by the negative control and were able to incorporate and metabolize MTS and hence, showed their viability. Therefore, the leachables released from the tested scaffolds could be considered as non-cytotoxic.

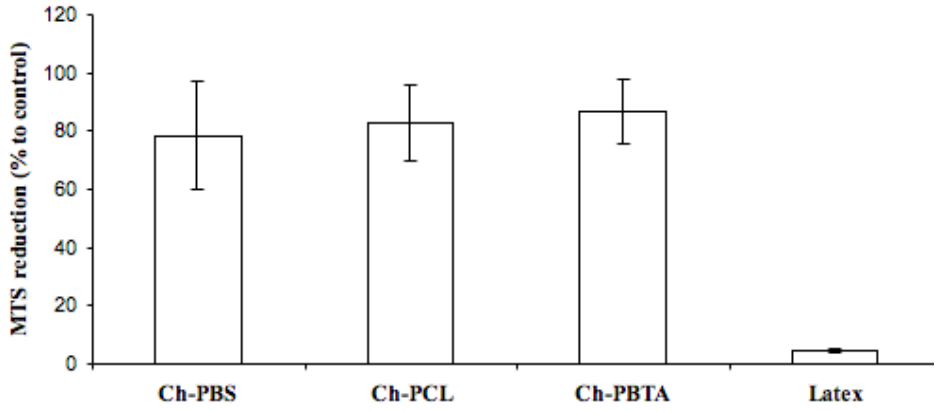

Figure 3. Cytotoxicity results of the 72 h extracts of the Ch-PBS, Ch-PCL and Ch-PBTA scaffolds. Results are based on optical density measurements, at O.D. of 490 nm and normalized for the negative control (n=6; ±sd; p<0.05).

3.4. Cell adhesion and morphology by SEM

Regarding the present experiment, SEM observations allowed to determine that mouse MSCs were able to adhere to the surface of the chitosan-polyester based scaffolds, where a monolayer of cells could be observed after 1 week in culture (Figures 4a, 4b, 4c). Furthermore it should be highlighted that there was no pore occlusion by the cells (Figure 4d), which demonstrated the adequacy of the pore size range within the scaffolds (250-500 μm).

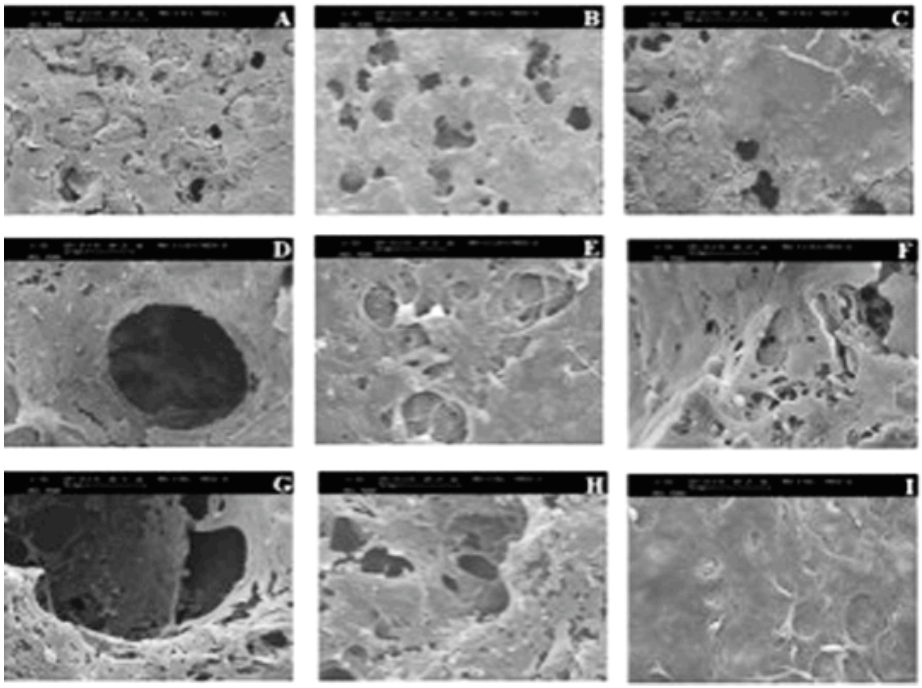

Figure 4. SEM micrographs of BMC9 cells adhesion and proliferation, under osteogenic stimulation, on the 50% wt Ch-PBS scaffolds after a) 1 b) 2 and c) 3 weeks of culture; on the 50% wt Ch-PCL scaffolds after d) 1 e) 2 and f) 3 weeks of culture and on the 50% wt Ch-PCL scaffolds after g) 1 h) 2 and i) 3 weeks of culture.

By week 2 it was possible to observe a higher degree of colonization, denoting a multilayer of cells and the onset of elaboration of extracellular matrix (ECM), at the surface of all the scaffolds obtained from different chitosan based blends (Figures 4e, 4f). A closer observation demonstrated that in the blend composed by chitosan and PBS there was a higher degree of proliferation of the cells including the ones in the inner regions of the scaffolds (Figure 4g). Furthermore, by observing the inside scaffold's inner regions (Figure 5)

it was shown that the cells were also capable of colonizing these areas, without occluding the pores of the scaffolds structure.

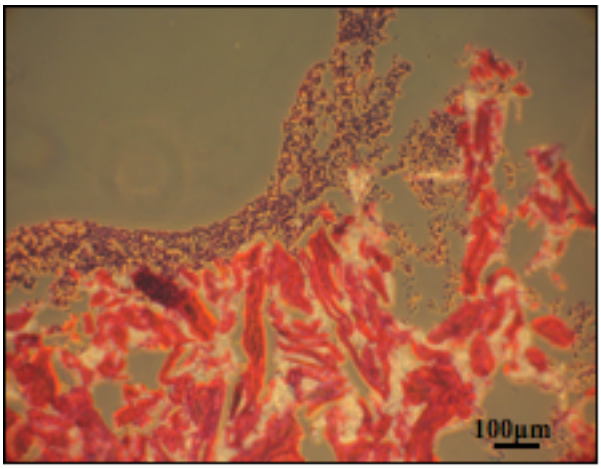

Figure 5. Light micrograph illustrating a representative section of the colonization of the MSCs onto the chitosan-PBS scaffolds for 21 days, after H&E staining. Original magnification 100X.

After 3 weeks, further development of the cell number and surface density were observed, indicating that the BMC9 cells massively adhered and proliferated within all the chitosan based scaffolds, also showing a calcified ECM elaboration (Figure 9).

The scaffolds composed by Ch-PBS showed cell adhesion and colonization of the surface and inner regions (Figure 5), and simultaneously evidencing the elaboration of a mineralized extracellular matrix, shown by the presence of Ca and P, by EDS analysis (Figure 9a).

3.5. Cell viability by MTS assay/ calcein AM staining

Tracking the survival/activity of the cells seeded on the scaffolds from the time of seeding until implantation might be helpful for the optimization on the development of bone tissue engineered constructs (37).

Results showed that the tested MSCs were able to reduce MTS, showing increasing metabolic rates with increasing time of culture (Figure 6), and denoting a high viability and proliferation profile.

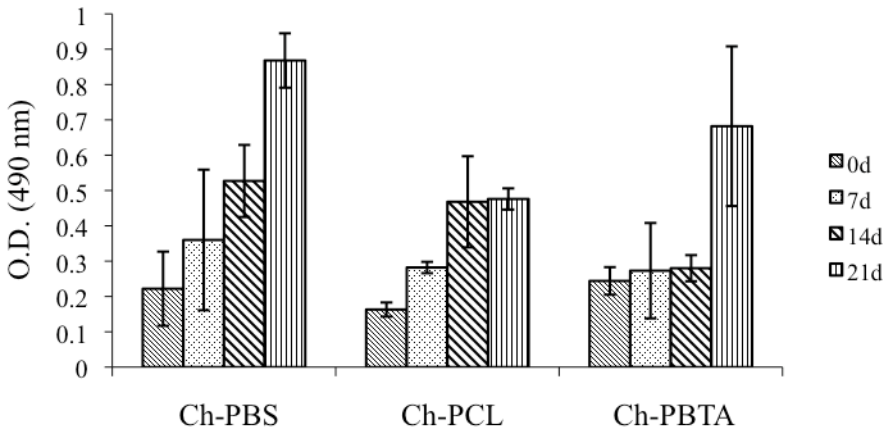

Figure 6. Viability of the BMC9 cells seeded and cultured onto the chitosan-PBS (Ch-PBS), chitosan-PCL (Ch-PCL) and chitosan-PBTA (Ch-PBTA) scaffolds following 3 hours after cell seeding, at 1, 2 and 3 weeks, by MTS assay (n=6; ±sd; p<0.05).

Cell viability assay with calcein AM staining (Figures 7a, 7b and 7c) confirmed the SEM results, where BMC9 cells were metabolically active in the scaffolds after 3 weeks in static culture. Moreover, with these results it can be established a time dependent cell proliferation, as it is notorious the presence of a higher number of cells for the latest time period.

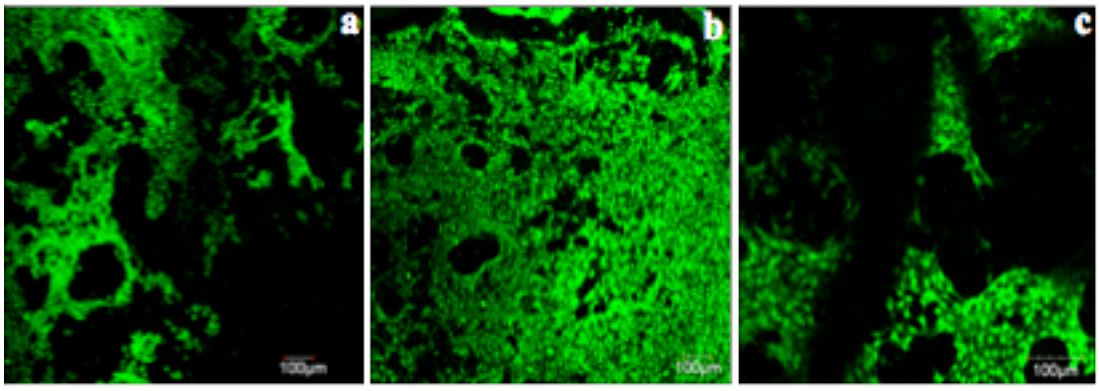

Figure 7. Confocal micrographs showing the cell adhesion and viability upon the scaffolds of 50% wt Chitosan-PBS scaffolds a); 50% wt Chitosan-PCL scaffolds b) and 50% wt Chitosan-PBTA scaffolds c), after 3 weeks of culture.

3.6. Alkaline phosphatase quantification

For all tested blends, ALP activity (Figure 8) increased until the second week, reflecting probably the early osteogenic differentiation stage of the MSCs. After this period, ALP activity decreased, presumably due to the onset of the mineralization process (36), denoting in this sense a positive indication of the transient character of the differentiation of the cells into the osteogenic lineage. Once more, the best results were evidenced by the scaffolds produced from the Ch-PBS blend, which showed the higher values of the ALP activity.

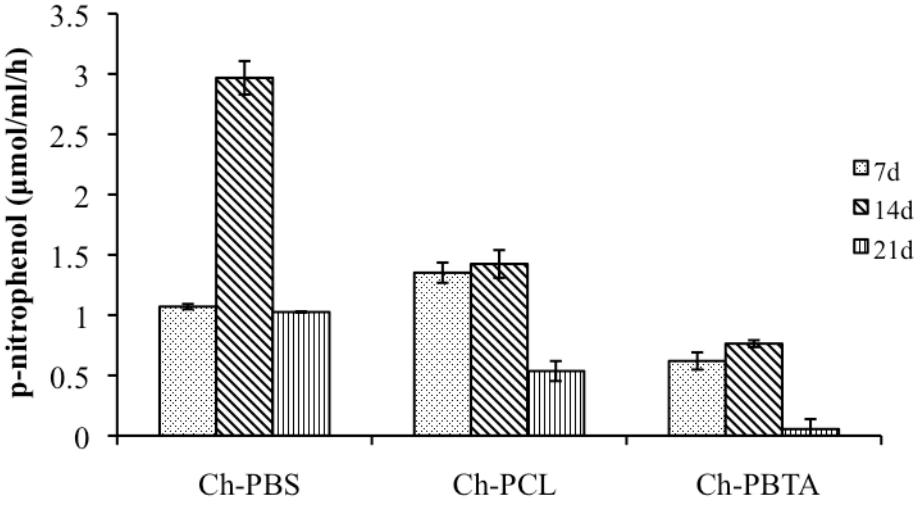

Figure 8. Alkaline phosphatase activity assay: supernatants were weekly collected and frozen. After 3 weeks, supernatants were thawed. The results are shown in p-nitrophenol (µmol/ml/h) as a function of days. On day 7, cells were stimulated with 10 mM glycerophosphate (Sigma), 50 mM ascorbic acid (Sigma) and 10^{-8} M dexamethasone (Sigma). The ALP levels increased, reaching the highest values after 2 weeks in culture (n=6; ±sd; p<0.05).

3.7. Mineralization content by EDS analysis

The EDS analysis of the surface of the seeded and cultured scaffolds with mouse MSCs under osteogenic conditions for 21 days (Figure 9) detected the presence of Ca and P elements on the surface, being therefore, a clear indication of the formation of a mineralized ECM.

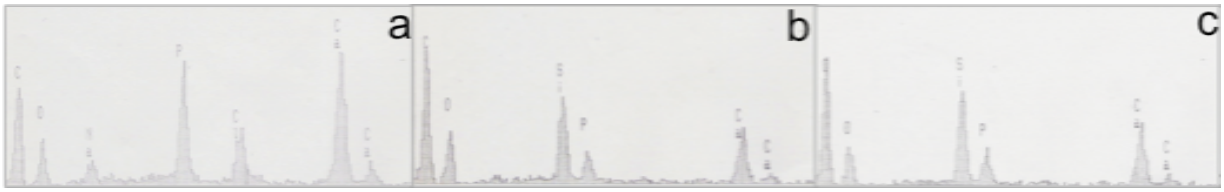

Figure 9. Energy dispersive spectra showed the presence of calcium and phosphorous at the surface of the seeded chitosan-PBS a), chitosan-PCL b) and chitosan-PBTA c) scaffolds, after 3 weeks under osteogenic culture conditions.

4. DISCUSSION

In the last few years, natural based polymers have been presented as biomaterials for tissue engineered scaffolding. Among these, chitosan has emerged as one of the most promising, namely by its biodegradability, biocompatibility and its resemblance to GAGs (23).

In this study we report the biological performance, in terms of cell adhesion, proliferation and differentiation of mouse MSCs seeded and cultured onto the newly developed chitosan based scaffolds.

The melt based approach used to produce the scaffolds allowed us to obtain 3D porous structures without the use of organic solvents that could remain in the structure and damage the transplanted cells or the surrounding tissues (after transplantation). The mechanical properties, in terms of compressive modulus, were in the range of those for trabecular bone properties (36).

The developed scaffolds revealed to be non-cytotoxic to fibroblast cells, since the leachables released during the extraction period did not affect cell viability as well as did not inflict changes in cell morphology.

Cells were able to colonize the scaffolds structure up to periods of 3 weeks. The cell proliferation was gradual and continuously increasing over time of culture, being more evident on the ch-PBS scaffolds. The differences observed for the different blends are probably related with the different surface chemistry and mechanical properties of the 3D scaffolds with the best results being noticed for the scaffolds produced from ch-PBS blend.

It is known that if cells are undergoing osteogenic differentiation, ALP is considered to be one of the early markers (38). Although not being specific for the osteoblast lineage, ALP

is used typically to illustrate the early differentiation into a bone related phenotype, which is noticed by the increase of the enzyme activity until the second week.

The presence of Ca and P elements on the surface of the cell-seeded scaffolds revealed the presence of a mineralized ECM. This fact is in agreement with the data obtained for alkaline phosphatase experiments, showing that cells had undergone an osteogenic differentiation and were elaborating mineralized ECM.

5. CONCLUSIONS

With the present study it was possible to show that the scaffolds based on 50:50 (wt%) blends of chitosan and synthetic polyesters (PBS, PCL and PBTA) present a range of properties that are considered to be adequate for bone tissue engineering applications.

Scaffolds produced by compression molding followed by salt leaching were shown to be non-cytotoxic and clearly cytocompatible. The results of the direct contact assays under osteogenic conditions revealed that the three types of chitosan-based scaffolds selected for this study promoted the attachment and proliferation of mouse mesenchymal stem cells. Furthermore, they also presented high indexes of alkaline phosphatase activity and the production of a calcified ECM, which is due to the differentiation towards the osteogenic pathway. From the three tested blends, the chitosan-PBS blend showed the best results, namely in terms of cell adhesion and proliferation. Nevertheless the other blends also presented adequate properties for bone tissue engineering.

Due to the good combination of properties and excellent biological performance, it is strongly believed that the scaffolds herein proposed will be a valid alternative to the currently used materials when considering bone regeneration/tissue engineering applications.

ACKNOWLEDGEMENTS

Ana Costa-Pinto was supported by scholarship SFRH/24735/2005 from the Portuguese research council “Fundação para a Ciência e a Tecnologia” (FCT).

This work was partially supported by the EU Integrated Project GENOSTEM (Adult Mesenchymal Stem Cells Engineering for connective tissue disorders: from the bench to the bed side), and the European Network of Excelence EXPERTISSUES.

REFERENCES

1. Langer R, Vacanti J. Tissue engineering Science. 1993;260(5110):920-6.
2. Yang S, Leong K-F, Du Z, Chua C-K. The Design of Scaffolds for Use in Tissue Engineering. Part I. Traditional Factors. Tissue Engineering. 2001;7(6):679-89.
3. Salgado AJ, Gomes ME, Reis RL. Tissue Engineering of Mineralized Tissues: The Essential Elements. In: Reis RL, Weiner S, editors. Learning from Nature How to Design New Implantable Biomaterialsis: From Biomineralization Fundamentals to Biomimetic Materials and Processing Routes: Springer Netherlands; 2005. p. 205-22.
4. Albrektsson T, Johansson C. Osteoinduction, osteoconduction and osseointegration. Eur Spine J. 2001;10:96-101.
5. Lind M, Bünger C. Factors stimulating bone formation. European Spine Journal. 2001;10(0):S102-S9.
6. Kneser U, Schaefer DJ, Munder B, Klemt C, Andree C, Stark GB. Tissue engineering of bone. Minimally Invasive Therapy & Allied Technologies. 2002;11(3):107-16.
7. Salgado A J. Bone tissue engineering: state of the art and future trends. Macromolecular Bioscience. 2004;4:743-5.
8. Mano JoF, Sousa RA, Boesel LF, Neves NM, Reis RL. Bioinert, biodegradable and injectable polymeric matrix composites for hard tissue replacement: state of the art and recent developments. Composites Science and Technology. 2004;64(6):789-817.
9. Sikavitsas V, van den Dolder, J, Bancroft,GN, Jansen,JA, , Mikos A. Influence of the in vitro culture period on the in vivo performance of cell/titanium bone tissue-engineered constructs using a rat cranial critical size defect model. J Biomed Mater Res. 2003;67A:944-51.
10. Holtorf HL, Jansen JA, Mikos AG. Ectopic bone formation in rat marrow stromal cell/titanium fiber mesh scaffold constructs: effect of initial cell phenotype. Biomaterials. 2005;26(31):6208-16.
11. Meretoja VV, Ruijter AED, Peltola TO, Jansen JA, N√§rhi TO. Osteoblast Differentiation with Titania and Titania‚ÄìSilica-Coated Titanium Fiber Meshes. Tissue Engineering. 2005;11(9-10):1489-97.
12. Petite H. Tissue-engineered bone regeneration. Nature Biotechnology. 2000;18:959-63.
13. Le Nihouannen D, Guehennec LL, Rouillon T, Pilet P, Bilban M, Layrolle P, et al. Micro-architecture of calcium phosphate granules and fibrin glue composites for bone tissue engineering. Biomaterials. 2006;27(13):2716-22.
14. Okamoto M, Dohi Y, Ohgushi H, Shimaoka H, Ikeuchi M, Matsushima A, et al. Influence of the porosity of hydroxyapatite ceramics on in vitro and in vivo bone formation by cultured rat bone marrow stromal cells. Journal of Materials Science: Materials in Medicine. 2006;17(4):327-36.
15. Ishaug SL, Crane GM, Miller MJ, Yasko AW, Yaszemski MJ, Mikos AG. Bone formation by three-dimensional stromal osteoblast culture in biodegradable polymer scaffolds. Journal of Biomedical Materials Research. 1997;36(1):17-28.
16. Pavlov MP, Mano JF, Neves NM, Reis RL. Fibers and 3D Mesh Scaffolds from Biodegradable Starch-Based Blends: Production and Characterization. Macromolecular Bioscience. 2004;4(8):776-84.
17. Mendes SC, Bezemer J, Claase MB, Grijpma DW, Bellia G, f. Degli-Innocenti, et al. evaluation of two biodegradable polymeric systems as substrates for bone tissue Engineering. Tissue Engineering. 2002;9:94-101.
18. Schantz JT, Hutmacher DW, Chim H, Ng KW, Lim TC, Teoh SH. Induction of Ectopic Bone Formation by Using Human Periosteal Cells in Combination With a Novel Scaffold Technology. Cell Transplantation. 2002;11:125-38.

19. Behravesh E, Yasko AW, Engel PS, Mikos AG. Synthetic Biodegradable Polymers for Orthopaedic Applications. Clinical Orthopaedics and Related Research. 1999;367:S118-S29.
20. Hutmacher DW. Scaffolds in tissue engineering bone and cartilage. Biomaterials. 2000;21(24):2529-43.
21. Gomes ME, Ribeiro AS, Malafaya PB, Reis RL, Cunha AM. A new approach based on injection molding to produce biodegradable starch-based polymeric scaffolds: morphology, mechanical and degradation behaviour. Biomaterials. 2001;22(9):883-9.
22. Marques AP, Reis RL, Hunt JA. Cytokine secretion from mononuclear cells cultured in vitro with starch-based polymers and poly-L-lactide. Journal of Biomedical Materials Research Part A. 2004;71A(3):419-29.
23. Di Martino A, Sittinger M, Risbud MV. Chitosan: a versatile biopolymer for orthopaedic tissue-engineering. Biomaterials. 2005;26(30):5983-90.
24. Ding Z, Chen J, Gao S, Chang J, Zhang J, Kang ET. Immobilization of chitosan onto poly--lactic acid film surface by plasma graft polymerization to control the morphology of fibroblast and liver cells. Biomaterials. 2004;25(6):1059-67.
25. Malafaya PB, Pedro AJ, Peterbauer A, Gabriel C, Redl H, Reis RL. Chitosan particles agglomerated scaffolds for cartilage and osteochondral tissue engineering approaches with adipose tissue derived stem cells. Journal of Materials Science: Materials in Medicine. 2005 ;16:1077-85.
26. Oliveira JM, Rodrigues MT, Silva SS, Malafaya PB, Gomes ME, Viegas CA, et al. Novel hydroxyapatite/chitosan bilayered scaffold for osteochondral tissue-engineering applications: Scaffold design and its performance when seeded with goat bone marrow stromal cells. Biomaterials. 2006;27(36):6123-37.
27. Seol YJ, Lee JY, Park YJ, Lee YM, Young-Ku, Rhyu IC, et al. Chitosan sponges as tissue engineering scaffolds for bone formation. Biotechnology Letters. 2004;26(13):1037-41.
28. Yin YJ, Luo XY, Cui JF, Wang CY, Guo XM, Yao KD. A Study on Biomineralization Behavior of N-Methylene Phosphochitosan Scaffolds. Macromolecular Bioscience. 2004;4(10):971-7.
29. Zhang Y, Ni M, Zhang M, Ratner B. Calcium phosphate-chitosan composite scaffolds for bone tissue engineering. Tissue Eng. 2003 Apr;9(2):337-45.
30. Correlo VM, Boesel, L.F., Bhattacharya, M., Mano,J.F., Neves, N.M., Reis, R.L.,. Hydroxyapatite reinforced chitosan and polyester blends for biomedical applications. Macromolecular Materials and Engineering 2005;290(12):1157-65.
31. Correlo VM, Boesel LF, Bhattacharya M, Mano JF, Neves NM, Reis RL. Properties of melt processed chitosan and aliphatic polyester blends. Materials Science and Engineering: A. 2005;403(1-2):57.
32. Correlo VM, Boesel LF, Pinho E, Costa-Pinto AR, Alves da Silva ML, Bhattacharya M, et al. Melt-based compression-molded scaffolds from chitosan-polyester blends and composites: Morphology and mechanical properties. J Biomed Mater Res A. 2009;91(2):489-504.
33. Correlo VM, Pinho ED, Pashkuleva I, Bhattacharya M, Neves NM, Reis RL. Water Absorption and Degradation Characteristics of Chitosan-Based Polyesters and Hydroxyapatite Composites. Macromolecular Bioscience. 2007;7(3):354-63.
34. Dennis JE, Merriam A, Awadallah A, Yoo JU, Johnstone B, AI. C. A quadripotential mesenchymal progenitor cell isolated from the marrow of an adult mouse. J Bone Miner Res. 1999;14(5):700-9.
35. Maniatopoulos C, Sodek J, AH. M. Bone formation in vitro by stromal cells obtained from bone marrow of young adult rats. cell Tissue Res. 1988;254(2):317-30.
36. Aubin J, Triffitt J. Mesenchymal Stem Cells and Osteoblast Differentiation. In: Bilezikian J, Raisz L, Rodan G, editors. Principles of Bone Biology. 1 ed. San Diego: Academic Press; 1996.

37. Wilson C, Dhert W, Van Blitterswijk C, Verbout A, Bruijn J. Evaluating 3D bone tissue enginered constructs with different seeding densities using the alamar blue assay and the effect on in vivo bone formation. Journal of Materials Science: Materials in Medicine. 2002;13:1265-9.
38. Lian JB, Stein GS. Concepts of Osteoblast Growth and Differentiation: Basis for Modulation of Bone Cell Development and Tissue Formation. Critical Reviews in Oral Biology & Medicine. 1992;3(3):269-305.

CHAPTER IV

Influence of chitosan content in the scaffold composition over the *in vitro* osteogenic differentiation of hBMSCs and *in vivo* tissue response

This chapter is based on the following publication: Costa-Pinto AR, Vargel I, Tuzlakoglu K, Battacharya M, Correlo VM, Sol PC, Piskin E, Reis RL, Neves NM. "Influence of chitosan content in the scaffold composition over the *in vitro* osteogenic differentiation of hBMSCs and *in vivo* tissue response". 2010; Submitted.

CHAPTER IV

Influence of chitosan content in the scaffold composition over the *in vitro* osteogenic differentiation of hBMSCs and *in vivo* tissue response

ABSTRACT

Chitosan has been showing promising results for bone tissue engineering applications, namely for modulating cell behaviour *in vitro* and promoting bone regeneration *in vivo*. Previous results from our group evidenced that chitosan poly(butylene succinate) melt based scaffolds showed remarkable biological performance. This fact brought up the question of the role of chitosan in this specific blend. For this purpose scaffolds with 50% of chitosan (Ch) and 50% poly(butylene succinate) (PBS), 25% of Ch and 75% of PBS and 100% PBS were produced by compression molding and salt leaching. These scaffolds were evaluated *in vitro* with human bone marrow mesenchymal stem cells (hBMSCs) and *in vivo* by implanting them in different anatomical regions (cranial defect model, iliac submuscular and auricular areas) in Wistar rats. Higher percentages of chitosan favoured better biological performance, when compared to PBS scaffolds alone. Cells showed enhanced viability over time, evidencing superior cell adhesion and proliferation. Moreover, alkaline phosphatase (ALP) activity and gene expression showed that cells were undergoing osteogenic differentiation in chitosan containing scaffolds. For all *in vitro* studies, PBS scaffolds presented inferior biological performance when compared to chitosan based scaffolds.

Scaffolds displayed a normal and mild inflammatory response after one month implantation and integrated well with the surrounding tissues. Connective tissue cells colonized the scaffolds structures. Tissue responses were milder in auricular and calvaria implantations when compared to the submuscular. Chitosan scaffolds evidenced better results, with enhanced cell penetration, without cell necrosis and large number of blood vessels in the proximity and inside the scaffolds.

The addition of chitosan positively influenced the osteogenic differentiation of hBMSCs, and also showed enhanced tissue biocompatibility, as compared to PBS alone. Considering the results herein reported it is reasonable to state that chitosan-PBS scaffolds demonstrate appropriate properties both *in vitro* and *in vivo* to be used in bone tissue engineering applications.

1. INTRODUCTION

A new field known as Tissue Engineering has recently emerged, having potential to overcome the increasing number of clinical needs for bone regeneration mainly due to the aging of population. This multidisciplinary approach involves the basic principles of engineering and life sciences, in order to develop biological substitutes aimed at restore, maintain or improve a tissue function or a whole organ (1). Firstly, a tissue construct is created, using cells and scaffolds. This scaffold is further matured *in vitro*, and then transplanted and integrated into the host defect site (2). Frequently, the cells are seeded and cultured onto a natural or synthetic biodegradable scaffold. The ideal scaffold must fulfill a number of requirements that include being biocompatible with specific biodegradability kinetics and should possess adequate porosity, pore size and mechanical properties compatible with the loads to which will be subjected (3).

Among the various natural polymers available, chitosan has emerged as a candidate biomaterial to produce biodegradable scaffolds for tissue engineering applications. The first report about the partially deacetylated form of chitin (chitosan) dates back from the 19^{th} century (4). Chitosan presents biological properties that makes it appropriated to develop scaffolds for tissue engineering, including its biodegradability (5, 6), antibacterial activity (7, 8), haemostatic and wound healing properties (9, 10), biocompatibility (11, 12) and easy accessibility. It is a linear polysaccharide composed of glucosamine and N-acetyl glucosamine with a β (1-4) link (13). Chitosan has a cationic character, which allows electrostatic interactions with anionic glycosaminoglycans (GAGs) and proteoglycans. Moreover, the chemical structure of chitosan has similarities with the structure of GAGs (14). These molecules play an important role in the modulation of cell function, morphology and differentiation.(13).

Interactions between cells and extracellular matrix (ECM) provide essential cues used by the cells to influence and adapt its intra and extracellular environment (15). Chitosan by itself or in combination with other biomaterials has been reported to have a positive effect over the cell behavior. Polystyrene coated with chitosan solution has shown cytocompatibility as a substrate for growth of human osteoblasts and chondrocytes (16). Poly-(*L*-lactide acid) (PLLA) films modified with chitosan evidenced improved cell adhesion, proliferation and biosynthetic activity, using articular chondrocytes (17). Commercially available chitosan supports the initial attachment and spreading of osteoblasts preferentially over fibroblasts (18). MC3T3-E1 osteoblastic-like cells proliferated and evidenced increased alkaline phosphatase activity, as well as up-regulation of osteogenic gene expression, in composite

chitosan/poly(lactic acid-glycolic acid) scaffolds as compared to poly(lactic acid-glycolic acid) scaffolds (19). In fact, in a recent study by Wu and co-workers, different proportions of poly(caprolactone)/chitosan scaffolds evidenced better results for the blends with higher chitosan content, using rat osteoblasts (20). Moreover, nanofibrous scaffolds containing chitosan revealed that stem cells adhere, proliferate and express phenotypic markers of osteogenic differentiation in a superior level than synthetic nanofibrous scaffolds without chitosan (21, 22). It has been described in the literature that combined chitosan–collagen matrices, with higher proportion of chitosan promoted osteoblastic differentiation of hBMSCs and improved the mechanical and physical properties of the sponges (23). Previous studies from our group, using chitosan particle aggregated scaffolds, evidenced good results favoring osteogenic and chondrogenic differentiation of adipose derived stem cells (24). Another work from our group reported that discs composed of chitosan-PBS and other biodegradable polyesters, obtained by injection molding, showed that chitosan had a positive effect over osteoblast-like cells activity *in vitro* (25).

Chitosan is difficult to be processed by methods that do not require the use of solvents. Accordingly, there is the need to combine it with other polymers to improve its processability. By this combination, the mechanical properties of the resulting biomaterial can also be improved to become adequate for load bearing tissues, such as bone (26). Previously, we proposed a methodology to process chitosan with aliphatic polyesters, facilitating its processing by melt and avoiding the need of solvents (27, 28). This processing route involves melt-based compression molding followed by particle leaching. Details about this technique were described elsewhere (28). Briefly, several aliphatic polyesters in different percentages were blended with chitosan. These various scaffold formulations were evaluated *in vitro* for osteogenic applications, using a mouse MSC cell line (BMC9). The composition having chitosan–PBS (50% wt) evidenced the strongest results, in terms of both cell adhesion and proliferation (29). These results raised the question of why this specific blend shows such enhanced cell behavior. We herein addressed this important question by studying different blends with two different concentrations of chitosan: chitosan-PBS (25-75% wt) and chitosan-PBS (50% wt), as well as, without chitosan, with only PBS (100% wt), with human MSCs seeded and cultured in osteogenic conditions. *In vivo* tissue response was evaluated by implanting scaffolds with the extreme compositions, chitosan-PBS (50% wt) and scaffolds without chitosan (PBS 100) in Wistar rats. The implantation locations were defined to evaluate the inflammatory response in regions with different degrees of vascularization. The regions were the cranial bone that is a region with relevance for the intended application, submuscular, a highly vascularized location and auricular area, which is a region with lower

vascularization.

2. MATERIALS AND METHODS

2.1. Scaffolds processing

The aim of this specific study required the production of scaffolds with different compositions of chitosan and PBS. Namely, we produced scaffolds having 100% of polyester (PBS 100); 25% of chitosan and 75% of PBS (Ch-PBS 25-75); and 50% of chitosan and 50% PBS (Ch-PBS 50-50). In both cases, the composition is in a weight basis.

Chitosan and PBS powder were melt blended by extrusion. The extrudate was subsequently grinded into powder. This powder was physically mixed with NaCl particles with controlled sizes (obtained by sieving) and processed by compression molding into large discs. These large discs were subsequently sectioned to obtain the required geometry for the final scaffolds. The sectioning was performed using a CNC equipment (3D Plotter MDX-20 – Roland), which allows cutting solid objects in a controlled and reproducible manner. In a first stage, the outer skin of the large disk produced initially by compression molding was removed. A plate with the final required thickness was obtained from where smaller discs were cut with the desired geometries to be used as scaffolds. A subsequent salt leaching process was performed by immersion in water during a sufficient period to allow all NaCl particles to be dissolved and leached out. In this way, porous scaffolds with controlled geometry are obtained. Specific details of the processing conditions are described elsewhere (28). Taking into account the final applications, we herein produced discs with diameters of 8 mm and two different thicknesses, 1 mm and 3 mm. Finally, the discs intended to be used in further cell culture studies or for *in vivo* implantation were sterilized by ethylene oxide.

2.1.1. Scaffolds characterization by micro computed tomography (μCT)

A micro computed tomography equipment μCT Skyscan 1072 scanner (Skyscan, Knotich, Belgium) was used to analyze the internal 3D structure of the scaffolds. Three scaffolds of each formulation were scanned in high-resolution, using a resolution pixel size of 8.79 μm and exposure time of 1.792 ms. The energy of scanner was selected to use 63 keV and 157 μA current. Approximately 400 projections were acquired over a rotation range of 180º with a rotation step of 0.45º. μCT scans were reconstructed using a cone-beam

reconstruction software (NRecon v1.4.3, also from SkyScan). Representative data sets of 200 sections were segmented into binary images with a dynamic threshold of 150 to 255 (grey values) and were used for morphometric analysis including porosity, pore interconnectivity and mean pore size (CT analyzer, v1.5.1.5, SkyScan) and to reconstruct 3D models (ANT 3D creator, v2.4, SkyScan).

2.1.2. Mechanical tests

Compression tests were performed for determining the compressive modulus of the developed scaffolds using a Universal tensile testing machine (Instron 4505 Universal Machine, USA). Tests were performed using a crosshead speed of 2 mm/min until 60% of strain was reached. Tested scaffolds were cylinders of approximately 8 mm in diameter and 3 mm in thickness. The results presented are the average of testing at least five specimens. The compressive modulus was determined by selecting the most linear region of the stress-strain graph.

2.2. Cell studies

The biological performance of the scaffolds was assessed by *in vitro* assessment of cell adhesion, viability and osteogenic differentiation. Biocompatibility was analyzed by implanting the scaffolds in different body regions of Wistar rats. The parameters and conditions used in those tests will be described in detail in the current section.

2.2.1. Cell seeding and cell culture

Human bone marrow mesenchymal stem cells (hBMSCs) cells were grown in a culture medium consisting of alpha medium (Sigma, St. Louis, MO), 10% fetal bovine serum (Biochrom AG, Germany), 5 mM L-glutamine (Sigma, St. Louis, MO), 1 ng/ml basic fibroblast growth factor (bFgF) (PeproTech, USA) and 1% of antibiotic-antimycotic mixture (Sigma, St. Louis, MO). When an adequate cell number was obtained, cells at passage 2 were detached with trypsin/EDTA. Cells were seeded by means of a cell suspension at a density of $2.8x10^5$ cells/scaffold under dynamic conditions (orbital shaker), during 24 h. The constructs were placed in new 24-well plates and 1 ml of osteogenic medium was added to each well. The

osteogenic culture medium consisted of DMEM without phenol red, dexamethasone 10^{-8} M (Sigma, St. Louis, MO), ascorbic acid 50 μg/ml (Sigma, St. Louis, MO) and ß-glycerophosphate 10 mM (Sigma, St. Louis, MO). The cell-constructs were cultured for periods of up to 7, 14 and 21 days in a humidified atmosphere at 37ºC, containing 5% CO_2. The culture medium was changed every 2 to 3 days until the end of the experiment.

2.2.2. Cell viability

Cell viability was assessed after 7, 14, and 21 days using the MTS test. The cell-scaffold constructs (*n*=3) were rinsed 3 times in phosphate buffered saline solution (Sigma, USA), and immersed in a mixture consisting of serum-free cell culture medium and MTS reagent in a 5:1 ratio. After that, the samples were incubated during 3 hours at 37ºC in a humidified atmosphere containing 5% CO_2. The optical density (O.D.) was measured on a microplate ELISA reader (BioTek, USA) using an absorbance of 490 nm.

2.2.3. Cell adhesion and morphology - scanning electron microscopy (SEM)

The adhesion, morphology and spatial distribution of cells on the scaffolds were analyzed by SEM. The constructs were washed in phosphate buffered saline solution and fixed in 2.5% glutaraldehyde. After that, the constructs were dehydrated with increasing percentages of ethanol and let to air dry. Afterwards, the constructs were sputter coated with gold (JEOL JFC-1100) and analyzed using a SEM Leica Cambridge S360.

2.2.4. Early osteogenic marker - alkaline phosphatase

Samples were collected as previously described. Alkaline phosphatase (ALP) activity of the constructs (*n*=3) was measured by the specific conversion of *p*-nitrophenyl phosphate (pNpp) (Sigma, USA) into *p*-nitrophenol (pNp). The constructs were thawed at room temperature and sonicated during 15 min. The enzymatic reaction was set up by mixing 100 μl of the sample with 300 μl of substrate buffer containing 1 M diethanolamine HCl (pH 9.8) and 2 mg/ml of pNpp. The solution was further incubated at 37ºC during 1 hour and the reaction was stopped by the addition of a solution containing 2 M NaOH and 0.2 mM EDTA

in distilled water. The O.D. was determined at 405 nm. A standard curve was prepared using pNp values ranging from 0 to 20 µmol/ml.

2.2.5. Osteogenic gene expression -– real time reverse transcriptase PCR (RT-PCR)

Samples were collected after 7, 14 and 21 days of culture and Trizol® (Invitrogen, Life Technologies Inc., UK) was added to the constructs and immediately placed at -80ºC. Total RNA was isolated from cells with Trizol according to the manufacturer protocol. A NanoDrop microspectrophotometer (NanoDrop ND-1000 Spectrophotometer, Alfagene, USA) was used to measure the total RNA concentration. The integrity of the RNA samples was checked using denaturing agarose 1.2% gel electrophoresis.

The real time PCR analysis used in this work consisted of a two-step fluorogenic assay using the SyberGreen system (BioRad, USA). All the reagents used in this procedure were obtained from Bio-Rad in accordance with the instructions of the manufacturer.

cDNA synthesis was performed using iScript^{TM}cDNA Synthesis Kit (BioRad, USA). Briefly, cDNA synthesis was carried out using a reaction mixture consisting of 1X iScript Reaction Mix, 1µL iScript Reverse Transcriptase, RNA template (1 µg of total RNA) and nuclease-free water was prepared to a final reaction volume of 40 µL. After that stage, the obtained cDNA was used as template for the amplification of the genes. Specific genes, primer sequences and annealing temperatures are listed in Table I.

Table I. Amplified genes, specific primer pair sequences and annealing temperatures.

Gene	Primer sequence	T_m (ºC)
Runx 2	R- 5'-CAG CGT CAA CAC CAT CAT TC - 3' F- 5'-TTC CAG ACC AGC AGC ACT C - 3'	58.1
Osterix	R- 5'-CCCTTTACAAGCACTAATGG - 3' F- 5'-ACACTGGGCAGACAGTCAG - 3'	57.1
Osteopontin	R- 5'-GGG GAC AAC TGG AGT GAA AA - 3' F- 5'-CCC ACA GAC CCT TCC AAG TA - 3'	58.4
Akaline Phosphatase	R- 5'-AGA CTG CGC CTG GTA GTT G - 3' F- 5'-CTC CTC GGA AGA CAC TCT G - 3'	58.8
Osteocalcin	R- 5'-CTG GAG AGG AGC AGA ACT GG- 3' F- 5'-GGC AGC GAG GTA GTG AAG AG- 3'	61.4
Bone sialoprotein	R- 5'-CCT CGT ATT CAA CGG TGG TG - 3' F- 5'-CAA CAG CAC AGA GGC AGA AAA - 3'	59.8
Type I collagen	R- 5´-TCA AAA ACG AAG GGG AGA TG-3 F- 5´-CCA AAT CTG TCT CCC CAG AA-3	58.4
GAPDH	R- 5'-GAC AAG CTT CCC GTT CTC AG - 3' F- 5'-ACA GTC AGC CGC ATC TTC TT - 3'	58.4

Each real time PCR run was carried out with an initial incubation at 95ºC for 10 min followed by forty cycles of denaturation (95ºC, 10 s), annealing (temperature accordingly with the specific primer used, 30 s) and extension (72ºC, 30 s) in the gradient thermocycler MiniOpticon real-time PCR detection system (BioRad, USA). At the end of each cycle, the fluorescent products were detected and quantified.

GAPDH was used as the housekeeping gene and the expression of all the target genes was normalized to the GAPDH of that sample in the respective time point. The obtained results were further analyzed with CFX Manager Software – version 1.5 (BioRad, USA).

2.3. Animal model and surgical protocols

Twelve Wistar rats weighing between 250-300 g were used in the *in vivo* studies. All rats were fed *ad libitum* during the experiments. The animals were maintained in a temperature and humidity controlled environment at the animal research center of Hacettepe University. The study was conducted after receiving approval from the Animal Ethical Committee of the Kırıkkale University. A sterile surgical technique was applied throughout the surgical procedures. The scaffolds (8 mm in diameter and 1 mm thick) were previously sterilized by ethylene oxide. Animals were anesthetized by intraperitoneal injection with a mixture of ketamine HCl (Parke Davis, 50 mg/ml, Taiwan) and Rompun (2%, Bayer, Germany). The implantation site of the tested animals was shaved and disinfected with Baticon solution (Droksan, 10%, Turkey). The scaffolds were implanted in 3 different anatomical regions (Figure 1) to analyze the inflammation extent in zones with different degrees of vascularization:

(i) Cranial critical size defect: the periosteum was pulled back from the cranial surface, the cranial bone was removed by using a circular driller and the scaffold was immediately placed in the defect (inlay model), covered by the periosteum;

(ii) Auricular – ear: a pocket was made between the perichondrium and the ear cartilage and the scaffold was placed on the 1/3 proximal cartilage in the pocket;

(iii) Submuscular: an incision of 10 mm was made to reach the iliac bone. The scaffold was placed between the periosteum and the iliac bone (onlay model). A total of 3 scaffolds per animal were implanted. In all cases, the incision was closed using 5.0 silk sutures.

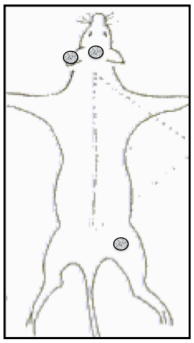

Figure 1. Scheme of the dorsal view of a rat showing the implantation sites.

2.4. Statistical analysis

Statistical analysis was performed using the SPSS statistic software (Release 15.0.0 for Windows). A Shapiro-Wilk test was used to ascertain about the data normality and variance equality. The normality was strongly rejected and for the results obtained for cell viability and ALP assays, the non-parametric test Kruskal-Wallis followed by Tukey's HSD test was applied to compare the three independent groups of samples for each variable. *P* values lower than 0.01 were considered statistically significant in the analysis of the results. In the case of gene expression results, the non-parametric Mann-Whitney U test was used.

3. RESULTS AND DISCUSSION

3.1. Scaffolds characterization by μCT

The morphological analysis of the scaffolds was performed by μCT, by reconstructing scaffolds' tridimensional morphology (Figure 2).

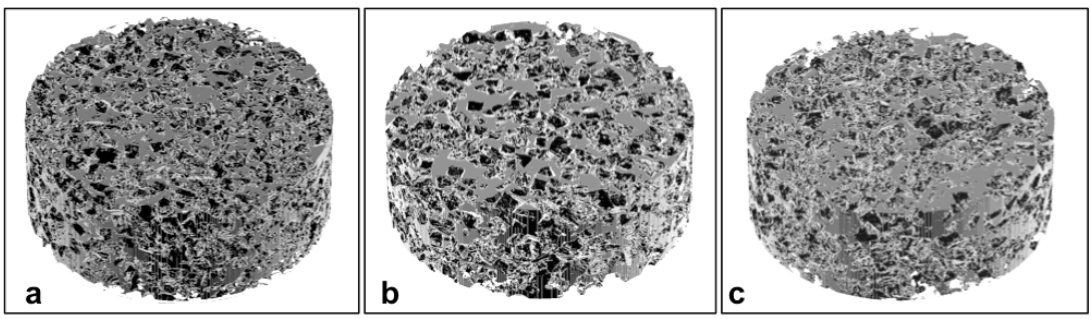

Figure 2. Tridimensional μCT reconstructions of the PBS 100 a), Ch-PBS 25-75 B), and Ch-PBS 50-50 scaffolds.

The qualitative analysis of scaffolds morphology showed the consistency of the porous morphology of the produced scaffolds. The material composition does not affect the morphology and structure of the scaffolds developed by compression molding followed by salt leaching.

Individual 2D analysis of the binary images obtained along the scaffold cross-section consisting of 300 slices was carried out for morphometric calculations (Table II).

Table II. Porosity, pore size, interconnectivity and compressive modulus of the produced scaffolds obtained by μCT

	Porosity (%)	**Pore size (μm)**	**Interconnectivity (%)**	**Compressive Modulus (MPa)**
100PBS	64.4±4.0	134.7±9.7	86.8±1.9	16.2±8.9
25Ch-75PBS	68.3±4.3	178.7±15.7	92.8±0.9	9.0±3.3
50Ch-50PBS	69.6±7.1	184.4±11.9	90.8±1.5	22.8±9.9

The analysis showed that the produced scaffolds have a very high open porous network. The level of interconnectivity of the porosity ranges from 86.8±1.9% to 92.8±0.9%, which is adequate to allow the diffusion of cells into the inner regions of the scaffolds. The percentage of porosity was directly proportional to the quantity of the porogen used (approximately 60%), with a small but not statistically significant increase for higher percentages of chitosan. Pore sizes were in general lower than the size range of the salt particles used. This is maybe due to the fact that compression molding process tends to break down some salt particles, resulting in a pore size in the scaffolds slightly lower than the original size of the porogen particles (28). The pore range of 100-250 μm was already shown in literature to be suitable for bone regeneration (30). The values for the compressive modulus of the various scaffolds are also shown in Table II.

We observed that the formulation with lower chitosan content (25% wt) has the lowest compressive modulus of all produced scaffolds. The formulation with higher amount of chitosan (50% wt) shows the highest elastic modulus. However, it should be noted that the pore size and level of porosity, as well as the interconnectivity of the scaffolds produced with formulations including chitosan have consistently larger values. These differences in

morphology may be responsible for the lower level of reinforcement achieved with chitosan compounds in this study. The mechanical properties are within the levels required for its application, as scaffolds for bone regeneration, since its values are compatible with those of trabecular bone (31).

3.2. Cell adhesion and morphology by SEM

The morphology of the cells and the extent of cell adhesion were analyzed by SEM (Figure 3).

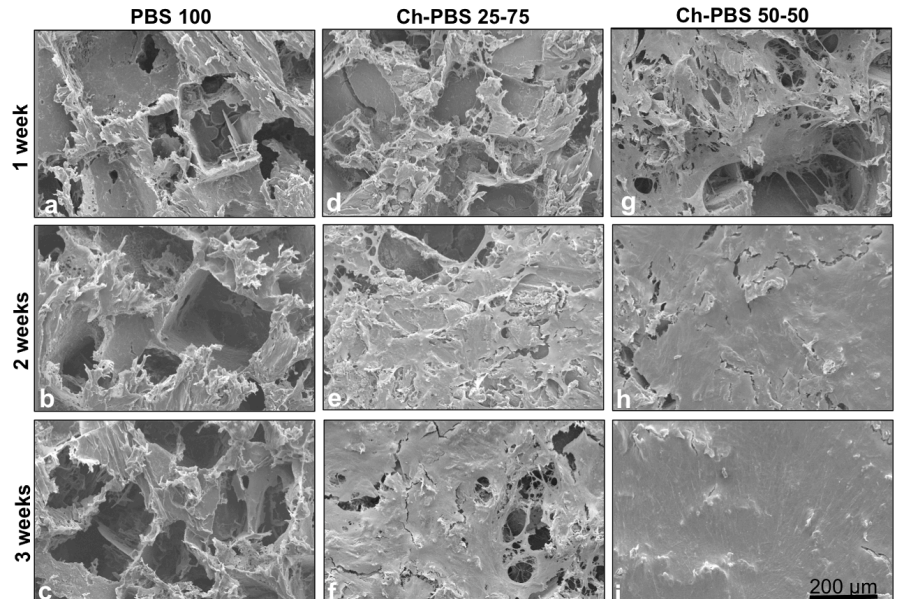

Figure 3. SEM micrographs showing the morphology of the seeded and cultured hBMSCs after 1, 2 and 3 weeks in PBS 100 scaffolds (a, b and c); Ch-PBS 25-75 (d, e and f); and Ch-PBS 50-50 (g, h and i), respectively.

Cells adhered in larger numbers to the chitosan containing scaffolds (Figures 3d and 3g) when compared to the PBS formulation (Figure 3a). Practically no cell colonization is visible in PBS 100 scaffolds (Figures 3a, 3b and 3c) for all time points. The formulation Ch-101the cultured scaffolds (Figures 3e and 3f). The stronger results in terms of cell adhesion were obtained for the formulation with the highest percentage of chitosan, showing that the presence of chitosan promoted cell adhesion and proliferation over time. Those results confirm our previous data (29) and clearly indicate a positive influence of chitosan over the adhesion and proliferation of hBMSCs seeded on the scaffolds. A study with chitosan-coralline scaffolds with a similar porosity evidenced a similar cell behavior (32).

3.3. Cell viability

Cell viability results (Figure 4) corroborate the SEM observation, showing that higher chitosan content has a positive influence on the viability of hMSCs. The absolute values obtained for chitosan based scaffolds were indeed high (Figure 4). At all time points, Ch-PBS 25-75 and Ch-PBS 50-50 displayed significantly higher cell viability than PBS 100. After 7 and 14 days of culture, Ch-PBS 50-50 scaffolds shown a significantly higher amount of cell viability than Ch-PBS 25-75. After 21 days of culture, no significant difference was obtained between Ch-PBS 25-75 and Ch-PBS 50-50. For PBS 100 scaffolds, the values of viability were quite low for all time points and even decreased with time, which correlates with the SEM images showing almost no cells at the surface of the scaffolds. The Ch-PBS 25-75 formulation evidenced increasing cell viability with time, even though the highest value obtained after 21 days of culture is still lower than the one obtained for the first time point (7 days) of the Ch-PBS 50-50 formulation. Ch-PBS 50-50 evidenced the highest values of cell viability, although there is a slight decrease of cell viability corresponding to the longer time point. This may be explained by the surface of the scaffold being already fully covered by the cells at this longer time point.

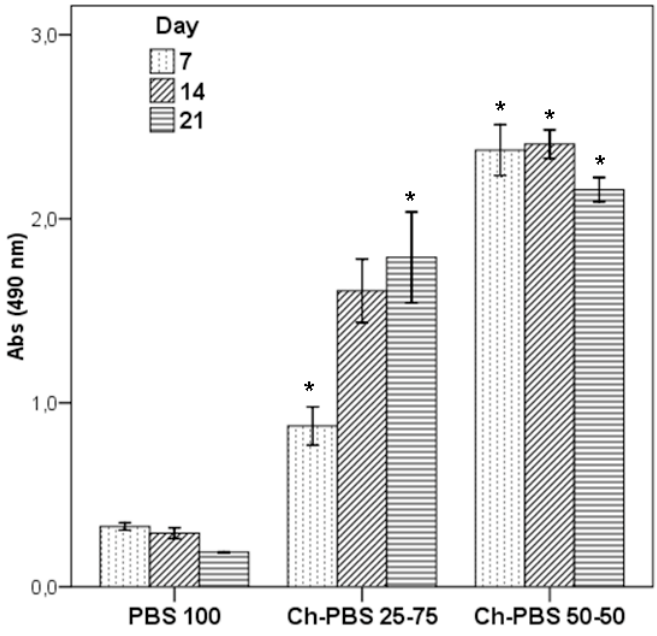

Figure 4. Cell viability (Abs 490 nm) in PBS 100, Ch-PBS 25-75 and Ch-PBS 50-50 after 7, 14 and 21 days of culture. Data were analyzed by nonparametric way of a Kruskal-Wallis test followed by Tukey's HSD test. (*) denotes significant differences compared to PBS 100.

3.4. Early osteogenic marker- ALP

ALP activity has been used as an indicator of osteogenic cell differentiation (33, 34). This membrane bound enzyme, which is expressed at relatively high levels in the osteoblasts, has long been recognized as a marker of osteoblastic differentiation, since it has been implicated in the mineralization process (35). ALP is upregulated in the early stages of biomineralization in order to form a large pool of inorganic phosphate, from which the ECM can be mineralized (36). An increasing ALP activity was observed over time for all scaffolds formulations. Similar trends were also observed for hMSCs cultured onto collagen-HA (37), silk (38) and chitosan (21, 23) 3D scaffolds. As expected from the SEM analysis and by data obtained from the viability tests, the seeded PBS 100 scaffolds presented the lowest values of ALP (Figure 5), corroborating the low cell adhesion detected in those scaffolds (Figures 3a, 3b and 3c).

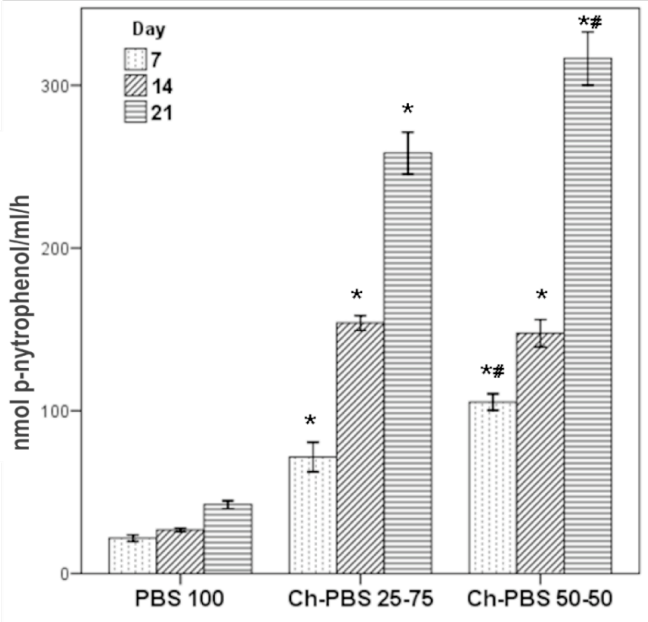

Figure 5. ALP activity of PBS 100, Ch-PBS 25-75 and Ch-PBS 50-50 after 7, 14, and 21 days of culture. Data were analyzed by nonparametric analysis using the Kruskal-Wallis test followed by Tukey's HSD test. (*) denotes significant differences compared to PBS 100, (**#**) denotes significant differences compared to Ch-PBS 25-75.

Formulations containing chitosan showed similar trends of ALP activity, increasing with time, as well as a high level of activity. Furthermore, the formulation with the largest

chitosan content showed also the highest values of the expression of ALP for the longest time point.

3.5. Osteogenic differentiation - gene expression

Bone cell differentiation is characterized by three different periods: proliferation, ECM maturation and mineralization (39). The osteogenic phenotype is recognized by cell maturation coordinated with the secretion of specific proteins, in a process that is asynchronously acquired and/or lost as the progenitor cells differentiate and the matrix matures and mineralizes (40). A preferred method to evaluate the transient state of the stem cells during differentiation is by analyzing gene expression profile during its culture in osteogenic differentiating conditions, as shown in Figure 6.

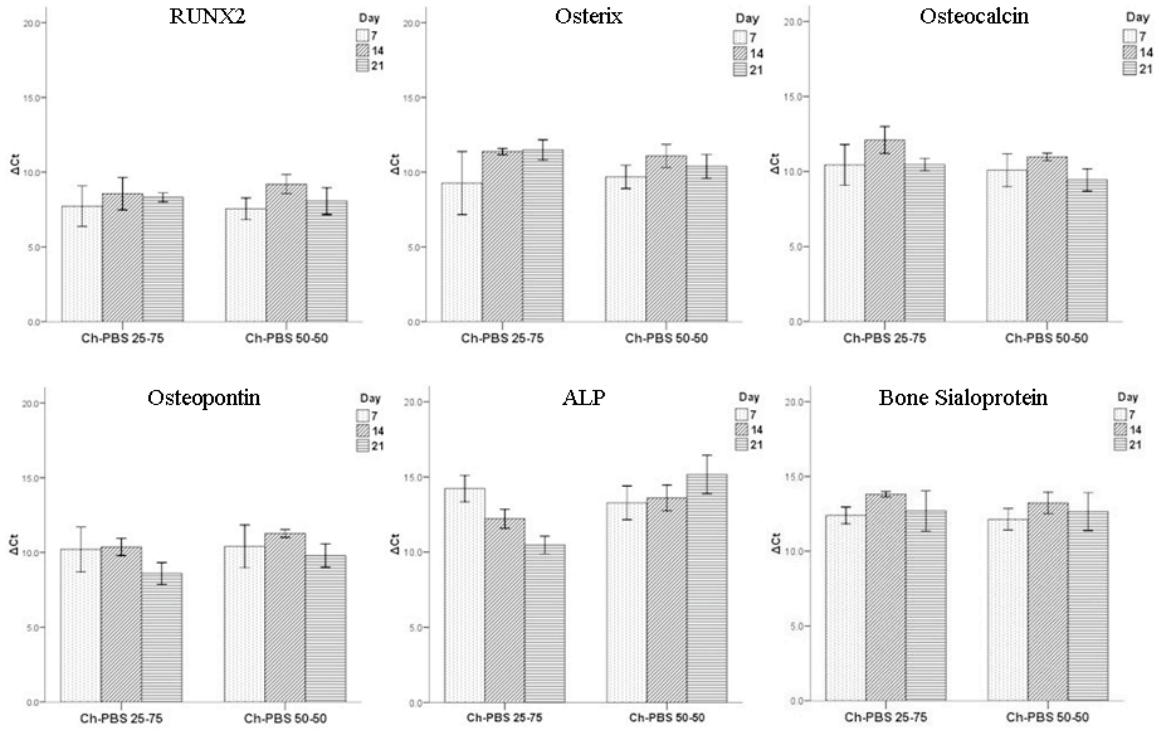

Figure 6. Relative gene expression of osteogenic related genes (Runx2, Oste0rix, Osteocalcin, Osteopontin, Alkaline phosphatase and Bone Sialoprotein) in hBMSCs cultures onto Ch-PBS 50-50, Ch-PBS 25-75 scaffolds in osteogenic conditions. The expression of these genes was normalized against the housekeeping gene GAPDH and calculated by ΔCT method. Data were analyzed by nonparametric Mann-Whitney U test.

We performed a real time quantitative PCR study to evaluate the level of the relative expression of osteogenic related genes. Gene expression for the formulation PBS 100 was not analyzed, due to the fact that these scaffolds did not support cell adhesion in sufficient amounts to obtain the quantity of mRNA to synthesize the minimum cDNA. The genes analyzed included Runx-2, Osterix, Alkaline phosphatase, Osteopontin, Bone Sialoprotein and Osteocalcin. The relative quantification of each gene was normalized against the expression of the housekeeping gene (GAPDH) for each time point. A constitutive expression of all mRNA transcripts was detected during the 21 days of the experiment. Runx-2 is expressed in an early multipotential mesenchymal cell population that can give rise to chondrogenic, osteogenic, and dentinogenic tissues as well as other lineages (41). Both chitosan scaffolds formulations presented a similar Runx-2 expression trend, with minor variation over time. Osterix is a transcription factor that is expressed in osteoblasts of all endochondral and membranous bones (42), acting during the stage of commitment of the osteoprogenitor cell into a pre-osteoblast (43). This gene was expressed in comparable levels for both Ch-PBS 25-75 and Ch-PBS 50-50 scaffolds. Osteocalcin gene is considered an important marker of the mineralization phase, reaching its maximum level before or during this process (39). In the present work this gene reached its maximum at 14 days of culture for both types of scaffolds. Osteopontin is one of the most abundant non-collagenous proteins in bone, binding to various extracellular molecules, including type I collagen, fibronectin or osteocalcin and contributes to the physical strength of the extracellular matrices (44). Osteopontin mRNA peak was at 14 days of hBMSCs culture, determining the end of the matrix deposition and the initiation of the mineralization stage. Higher values were obtained for Ch-PBS 50-50 formulation. Both osteocalcin and osteopontin mRNA maximum transcripts determine the presence of mature ostoblasts and the beginning of the mineralization. Alkaline phosphatase is localized in the plasma membrane of osteoblasts and although its precise function is not clearly understood, there are studies suggesting its involvement in mineralization process (33). It is an enzyme expressed by osteoblasts and it is considered a marker of osteogenic differentiation (45). Alkaline phosphatase has been shown to be responsible for the cleavage of pyrophosphate, a molecule that binds to hydroxyapatite crystals preventing further incorporation of phosphate into the crystals (46). This mRNA transcript evidenced opposed trends for the different scaffolds formulations, *i.e.*, for Ch-PBS 25-75, ALP expression decreased with time, whereas for Ch-PBS 50-50 increased with time, also presenting higher absolute values for the latest culture periods. Bone sialoprotein is an adhesive bone ECM protein exclusively associated with mature osteoblasts and suggested to be also involved in the mineralization phase of bone formation (47). This mRNA transcript

showed a similar profile for both types of scaffolds, increasing from 7 to 14 days and with a slight decrease at 21 days. This decrease can be considered relative, given the standard deviation associated. This is in accordance of what was expected, since this protein is expressed by mature osteoblasts (43). The whole set of genes consistently upregulated, strongly evidences a successful osteogenic differentiation of hBMSCs at the surface of chitosan containing scaffolds.

3.6. Host tissue response to the implanted scaffolds

The implantation of a biomaterial scaffold in a tissue is performed to verify the local effects on host tissues. The biocompatibility of a device in a tissue is assessed in terms of acute and chronic inflammatory responses, granulation tissue development, foreign body host reaction and potential of integration of the implanted scaffold with host tissue (49). The evaluation of the local pathological effects was carried out at both tissue level (macroscopic) and at microscopic level. The histological evaluation is used to characterize various important biological response parameters (50).

The tissue biocompatibility was evaluated *in vivo* by implanting Ch-PBS 50-50 and PBS 100 scaffolds in relevant tissue locations, including hard tissue in the cranial defect (Figure 7) and soft tissues in auricular (Figure 8) and submuscular (Figure 9) regions. The Ch-PBS 25-75 condition was excluded based on the *in vitro* results, since this condition evidenced a similar performance to Ch-PBS 50-50 and to minimize the number of animals used. All surgical incisions healed without evidence of infection or other complications. Retrieved implants showed no signs of serious inflammation.

Tissue reaction to an implanted biomaterial is often characterized by an initial acute inflammatory response, with the presence of polymorphonuclear cells (PMNs or neutrophils) that migrate from blood to the tissue (51). Acute inflammation is the immediate response to injury and most of the times destroy the foreign material. However, the implant may act as a persistent stimulus to inflammation, and the host response will evolve into a chronic inflammation response. The chronic inflammation is associated to angiogenesis, fibrosis or eventually, tissue necrosis (52). The leukocyte infiltration is composed by lymphocytes, macrophages and plasma cells, that in combination with angiogenesis and fibroplasia constitutes the granulation tissue (53). This chronic reaction has also another particularity, the possibility of recruiting giant cells (G), formed by macrophage fusion, mostly associated

to the failure of phagocytosis of large particles released from the device (54). This reaction is denominated by foreign body reaction (FBR).

After one month of implantation, an invasion of host cells throughout the implanted porous structures was visible for all tissue locations (Figures 7, 8 and 9). The implanted scaffolds caused mild inflammation, characterized by infiltration of mononuclear phagocytic cells, macrophages, lymphocytes, fibroblasts and some polymorphonuclear leukocytes in hard and soft tissues at the implantation site. For each implantation location:

i) Cranial defect

Both types of scaffolds were placed in close contact with the cortical bone of the calvaria. It is visible a significant ingrowth of connective tissue cells into the scaffolds porous structure (Figures 7a and 7d). Furthermore, new blood vessels were present (Figures 7b and 7e) and collagen is present in both type of scaffold (Figures 7c and 7f) formulations but in a higher amount for chitosan based scaffolds (Figures 7c). Foreign body giant cells were observed, being more pronounced for chitosan based scaffolds (Figure 7b) and it was already reported that chitosan may induce the formation of granulation tissue *in vivo* (55).

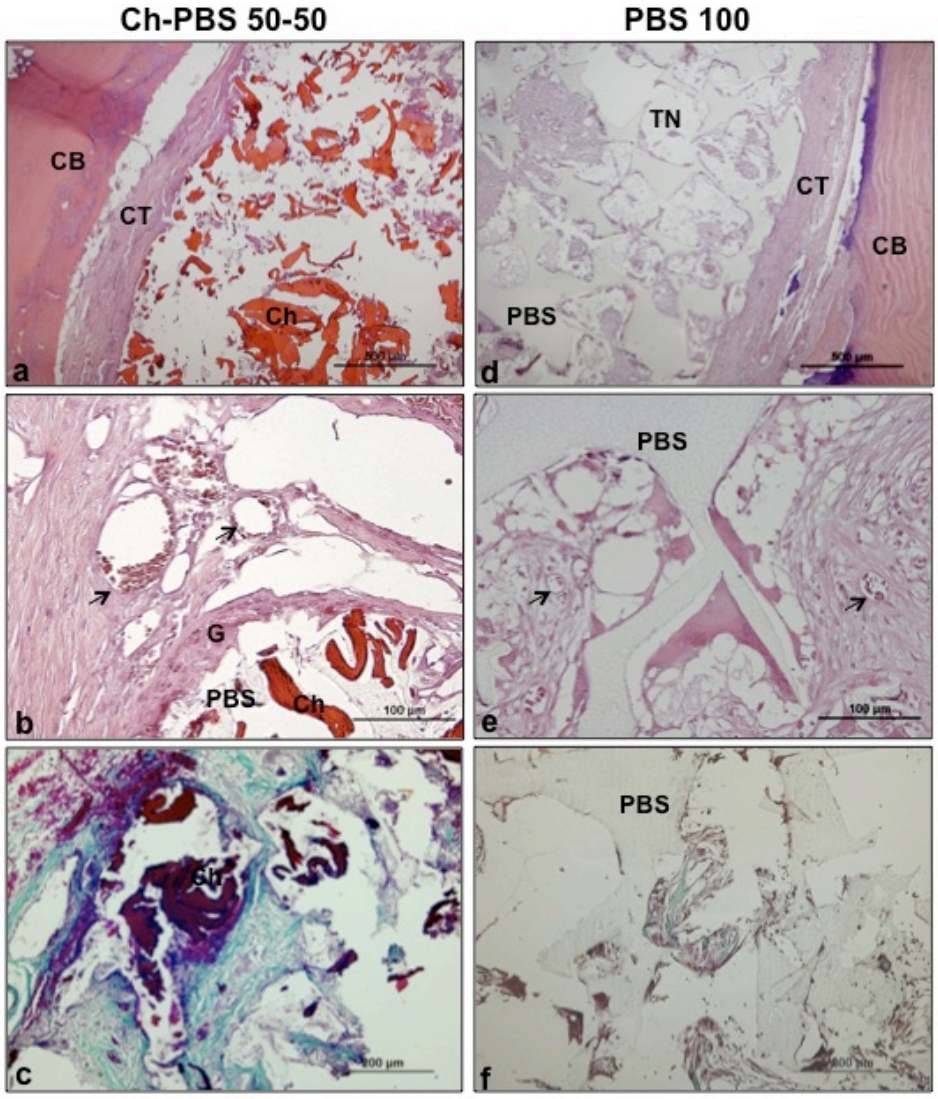

Figure 7. H&E histological sections of Ch-PBS 50-50 (a and b) and PBS 100 (d and e) implants in cranial defects. Masson trichrome stained sections of Ch-PBS 50-50 (c) and PBS 100 (f) implants in the same region, showing collagen in green. CB-Compact bone; CT-Connective tissue; TN- Tissue necrosis; Ch-Chitosan; PBS-Poly(butylene succinate).

ii) Auricular implantation

In this region scaffolds show, as in the cranial defect, a mild inflammatory response (Figure 8). This lower tissue response may be in part related to the fact that ear tissue is not intensely vascularized. PBS scaffolds evidenced lower cell colonization (Figures 8d and 8e), than Ch-PBS scaffolds. At high magnifications it was possible to observe cell necrosis inside the pores of PBS implants (Figure 8e). On the other hand, it was visible a massive colonization of inflammatory giant cells in chitosan implants (Figure 8b). Previous results

using chitosan and ovine MSCs with TGFβ-3 implanted into partial thickness lesions created in sheep legs, evidenced a hyaline-like cartilaginous matrix, well integrated into the host cartilage what provides further confidence for the potential of the present chitosan-based material also for cartilage regeneration (56).

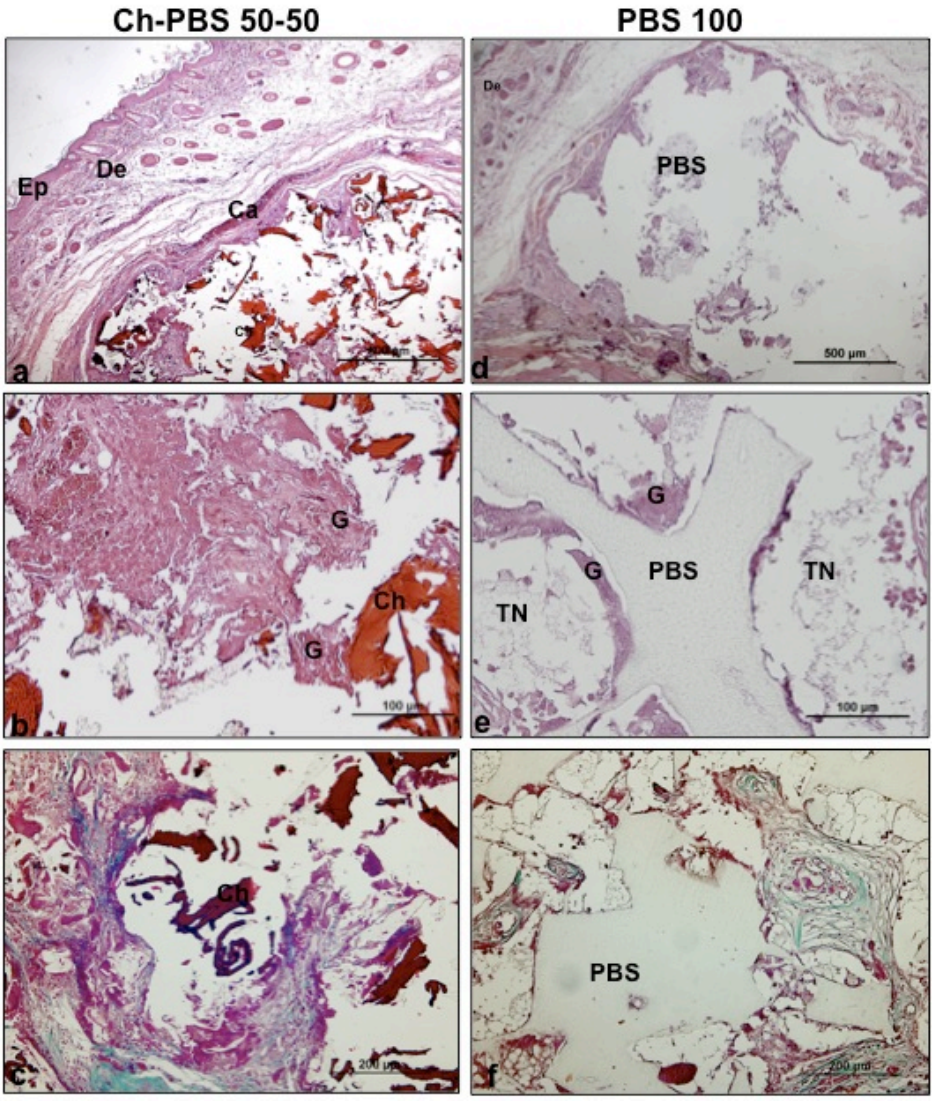

Figure 8. H&E histological sections of Ch-PBS 50-50 (a and b) and PBS 100 (d and e) implants in auricular area. Masson trichrome stained sections of Ch-PBS 50-50 (c) and PBS 100 (f) implants in the same region, showing collagen in green. Ep-Epidermis; De-Dermis; Ca-Cartilage; G-Giant cell; TN- Tissue necrosis; Ch-Chitosan; PBS-Poly(butylene succinate).

iii) Iliac submuscular implantation

In the submuscular region the scaffold was connected with bone at the bottom, and with periosteum-muscle at the top surface. In general, this implantation site showed more

inflammatory cells, namely neutrophils (Figure 9). This result may be due to the fact that this particular region has higher tissue vascularization, as well as higher tissue stresses caused by locomotion. Ch-PBS scaffolds evidenced robust infiltration by the host cells (Figures 9a and 9b), compared to PBS scaffolds that showed also in this implantation site some cell necrosis inside the implant (Figures 9d and 9f). Residual neutrophils were present in Ch-PBS scaffold implants (Figure 9b) caused by the presence of chitosan that is known to be attractive to neutrophils upon implantation (12, 57). It was also visible more collagen in chitosan based scaffolds (Figure 9c) in comparison with the PBS ones, where only residual collagen is observed (Figure 9f).

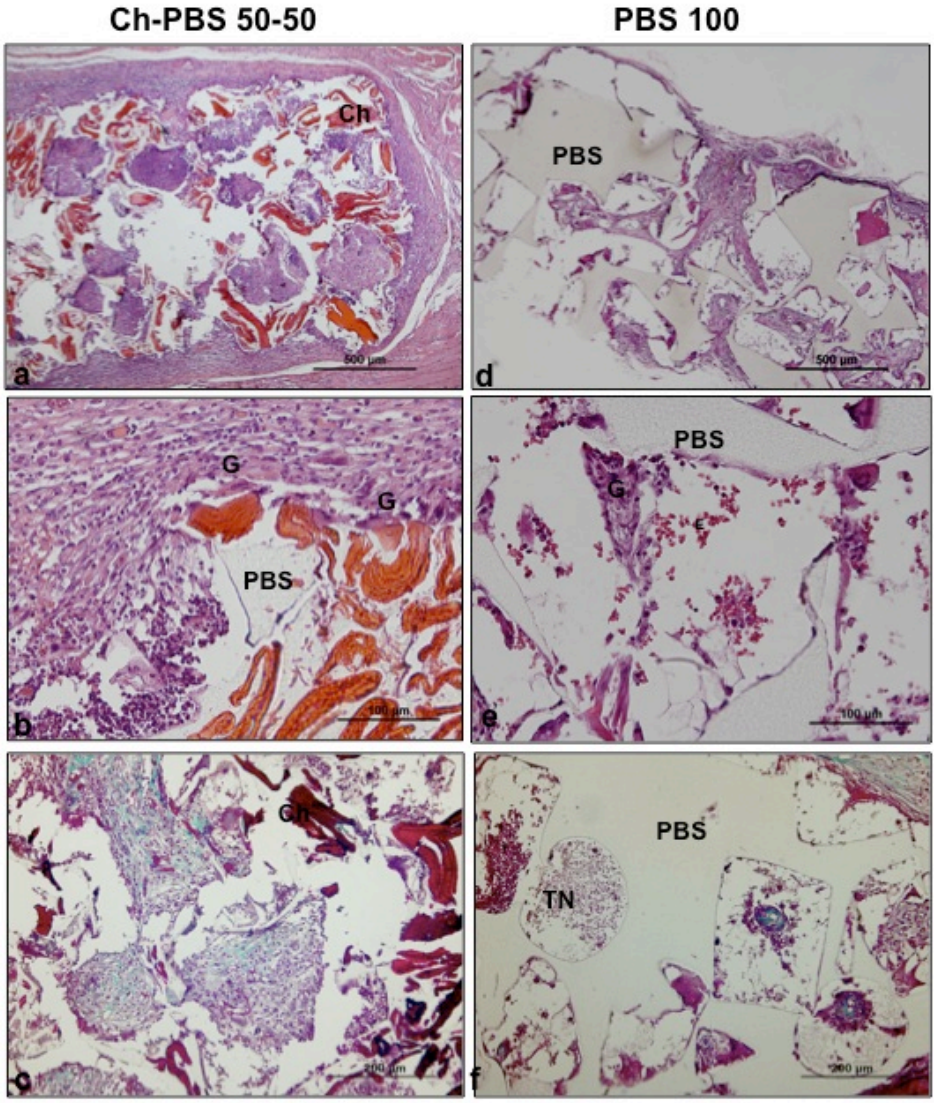

Figure 9. H&E histological sections of Ch-PBS 50-50 (a and b) and PBS 100 (d and e) implants in submuscular zone. Masson trichrome stained sections of Ch-PBS 50-50 (c) and PBS 100 (f) implants in the same location, showing collagen in green. G-Giant cell; TN-Tissue necrosis; Ch-Chitosan; PBS-Poly(butylene succinate).

4. CONCLUSIONS

Different chitosan and poly(butylene succinate) formulations were used to produce scaffolds by compression molding followed by salt leaching. The aim was to study the influence of chitosan over the viability, adhesion and osteogenic differentiation of hMSCs and *in vivo* tissue biocompatibility. Chitosan based scaffolds evidenced superior results in terms of *in vitro* cell performance, with PBS 100 scaffolds showing consistently inferior results.

Overall, a higher content of chitosan induce a stronger cellular performance in terms of cell adhesion, proliferation and differentiation, when using the produced scaffolds for the strategy presented in this work.

For all types of scaffolds tested *in vivo*, the tissue response was lower in calvaria and in auricular implantations when compared to the submuscular region. Chitosan based scaffolds evidenced more cell penetration, without any signs of cell necrosis. Furthermore, many blood vessels were observed in the immediacy of the scaffolds. A chronic inflammatory response without fibrosis was developed. Therefore, it is concluded that chitosan exerts a strongly positive effect over the cell performance *in vitro* as well as *in vivo*. Thus, the developed chitosan based scaffolds are strong candidates to be used in the bone tissue engineering field.

ACKNOWLEDGEMENTS

Ana Costa-Pinto was supported by scholarship SFRH/24735/2005 from the Portuguese research council “Fundação para a Ciência e a Tecnologia” (FCT). This work was partially supported by the European Network of Excelence EXPERTISSUES.

Professor Erhan Piskin was supported by Turkish Academy of Sciences (TÜBA) as a full member. The authors would also like to acknowledge for the supports of Biyomedtek and H.U.- Center for Bioengineering.

References

1. Langer R., Vacanti JP. Tissue engineering Science. 1993;260(5110):920-6.
2. Laurencin CT. Tissue Engineering:Orthopedic Applications. Annu Rev Biomed Eng. 1999;1:19-46.
3. Petite H. Tissue-engineered bone regeneration. Nature Biotechnology. 2000;18:959-63.
4. Dodane V, Vilivalam VD. Pharmaceutical applications of chitosan. Pharmaceutical Science & Technology Today. 1998;1(6):246-53.
5. Vârum KM, Kristiansen Holme H, Izume M, Torger Stokke Br, Smidsr¯d O. Determination of enzymatic hydrolysis specificity of partially N-acetylated chitosans. Biochimica et Biophysica Acta (BBA) - General Subjects. 1996;1291(1):5-15.
6. Tomihata K, Ikada Y. In vitro and in tivo degradation of films of chitin and its deacetylated derivatives. Biomaterials. 1997;18:261-8.
7. Muzzarelli R., Tarsi R, Filippini O, Giovanetti E, Biagini G, Varaldo PE. Antimicrobial properties of N-carboxybutyl chitosan. Antimicrob Agents Chemother. 1990;34(10):2019-23.
8. No HK, Park NY, Lee SH, Meyers SP. Antibacterial activity of chitosans and chitosan oligomers with different molecular weights. Int J Food Microbiol. 2002;74(1-2):65-72.
9. Prudden JF, Migel P, Hanson P, Friedrich L, Balassa L. The discovery of a potent pure chemical wound-healing accelerator. The American Journal of Surgery. 1970;119(5):560-4.
10. Malette WG, Quigley HJ, Gaines RD, Johnson ND, Rainer WG. Chitosan: a new hemostatic. Ann Thorac Surg. 1983;36(1):55-8.
11. Molinaro G, Leroux JC, Damas J, Adam A. Biocompatibility of thermosensitive chitosan-based hydrogels: an in vivo experimental approach to injectable biomaterials. Biomaterials. 2002;23(13):2717-22.
12. VandeVord PJ, Matthew HW, DeSilva SP, Mayton L, Wu B, Wooley PH. Evaluation of the biocompatibility of a chitosan scaffold in mice. J Biomed Mater Res. 2000;59(3):585-90.
13. Di Martino A, Sittinger M, Risbud MV. Chitosan: a versatile biopolymer for orthopaedic tissue-engineering. Biomaterials. 2005;26(30):5983-90.
14. Nishikawa H, Ueno A, Nishikawa S, Kido J-i, Ohishi M, Inoue H, et al. Sulfated Glycosaminoglycan Synthesis and Its Regulation by Transforming Growth Factor-[beta] in Rat Clonal Dental Pulp Cells. Journal of Endodontics. 2000;26(3):169-71.
15. Werb Z. ECM and Cell Surface Proteolysis: Regulating Cellular Ecology. Cell. 1997;91(4):439-42.
16. Lahiji A, Sohrabi A, Hungerford DS, Frondoza CG. Chitosan supports the expression of extracellular matrix proteins in human osteoblasts and chondrocytes. J Biomed Mater Res. 2000 Sep 15;51(4):586-95.
17. Cui YL, Qi AD, Liu WG, Wang XH, Wang H, Ma DM, et al. Biomimetic surface modification of poly(-lactic acid) with chitosan and its effects on articular chondrocytes in vitro. Biomaterials. 2003;24(21):3859-68.
18. Fakhry A, Schneider GB, Zaharias R, Senel S. Chitosan supports the initial attachment and spreading of osteoblasts preferentially over fibroblasts. Biomaterials. 2004 May;25(11):2075-9.
19. Jiang T, Abdel-Fattah WI, Laurencin CT. In vitro evaluation of chitosan/poly(lactic acid-glycolic acid) sintered microsphere scaffolds for bone tissue engineering. Biomaterials. 2006;27(28):4894.
20. Wu H, Wan Y, Dalai S, Zhang R. Response of rat osteoblasts to polycaprolactone/chitosan blend porous scaffolds. Journal of Biomedical Materials Research Part A. 2009;92A(1):238-45.

21. Yang X, Chen X, Wang H. Acceleration of Osteogenic Differentiation of Preosteoblastic Cells by Chitosan Containing Nanofibrous Scaffolds. Biomacromolecules. 2009;10(10):2772-8.
22. Mohammadi Y, Soleimani M, Fallahi-Sichani M, Gazme A, Haddadi-Asl V, Arefian E, et al. Nanofibrous poly(epsilon-caprolactone)/poly(vinyl alcohol)/chitosan hybrid scaffolds for bone tissue engineering using mesenchymal stem cells. Int J Artif Organs. 2007;30(3):204-11.
23. Arpornmaeklong P, Pripatnanont P, Suwatwirote N. Properties of chitosan-collagen sponges and osteogenic differentiation of rat-bone-marrow stromal cells. International Journal of Oral and Maxillofacial Surgery. 2008;37(4):357-66.
24. Malafaya P, Pedro A, Peterbauer A, Gabriel C, Redl H, Reis R. Chitosan particles agglomerated scaffolds for cartilage and osteochondral tissue engineering approaches with adipose tissue derived stem cells. Journal of Materials Science: Materials in Medicine. 2005;16:1077-85.
25. Coutinho D, Pashkuleva I, Alves C, Marques A, Neves N, Reis R. The Effect of Chitosan on the In Vitro Biological Performance of Chitosan-Poly(butylene succinate) Blends. Biomacromolecules. 2008;9(4):1139-45.
26. Zhang Y, Zhang M. Synthesis and characterization of macroporous chitosan/calcium phosphate composite scaffolds for tissue engineering. J Biomed Mater Res. 2001;55(3):304-12.
27. Correlo VM, Boesel LF, Bhattacharya M, Mano JF, Neves NM, Reis RL. Properties of melt processed chitosan and aliphatic polyester blends. Materials Science and Engineering: A. 2005;403(1-2):57.
28. Correlo VM, Boesel LF, Pinho E, Costa-Pinto AR, Alves da Silva ML, Bhattacharya M, et al. Melt-based compression-molded scaffolds from chitosan-polyester blends and composites: Morphology and mechanical properties. J Biomed Mater Res A. 2009;91(2):489-504.
29. Costa-Pinto AR, Salgado AJ, Correlo VM, Sol P, Bhattacharya M, Charbord P, et al. Adhesion, proliferation, and osteogenic differentiation of a mouse mesenchymal stem cell line (BMC9) seeded on novel melt-based chitosan/polyester 3D porous scaffolds. Tissue Eng Part A. 2008;14(6):1049-57.
30. Burg KJL, Porter S, Kellam JF. Biomaterial developments for bone tissue engineering. Biomaterials. 2000;21(23):2347-59.
31. Keaveny T, Morgan E, Niebur G, Yeh O. Bomechanics of trabecular bone. Annu Rev Biomed Eng 2001;3:307-33.
32. Mylene Gravel, Talia Gross, Razi Vago, Tabrizian M. Responses of mesenchymal stem cell to chitosan–coralline composites microstructured using coralline as gas forming agent. Biomaterials. 2006;27:1899-906.
33. van Straalen JP, Sanders E, Prummel MF, Sanders GTB. Bone-alkaline phosphatase as indicator of bone formation. Clinica Chimica Acta. 1991;201(1-2):27-33.
34. Lian J, Stein G. The developmental stages of osteoblast growth and differentiation exhibit selective responses of genes to growth factors (TGF beta 1) and hormones (vitamin D and glucocorticoids). J Oral Implantol 1993;19(2):95-105.
35. Stucki U, Schmid J, Ha¨mmerle CF, Lang NP. Temporal and local appearance ofalkaline phosphatase activity in early stages of guided bone regeneration. Clin Oral Impl Res. 2001;12:121-7.
36. Anderson HC. Molecular Biology of Matrix Vesicles. Clinical Orthopaedics and Related Research. 1995;314:266-80.
37. Bernhardt A, Lode A, Mietrach C, Hempel U, Hanke T, Gelinsky M. In vitro osteogenic potential of human bone marrow stromal cells cultivated in porous scaffolds from mineralized collagen. Journal of Biomedical Materials Research Part A. 2009;90A(3):852-62.

38. Zhang Y, Wu C, Friis T, Xiao Y. The osteogenic properties of CaP/silk composite scaffolds. Biomaterials.31(10):2848-56.
39. Lian JB, Stein GS. Concepts of Osteoblast Growth and Differentiation: Basis for Modulation of Bone Cell Development and Tissue Formation. Critical Reviews in Oral Biology & Medicine. 1992 January 1, 1992;3(3):269-305.
40. Madras N, Gibbs AL, Zhou Y, Zandstra PW, Aubin JE. Modeling Stem Cell Development by Retrospective Analysis of Gene Expression Profiles in Single Progenitor-Derived Colonies. Stem cells. 2002;20(3):230-40.
41. Bronckers AL, Sasaguri K, Cavender AC, D'Souza RN, Engelse MA. Expression of Runx2/Cbfa1/Pebp2alphaA During Angiogenesis in Postnatal Rodent and Fetal Human Orofacial Tissues. Journal of Bone and Mineral Research. 2005;20(3):428-37.
42. Tu Q, Valverde P, Chen J. Osterix enhances proliferation and osteogenic potential of bone marrow stromal cells. Biochemical and Biophysical Research Communications 341 (2006) 1257–1265. 2006;341:1257-65.
43. Siddappa R, Fernandes H, Liu J, Blitterswijk Cv, de Boer J. The Response of Human Mesenchymal Stem Cells to Osteogenic Signals and its Impact on Bone Tissue Engineering. Current Stem Cell Research and Therapy. 2007;2:209-20.
44. Denhardt DT, M N. Osteopontin expression and function: role in bone remodeling. J Cell Biochem Suppl. 1998;30-31:92-102.
45. Toquet J, Rohanizadeh R, Guicheux J, Couillaud S, Passuti N, Daculsi G, et al. Osteogenic potential in vitro of human bone marrow cells cultured on macroporous biphasic calcium phosphate ceramic. Journal of Biomedical Materials Research. 1999;44(1):98-108.
46. Murshed M, Harmey D, Millan JL, McKee MD, Karsenty G. Unique coexpression in osteoblasts of broadly expressed genes accounts for the spatial restriction of ECM mineralization to bone. Genes & development. 2005;19(9):1093-104.
47. Bianco P, Robey PG. Marrow stromal cells. Journal of Clinical Investigation. 2000;105(12):1663-8.
48. Anderson JM. Mechanisms of inflammation and infection with implanted devices. Cardiovascular Pathology. 1993 1993/9//;2(3, Supplement 1):33-41.
49. Anderson JM. Biological Responses to Materials. Annu Rev Mater Res. 2001;31:81-110.
50. Babensee J, Anderson J, Mcintire L, Mikos A. Host response to tissue engineered devices. Advanced Drug Delivery Reviews 1998;33:111-39.
51. Anderson JM. Inflammatory Response to Implants. ASAIO Journal. 1988;34(2):101-7.
52. Kumar V, Abbas K, Fausto N, Aster J. Acute and Chronic Inflammation. Robbins & Cotran Pathologic Basis of Disease: Saunders; 2010.
53. Anderson JM. Biological responses to materials Annu Rev Mater Res. 2001;31:81-110.
54. Kojima K, Okamoto Y, Miyatake K, Tamai Y, Shigemasa Y, Minami S. Optimum dose of chitin and chitosan for organization of non-woven fabric in the subcutaneous tissue. Carbohydrate Polymers. 2001;46(3):235-9.
55. Mrugala D, Bony C, Neves N, Caillot L, Fabre S, Moukoko D, et al. Phenotypic and functional characterisation of ovine mesenchymal stem cells: application to a cartilage defect model. Ann Rheum Dis 2008;67:288-95.
56. Usami Y., Okamoto Y, Minami S, Matsuhashi A, Kumazawa NH, Tanioka S, et al. Migration of canine neutrophils to chitin and chitosan. J Vet Med Sci. 1994;56(6):1215-6.

SECTION 4

CHAPTER V

Osteogenic differentiation of human bone marrow mesenchymal stem cells seeded on melt based chitosan scaffolds for bone tissue engineering applications

This chapter is based on the following publication: Costa-Pinto AR, Correlo VM, Sol PC, Bhattacharya M, Charbord P, Delorme B, Reis RL, Neves NM. "Osteogenic Differentiation of Human Bone Marrow Mesenchymal Stem Cells Seeded on Melt based Chitosan scaffolds for Bone Tissue Engineering Applications". Biomacromolecules, 2009 10: 2067–72

CHAPTER V

Osteogenic Differentiation of Human Bone Marrow Mesenchymal Stem Cells Seeded on Melt based Chitosan scaffolds for Bone Tissue Engineering Applications

ABSTRACT

The purpose of this study was to evaluate the growth patterns and osteogenic differentiation of human bone marrow mesenchymal stem cells (hBMSCs) when seeded onto new biodegradable chitosan/polyester scaffolds.

Scaffolds were obtained by melt blending chitosan with poly(butylene succinate) in a proportion of 50% (wt) each, and further used to produce a fiber mesh scaffold. hBMSCs were seeded on those structures and cultured for 3 weeks under osteogenic conditions. Cells were able to reduce MTS and demonstrated increasing metabolic rates over time. SEM observations showed cell colonization at the surface as well as within the scaffolds. The presence of mineralized extracellular matrix (ECM) was successfully demonstrated by peaks corresponding to calcium and phosphorous elements detected in the EDS analysis. A further confirmation was obtained when carbonate and phosphate group peaks were identified in Fourier Transformed Infrared (FTIR) spectra. Moreover, by Reverse transcriptase (RT)-PCR analysis it was observed the expression of osteogenic gene markers, namely Runt related transcription factor 2 (Runx2), type 1 collagen, bone sialoprotein (BSP) and osteocalcin.

Chitosan-PBS (Ch-PBS) biodegradable scaffolds support the proliferation and osteogenic differentiation of hBMSCs cultured at their surface *in vitro*, enabling future *in vivo* testing for the development of bone tissue engineering therapies.

1.INTRODUCTION

Mesenchymal Stem Cells (MSCs) isolated from bone marrow stroma have the capacity to differentiate into cells of connective tissues, namely into osteoblasts, chondrocytes and adipocytes (1-4). However, recent studies (5), indicate that they may have a much broader differentiation potential. Accordingly, the multipotential capacity of MSCs, their accessible origin, high *ex vivo* expansive potential, and ethical acceptance, make these cells attractive tools for tissue engineering and cell-based therapies.

Annually, more than 2.2 million bone grafting procedures (autologous bone graft and banked bone) are performed worldwide to ensure adequate bone healing in many skeletal problems, such as nonunion fractures, cervical and lumbar spine fusion, joint arthrodesis, revision arthroplasty (6). Unfortunately, the gold standard of bone grafting (autologous bone) requires an extra surgery to retrieve it from the patient. This leads to an increase in surgical and recovery times. Potential complications, such as chronic pain at the donor site, infections, and eventual disability (7) can occur. Tissue engineering offers a strategy to circumvent those problems. The concept involves the use of a porous and biodegradable scaffold, allowing cells to adhere and proliferate, creating conditions for the formation of ECM-like structures (8-10). Previous studies have shown that natural based polymers such as starch (11-18) or chitosan (19-28) have great potential for bone tissue engineering applications. The main advantages of these materials include low immunogenic potential, bioactive behavior, good interaction with host tissues, chemical versatility and high availability in nature (7).

Chitosan has already shown a range of properties, including its non-antigenicity (24) and cytocompatibility (21, 29), that suggest having adequate properties for bone tissue engineering applications. However the material offers limited versatility in its processability. To overcome this problem, we propose a novel methodology to process chitosan by compounding this material with biodegradable aliphatic polyesters (26). The blend combines the favorable biological properties of chitosan with the good mechanical properties and processability of polyesters (26, 28, 30-33), leading to a chitosan based material with adjustable properties for tissue engineering applications (30-32).

The purpose of the present work is to evaluate the performance of the developed microfiber mesh scaffolds. For that, we assess the cell adhesion, proliferation and osteogenic differentiation of human MSCs isolated from bone marrow and seeded onto novel chitosan/polyester micro fiber mesh scaffolds aimed to be used in bone tissue engineering field.

2. MATERIALS AND METHODS

2.1. Scaffold processing

New chitosan based scaffolds were, developed by a fiber bonding technique. The processing methodology is entirely melt based, thus avoiding the limitations of solvent-based

processing, and it is described in detail elsewhere (26). Briefly, chitosan was melt blended with polybutylene succinate (PBS) (50/50 wt%) in a twin-screw extruder. The extrudate was grinded into powder and further processed into microfibers, using a microextruder. The diameter of the fibers was controlled by the diameter of the die. After that, Ch-PBS fibers were cut and submitted to hot compression. This last step (15) consisted in applying temperature and pressure to obtain a fiber mesh scaffold with inherent porosity and interconnectivity. The scaffolds were sterilized by ethylene oxide and used for cell culture studies.

2.2. Scaffolds characterization

Chitosan-based fiber mesh scaffolds were analysed using a high-resolution micro-computed tomography Skyscan 1072 scanner (Skyscan, Kontich, Belgium). Five scaffolds were scanned in high resolution mode using a pixel size of 8.24 µm and integration time of 2.0 ms. The X-ray source was set at 80 keV of energy and 124 µA of current. For all the scanned specimens representative data sets of 150 slices were transformed into binary using a dynamic threshold of 60-255 (grey values) to distinguish polymer material from pore voids. This data was used for morphometric analysis (CT Analyser v1.5.1.5, SkyScan). The morphometric analysis included porosity, scaffolds interconnectivity and mean pore size quantification. Three dimensional (3D) virtual models of representative regions in the bulk of the scaffolds were also created, visualized and registered using the image processing software (ANT 3D creator v2.4, SkyScan).

The mechanical properties of the scaffolds were tested on compression tests carried out in a universal tensile testing machine (Instron 4505, Universal Machine). A crosshead speed of 5 mm/min was used and the compression modulus was determined from the most linear region of the stress-strain curve and averaged from the results obtained with five specimens.

2.3. Cell culture studies

2.3.1. *In vitro* cytotoxicity tests

A rat lung fibroblast cell line (L929), acquired from the european collection of cell cultures (ECACC), was used for the initial standard cytotoxicity assays. Tests were carried

out following the international standard ISO 10993. The procedure and methods are described elsewhere (27).

2.3.2. hBMSCs seeding and culture onto the scaffolds

Primary cultures of hBMSCs were used. The cells were characterized by flow cytometry for MSCs markers (CD31, CD34, CD45-negative and CD13, CD29, CD73, CD90, CD105, CD166-positive cells) and differentiation studies into osteogenic, chondrogenic and adipogenic lineage (34). The cells were grown in a culture medium consisting of alpha medium (Sigma, St. Louis, MO), 10% fetal bovine serum (Biochrom AG, Germany), 5 mM L-glutamine (Sigma, St. Louis, MO), 1 ng/ml basic fibroblast growth factor (bFgF) (PeproTech, USA) and 1% of antibiotic-antimycotic mixture (Sigma, St. Louis, MO). When an adequate cell number was obtained, cells at passage 2 were detached with trypsin/EDTA. Cells were seeded at a density of $2.5x10^5$ cells/scaffold under static conditions, by means of a cell suspension. After 24 hours of attachment, constructs were placed in new 24-well plates and 1 ml of osteogenic medium was added to each well. The osteogenic culture medium consisted of DMEM without phenol red, dexamethasone 10^{-8} M (Sigma, St. Louis, MO), ascorbic acid 50 µg/ml (Sigma, St. Louis, MO) and ß-glycerophosphate 10 mM (Sigma, St. Louis, MO). The constructs were cultured for periods of up to 7, 14 and 21 days in a humidified atmosphere at 37ºC, containing 5% CO_2. The culture medium was changed every 2 to 3 days until the end of the experiment.

2.3.3. Cellular viability assay - MTS test

Cell viability was assessed after 3 hours, 7, 14 and 21 days, using the MTS test. The constructs (*n*=3) were rinsed 3 times in phosphate buffered saline (Sigma, St. Louis, MO), and immersed in a mixture consisting of serum-free cell culture medium and MTS reagent in a 5:1 ratio and incubated for 3 hours at 37ºC in a humidified atmosphere containing 5% CO_2. After this, 200 μl (*n*=3) were transferred to 96 well plates and the optical density (O.D.) was measured on a microplate ELISA reader (BioTek, USA) using an absorbance of 490 nm.

2.3.4. Cell adhesion and cell viability stained with calcein-AM using confocal laser microscopy

Cells were incubated with calcein AM (Molecular Probes, Invitrogen, USA). Inside the cells, calcein-AM is hydrolyzed by endogenous esterases into the highly negatively charged green fluorescent calcein, which is retained inside the cytoplasm. The constructs were sectioned and cell adhesion, proliferation and viability were observed in the inner regions of the scaffolds using an Olympus FluoView FV1000 confocal laser scanning microscope.

2.3.5. Cell adhesion and morphology by scanning electron microscopy (SEM)

Cell adhesion, morphology, and spatial distribution were observed by SEM. The constructs were washed in 0.15 M phosphate buffered saline and fixed in 2.5% glutaraldehyde. After that, the constructs were dehydrated using a graded series of ethanol (30, 50, 70, 90, 100%) for 15 minutes, twice. Then, the samples were immersed in hexamethyldisilazane (35) (HDMS; Electron Microscopy Sciences, Washington, USA), and let to air dry for 2 h. Afterwards, the constructs were sputter coated with gold (JEOL JFC-1100) and analyzed using a Leica Cambridge S360 scanning electron microscope.

2.3.6. Cell proliferation by DNA quantification

hBMSCs proliferation on the Ch-PBS scaffolds was determined using a fluorimetric dsDNA quantification kit (PicoGreen, Molecular Probes, Invitrogen, USA). Samples collected at days 7, 14 and 21, were washed twice with a sterile phosphate buffered saline solution and transferred into 1.5 ml microtubes containing 1ml of ultra-pure water. Constructs were cryopreserved at -80ºC for further analysis. Prior to DNA quantification, samples were thawed and sonicated for 15 min. Standards were prepared with concentrations ranging between 0 and 2 mg/ml. Per each well of an opaque 96-well plate were added 28.7 μl of sample (n=3) or standard, 71.3 μl of PicoGreen solution, and 100 μl of Tris–EDTA buffer. The plate was incubated for 10 minutes in the dark and fluorescence was measured using an excitation wavelength of 480 nm and an emission wavelength of 528 nm.

2.3.7. Alkaline phosphatase quantification

Samples were collected as previously described. Alkaline phosphatase (ALP) activity of the scaffolds/cells constructs (*n*=3) was measured by the specific conversion of p-nitrophenyl phosphate (pNpp) (Sigma, St. Louis, MO, USA) into p-nitrophenol (pNp). The constructs were thawed at room temperature and sonicated for 15 min. The enzymatic reaction was set up by mixing 100 ml of the sample with 300 ml of substrate buffer containing 1 M diethanolamine HCl (pH 9.8) and 2 mg/ml of pNpp. The solution was further incubated at 37ºC for 1 hour and the reaction was stopped by the addition of a solution containing 2 M NaOH and 0.2 mM EDTA in distilled water. The O.D. was determined at 405 nm. A standard curve was made using pNp values ranging from 0 to 20 µmol/ml. The results were normalized by DNA values and expressed in µmol of pNp produced/µg ds DNA. A detailed description of the assay can be found elsewhere (36).

2.3.8. Mineralization content by energy dispersive spectroscopy (EDS)

The constructs were processed as described previously for SEM. The samples (*n*=3) were sputter coated with carbon (JEOL JFC-1100) with the purpose of analyzing the presence of Ca and P elements at the surface by EDS with a Leica Cambridge S360 scanning electron microscope. Sputter coating with carbon avoids overlapping of signals of the coating with the elements being analyzed.

2.3.9. Mineralization crystallinity by fourier transform infra-red spectroscopy (FTIR)

The constructs were washed in phosphate buffered saline and fixed in 2.5% glutaraldehyde. The samples were pressed into pellets with potassium bromide (KBr; Riedel-de Haen, Germany). The IR spectrum was measured using a FTIR Spectrometer (model IRPrestige-21, Shimadzu; Germany) in the wavelength range of 4000–400 cm^{-1}.

2.3.10. Osteogenic differentiation by reverse transcriptase PCR

Total RNA was isolated from cells with Trizol (Sigma, St Louis, USA), according to the manufacturer protocol. A NanoDrop Microspectrophotometer (NanoDrop ND-1000

Spectrophotometer, Alfagene, USA) was used to measure the total RNA amounts (ng/μl). Aliquots of the total RNA (100 ng/μl) were transcripted into cDNA and amplified in each PCR in one step RT-PCR beads (Amersham Biosciences) and gene specific primers were added. Each cDNA sample was run in triplicate for every PCR. Amplification was performed using a Mastercycler gradient (MyCycler™, Thermal Cycler, Biorad). The first reverse transcription step at 42ºC for 30 min was followed by a step of denaturation at 95ºC during 5 min. After this, 35 cycles of PCR were performed, each consisting of a denaturation stage at 95ºC for 1 min, annealing at a given temperature accordingly with the specific primer used, and then an extension stage at 72ºC for 2 min. In all cases, a final extension at 72ºC for 5 min was performed before storing the samples at 4ºC. Specific primers used were: for human Runx2, osteocalcin, type 1 collagen, BSP and for the house keeping gene glyceraldehyde-3-phosphate dehydrogenase (GAPDH). PCR products were separated by 1% agarose (Biorad, USA) at least twice. The separated DNA fragments were visualized by ethidium bromide (Sigma, St Louis, MO) staining and observed with an Eagleye software (Alpha Innotech, USA) using excitation at 514 nm and emission at 610 nm.

2.3.11. Statistical analysis

Results of MTS and ALP are expressed as mean ± standard deviation with n=3 for each group. Statistical significance of differences was determined using Student's t-test multiple comparison procedure at a confidence interval of 95% ($p < 0.05$).

3. RESULTS

3.1. Scaffolds characterization

Porous chitosan based fiber mesh scaffolds used in this study were produced with a blend of 50% chitosan and 50% of poly(butylene succinate). The scaffolds were prepared using melt extrusion, followed by hot compression (fiber bonding). Scaffolds were cut into cylinders of approximately 6.5 mm diameter and thickness of 1.5 mm. Figure 1 shows the top surface of the novel chitosan based fiber mesh scaffold produced by the described melt based process. Scaffolds show a large porosity and inherent interconnectivity, as well as an irregular distribution of the fiber orientation as intended.

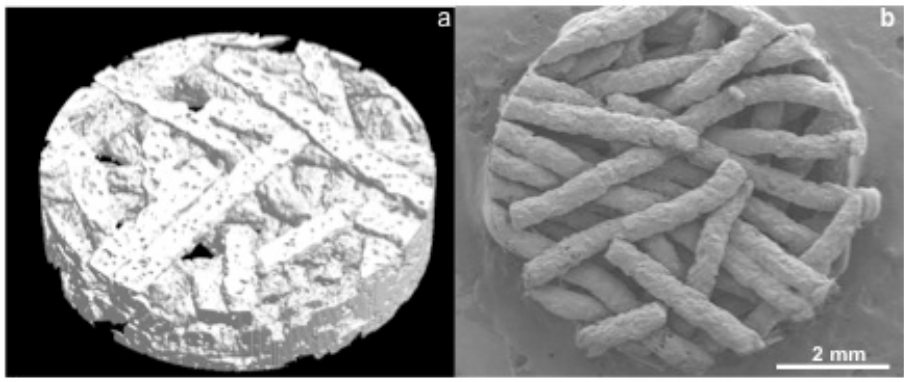

Figure 1. Three-dimensional (3D) images obtained by μ-CT reconstruction model (a) and SEM photomicrograph of Ch-PBS (50% wt) fiber mesh scaffold (b).

The μCT technology allows obtaining series of X-ray slice images covering a representative volume region of the porous scaffold. The solid volume representation and the quantitative data is obtained following image processing using specific software and the X-rays micrographs obtained in each slice. This technique was used to obtain 3D images of the novel chitosan fiber mesh scaffolds (Figure 1a) and to quantitatively determine the average porosity (44.8% ± 2.1) and the interconnectivity of 89.6% ± 1.9. Compression mechanical tests have shown that scaffolds have a compression modulus of 32.6 ± 12.8 MPa, which is within the range of interest for bone applications (37).

The fibers used to produce these scaffolds have an average diameter of 450 μm and as can be seen in Figure 1b, evidence an interesting surface roughness that may contribute to enhance the cell adhesion by increasing the surface area. Moreover, detailed observations using μCT equipment show that microfibers in addition to the surface roughness also possess some microporosity at the surface that further enhances the surface area (Figure 1a).

3.2. *In vitro* cytotoxicity tests

In the MTS test (data not shown), L929 fibroblasts metabolized MTS into brown formazan product after incubation with the scaffold's extract. This fact evidences that the cells have metabolic activities (around 80%) similar to those obtained by cells grown in DMEM (negative control). Moreover, they were able to incorporate and metabolize MTS,

showing very high viability. Therefore, the leachables released from the tested scaffolds can be considered as non-cytotoxic.

3.3. Cell viability by MTS and Calcein-AM staining

Results showed that the tested hBMSCs were also able to reduce MTS (Figure 2), demonstrate high metabolic rates as a function of time, and denote a high viability and proliferation profile. Moreover, a cell viability assay with calcein-AM staining (Figure 3) demonstrated that hBMSCs were metabolically active and well distributed throughout the scaffold surfaces after 3 weeks.

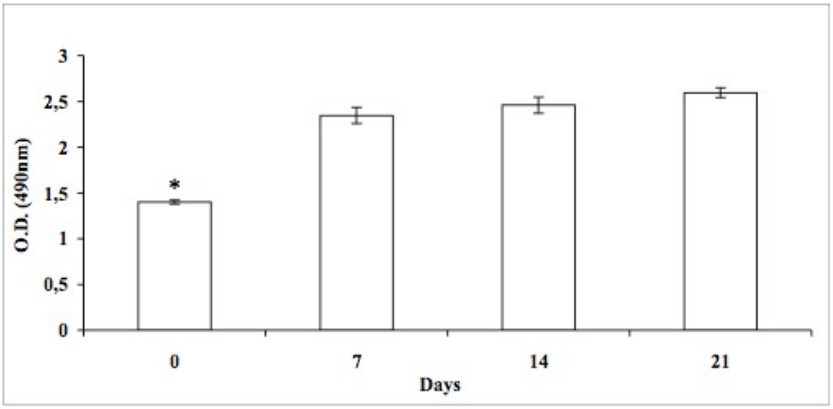

Figure 2. MTS viability assay of constructs and cultured Ch-PBS scaffolds following 3 hours (0 days), 7, 14 and 21 days, after cell seeding. Results are expressed as means ± standard deviation with n=3 for each bar, (*) indicate a significant difference ($p < 0.05$) between testing conditions as a function of time.

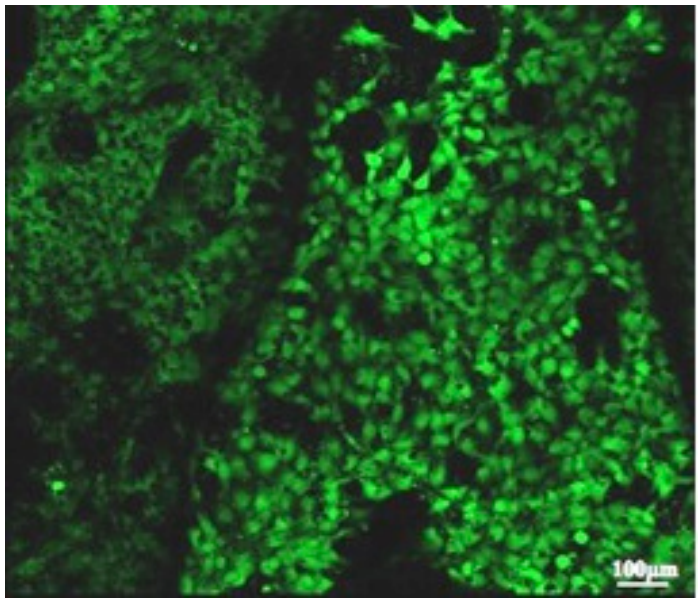

Figure 3. Cell viability after three weeks of cell-culture in the scaffolds analyzed by calcein-AM staining. Confocal micrograph showing cell adhesion and viability on the Ch-PBS fiber mesh scaffolds after 3 weeks in culture.

3.4. Cell adhesion and morphology by SEM

After 1 week, hBMSCs cultured under osteogenic conditions, were able to adhere to the fibrous surface and inner pores of the scaffolds and to proliferate during the subsequent periods in culture (Figures 4A, 4D and 4G). The production of ECM can be analyzed in more depth at higher magnifications (Figures 4C, 4F and 4I). Furthermore, it is observed that the cells were able to create “bridges” between neighboring fibers, but without occluding the pores (Figures 4B and 4E). Cells were also capable of colonizing the inner regions of the scaffolds, keeping the viability on those inner pores (Figures 4J, 4K and 4L).

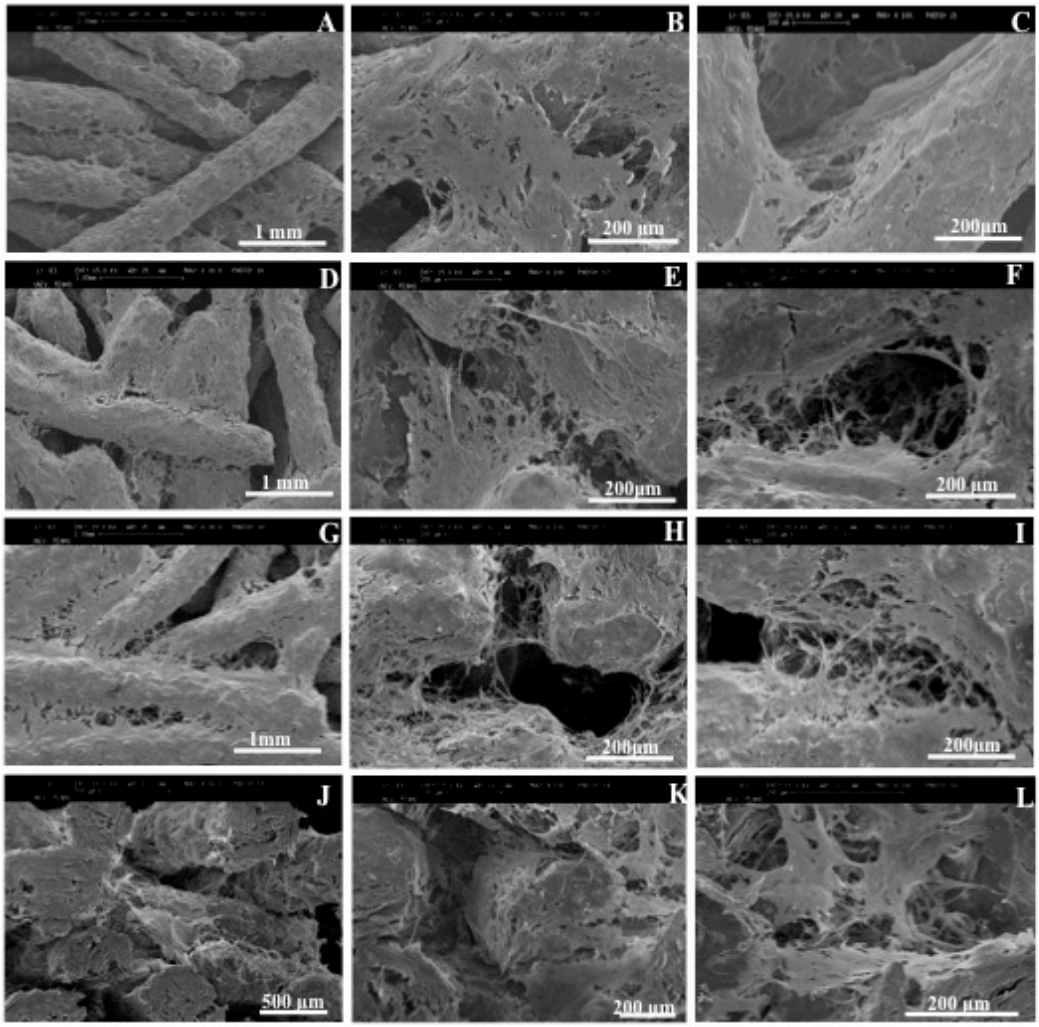

Figure 4. SEM micrographs of the adhesion and proliferation of hBMSCs, under osteogenic induction, on the 50 % wt Ch-PBS fiber mesh scaffolds at the surface after 1 week (Figures A, B, C), 2 weeks (Figures D, E, F) and 3 weeks (Figures G, H, I). The micrographs J, K and L correspond to cross sections of the cell seeded scaffolds after 3 weeks, showing the bulk colonization by the cells.

3.5. Alkaline phosphatase quantification

The expression of ALP is typically used as an early marker of the osteogenic phenotype. The ALP expression shows the typical pattern of expression (Figure 5), increasing until the second week, where it reached its maximum. This observation reflects the early osteogenic differentiation stage of the MSCs. After this period, ALP activity decreased, probably due to the onset of the mineralization process (36). This observation is a

positive indication of the transient character of the differentiation of cells into the osteogenic lineage.

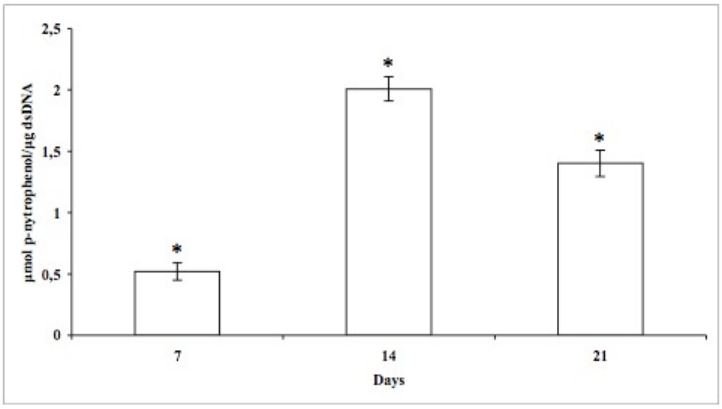

Figure 5. Alkaline phosphatase activity of hBMSCs cultured on the scaffolds at time points, 1, 2 and 3 weeks, under osteogenic induction. The results are normalized by μg of dsDNA, and presented in amount of p-nitrophenol (μmol/ml/h/μg dsDNA). Results are expressed as average ± standard deviation with *n*=3 for each bar, (*) indicates a significant difference ($p<0.05$) between conditions as a function of time.

3.6. Mineralization content of ECM by EDS and FTIR analysis

EDS analysis of the surface of constructs detected the presence of Ca and P elements (Figure 6 A). Acellular scaffolds (control) do not show any presence of those two elements during the same period of immersion in osteogenic inducing culture medium. These results clearly indicate the formation of mineralized ECM at the surface of cell seeded scaffolds. These results were further confirmed by FTIR analysis (Figure 6C), showing the presence of phosphate and carbonate groups, which are typical for carbonated apatite (38).

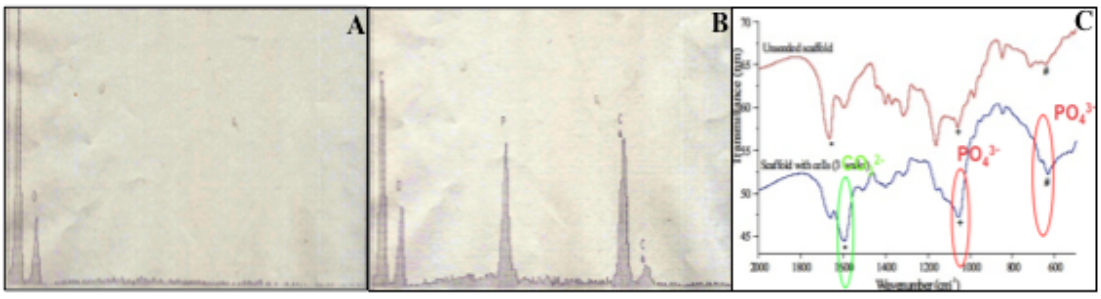

Figure 6. EDS spectra of the acellular scaffolds (A), 3 weeks in culture of hBMSCs on Ch-PBS scaffolds (B), and FTIR spectra of the control and constructs (C) (*CO_3^{2-} , + # PO_4^{3-}).

3.7. Osteogenic differentiation of hMSCs upon chitosan based scaffolds

To further analyze the differentiation towards the osteogenic phenotype, the RNA of the cell cultured in the scaffolds is analysed by reverse transcriptase PCR (Figure7).

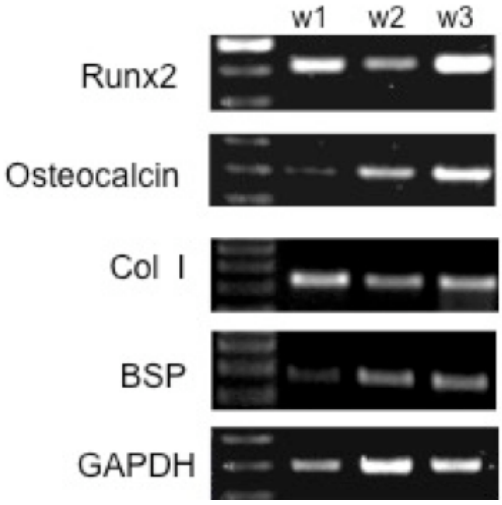

Figure 7. PCR analysis of the genes that encode for the transcription factor Runx2, the bone ECM protein osteocalcin, type I collagen, bone sialoprotein (BSP) and the house keeping gene GAPDH on hBMSCs grown under osteogenic conditions on Ch-PBS fiber mesh scaffolds for 21 days.

PCR analysis show the expression of specific genes related to the osteogenic lineage, namely the transcription factor Runx2, considered to be a crucial transcription gene within the osteogenic phenotype (39, 40). Its expression was detected at all time points, being more pronounced at the third week of culture. The gene expression patterns of the various extracellular proteins, including osteocalcin, type 1 collagen and BSP, was detected at all time points and in increased levels at the latest time point. This indicates a successful differentiation into the osteogenic phenotype.

4. DISCUSSION

The demand for new therapies for diseases affecting musculoskeletal tissues is continuously increasing, especially considering the high number of patients suffering from skeletal degenerative diseases. Bone tissue engineering has been proposing solutions to

address those clinical problems. The strategy could combine cells with a 3D scaffold and growth factors, seeking to achieve the regeneration of bone tissue.

Natural-based polymers such as chitosan, a polymer produced by partial deacetylation of chitin, have been proposed as having potential for tissue engineering applications. Chitosan is characterized by its good biocompatibility, low immunogeneicity, non-cytotoxicity and wound healing capability. These properties make chitosan a strong candidate material for bone tissue engineering applications. Due to its limited mechanical properties and process ability, scaffolds produced only with chitosan are more difficult to optimize for hard tissue applications. An alternative methodology to overcome those limitations consists in blending chitosan with synthetic and biodegradable aliphatic polyesters (26, 33). Thermoplastic biodegradable polymers have already shown great potential in the clinic as implantable biomaterials due to their reported non-cytotoxicity and biodegradability. Their degradation products are also non-cytotoxic, although they lack the cell recognition affinity typically provided by natural polymers. Thus by blending chitosan with synthetic polyesters it is possible to obtain a good balance between biological affinity (30-32) and processability, not compromising the biodegradability.

The developed fibrous scaffolds showed a significant interconnectivity (Figure 1), which is known to be a critical condition for successful cell colonization and viability. Extracts from the developed scaffolds are non-cytotoxic in contact with L929 cells (data not presented herein).

Human MSCs showed high metabolic levels when adhered onto the scaffolds both by the reduction of the MTS substrate (Figure 2) and also by the calcein-am staining (Figure 3).

SEM micrographs (Figure 4) show that hBMSCs adhered at the surface of the scaffolds and were able to “bridge” between fibers without occluding the pores (Figure 4C). The proliferation of hBMSCs and the production of ECM showed increased levels over time (Figures 4A, 4D and 4G). SEM observations and cell viability results can help to establish a time dependent cell proliferation patterns as showing the presence of higher number of cells at late time periods. It was also observed that cells proliferated and colonized the inner regions (Figures 4J, 4K and 4L) of the scaffolds, which demonstrate that porosity and interconnectivity exhibited by the scaffolds are adequate for cell infiltration and ingrowth.

ALP activity measurements (Figure 5) showed a maximum at the second week of culture, reflecting the early osteogenic differentiation stage of hMSCs (36). After this period,

ALP activity decreased due to the onset of the mineralization process, which is a typical positive indication.

hBMSCs were able to produce mineralized ECM confirmed by the presence of Ca and P elements (Figure 6a). Furthermore, the existence of characteristic peaks of carbonate and phosphate groups in FTIR spectra (Figure 6C) indicates the presence of carbonated apatite at the surface of constructs.

The differentiation of the hBMSCs towards the osteogenic lineage was ultimately demonstrated by the expression of genes that are usually associated with the mineralization during osteogenesis, such as the transcription factor Runx2, and the matrix proteins osteocalcin, type 1 collagen and BSP (Figure 7). Runx2 is essential for the differentiation of MSCs into mature osteoblasts in the skeletal development of numerous mammalian organisms (39, 40). Osteocalcin, one of the few osteogenic specific genes, is a bone matrix protein and it is known to play an important role in the differentiation of osteoblast progenitor cells, with significant up-regulation observed both in matrix synthesis and in the mineralization process (39). BSP is secreted, bind cell surface integrin receptors, and regulate mineralization and type I collagen represents the majority of the organic part of bone matrix (41).

5. CONCLUSIONS

Chitosan–poly(butylene succinate) fiber mesh scaffolds were successfully produced by a melt based routine, avoiding the use of solvents. The scaffolds presented a high degree of interconnectivity (89,6% ± 1.9) and adequate mechanical properties (32.6 ± 12.8 MPa) for bone tissue engineering applications.

It was demonstrated that chitosan-PBS scaffolds are cytocompatible, both with L929 cells and hBMSCs. The scaffolds support hBMSCs adhesion and proliferation under osteogenic inducing conditions. The cells presented high levels of viability, demonstrating that besides the remarkable colonization of the scaffold structure, the cells were metabolically active.

ALP expression a mineralized ECM is detected by the presence of Ca and P elements in EDS spectra, and also confirmed by FTIR. The expression of osteogenic related genes (Runx2, osteocalcin, type 1 collagen and bone sialoprotein) show successful differentiation of the cells in the scaffolds towards an osteogenic phenotype.

Due to the extremely well balanced combination of properties and excellent biological performance, it is strongly believed that the scaffolds herein proposed in combination with human adult mesenchymal stem cells will provide new therapies for the development of tissue engineering solutions for bone regeneration.

ACKNOWLEDGEMENTS

Ana Costa-Pinto was supported by a grant (SFRH/24735/2005) from the Portuguese Foundation for Science and Technology “Fundação para a Ciência e a Tecnologia” (FCT).

This work was partially supported by the EU Integrated Project GENOSTEM (Adult Mesenchymal Stem Cells Engineering for connective tissue disorders: from the bench to the bedside, LSHB-CT-2003-5033161), and the European Network of Excellence EXPERTISSUES (NMP3-CT-2004-500283). The authors would like to acknowledge to the School of Health Sciences of the University of Minho for the opportunity of using its facilities.

REFERENCES

1. Friedenstein A, Deriglasova U, Kulagina N, Panasuk A, Rudakowa S, Luriá E, et al. Precursors for fibroblasts in different populations of hematopoietic cells as detected by the in vitro colony assay method. Exp Hematol. 1974;2(2):83-92.
2. Owen M. Marrow Stromal Stem Cells. J Cell Sci Suppl. 1988;10:63-76.
3. Bianco P, Robey P. Marrow stromal cells. Journal of Clinical Investigation. 2000;105(12):1663-8.
4. Bianco P, Robey P. Stem cells in tissue engineering. Nature 2001;414(6589):118-21.
5. Delorme B, Ringe J, Pontikoglou C, Gaillard J, Langonné A, Sensebé L, et al. Specific Lineage-Priming of Bone Marrow Mesenchymal Stem Cells Provides the Molecular Framework for Their Plasticity. Stem Cells 2009;27(5):1142-51.
6. Giannoudis PV, Dinopoulos H, Tsiridis E. Bone substitutes: An update. Injury, Int J Care Injured. 2005;36S:20-7.
7. Salgado A, Coutinho O, Reis R. Bone tissue engineering: state of the art and future trends. Macromolecular Bioscience. 2004;4:743-5.
8. Langer R, Vacanti J. Tissue engineering Science. 1993;260(5110):920-6.
9. Cancedda R. Tissue engineering and cell therapy of cartilage and bone. Matrix Biology. 2003;22:81-91.
10. Hutmacher DW, Schantz JT, Lam CXF, Tan KC, Lim TC. State of the art and future directions of scaffold-based bone engineering from a biomaterials perspective. JTERM. 2007;1(4):245-60.
11. Reis RL, Cunha, A. M. , Allan, P. S., Bevis,M. J. . Mechanical Behaviour of Injection Moulded Starch Based Polymers. Journal of Polymers for Advanced Technologies. 1996;7:784-90.
12. Mendes S, Reis R, Bovell Y, Cunha A, van Blitterswijk C, de Bruijn J. Biocompatibility testing of novel starch-based materials with potential application in orthopaedic surgery: a preliminary study. Biomaterials. 2001;22:2057-64.
13. Salgado A, Gomes M, Chou A, Coutinho O, Reis R, Hutmacher D. Preliminary study on the adhesion and proliferation of human osteoblasts on starch-based scaffolds. Materials Science and Engineering C. 2002;20(2002):27-33.
14. Alves CM, Reis RL, Hunt JA. Preliminary Study on Human Protein Adsorption and Blood Cells Adhesion to Starch-Based Biomaterials. J Materials Science: Materials in Medicine. 2003;14:157-65.
15. Gomes M, Sikavitsas V, Behravesh E, Reis R, Mikos A. Effect of flow perfusion on the osteogenic differentiation of bone marrow stromal cells cultured on starch-based three-dimensional scaffolds. Journal of biomedical materials research. 2003;67A:87-95.
16. Salgado A, Coutinho OP, Reis RL. Novel Starch-Based Scaffolds for Bone Tissue Engineering: Cytotoxicity, Cell Culture, and Protein Expression. Tissue Engineering. 2004;10(3/4):465-74.
17. Leonor IB, Kim HM, Balas F, Kawashita M, Reis RL, Kokubo T, et al. Alkaline treatments to render starch-based biodegradable polymers self-mineralizable. Journal of Tissue Engineering and Regenerative Medicine. 2007;1(6):425-35.
18. Gomes ME, Azevedo HS, Moreira AR, Ellä V, Kellomäki M, Reis RL. Starch–poly(ε-caprolactone) and starch–poly(lactic acid) fibre-mesh scaffolds for bone tissue engineering applications: structure, mechanical properties and degradation behaviour. Journal of Tissue Engineering and Regenerative Medicine. 2008;2(5):243-52.
19. Peluso G, Petillo O, Ranieri M, Santin M, Ambrosio L, Calabró D, et al. Chitosan-mediated stimulation of macrophage function. Biomaterials. 1994;15:1215-20.
20. Madihally SV, Matthew HWT. Porous chitosan scaffolds for tissue engineering. Biomaterials. 1999;20(12):1133-42.

21. Chatelet C, Damour O, Domard A. Influence of the degree of acetylation on some biological properties of chitosan films. Biomaterials. 2001 Feb;22(3):261-8.
22. VandeVord PJ, Matthew HW, DeSilva SP, Mayton L, Wu B, Wooley PH. Evaluation of the biocompatibility of a chitosan scaffold in mice. Journal of biomedical materials research. 2002;59(3):585-90.
23. Kumar MNVR, Muzzarelli RAA, Muzzarelli C, Sashiwa H, Domb AJ. Chitosan Chemistry and Pharmaceutical Perspectives. Chemical Reviews. 2004;104(12):6017-84.
24. Seol YJ, Lee JY, Park YJ, Lee YM, Young-Ku, Rhyu IC, et al. Chitosan sponges as tissue engineering scaffolds for bone formation. Biotechnology Letters. 2004;26(13):1037-41.
25. Tuzlakoglu K, Alves C, Mano J, Reis R. Production and characterization of chitosan fibers and 3-D fiber mesh scaffolds for tissue engineering applications. Macromol Biosci. 2004;4(8):811-9.
26. Correlo VM, Boesel LF, Bhattacharya M, Mano JF, Neves NM, Reis RL. Properties of melt processed chitosan and aliphatic polyester blends. Materials Science and Engineering: A. 2005;403(1-2):57.
27. Oliveira JM, Rodrigues MT, Silva SS, Malafaya PB, Gomes ME, Viegas CA, et al. Novel hydroxyapatite/chitosan bilayered scaffold for osteochondral tissue-engineering applications: Scaffold design and its performance when seeded with goat bone marrow stromal cells. Biomaterials. 2006;27(36):6123-37.
28. Correlo VM, Pinho ED, Pashkuleva I, Bhattacharya M, Neves NM, Reis RL. Water Absorption and Degradation Characteristics of Chitosan-Based Polyesters and Hydroxyapatite Composites. Macromolecular Bioscience. 2007;7(3):354-63.
29. Heinemann C, Heinemann S, Bernhardt A, Worch H, Hanke T. Novel textile chitosan scaffolds promote spreading, proliferation, and differentiation of osteoblasts. Biomacromolecules. 2008;9(10):2913-20.
30. Costa-Pinto AR, Salgado AJ, Correlo VM, Sol P, Bhattacharya M, Charbord P, et al. Adhesion, proliferation, and osteogenic differentiation of a mouse mesenchymal stem cell line (BMC9) seeded on novel melt-based chitosan/polyester 3D porous scaffolds. Tissue Eng Part A. 2008;14(6):1049-57.
31. Coutinho D, Pashkuleva I, Alves C, Marques A, Neves N, Reis R. The Effect of Chitosan on the In Vitro Biological Performance of Chitosan-Poly(butylene succinate) Blends. Biomacromolecules. 2008;9(4):1139-45.
32. Oliveira JT, Correlo VM, Sol PC, Costa-Pinto AR, Malafaya PB, Salgado AJ, et al. Assessment of the suitability of chitosan/polybutylene succinate scaffolds seeded with mouse mesenchymal progenitor cells for a cartilage tissue engineering approach. Tissue Eng Part A. 2008;14(10):1651-61.
33. Correlo VM, Boesel LF, Pinho E, Costa-Pinto AR, Alves da Silva ML, Bhattacharya M, et al. Melt-based compression-molded scaffolds from chitosan-polyester blends and composites: Morphology and mechanical properties. J Biomed Mater Res A. 2009;91(2):489-504.
34. Delorme B, Charbord P. Culture and characterization of human bone marrow mesenchymal stem cells. Methods Mol Med. 2007;140:67-81.
35. Bray D, Bagu J, Koegler P. Comparison of hexamethyldisilazane (HMDS), Peldri II, and critical-point drying methods for scanning electron microscopy of biological specimens. Microsc Res Tech 1993 26(6):489-95.
36. Maniatopoulos C, Sodek J, Melcher A. Bone formation in vitro by stromal cells obtained from bone marrow of young adult rats. Cell Tissue Res. 1988;254(2):317-30.
37. Yang S, Leong K-F, Du Z, Chua C-K. The Design of Scaffolds for Use in Tissue Engineering. Part I. Traditional Factors. Tissue Engineering. 2001;7(6):679-89.
38. Rehman I, Bonfield W. Characterization of hydroxyapatite and carbonated apatite by photo acoustic FTIR spectroscopy. Journal of Materials Science: Materials in Medicine. 1997;8(1):1-4.

39. Viereck V, Siggelkow H, Tauber S, Raddatz D, Schutze N, Hüfner M. Differential regulation of Cbfa1/Runx2 and osteocalcin gene expression by vitamin-D3, dexamethasone, and local growth factors in primary human osteoblasts. Journal of Cellular Biochemistry. 2002;86(2):348-56.
40. Lian J, Stein G. Runx2/Cbfa1: a multifunctional regulator of bone formation. Curr Pharm Des. 2003;9(32):1677-85.
41. Liu F, Akiyama Y, Tai S, Maruyama K, Kawaguchi Y, Muramatsu K, et al. Changes in the expression of CD106, osteogenic genes, and transcription factors involved in the osteogenic differentiation of human bone marrow mesenchymal stem cells. Journal of Bone and Mineral Metabolism. 2008;26(4):312-20.

CHAPTER VI

In vitro degradation and biocompatibility assessment of chitosan-poly(butylene succinate) fiber mesh scaffolds

This chapter is based on the following publication: Costa-Pinto AR, Martins AM, Castelhano-Carlos MJ, Correlo VM, Sol PC, Bhattacharya M, Reis RL, Neves NM. "*In vitro* degradation and biocompatibility assessment of chitosan-poly(butylene succinate) fiber mesh scaffolds". 2010 *Submitted*.

CHAPTER VI

In vitro degradation and biocompatibility assessment of chitosan-poly(butylene succinate) fiber mesh scaffolds

ABSTRACT

In a tissue engineering approach it is important to determine the kinetics of the biodegradation of biomaterials *in vitro*, as well as *in vivo.* Furthermore, the evaluation of a host response to the implantation of the biomaterials must be performed to understand the extent of the inflammatory reaction.

Chitosan-poly(butylene succinate) fiber mesh scaffolds, in previous studies evidenced enhanced biological performance, not only in terms of cell adhesion and proliferation, but also as supporting the osteogenic differentiation of mouse and human MSCs. The following step consisted on the study of the degradation process *in vitro* using relevant enzymes, lipase and lysozyme, responsible for the degradation of the poly(butylene succinate) and chitosan, respectively. Moreover, subcutaneous implantation of the scaffolds was performed to assess the tissue response. Histology and immunoshistochemistry were used to visualize the type of inflammatory cells present in the surrounding tissue, as well as within the scaffold..

In the presence of lipase, or with lysozyme, water uptake of the scaffolds increased. This phenomenon is probably due to the degradation of scaffolds by the enzymes. Weight loss results and scanning electron micsoscopy (SEM) analysis evidenced that lysozyme combined with lipase have a notable effect on the degradation of the scaffolds *in vitro.*

In vivo implantation showed a normal inflammatory response with the typical presence of neutrophils in a first stage and macrophages, lymphocytes and giant cells in a later stage. Vascularization was observed, increasing with time, by the presence of blood vessels in the surrounding tissue and within the implant. Moreover, collagen deposition, vizualized by Masson trichrome stain, increased over time inside of the implant. During the entire *in vivo* experiment the scaffolds maintained the structural integrity, although after 12 weeks it was possible to observe cell colonization inside the fibrous structure. *In vitro* results showed a faster and greater degradation compared to those observed *in vivo.*

1. INTRODUCTION

Many biodegradable polymers have been proposed to produce scaffolds in Tissue Engineering field. These structures sustain the extracellular matrix (ECM) production by cells and at the same time, it is expected to degrade gradually to allow the surrounding tissue to replace the supporting function of the scaffold (1).

Biodegradable polymers are able to act as a a temporary substrate that will degrade over time, in a controlled way into products, which will be eliminated by regular metabolic pathways in the body (biodegradation) (2). Furthermore, the biological performance of some biomaterials depends on their degradation behavior, since this process influences cell performance and inflammatory response. Therefore, it is crucial to study the degradation properties of the scaffold for a long term success of the tissue engineered construct (3).

In the last years, natural biodegradable polymers have been used to produce scaffolds for tissue engineering. Due to their resemblance with the ECM, natural polymers may avoid the stimulation of chronic inflammation or toxicity, generally found out for synthetic polymers (4). Chitosan, the partially deacetylated product of chitin, has emerged as one of the favorites, mainly because of the similarity to glycosaminoglycans (GAGs), native components of ECM (5). Additionally, the cationic nature of chitosan allows electrostatic interactions with anionic GAGs and proteoglycans (6).

In our group, we have been working with chitosan based scaffolds (7-15). One of the most promising biomaterials is the chitosan-poly(butylene succinate) processed into scaffolds by melt based technology (16-18). These scaffolds combine the biological properties of chitosan and the mechanical properties of aliphatic polyesters (17, 18). *In vitro* studies performed with different cell types showed a remarkable cell colonization of these scaffolds (10, 13, 14, 19). Chitosan has been proposed as a biomaterial for biomedical applications mainly due to its biocompatibility (20). Furthermore, it has been described as a potent wound healing accelerator (21-26), as well as to modulate the immune system by activating macrophages (27) to produce cytokines (28) and to inhibit infection (29).

Poly(butylene succinate) is a biodegradable synthetic polymer with good processability when compared to poly(lactic acid) or poly(glycolic acid) (30). Moreover, it shows good mechanical properties for bone tissue engineering, comparable to those of poly-caprolactone (31). The degradation profile of poly(butylene succinate) in the environment has been widely studied (32-34). Succinic acid is the main degradation product, which is an

intermediate of the tricarboxilic acid cycle, that ultimately degrades into carbon dioxide and water (32, 34).

Some biomaterials are degraded by hydrolysis, a non-enzymatic degradation, whose materials are mainly decomposed by contact with water or serum, being this process non specifically regulated (35). Biodegradation of polymeric biomaterials requires cleavage of hydrolytically and/or enzymatically sensitive bonds in the polymer, leading to polymer erosion (36). Degradation products should be non-toxic and free of immunogenicity. The resulting products should be small enough to dissolve in the body fluids and, after transportation via lymphatic system, the kidneys should be able to excrete them from the body (37). The degradation behavior of polymers can be tested previously *in vitro*, in order to predict their behavior when implanted *in vivo*. Usually, biomaterials are incubated in phosphate buffered solution, with or without enzymes, at 37ºC, under static and/or dynamic conditions to better simulate the *in vivo* conditions. It is common that degradation studies are performed in parallel with biocompatibility tests, both *in vitro* and *in vivo.* This close relation is due to the fact that the degradation of a biomaterial implanted in a host is influenced by the presence and recruitment of inflammatory cells and, consequently, by the production of inflammatory mediators.

In vivo, chitosan was shown to be degraded mainly by lysozyme (38-40). The degradation kinetics of chitosan is inversely related to the degree of deacetylation (39, 41), since this enzyme targets the acetylated residues of chitosan polymer (38, 40). Human lysozyme is found in several body fluids, including serum (42, 43), tears (42, 43), saliva (42, 43) and other fluids, like those surrounding cartilage (44). It is also important to highlight the fact that during inflammation process, neutrophils and macrophages cells will release enzymes, namely lysozyme and reactive oxygen species (45). On the other hand, PBS is an aliphatic polyester and these polymers are known to be degraded by lipases (46). This enzyme is water soluble, hydrolyzing ester bonds of triglycerides, phospholipids and cholesteryl esters (47, 48). Human lipases include pre-duodenal lingual, gastric, extra-duodenal pancreatic, hepatic, lipoprotein and endothelial lipases (49). Serum lipase is mainly derived from pancreatic cells, but tissues such as digestive track, adipose tissue, lungs and leucocytes also contain lipase (50, 51).

One of the most important requisites for clinical application of a biomaterial is its biocompatibility, that is defined as the ability of a material to perform, with an appropriate host response, in a specific application (52). The implantation of a biomaterial device sets off

a cascade of events that starts with an acute inflammatory response that may lead to a chronic inflammatory response. Polymorphonucleated cells (PMNs), macrophages and new blood vessels are present and granulation tissue can be developed, with subsequent foreign body reaction and fibrous capsule development (53). The inflammation process serves to contain, neutralize or dilute the injurious agent or process. Thus, the intensity and the duration of the inflammatory reaction may characterize the biocompatibility of a biomaterial (54). In the case of biodegradable polymers, the intensity of these responses may be modulated by the biodegradation process that can cause changes in shape, size, surface roughness, porosity and release of degradation products (54). Generally, the local reaction of an implant is studied after a 3 months implantation period, as described in the ISO standard 10993-6 (55). This time frame usually reflects a steady state, where the local acceptance/rejection can be evaluated.

In this work we studied the biodegradation process, as well as the biocompatibility of chitosan-poly(butylene succinate) fiber mesh scaffolds. The tests *in vitro* involved enzymes responsible for the degradation of chitosan and PBS, lysozyme and/or lipase, respectively. The *in vitro* degradation studies were carried out using the enzymes in concentrations similar to those present in the human blood serum. *In vivo* studies were performed with the main aims of studying the biodegradation and the biocompatibility of these scaffolds, using a subcutaneous model in Wistar rats during 3 months of implantation.

2. MATERIALS AND METHODS

2.1. Scaffolds production

The processing methodology is described in previous works from our group (19). Briefly, chitosan was melt blended with polybutylene succinate by extrusion (50% wt). The resulting extrudate was grinded into powder and processed into microfibers also by extrusion. The fibers were cut and submitted to hot compression. In this study the scaffolds dimensions were 6.5 mm diameter and 1 mm. The scaffolds were sterilized by ethylene oxide to be further used in subsequent tests.

2.2. *In vitro* degradation studies

Degradation studies were performed in triplicate by incubating the scaffolds in phosphate-buffered saline solution (pH 7.4) (control), with lipase from *aspergillus oryzal* (Fluka) (110 U/L) and/or lysozyme chicken egg white (Sigma) (13 mg/L). The concentrations used were similar those found in human blood serum, at 37ºC in dynamic conditions (60 rpm) for 1, 3, 6 and 12 weeks. At the end of each degradation period, the samples were removed and immediately weighed to determine the water uptake and dried for later calculation of the weight loss.

2.2.1. Water uptake and weight loss measurements

All samples were weighed before incubation in phosphate buffered saline or enzymatic solutions (initial weight). After 1, 3, 6 and 12 weeks, three samples of each condition were removed and immediately weighed for determination of water uptake (Equation 1), washed thoroughly with distilled water and dried for later calculation of weight loss (Equation 2),

$$\text{Water uptake (\%)} = [(w_w - w_i)/ w_i] \times 100 \qquad \text{(Equation 1)}$$

$$\text{Weight loss (\%)} = [w_i - w_f)/ w_i] \times 100 \qquad \text{(Equation 2)}$$

where w_i is the initial weight, w_w is the wet weight and w_f is the final weight of the sample.

2.2.2. Analysis of sample morphology by scanning electron microscopy

The samples morphology, before and after degradation with the different solutions was analyzed by scanning electron microscopy (NanoSEM, FEI company, USA).

2.3. *In vivo* degradation studies

One day before subcutaneous implantation surgery the implants were immersed in phosphate buffered saline solution under sterile conditions. Twelve adult male Wistar Han rats (41-44 days old at the beginning of the experiment), *Specified Pathogen Free*, were

purchased from Charles River Laboratories, France. The animals were kept one week in a quarantine room and transferred to a conventional maintenance room of the experimental unit of the animal facility, where they were housed for the all period of the experiment.

For the present study, 12 animals were used for subcutaneous implantation of acellular scaffolds. At 1, 3, 6 and 12 weeks, samples were retrieved for further analysis. Animals were anesthetized by an intraperitoneal injection of a solution of 75//0.5 mg/kg body weight ketamine/metedomidine (Imalgene®/Dorbenvet®). After confirming depth of anesthesia by pedal reflex, the dorsum of the animals was shaved and they were placed in ventral position. The incision site at the dorsal skin was disinfected with clorohexidine and 2 medial longitudinal incisions were performed. Subcutaneous pockets were created and 4 scaffolds were placed in each animal, away from the suture site (incision) to avoid inflammation of the wound. The incisions were closed with a 4.0 silk suture (Look, Harvard, USA), which was removed 10 days after surgery in the animals with longer implantation periods. The anesthesia was then reverted with a subcutaneous injection of 0.25 mg/kg Atipamezol (Antisedan®). Once animals become active, they were placed in their home cages and water and food were supplied *ad libitum*. Each animal received a subcutaneous injection of 1mg/kg analgesic Butorphanol (Torbugesic®) administered immediately after surgery and 24h later, to avoid post-operative pain. At each time point, animals were euthanized by intraperitoneal injection of sodium penthobarbital, at a lethal dose, and the respective implants retrieved.

All procedures were conducted in accordance with European regulations for animal laboratory testing (European Union Directive 86/609/EEC).

2.4. Histological evaluation

2.4.1. Implants processing and H&E staining

The implants were collected with the surrounding tissues and processed for histology. The retrieved implants together with the surrounding tissue were fixed in 10% neutral buffered formalin. The specimens were cut to obtain 3 μm thickness longitudinal and transverse sections to analyse the kinetics of degradation of the scaffolds. Sections were stained with hematoxylin and eosin (H&E) to evaluate the *in vivo* degradation and cellular infiltration throughout the implants.

2.4.2. Masson's trichrome staining

Masson's trichrome stain was used to evaluate the amount and the distribution of mature collagen. This stain is useful to differentiate collagen fibers from other fibers, particularly smooth muscle and elastin. Masson trichrome stains collagen green, nuclei black and cytoplasm red.

2.4.3. Immunohistochemistry

Immunostaining for α-smooth muscle actin (α-SMA) antibody was performed to assess the vascularization degree. Antigen retrieval was heat induced in a water bath at 96ºC for 20 min, with incubation of the slides in citrate buffer (pH=6). The slides were washed with phosphate buffer saline and endogenous peroxidase was blocked with 0.6% hydrogen peroxide (H_2O_2) in methanol, at room temperature (RT) for 30 min. R.T.U. Vectastain® Universal Elite ABC Kit (Vector, VCPK-7200) was used for antibody incubation, according to the instructions of the manufacturer. Briefly, sections were incubated with primary antibody (Abcam, ab5694) overnight at 4ºC, in a humidified atmosphere. After washing with phosphate bufferes saline, antibody detection was revealed by using the Peroxidase Substrate Kit DAB (Vector, VCSK-4100). Slides were washed in water for 5 minutes and then counterstained with Harris' haematoxylin for nuclear contrast. All images were obtained using an Olympus BX61 Motorized System Microscope and attached video camera (Olympus DP70).

3. RESULTS AND DISCUSSION

3.1. Weight loss and water uptake

In this study, scaffolds based on chitosan-poly(butylene succinate) were prepared by melt spinning and fiber bonding (18, 19). The main aim of the *in vitro* degradation studies was to simulate physiological conditions using enzymes present in human serum, which are responsible for the degradation of chitosan-poly(butylene succinate) fiber mesh scaffolds.

Degradation studies using lysozyme and/or lipase were performed using dynamic (60 rpm). No differences were observed in the pH of the different degradation solutions after each incubation time.

The ability of a material to absorb water and its water permeability are important parameters to be studied, since it will influence the absorption of body fluids and the transfer of cell nutrients and metabolites throughout the materials. The water uptake data (Figure 1) shows that scaffolds immersed in phosphate buffered saline solution (control) in dynamic conditions without changing the solutions, have a hydration degree of approximately 40%. Those scaffolds were blends of chitosan (50% wt), an extremely hydrophilic material and poly(butylene succinate), known to be more hydrophobic than chitosan. When only lysozyme was present, the degradation of the scaffolds was quite similar to the control (Figure 1). However, in the presence of lipase or lipase with lysozyme, the water uptake of the materials had a remarkable increase (Figure 1). This behaviour might be due to degradation of the scaffolds in the presence of these enzymes.

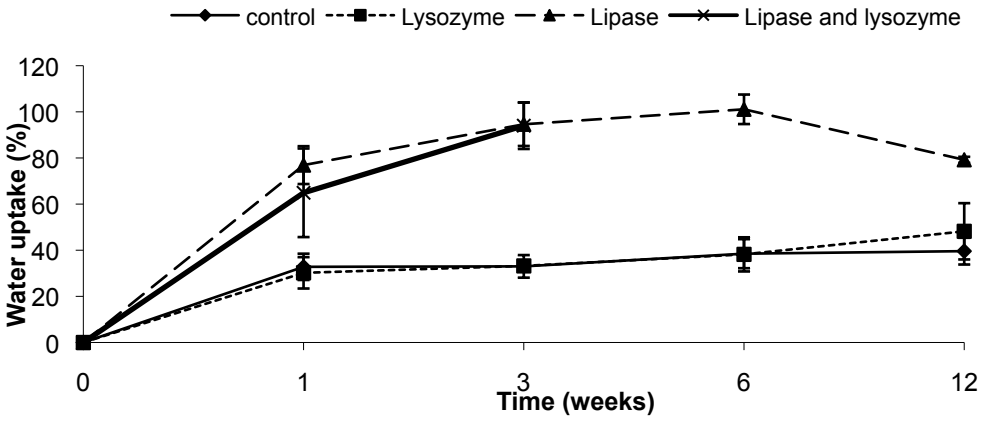

Figure 1. Water uptake of the scaffolds as a function of immersion time in PBS with lysozyme (13 mg/L), lipase (110 U/L) and both lipase and lysozyme. PBS alone was used as a control (pH 7.4, T=37ºC), in dynamic conditions.

When analyzing the weight loss profile using lysozyme or lipase, few differences were observed (Figure 2). The degradation of chitosan in the human body has been reported to be mediated by lysozyme (39, 40). The scaffolds immersed in phosphate buffered saline supplemented with lysozyme presented the highest weight loss (5%) in the first week, as compared with the other conditions. The weight loss remained constant until the end of the experiment (Figure 2). It was clear that degradation of the scaffolds in the presence of lysozyme it was not pronounced. This result might be explained by the degree of deacetylation of chitosan used in this study. This chitosan has 85% deacetilation degree and

it is well documented in the literature that the degree of deacetylation is inversely related to the degradation rate (38, 41, 43).

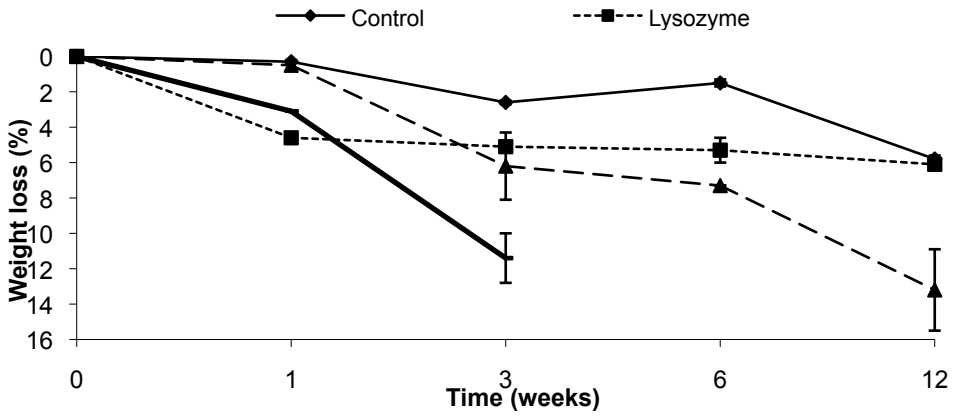

Figure 2. Weight loss of the scaffolds as a function of immersion time in PBS with lysozyme (13 mg/L), lipase (110 U/L), and both lipase and lysozyme. PBS alone was used as a control (pH 7.4, T=37ºC), in dynamic conditions.

Lipase is an enzyme responsible for the hydrolysis of ester bonds in polyesters (46, 56). In the presence of lipase the values of weight loss were higher than those obtained in the presence of lysozyme, increasing as a function of immersion time (Figure 2). Nevertheless, immersion periods up to 12 weeks did not cause the scaffolds to loose their structural integrity in the presence of either lysozyme or lipase.

In order to investigate the effect of an enzyme cocktail containing lipase and lysozyme, the scaffolds were also incubated with both enzymes. The highest weight loss was observed in the presence of lipase and lysozyme together (Figure 2). These results are in agreement with previous studies using different enzymatic cocktails (57, 58). In contrast with the other conditions, lipase and lysozyme together induced the loss of structural integrity of the scaffolds after 3 weeks. At the 6th week, all scaffolds lost their structural integrity in the presence of both enzymes.

3.2. Morphology of the scaffolds before and after *in vitro* degradation

The morphology of the scaffolds was studied before and after degradation with the different solutions by SEM (Figure 3). It is possible to observe the surface of the fibers before

degradation (Figures 3A and 3B). The surface of the fibers showed fractures as a result of degradation (Figures 3C, 3D, 3E, 3F, 3G, 3H, 3I and 3J). It is possible to observe that the samples incubated in phosphate buffered saline, evidence a rougher surface (Figures 3C and 3D). The scaffolds incubated with lysozyme solution (Figures 3E and 3F) presented cracks at the surface of the fiber, at the same level than in those incubated in phosphate buffered saline. This result may be explained by the fact that the chitosan used has a high level of deacetylation and it is well documented in the literature that for high degrees of deacetylation, lysozyme has a minimal effect on the polymer degradation (38). However for scaffolds incubated with lipase solution (Figures 3G and 3H) more cracks are visible at the surface of the fibers, which confirms that lipase, is attacking the polyester phase. The combination of both lysozyme and lipase (Figures 3I and 3J), as expected by the water uptake and weight loss results, evidenced larger cracks at the surface of the fibers.

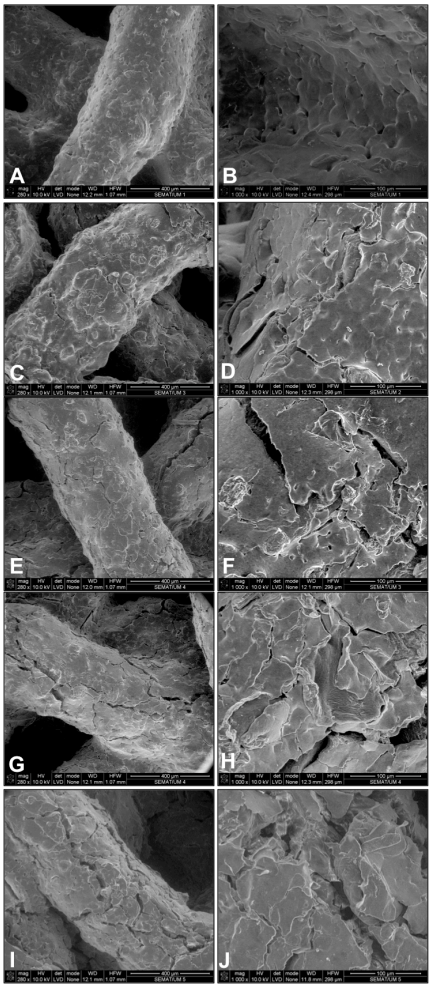

Figure 3. SEM micrographs showing the morphology of chitosan-poly(butylene succinate) scaffolds before degradation (A and B), after 12 weeks in PBS (C and D), plus lysozyme (E and F), lipase (G and H) and both lysozyme and lipase (I and J).

3.3. Biocompatibility assessment by histological analysis

No signs of infection were observed during the study or after surgery. Scaffolds were implanted subcutaneously and explants were retrieved after 1, 3, 6 and 12 weeks. Local tissue integration, inflammatory response and degradation behavior were assessed by histological stains (H&E and Masson´s thricrome).

The implantation of a biomaterial may result in injury to tissues or organs (53, 59). The tissue response to injury depends on various factors, including the extent of the injury, blood-material interactions, extent or degree of cellular necrosis, provisional matrix formation and the inflammatory response (54). Materials currently used in clinical applications considered non-immunogenic, non-toxic and chemically inert, elicit frequently acute and potential chronic inflammatory response (60).

Chitin and chitosan have been shown to accelerate wound healing and the attainment of a good healing surface. Histological findings suggest that these substances stimulate migration of polymorphonuclear and mononuclear cells and accelerate connective tissue regeneration and angiogenesis (61). It is also known that chitosan has the ability to attract neutrophils and activate macrophages (27, 62).

Histological sections of implanted scaffolds revealed that the porous morphology of the scaffolds is maintained after 7 days of implantation (Figure 4).

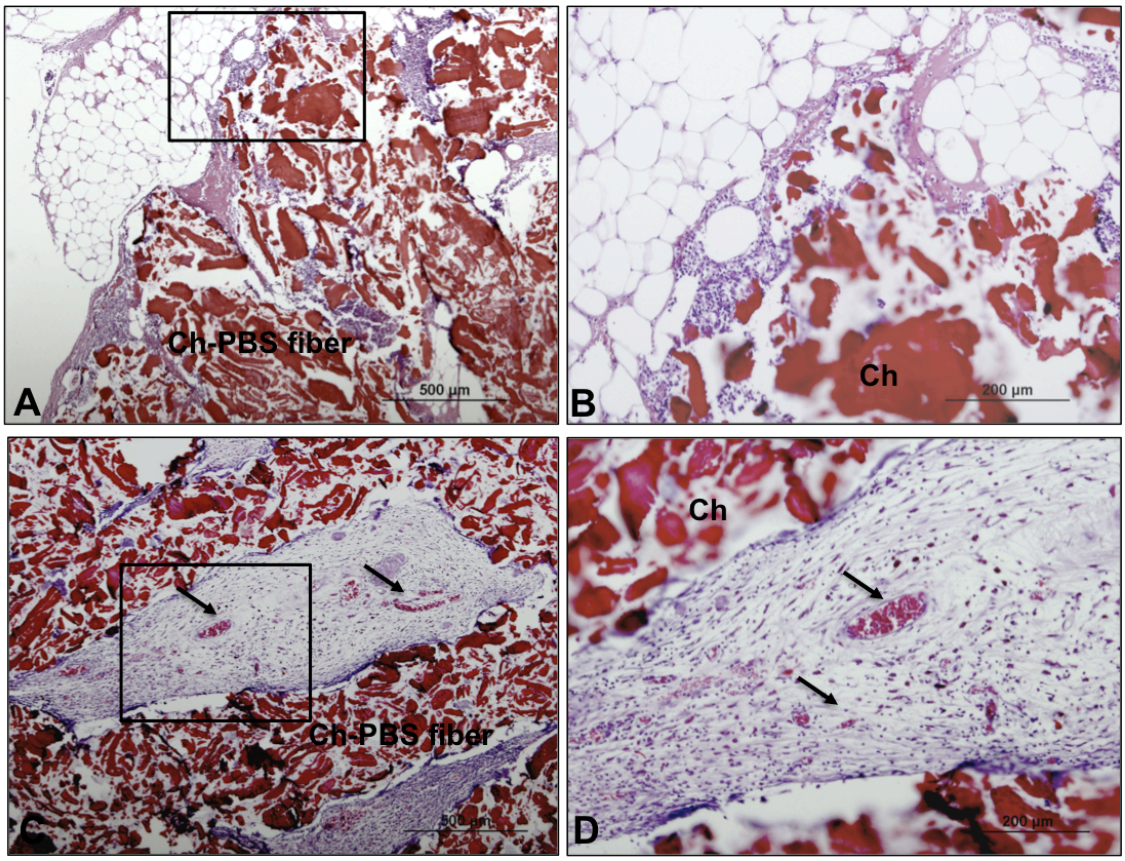

Figure 4. Representative H&E stained histological sections of tissues surrounding chitosan-based implants after (A, B) 1 week and (C, D) 3 weeks of subcutaneous implantation in Wistar rats. B and D represent the magnified sections of selected areas (squares) of A and B, respectively. Black arrows point to blood vessels. Ch – chitosan, PBS – poly(butylene succinate).

A detailed observation of the sections evidenced that the inflammatory infiltrate is mainly constituted of neutrophils (Figure 4B). Those cells are characterized by multilobulated nuclei, recruited from blood circulation, reacting to the implantation of chitosan-poly(butylene succinate) scaffolds. These cells are characteristic of the acute inflammatory response, which is the initial process of inflammation process. Acute inflammation has short duration (hours to days) and is characterized by exudation of fluid and plasma proteins (edema) and the emigration of leukocytes, mainly neutrophils. The major role of these cells in acute inflammatory response is to phagocytose microorganisms and foreign materials. In the case of biomaterials, neutrophils are not able to phagocytose them because of the size disparity (Figure 4B).

At 3 weeks of implantation, the presence of neutrophils was almost residual. It was clear the presence of blood vessels within the scaffold structure (Figures 5C and 5D). Furthermore, smooth muscle actin immunostaining is visible inside the fibers of the scaffold (Figure 5B), which indicates that connective tissue is growing and vascularization is increasing throughout the scaffold (11). At the same time, collagen is being deposited by fibroblasts (Figure 6B). The appearance of blood vessels and fibrosis is an indication of a chronic inflammatory response. This type of response emerges when a persistent stimulus is present (59).

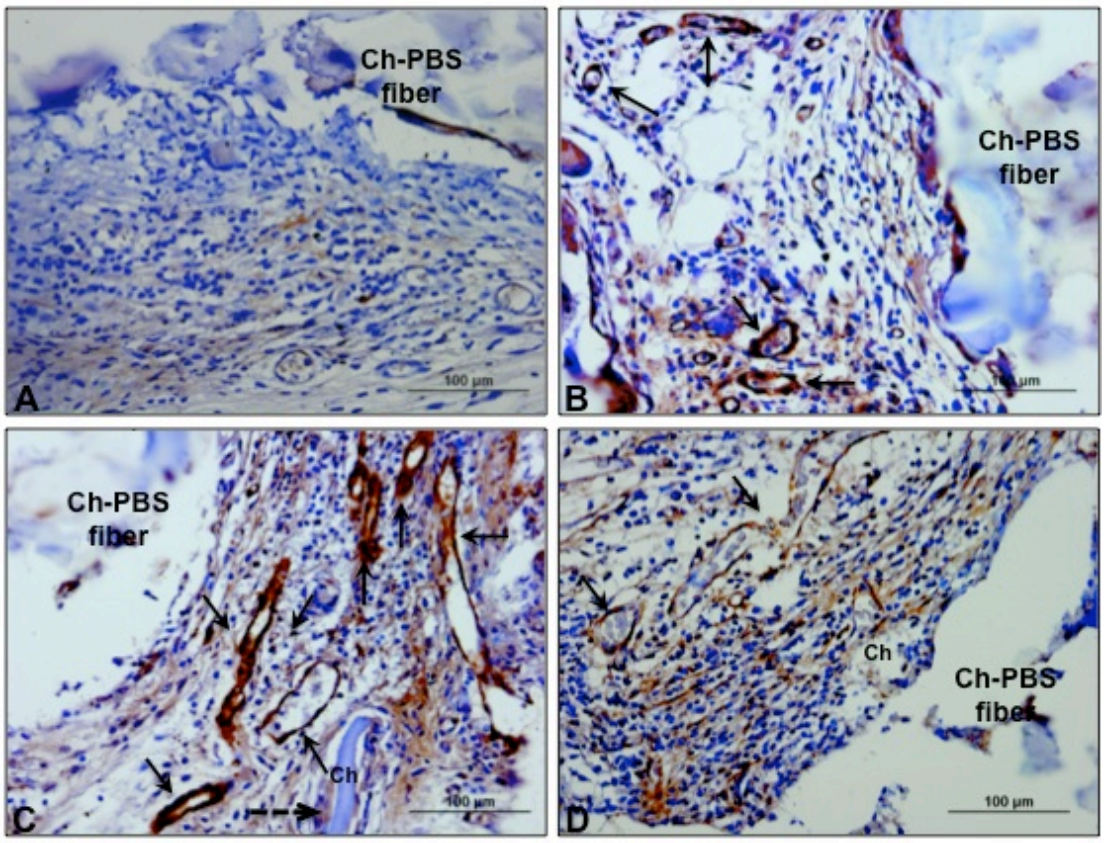

Figure 5. Representative α-SMA immunostained sections of tissues inside fibers of chitosan-poly(butylene succinate) mesh scaffolds after (B) 3 week, (C) 6 weeks and (D) 12 weeks of implantation. (A) Negative control. Black arrows point to new blood vessels. Dashed arrow points to a phagocyted chitosan particle. Ch – chitosan, PBS – poly(butylene succinate).

After 6 weeks of implantation (Figures 7A and 7B), it was possible to observe the evolution of the acute inflammatory response into a chronic response, by the presence of granulatomous tissue and giant cells. Chronic inflammatory response is longer than acute

and it is characterized by the presence of mononuclear cells, which includes macrophages, lymphocytes and plasma cells (63). Implantation of foreign materials elicits the normal foreign body reaction (FBR), *i.e.*, foreign body reaction composed of foreign body giant cells and granulation tissue development, constituted by macrophages, fibroblasts and capillaries (54). Biodegradable materials elicit a FBR that, with time will become chronic until final degradation. In the case of non-degradable materials, the reaction continues until a capsule is formed around the implant, isolating it and FBR from the local tissue environment (60). Foreign body giant cells are formed when material particles are too large to be phagocytosed by macrophages and these cells fuse. In figure 5C it could be observed the phagocytosis of a chitosan particle by giant cells (dashed arrow). A major organization of the tissue within the implant was observed, with marked presence of α-SMA (Figure 5C) and collagen deposition (Figure 6C).

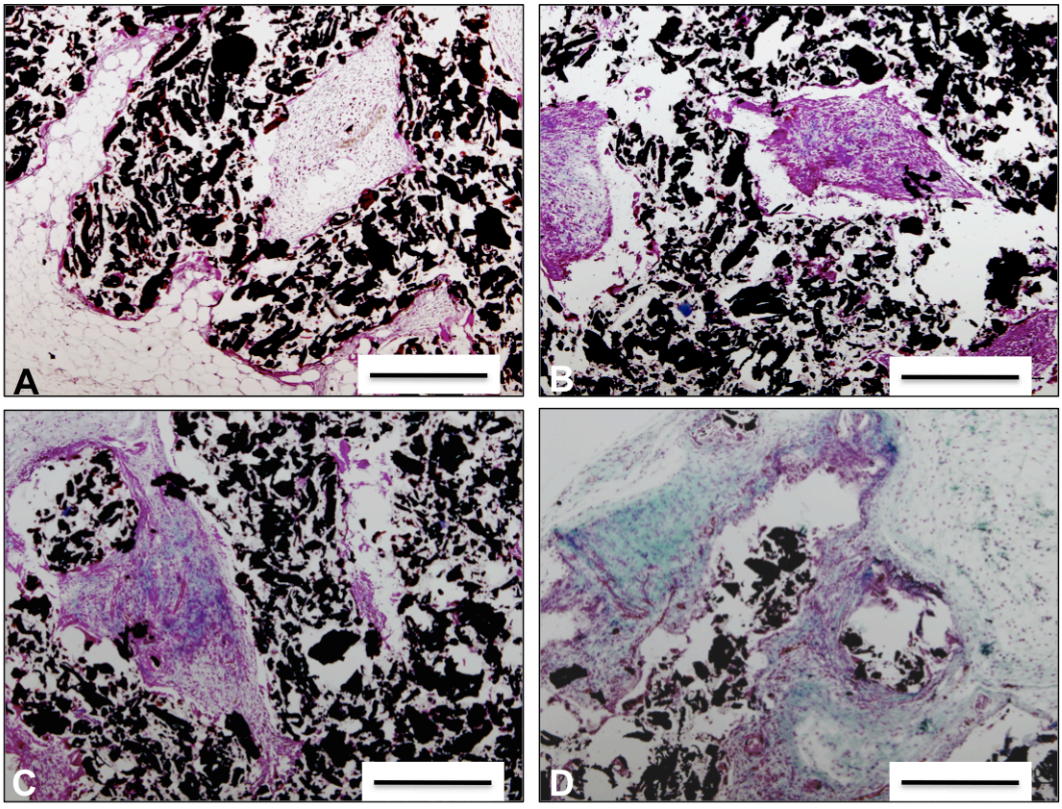

Figure 6. Masson´s thricrome stained sections of tissues of chitosan-poly(butylene succinate) mesh scaffolds after (A) 1 week, (B) 3 weeks, (C) 6 weeks and (D) 12 weeks of implantation. Green stain is collagen. Ch – chitosan, PBS – poly(butylene succinate). Bar correspond to 500 μm.

Up to 3 months, implanted scaffolds did not show evident signs of significant degradation. Histological findings only presented the ingrowth of cells within each fiber of the scaffold (Figures 8C and 8D). Giant cells attempted to phagocytose the particles of the scaffold, with some evidence, as presented in figure 6C.

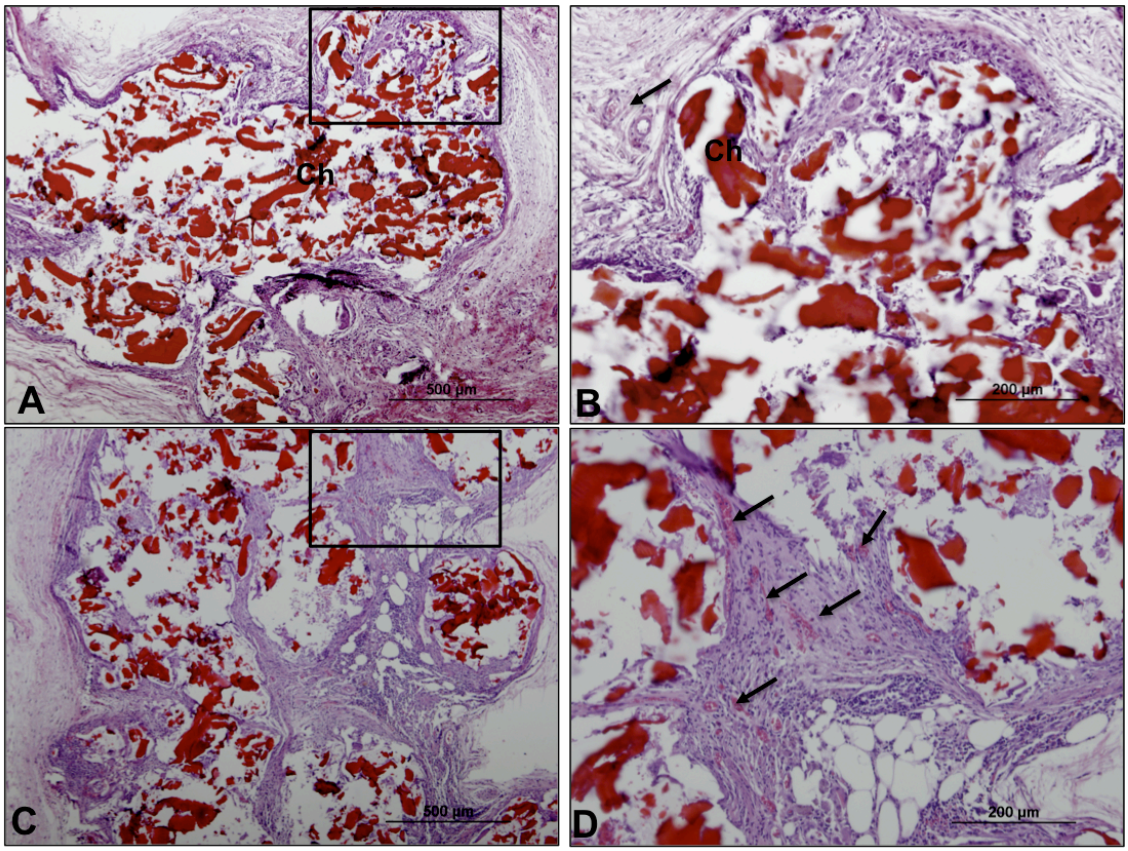

Figure 7. Representative H&E stained histological sections of tissues surrounding chitosan-based implants after (A, B) 6 week and (C, D) 12 weeks of subcutaneous implantation in Wistar rats. B and D represent the magnified sections of selected areas (square) of A and B, respectively. Black arrows point to new blood vessels. Ch – chitosan, PBS – poly(butylene succinate).

After 12 weeks of implantation (Figures 7C and 7D), all scaffolds maintained its shape and structure, in contrast with the *in vitro* results, which after 6 weeks incubated in lipase and lysozyme, the scaffolds lost their structural integrity (Figure 2). Thus, it is clear that *in vitro* degradation was much faster than *in vivo* degradation. One fact that must be highlighted is that the magnitude of tissue response to a biodegradable material depends upon the site of implantation (64). Another issue is the type of the enzymes used, that even at concentrations

similar to the ones found in human serum, are not from human origin and its action may be slightly different. Furthermore, in vitro tests provide a much more hydrated environment than the host environment in vivo. It is important to state as well that pH did not change during the entire in vitro experiment, being this a major factor contributing to medium acidification and accelerating the degradation effects (autocatalytic effect) (65). Since *in vivo* the degradation was slower it seems that pH also did not change, otherwise the scaffolds would evidence a higher degree of degradation.

4. CONCLUSIONS

The degradation rate of the scaffolds must be tailored appropriately accordingly with the growth rate of the new tissue. It was shown that an enzymatic cocktail with lysozyme and lipase (in concentrations equivalent at the ones found in human body) had a strong positive effect on the scaffolds degradation *in vitro*. After 12 weeks of implantation, scaffolds did not lose their structural integrity. It should be noted the difference in kinetics of biodegradation *in vitro* and *in vivo*. A fast degradation *in vivo* is not desirable, since the degradation should be compatible with the rate of tissue formation and bone defects may require some months to heal.

The implanted scaffolds displayed a normal and mild tissue response, with the development of chronic inflammatory response and foreign body reaction.

It is therefore worthwhile continuing to investigate the functional performance potential of chitosan-poly(butylene succinate) fiber mesh scaffolds for bone tissue engineering and regenerative medicine.

ACKNOWLEDEGMENTS

Ana Costa-Pinto was supported by a grant (SFRH/24735/2005) from the Portuguese Foundation for Science and Technology “Fundação para a Ciência e a Tecnologia” (FCT).

This work was partially supported by the European Network of Excellence EXPERTISSUES (NMP3-CT-2004-500283). The authors would like to acknowledge to Dr. Fernando Schmitt and Prof. Adhemar Longhatto for helping with the histological evaluation. The authors would also like to acknowledge to the School of Health Sciences of the University of Minho for the opportunity of using its facilities.

REFERENCES

1. De Jong W, Eelco B, Robinson J, Bos R. Tissue response to partially in vitro predegraded poly-L-lactide implants. Biomaterials. 2005;26(14):1781-91.
2. Azevedo H, Reis R. Understanding the enzymatic degradation of biodegradable polymers and strategies to control their degradation rate. In: Reis R, San Roman J, editors. Biodegradable systems in tissue engineering and regenerative medicine. Boca Raton: CRC Press; 2005. p. 177-201.
3. Babensee J, Anderson J, Mcintire L, Mikos A. Host response to tissue engineered devices. Advanced Drug Delivery Reviews 1998;33:111-39.
4. Mano J, Silva G, Azevedo H, Malafaya P, Sousa R, Silva S, et al. Natural origin biodegradable systems in tissue engineering and regenerative medicine:present status and some moving trends. Journal of Royal Society Interface. 2007;4:999-1030.
5. Nishikawa H, Ueno A, Nishikawa S, Kido J-i, Ohishi M, Inoue H, et al. Sulfated Glycosaminoglycan Synthesis and Its Regulation by Transforming Growth Factor-[beta] in Rat Clonal Dental Pulp Cells. Journal of Endodontics. 2000;26(3):169-71.
6. Di Martino A, Sittinger M, Risbud MV. Chitosan: a versatile biopolymer for orthopaedic tissue-engineering. Biomaterials. 2005;26(30):5983-90.
7. Tuzlakoglu K, Alves C, Mano J, Reis R. Production and characterization of chitosan fibers and 3D fiber mesh scaffolds for tissue engineering applications. Macromol Biosci. 2004;4(8):811-9.
8. Malafaya P, Pedro A, Peterbauer A, Gabriel C, Redl H, Reis R. Chitosan particles agglomerated scaffolds for cartilage and osteochondral tissue engineering approaches with adipose tissue derived stem cells. Journal of Materials Science: Materials in Medicine. 2005;16:1077-85.
9. Oliveira JM, Rodrigues MT, Silva SS, Malafaya PB, Gomes ME, Viegas CA, et al. Novel hydroxyapatite/chitosan bilayered scaffold for osteochondral tissue-engineering applications: Scaffold design and its performance when seeded with goat bone marrow stromal cells. Biomaterials. 2006;27(36):6123-37.
10. Costa-Pinto AR, Salgado AJ, Correlo VM, Sol P, Bhattacharya M, Charbord P, et al. Adhesion, proliferation, and osteogenic differentiation of a mouse mesenchymal stem cell line (BMC9) seeded on novel melt-based chitosan/polyester 3D porous scaffolds. Tissue Eng Part A. 2008;14(6):1049-57.
11. Malafaya PB, Santos TC, van Griensven M, Reis RL. Morphology, mechanical characterization and in vivo neo-vascularization of chitosan particle aggregated scaffolds architectures. Biomaterials. 2008;29(29):3914-26.
12. Martins AM, Santos MI, Azevedo HS, Malafaya PB, Reis RL. Natural origin scaffolds with in situ pore forming capability for bone tissue engineering applications. Acta Biomater. 2008;4(6):1637-45.
13. Oliveira JT, Correlo VM, Sol PC, Costa-Pinto AR, Malafaya PB, Salgado AJ, et al. Assessment of the suitability of chitosan/polybutylene succinate scaffolds seeded with mouse mesenchymal progenitor cells for a cartilage tissue engineering approach. Tissue Eng Part A. 2008;14(10):1651-61.
14. Alves da Silva M, Crawford A, Mundy J, Correlo V, Sol P, Bhattacharya M, et al. Chitosan/polyester-based scaffolds for cartilage tissue engineering: Assessment of extracellular matrix formation. Acta Biomater, 2010;6:1149–1157.
15. Martins AM, Pereira RC, Leonor IB, Azevedo HS, Reis RL. Chitosan scaffolds incorporating lysozyme into CaP coatings produced by a biomimetic route: a novel concept for tissue engineering combining a self-regulated degradation system with in situ pore formation. Acta Biomater. 2009;5(9):3328-36.

16. Correlo VM, Boesel LF, Bhattacharya M, Mano JF, Neves NM, Reis RL. Properties of melt processed chitosan and aliphatic polyester blends. Materials Science and Engineering: A. 2005;403(1-2):57.
17. Correlo VM, Boesel LF, Pinho E, Costa-Pinto AR, Alves da Silva ML, Bhattacharya M, et al. Melt-based compression-molded scaffolds from chitosan-polyester blends and composites: Morphology and mechanical properties. J Biomed Mater Res A. 2009;91(2):489-504.
18. Correlo VM, Costa-Pinto AR, Sol P, Covas JA, Bhattacharya M, Neves NM, et al. Melt Processing of Chitosan-Based Fibers and Fiber-Mesh Scaffolds for the Engineering of Connective Tissues. Macromolecular Bioscience. 2010; DOI: 10.1002/mabi.201000011.
19. Costa-Pinto AR, Correlo VM, Sol PC, Bhattacharya M, Charbord P, Delorme B, et al. Osteogenic differentiation of human bone marrow mesenchymal stem cells seeded on melt based chitosan scaffolds for bone tissue engineering applications. Biomacromolecules. 2009;10(8):2067-73.
20. Shigemasa Y, Minami S. Applications of chitin and chitosan for biomaterials. Biotechnology & genetic engineering reviews. 1996;13:383-420.
21. Prudden JF, Migel P, Hanson P, Friedrich L, Balassa L. The discovery of a potent pure chemical wound-healing accelerator. The American Journal of Surgery. 1970;119(5):560-4.
22. Ishihara M, Ono K, Sato M, Nakanishi K, Saito Y, Yura H, et al. Acceleration of wound contraction and healing with a photocrosslinkable chitosan hydrogel. Wound Repair Regen. 2001;9(6):513-21.
23. Katsuaki O. Experimental evaluation of photocrosslinkable chitosan as a biologic adhesive with surgical applications. Surgery 2001;130:844-50.
24. Masayuki Ishihara, Kuniaki Nakanishi, Katsuaki Ono, Masato Sato, Makoto Kikuchi, Yoshio Saito, et al. Photocrosslinkable chitosan as a dressing for wound occlusion and accelerator in healing process. Biomaterials 2002;23:833-40.
25. Wang L, Khor E, Wee A, Lim LY. Chitosan-alginate PEC membrane as a wound dressing: Assessment of incisional wound healing. J Biomed Mater Res. 2002;63(5):610-8.
26. Azad AK, Sermsintham N, Chandrkrachang S, Stevens WF. Chitosan membrane as a wound-healing dressing: characterization and clinical application. J Biomed Mater Res B Appl Biomater. 2004;69(2):216-22.
27. Peluso G, Petillo O, Ranieri M, Santin M, Ambrosio L, Calabró D, et al. Chitosan-mediated stimulation of macrophage function. Biomaterials. 1994;15:1215-20.
28. Mori. Effects of chitin and its derivatives on the proliferation and cytokine production of fibroblasts in vitro. Biomaterials. 1997;18:947-51.
29. Nishimura K, Nishimura S, Nishi N, Saiki I, Tokura S, Azuma I. Immunological activity of chitin and its derivatives. Vaccine. 1984;2(1):93-9.
30. Haiyan L, Jiang C, Amin C, Junying W. In vitro evaluation of biodegradable poly(butylene succinate) as a novel biomaterial. Macromol Biosci. 2005;5:433-50.
31. Hutmacher DW, Schantz T, Zein I, Ng KW, Teoh SH, Tan KC. Mechanical properties and cell cultural response of polycaprolactone scaffolds designed and fabricated via fused deposition modeling. Journal of Biomedical Materials Research. 2001;55(2):203-16.
32. Bahari K, Mitomo H, Enjoji T, Yoshi F, Makuuchi K. Degradability of poly (3-hydroxybutyrate) and its copolymer grafted with styrene by radiation. Polymer Degradation and Stability. 1998;62:245-52.
33. Hirotsu T, Tsujisaka T, Masuda T, Nakayama K. Plasma surface treatments and biodegradation of poly(butylene succinate) sheets. Journal of Applied Polymer Science. 2000;78(5):1121-9.
34. Hashitani T, Yano E, Ando Y. Biodegradable Packing Materials for LSIs. Fujitsu Sci Tech J. 2002;38(1):112-8.
35. Hubbell JA. Biomaterials in Tissue Engineering. Nat Biotech. 1995;13(6):565-76.

36. Katti DS, Lakshmi S, Langer R, Laurencin CT. Toxicity, biodegradation and elimination of polyanhydrides. Advanced Drug Delivery Reviews. 2002;54(7):933-61.
37. van Dijkhuizen-Radersma R, Moroni L, Apeldoorn Av, Zhang Z, Grijpma D, Blitterswijk Cv, et al. Degradable polymers for tissue engineering. Tissue Engineering. Burlington: Academic Press; 2008. p. 193-221.
38. Hirano S, Tsuchida H, Nagao N. N-acetylation in chitosan and the rate of its enzymic hydrolysis. Biomaterials. 1989;10(8):574-6.
39. Tomihata K, Ikada Y. In vitro and in vivo degradation of films of chitin and its deacetylated derivatives. Biomaterials. 1997;18:261-8.
40. Varum. In vitro degradation rates of partially N-acetylated chitosans in human serum. Carbohydrate res. 1997;299:99-101.
41. Sashiwa H, Saimoto H, Shigemasa Y, Ogawa R, Tokura S. Lysozyme susceptibility of partially deacetylated chitin. International Journal of Biological Macromolecules. 1990;12(5):295-6.
42. Hankiewicz J, Swierczek E. Lysozyme in human body fluids. Clinica Chimica Acta. 1974;57(3):205-9.
43. Nordtveit RJ, Vârum KM, Smidsrd O. Degradation of partially N-acetylated chitosans with hen egg white and human lysozyme. Carbohydrate Polymers. 1996;29(2):163-7.
44. Muzzarelli RAA. Biochemical significance of exogenous chitins and chitosans in animals and patients. Carbohydrate Polymers. 1993;20(1):7-16.
45. Griffiths MM, Langone JJ, Lightfoote MM. Biomaterials and Granulomas. Methods. 1996;9(2):295-304.
46. Tokiwa Y, Suzuki T. Hydrolysis of polyesters by lipases. Nature. 1977;270(5632):76-8.
47. Wong H, Schotz MC. The lipase gene family. J Lipid Res. 2002 July 1, 2002;43(7):993-9.
48. Hasham SN, Pillarisetti S. Vascular lipases, inflammation and atherosclerosis. Clinica Chimica Acta. 2006;372(1-2):179-83.
49. Mukherjee M. Human digestive and metabolic lipases--a brief review. Journal of Molecular Catalysis B: Enzymatic. 2003;22(5-6):369-76.
50. Tietz N, Shuey D. Lipase in serum--the elusive enzyme: an overview. Clin Chem. 1993 May 1, 1993;39(5):746-56.
51. Azevedo HS, Gama FM, Reis RL. In Vitro Assessment of the Enzymatic Degradation of Several Starch Based Biomaterials. Biomacromolecules. 2003;4(6):1703-12.
52. Williams DF, A. R. Immune response in biocompatibility. Biomaterials. 1992;13(11):731-41.
53. Anderson JM. Mechanisms of inflammation and infection with implanted devices. Cardiovascular Pathology. 1993;2(3, Supplement 1):33-41.
54. Anderson JM. Biological responses to materials Annu Rev Mater Res. 2001;31:81-110.
55. ISO IOfS. Biological evaluation of medical devices. Part 6: tests for local efects after implantation. Geneva: International Organization for Standardization; 1994.
56. Marten E, M¸ller R-J, Deckwer W-D. Studies on the enzymatic hydrolysis of polyesters I. Low molecular mass model esters and aliphatic polyesters. Polymer Degradation and Stability. 2003;80(3):485-501.
57. Balmayor E, Tuzlakoglu K, Marques A, Azevedo H, Reis R. A novel enzymatically-mediated drug delivery carrier for bone tissue engineering applications: combining biodegradable starch-based microparticles and differentiation agents. Journal of Materials Science: Materials in Medicine. 2008;19(4):1617-23.
58. Gomes ME, Azevedo HS, Moreira AR, Ellä V, Kellomäki M, Reis RL. Starch–poly(ε-caprolactone) and starch–poly(lactic acid) fibre-mesh scaffolds for bone tissue engineering

applications: structure, mechanical properties and degradation behaviour. Journal of Tissue Engineering and Regenerative Medicine. 2008;2(5):243-52.
59. Anderson JM. Inflammatory Response to Implants. ASAIO Journal. 1988;34(2):101-7.
60. Luttikhuizen DIT, Harmsen MC, Luyn MJAV. Cellular and Molecular Dynamics in the Foreign Body Reaction. Tissue Engineering. 2006;12(7):1955-70.
61. Muzzarelli R, Baldassarre V, Conto F, Ferrara P, Biagini G, Gazzanelli G, et al. Biological activity of chitosan: ultrastructural study. Biomaterials. 1988;9(3):247-52.
62. Usami Y, Okamoto Y, Takayama T, Shigemasa Y, Minami S. Chitin and chitosan stimulate canine polymorphonuclear cells to release leukotriene B4 and prostaglandin E2. Journal of Biomedical Materials Research. 1998;42(4):517-22.
63. Kumar V, Abbas K, Fausto N, Aster j. Acute and Chronic Inflammation. Robbins & Cotran Pathologic Basis of Disease: Saunders; 2010.
64. Ferreira L, Rafael A, Lamghari M, Barbosa MA, Gil MH, Cabrita AMS, et al. Biocompatibility of chemoenzymatically derived dextran-acrylate hydrogels. Journal of Biomedical Materials Research Part A. 2004;68A(3):584-96.
65. Lu L, Peter SJ, D. Lyman M, Lai H-L, Leite SM, Tamada JA, et al. In vitro and in vivo degradation of porous poly(-lactic-co-glycolic acid) foams. Biomaterials. 2000;21(18):1837-45.

SECTION 5

CHAPTER VII

Chitosan-poly(butylene succinate) scaffolds and human bone marrow stromal cells induce bone repair in a mouse calvaria model

This chapter is based on the following publication: Costa-Pinto AR, Correlo VM, Sol PC, Bhattacharya M, Srouji S, Livne E, Reis RL, Neves NM. "Chitosan-poly(butylene succinate) scaffolds and human bone marrow stromal cells induce bone repair in a mouse calvaria model". JTERM. 2010; Accepted for publication.

CHAPTER VII

Chitosan-poly(butylene succinate) scaffolds and human bone marrow stromal cells induce bone repair in a mouse calvaria model

ABSTRACT

Tissue Engineering sustains the need of a tridimensional (3D) scaffold to promote the regeneration of tissues in volume. Usually, scaffolds are seeded with an adequate cell population allowing its growth and maturation upon implantation *in vivo*.

Previous studies obtained by our group evidenced significant growth patterns and osteogenic differentiation of human bone marrow mesenchymal stem cells (hBMSCs) when seeded and cultured on melt based porous chitosan fiber mesh scaffolds. Therefore, it is crucial to test the *in vivo* performance of the *in vitro* 3D constructs.

In this study, chitosan based scaffolds were seeded and cultured *in vitro* with hBMSCs for 3 weeks under osteogenic stimulation conditions and analyzed for cell adhesion, proliferation and differentiation. Implantation of 2 weeks pre-cultured constructs in osteogenic culture conditions was performed into critical cranial sized defects in nude mice. The objective of this study was to verify the scaffold integration and new bone formation. At 8 weeks of implantation, scaffolds were harvested and prepared for micro computed tomography analysis (μCT). Retrieved implants showed good integration with the surrounding tissue and significant bone formation, more evident for the scaffolds cultured and implanted with human cells.

Results of this work demonstrated that chitosan based scaffolds, besides supporting *in vitro* proliferation and osteogenic differentiation of hBMSCs, induced bone formation *in vivo*. Thus, it was validated its osteogenic potential in orthotopic location in immunodeficient mice, evidencing good prospects for its use in bone tissue engineering therapies.

1. INTRODUCTION

Tissue Engineering has emerged in the last 17 years as a new regenerative approach for the treatment of a variety of tissues, including bone. The concept is based on the development of strategies aimed at obtaining tissue and organ equivalents, that can replace or restore the natural features and physiological functions of natural tissues *in vivo* (1). One of the fundamental principles relies on the need of a specific cell population in combination with a 3D structure, in order to promote, in volume, tissue regeneration (2)

The ideal cell population is considered to be autologous undifferentiated stem cells that can be isolated from adult sources. Although embryonic stem cells display an enormous potential, they raise ethical and moral issues, mainly because of the removal and destruction of human embryos (3). In this context, adult stem cells present an alternative option, being isolated from several sources, such as bone marrow (4), brain, liver, skin, skeletal muscle, intestine, pancreas, peripheral blood, dental pulp (3), adipose tissue (5) or fetal tissues such as umbilical cord (6) or amniotic fluid. Stem cells are defined as cells that have clonogenic and self-renewing capabilities and that differentiate into multiple cell lineages (7).

Mesenchymal stem cells (MSCs) can be combined with appropriate carriers – scaffolds – where a cell population will be grown and further implanted *in vivo*. Scaffolds used for tissue engineering purposes mimic the extracellular matrix (ECM) of the regenerating bone environment. Selection of the material for scaffold production in bone related applications is a very important step towards the creation of a tissue-engineered construct (8).

In the last years, natural polymers emerged as an alternative to synthetic polymers, mainly due to their biocompatibility and biodegradability. Most of the synthetic biomaterials are effective in supporting bone regeneration, either alone or in conjunction with growth factors, although they display limitations. Ideally this structure should be biodegradable, allowing cells to adhere and proliferate, leading to the formation of ECM (9). Different natural based polymers have been proposed for this demanding application, such as starch (10, 11) and chitosan (12-15). Chitosan has shown an excellent combination of properties, including non-antigenicity and non-cytotoxicity, making this biomaterial quite attractive for bone tissue engineering applications (16, 17).

We have developed a set of biomaterials using the thermal based processing of thermoplastic polymers, by blending chitosan (Ch) with different aliphatic polyesters such as, poly-(ε-caprolactone) (PCL), poly(butylene succinate) (PBS), poly(butylene terephthalate adipate) (PBTA), and poly(butylene succinate adipate) (PBSA) (18, 19). After testing the

eventual cytotoxicity of the developed scaffolds, the next step consisted on the biological screening of the most suitable scaffold formulation for bone tissue engineering applications. For that, we tested several blends with a mouse mesenchymal stem cell line (BMC9), promoting the differentiation into the osteogenic lineage. Results evidenced that the chitosan–PBS blend formulation, 50% wt, and 60% porosity, showed the best performance in terms of cell behavior (13). Further studies were performed using human bone marrow mesenchymal stem cells (hBMSCs) in fiber mesh scaffold morphology, with excellent results, in terms of cell adhesion, proliferation and osteogenic differentiation (15). Also, osteogenic differentiation of these cells onto the scaffolds was consistently detected by the presence of mineralized ECM (20, 21). Therefore, the fibrous morphology enhanced conditions to promote cell infiltration into the inner regions of the scaffold.

Thus, the next step is to evaluate this tissue engineering strategy *in vivo,* using a feasible animal model. For that, we have selected the cranial defect in nude mice (22, 23) since it enables testing several aspects of this strategy. Calvaria is a flat bone, which allows the creation of a uniform circular defect with an adequate size for easier surgical procedure and specimen handling. Fixation is provided by the *dura mater* and the overlying skin. The model has been thoroughly used and studied and is well reproduced (22-24). The low vascularization in cranial area turns this model one of the toughest to evaluate the *in vivo* performance of tissue engineered constructs (25). The nude mouse model is required since human cells will be implanted, avoiding graft rejection responses from the host (20). The critical size defect (CSD) for this model is 4-5 mm. A CSD is defined as the intraosseous wound in a specifically bone and species of animal without spontaneous healing during the lifetime of the animal (21).

Herein, we have selected compression molded - salt leaching scaffolds. We considered this production method as the most appropriate for the development of scaffolds that meet the required dimensions to fit into the animal calvaria defect. In the present study, we have assessed the *in vitro* biological behavior of hBMSCs cultured on Ch-PBS scaffolds, and these 3D constructs were validated in an *in vivo* model of a critical cranial defect in nude mice.

2. MATERIALS AND METHODS

2.1. Scaffolds production

The scaffolds used in this study were produced by melt based compression molding followed by salt leaching. Briefly, chitosan was melt blended with PBS (50% in weight) by extrusion and further grinded into a powder. This powder was subjected to a solid mixing with salt particles with size between 250 and 500 μm, and a salt content of 60%. Details on the processing methodology can be found elsewhere (19).

2.2. Scaffolds characterization

Cross-sections of all the developed scaffolds were analyzed using a Leica-Cambridge S-360 Scanning Electron Microscope (SEM) for preliminary assessment on their morphology. All the samples were sputter-coated with gold prior to the SEM analysis.

To evaluate the internal 3D structure of the scaffolds, micro computed tomography equipment (SkyScan, Belgium) was used as a non-destructive characterization methodology. Three scaffolds were scanned in high resolution mode of 8.7 μm x/y/z and an exposure time of 1792 ms. The scanner energy was set to 63 keV with 157 μA current. μCT scans followed by 3-D reconstruction (μCT analyzer and a μCT Volume Realistic 3D Visualization, from SkyScan) of serial image sections allowed to reconstruct and analyze the 3D microarchitecture of the scaffolds, pore morphology, determination of porosity and interconnectivity.

2.3. *In vitro* cell culture

Human bone marrow mesenchymal stem cells were isolated from bone marrow and characterized for the MSC phenotype (26). Cells were expanded in alpha minimum essential medium (α-MEM) (Sigma, St. Louis, MO) with 10% fetal bovine serum (Biochrom AG, Germany), 1 ng/ml basic fibroblast growth factor (bFGF) (PeproTech, USA) and 1% of antibiotic/antimycotic mixture (Sigma, St. Louis, MO). When a sufficient cell number was obtained, cells at passage 2 were seeded onto scaffolds at a density of $2.5x10^5$ cells/scaffold. After 24 hours of attachment, constructs were placed in new 24-well plates and 1 ml of osteogenic medium containing dexamethasone 10^{-8} M (Sigma, St. Louis, MO), ascorbic acid

50 µg/ml (Sigma, St. Louis, MO) and β-glycerophosphate 10 mM (Sigma, St. Louis, MO) was added to each well. The constructs were cultured for 7, 14, and 21 days in a humidified atmosphere at 37ºC, containing 5% CO_2.

2.3.1. Cell adhesion and morphology by scanning electron microscopy (SEM)

Cell adhesion, morphology and distribution throughout the scaffolds were analyzed by SEM. Constructs were fixed and dehydrated using a sequence of ethanol gradients and further sputter coated with gold (JEOL JFC-1100) to analyze using a Leica Cambridge S360 scanning electron microscope.

2.3.2. Cell viability assay - MTS test

Cell viability was assessed after 3 hours, 7, 14, and 21 days using the MTS test. Constructs (*n*=3) were washed in phosphate buffered saline (Sigma, St. Louis, MO), immersed in a mixture consisting of serum-free cell culture medium and MTS reagent in a 5:1 ratio and incubated for 3 hours at 37 ºC in a humidified atmosphere containing 5% CO_2. Scaffolds alone incubated for the same time in osteogenic medium were used as controls. After this, 200 *µ*l (*n*=3) were transferred to 96 well plates and the optical density (O.D.) was measured on a microplate ELISA reader (BioTek, USA) using an absorbance of 490 nm.

2.3.3. Alkaline phosphatase (ALP) quantification

Samples were washed with phosphate buffered saline solution and transferred to 1.5 ml microtubes containing 1ml of ultra-pure water. Constructs (*n*=3) were cryopreserved at -80ºC for further analysis. Prior to ALP quantification, samples were thawed and sonicated for 15 min.

Alkaline phosphatase (ALP) activity was measured by the specific conversion of p-nitrophenol phosphate (pNpp) (Sigma, St. Louis, MO, USA) into p-nitrophenol (pNp). The enzymatic reaction was set up by mixing 100 ml of the sample with 300 ml of substrate buffer containing 1 M diethanolamine HCl (pH 9.8) and 2 mg/ml of pNp. The solution was further incubated at 37ºC for 1 hour and the reaction was stopped by adding a solution containing 2

M NaOH and 0.2 mM EDTA. The O.D. was determined at 405 nm. A standard curve was made using pNp values ranging from 0 to 20 μmol/ml.

2.4. *In vivo* cranial defect in nude mice

Athymic nude mice with 7 weeks old (Harlan, Jerusalem, Israel) were used to examine the healing of cranial critical size bone defects in response to transplants in the defects according to the method described previously (20). All procedures involving the use of animals were conducted in accordance with the guidelines of the Institutional Animal Care and Use Committee of the Technion, Israel.

The *in vitro* cell-scaffold constructs were cultured in osteogenic inducing medium for 2 weeks prior implantation. Each scaffold was seeded with $1x10^6$ cells. All surgeries were performed under a protocol approved by Animal Care and Use Committee of the Technion, Israel.

Two bilateral critical-size circular defects (5 mm diameter and 1 mm thick) were performed with a hand drill and trephine bit in the parietal bones of the skull on either side of the sagittal suture line (Figure 1). Care was taken not to damage the sagittal suture or to interrupt the *dura mater* beneath the bone. During the procedure, sterile saline was dripped over the drilling site in order to avoid extensive heating and to protect the brain. Figure 1 illustrates the location of the defects in the mice crania. Surgeries were performed under general anesthesia (xylazine:ketamine, 1:1 solution in saline) by intra peritoneal injection.

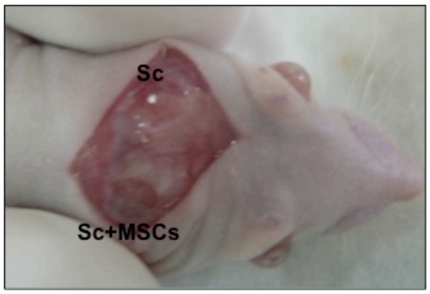

Figure 1. Low magnification image of cranial defects immediately after implantation. Cell/constructs (Sc+MSCs) and scaffolds without cells (Sc).

Scaffolds were randomly implanted into the defects and divided into 2 experimental groups that received the following implants: scaffolds seeded and cultured for 2 weeks with $1x10^6$ hBMSC and scaffold without cells A total of 6 nude mice were used and 12 cranial

defects were created. Animals were kept under aseptic conditions. After 8 weeks post-surgery, animals were euthanized and crania were removed, cleaned, and fixed immediately in formalin for 24 h to be analyzed by μCT analysis. Briefly, the mice crania (with or without cells) were also analyzed using a high-resolution μCT Skyscan 1072 scanner (Skyscan, Kontich, Belgium). Six specimens were scanned in high resolution mode using a pixel size of 19.13 μm and integration time of 1.7 ms. The X-ray source was set at 91 keV of energy and 110 μA of current. For all the scanned specimens representative data sets of 1023 slices were transformed into binary using a dynamic threshold of 255-120, to distinguish bone from polymeric material. This data was used for morphometric analysis (CT Analyzer v1.5.1.5, SkyScan). 3D virtual models of the mice crania were created, visualized, and registered using image processing software (ANT 3D creator v2.4, SkyScan).

2.5. Statistical analysis

Results of MTS and ALP are expressed as mean ± standard deviation with n=3 for each group. Statistical significance of differences was determined using Student's t-test multiple comparison procedure at a confidence interval of 95% (p<0.01).

3. RESULTS AND DISCUSSION

3.1. Scaffolds characterization

SEM micrographs of the porous scaffolds are presented in Figure 2. Figure 2a shows scaffolds morphology with 4 mm diameter and 1 mm thick. Previous studies (13, 27, 28) demonstrated that these scaffolds had adequate porosity to allow extensive cell proliferation (Figure 2b).

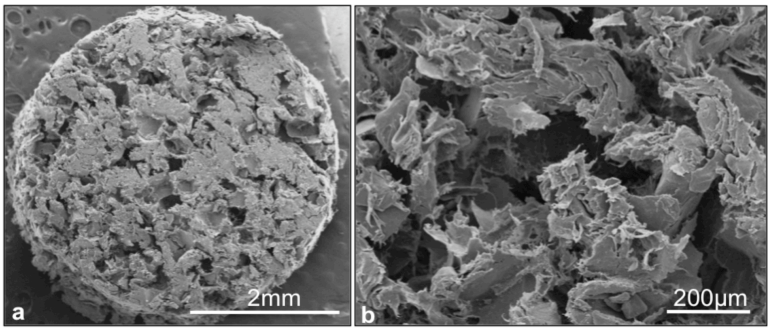

Figure 2. SEM micrographs showing a general a) and magnified views b) of Ch-PBS (50% wt) salt leaching scaffold.

For a detailed characterization of the scaffolds' internal structure, μCT studies were conducted. Images of the region of interest were acquired and transformed into binary images (Figure not shown). For all scaffolds, a dynamic threshold ranging from 255–150 gray scale values was used to distinguish polymer material from pore voids. Individual 2D analysis of the binary images (with a circle of interest of 4.5 mm^2) (Figure 2a) was obtained from the scaffold cross-sections (Figure 2a), consisting of 300 slices (Figure 2b) and used for morphometric analysis (Table I).

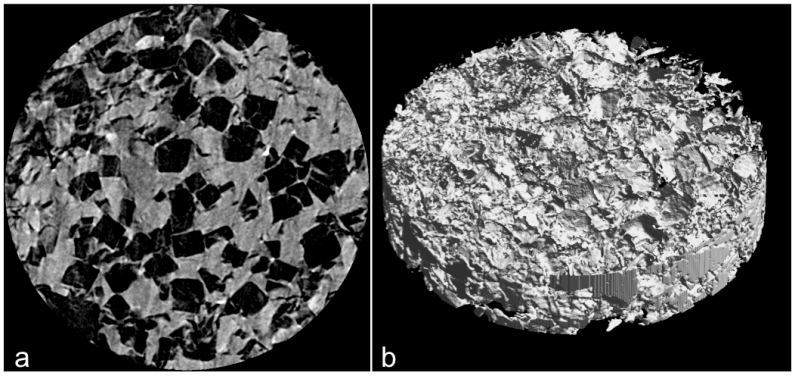

Figure 3. Representative 2D μCT image (a) and 3D μCT image of the scaffold obtained from the sequence of 2D sections (b).

Table I. Porosity, pore size and interconnectivity of the scaffolds produced from chitosan–PBS blend and salt particle size ranging from 250 to 500 μm

Porosity (%)	Pore size (mm)	Interconnectivity (%)
59.0±11.4	144.9±33.4	60.9±25.7

The overall porosity of approximately 60% is consistent with the amount of leachable NaCl particles used in scaffolds' preparation. The average pore size is lower than expected, since the selected range of NaCl particles used was between 250 and 500 micrometers. However, the mixing in the solid phase and the subsequent compression molding may cause significant reduction of the leachable particles, and consequently of the pore size. The level of interconnectivity indicates that most of the pores are open and probably allow cell infiltration into the scaffold' inner pores.

3.2. *In vitro* cell culture studies

3.2.1. Scanning electron microscopy (SEM)

SEM analysis showed that cells present a great affinity to the scaffolds surface, which is evident by the massive cell adhesion at the surface of the scaffolds (Figure 4).

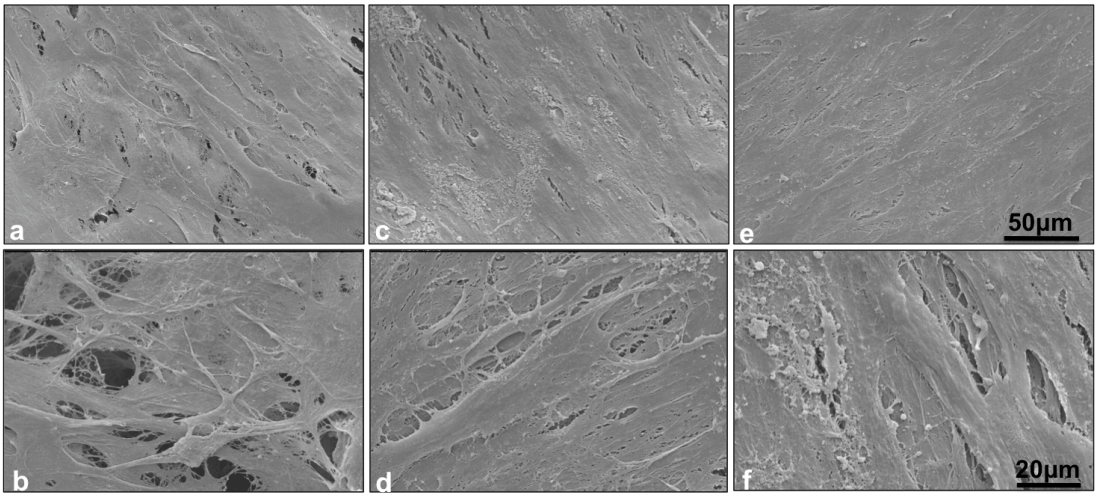

Figure 4. SEM micrographs of the seeded scaffolds cultured under osteogenic induction, after 1 week (a and b), 2 weeks (c and d) and 3 weeks (e and f).

Previous results also showed this cell behavior at the surface of similar scaffolds (15). After only 1 week of culture (Figures 4a and 4b) it was already visible a remarkable cell proliferation on the 3D structures. At the second week of culture, it was shown that a multilayer of cells is covering the surface of the 3D scaffold (Figures 4c and 4d). After 3 weeks of culture, it was visible that cell proliferation further developed into a dense multilayer cell structure (Figure 4e). Furthermore, it was clear the presence of Ca-P deposits (Figure 4f), corresponding to the produced mineralized ECM that was visible at higher magnifications. These results were confirmed by EDS analysis performed in samples cultured up to 21 days (Figure 5). Unseeded scaffolds (kept immersed in osteogenic medium for the same period of time) were used as control of EDS analysis. The presence of Ca and P peaks in the spectrum confirmed the presence of Ca and P elements at the surface of the cell seeded scaffolds, which indicated that cells are producing mineralized ECM and thus confirming the osteogenic differentiation after 21 days of culture.

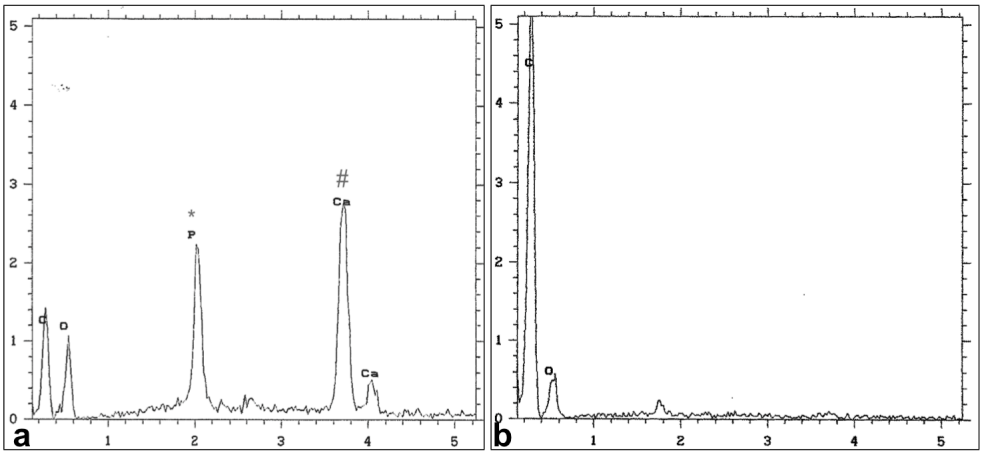

Figure 5. Energy dispersive spectra (EDS) showing the presence of calcium (#) and phosphorous (*) at the surface of the seeded chitosan-PBS (a), and scaffolds without cells (control) (b), after 3 weeks under osteogenic culture conditions.

3.2.2. Cell viability (MTS)

Cell viability assay (MTS) was used to assess the activity of the cells over time. Results demonstrated that hBMSCs seeded onto chitosan-PBS scaffolds were able to reduce MTS substrate and progressively increased its metabolic activity during the time of culture (Figure 6).

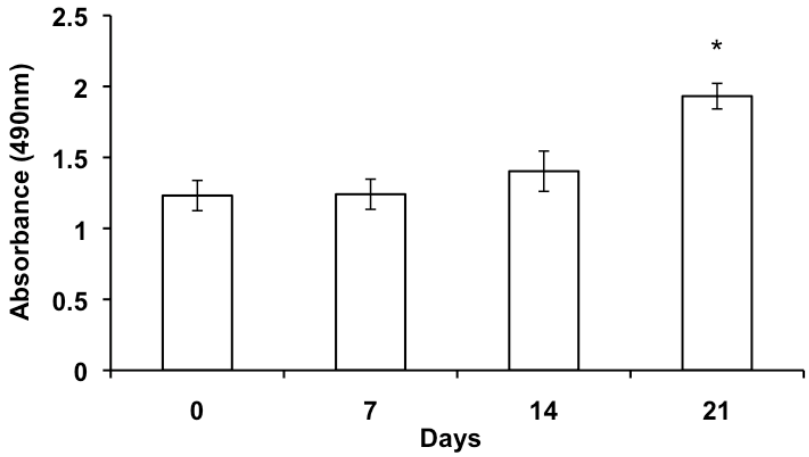

Figure 6. MTS viability assay of constructs and cultured Ch-PBS scaffolds following 3 hours (0 days), 7, 14 and 21 days, after cell seeding. Results are expressed as mean ± standard deviation with *n=3* for each bar, (*) indicate a significant difference ($p < 0.01$) between testing conditions as a function of time.

Cell viability assay (MTS) was used to assess the activity of the cells over time. Results demonstrated that hBMSCs seeded onto chitosan-PBS scaffolds were able to reduce MTS substrate and progressively increased its metabolic activity during the time of culture (Figure 6). The obtained optical density values show a significant increase after 21 days of culture. These results were corroborated by SEM images (Figure 4), with the increase of cell colonization over time. Furthermore, the presence of such active cells just after seeding (time 0), corresponded to a great seeding efficacy, which was due to the preference of the cells for these scaffolds, instead of the tissue culture plate. These results were in accordance with previous results using different cells cultured onto similar scaffold (13, 15, 27, 28).

3.2.3 Alkaline phosphatase activity (ALP)

The ALP activity of human MSCs cultured onto the scaffolds did not follow the typical trend of this marker of osteogenic differentiation, as it is demonstrated after 21 days (Figure 7). After this time point, a significant increase in ALP activity was observed (Figure 7). Usually, ALP reaches a peak at an earlier time point. However, the presence of visible deposits of mineralized matrix after 21 days (SEM images, cell viability and EDS results) suggests that cells were viable and continued to deposit matrix, thereby indicating the cells' osteogenic differentiation.

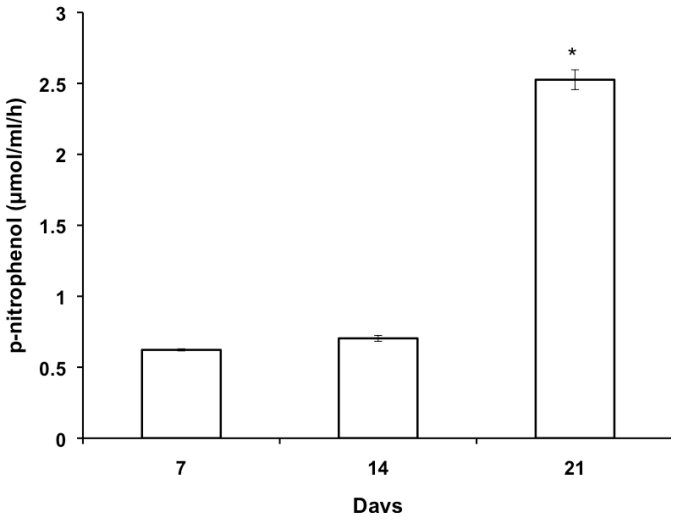

Figure 7. Alkaline phosphatase activity of hBMSCs cultured on the scaffolds after 1, 2 and 3 weeks under osteogenic induction. Results are expressed as mean ± standard deviation with n=3 for each bar, (*) indicates a significant difference ($p < 0.01$) between conditions as a function of time.

3.3. *In vivo* cranial defect in nude mice

After *in vitro* studies, the following step involved the *in vivo* validation, using a suitable animal model. For that, constructs were tested using a critical size cranial defect. Briefly, we planned a study using the critical size calvaria bone defect in nude mice, using Ch-PBS scaffolds and human cells. In this way, we were able to test both the viability of the 3D cell-construct *in vivo*, as well as the ability of those constructs to regenerate bone tissue. Cranial reconstruction represents a unique model to study bone regeneration, mainly because the calvaria is an anatomic area under limited mechanical stress, quite unlike the axial skeleton, which is subjected to long periods of compressive load (29). We used a 5 mm diameter defect, based in previous data found in the literature, showing that adult nude mice did not demonstrate significant calvaria bone healing in defects of 3, 4 and 5 mm in diameter (20).

Scaffolds' diameter was optimized to enable some swelling before implantation. Previous studies showed that these scaffolds have approximately 21% of water uptake. Based on these findngs, we have implanted scaffolds with 4.5mm of diameter to match the size of the defect at the time of implantation.

Bone formation was evaluated by μCT. This methodology is a low radiation and a non invasive method for studying the structure of bone samples. This technique can generate high-resolution images and provide the accurate quantitative analysis of the bone structure parameters (30).

Bone possesses some self-healing capacity. However, there is a limit to the size of bone fractures and defects that can be self-repaired. This limit is designated "critical size defect" (21, 23) and will not heal completely during the lifetime of the patient. For large bone defects, medical intervention is often necessary to repair the bone. In this study we have used hBMSCs cultured onto chitosan based scaffolds, in order to assess the ability of these tissue engineered constructs to induce bone regeneration in nude mice cranial critical size defects. To our knowledge, there are few studies documenting the use of xenogeneic grafs (*i.e.*, human cells and scaffolds) on the athymic nude mouse model (31-34). We have used nude mice in order to study the osteogenic potential of the hBMSCs seeded and cultured on Ch-PBS scaffolds, when implanted in a critical size defect. The μCT results suggested that after 8 weeks of implantation, constructs promoted bone regeneration of the calvaria critical size defect (Figure 8).

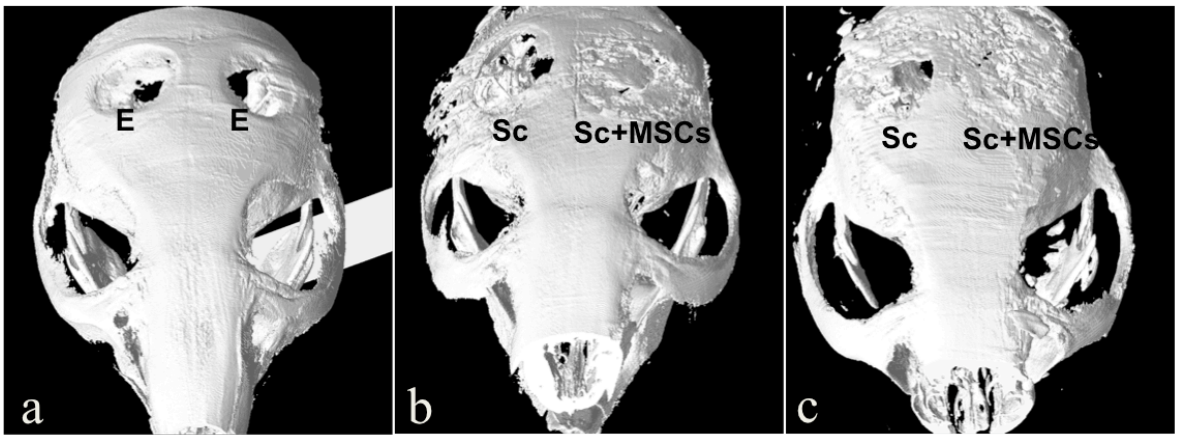

Figure 8. Micro computed tomography analysis of calvaria defects in nude mice. Images show the endpoint result after 8 weeks, of bone healing upon implantation of scaffolds in the cranial defect of nude mice. E – empty; Sc – scaffold alone; Sc+MSCs – scaffolds with hBMSCs pre-cultured *in vitro* in osteogenic medium.

Micro CT images also support that scaffolds cultured with MSCs presented enhanced bone ingrowth. Some of the images clearly show an almost complete healing of the defect (Figures 8b and 8c). These findings are in accordance with previous results where scaffolds seeded with pre-induced osteogenic MSCs enhanced bone regeneration in critical size defect when the same animal model was used (32). Scaffolds *per se* were able to induce some bone regeneration/ingrowth (Figure 8c). New bone formation could be due to invading reparative cells from the dura or from adjacent host tissues. The selected implantation time seemed to be adequate for assessing the complete bone healing at the site defect, as shown in figure 8c. Further studies need to be addressed using these scaffolds without cells, in immunocompetent animals, to confirm the tissue regeneration ability of Ch-PBS scaffolds.

4. CONCLUSIONS

In the present study, chitosan-poly(butylene succinate) scaffolds were successfully produced by melt-based compression molding followed by salt leaching. The microarchitecture of the scaffolds was assessed by SEM and μCT, revealing a fully porous and interconnected 3D structure.

In vitro cell culture studies using hBMSCs have shown properties compatible with

bone engineering applications. Cells evidenced high levels of viability as a function of cultured time and well correlated with SEM images that showed extensive cell colonization of the scaffolds. The produced ECM showed the presence of Ca and P elements, detected in EDS spectra of cultured scaffolds' surface, which confirmed the mineralization. Successful bone regeneration was achieved using the critical size defect in calvaria of nude mice, with prominent results for the *in vitro* cell construct compared to the scaffold without cells.

The combination of good biological performance of hBMSCs cultured onto chitosan based scaffolds and the ability to regenerate bone tissue in a critical size defect, significantly expands previous evidences that these materials can and will have a role to play in bone tissue engineering strategies.

This study evidenced very positive results that highlight the possibility of chitosan-PBS-hBMSCs constructs to be used as implants for non load-bearing bone defects.

ACKNOWLEDGMENTS

Ana Costa-Pinto was supported by the scholarship SFRH/24735/2005 from the Portuguese research council ''Fundação para a Ciência e a Tecnologia'' (FCT).

This work was partially supported by the EU Integrated Project GENOSTEM (Adult Mesenchymal Stem Cells Engineering for connective tissue disorders: from the bench to the bedside, LSHB-CT-2003-5033161) and the European Network of Excellence EXPERTISSUES (NMP3-CT-2004-500283).

REFERENCES

1. Langer R, Vacanti J. Tissue engineering Science. 1993;260(5110):920-6.
2. Hutmacher D, Schantz J, Lam C, Tan K, Lim C. State of the art and future directions of scaffold-based bone engineering from a biomaterials perspective. Journal of Tissue Eengineering and Regenerative Medicine. 2007;1:245-60.
3. Hipp J, Atala A. Sources of Stem Cells for Regenerative Medicine. Stem Cell Rev. 2008;4:3-11.
4. Bianco P, Robey P. Stem cells in tissue engineering. Nature 2001;414(6589):118-21.
5. Gimble J, Guilak F. Adipose-derived adult stem cells: isolation, characterization, and differentiation potential. Cytotherapy. 2003;5(5):362-9.
6. Sarugaser R, Lickorish D, Baksh D, Hosseini M, Davies J. Human Umbilical Cord Perivascular (HUCPV) Cells: A Source of Mesenchymal Progenitors. Stem cells. 2005;23:220-9.
7. Weissman I. Stem cells: units of development, units of regeneration, and units in evolution. Cell. 2000;100(157-168).
8. Martins A, Alves C, Reis R, Mikos A, Kasper F. Toward Osteogenic Differentiation of Marrow Stromal Cells and In Vitro Production of Mineralized Extracellular Matrix onto Natural Scaffolds. In: Puleo D, Bizios R, editors. Biological Interactions on Materials Surfaces. New York: Springer; 2009.
9. Salgado AJ, Coutinho OP, Reis RL. Bone tissue engineering: state of the art and future trends. Macromol Biosci. 2004 Aug 9;4(8):743-65.
10. Gomes M, Reis RL, Cunha AM, Blitterswijk CA, de Bruijn JD. Cytocompatibility and response of osteoblastic-like cells to starch-based polymers: effect of several additives and processing conditions. Biomaterials. 2001 Jul;22(13):1911-7.
11. Salgado A, Gomes M, Chou A, Coutinho O, Reis R, Hutmacher D. Preliminary study on the adhesion and proliferation of human osteoblasts on starch-based scaffolds. Materials Science and Engineering C. 2002;20:27-33.
12. Malafaya P, Pedro A, Peterbauer A, Gabriel C, Redl H, Reis R. Chitosan particles agglomerated scaffolds for cartilage and osteochondral tissue engineering approaches with adipose tissue derived stem cells. Journal of Materials Science: Materials in Medicine. 2005;16:1077-85.
13. Costa-Pinto AR, Salgado AJ, Correlo VM, Sol P, Bhattacharya M, Charbord P, et al. Adhesion, proliferation, and osteogenic differentiation of a mouse mesenchymal stem cell line (BMC9) seeded on novel melt-based chitosan/polyester 3D porous scaffolds. Tissue Eng Part A. 2008;14(6):1049-57.
14. Martins AM, Santos MI, Azevedo HS, Malafaya PB, Reis RL. Natural origin scaffolds with in situ pore forming capability for bone tissue engineering applications. Acta Biomater. 2008;4(6):1637-45.
15. Costa-Pinto AR, Correlo VM, Sol PC, Bhattacharya M, Charbord P, Delorme B, et al. Osteogenic differentiation of human bone marrow mesenchymal stem cells seeded on melt based chitosan scaffolds for bone tissue engineering applications. Biomacromolecules. 2009;10(8):2067-73.
16. Zarzycki R, Modrzejewska Z. Use of chitosan in medicine and biomedical engineering. Polim Med. 2003;33(1-2):47-58.
17. Di Martino A, Sittinger M, Risbud MV. Chitosan: a versatile biopolymer for orthopaedic tissue-engineering. Biomaterials. 2005 Oct;26(30):5983-90.
18. Correlo VM, Boesel LF, Bhattacharya M, Mano JF, Neves NM, Reis RL. Properties of melt processed chitosan and aliphatic polyester blends. Materials Science and Engineering: A. 2005;403(1-2):57.
19. Correlo VM, Boesel LF, Pinho E, Costa-Pinto AR, Alves da Silva ML, Bhattacharya M, et al. Melt-based compression-molded scaffolds from chitosan-polyester blends and

composites: Morphology and mechanical properties. J Biomed Mater Res A. 2009;91(2):489-504.
20. Gupta D, Kwan M, Slater B, Wan D, Longaker M. Applications of an athymic nude mouse model of nonhealing critical-sized calvarial defects. J Craniofac Surg 2008;19:192-7.
21. Wu X, Downes S, Watts DC. Evaluation of critical size defects of mouse calvarial bone: An organ culture study. Microscopy Research and Technique. 2010;73(5):540-7.
22. Schmitz J, Hollinger J. The Critical Size Defect as an Experimental Model for Craniomandibulofacial Nonunions. Clinical Orthopaedics and Related Research. 1986;205:299-308.
23. An Y, Freidman R. Animal Models in Orthopaedic Research. In: An Y, Freidman R, editors. 1st edition ed. Boca Raton, FL 1999,: CRC Press; 1998. p. 241.
24. Montjovent M, Mathieu L, Schmoekel H, Mark S, Bourban P, Zambelli P, et al. Repair of critical size defects in the rat cranium using ceramic-reinforced PLA scaffolds obtained by supercritical gas foaming. Journal of Biomedical Materials Research Part A. 2007;83A(1):41-51.
25. Castano-Izquierdo H, Alvarez-Barreto J, van den Dolder J, Jansen J, Mikos A, Sikavitsas V. Pre-culture period of mesenchymal stem cells in osteogenic media influences their in vivo bone forming potential. Journal of Biomedical Materials Research Part A. 2007;82:129-38.
26. Delorme B, Charbord P. Culture and characterization of human bone marrow mesenchymal stem cells. Methods Mol Med. 2007;140:67-81.
27. Oliveira JT, Correlo VM, Sol PC, Costa-Pinto AR, Malafaya PB, Salgado AJ, et al. Assessment of the suitability of chitosan/polybutylene succinate scaffolds seeded with mouse mesenchymal progenitor cells for a cartilage tissue engineering approach. Tissue Eng Part A. 2008;14(10):1651-61.
28. Alves da Silva M, Crawford A, Mundy J, Correlo V, Sol P, Bhattacharya M, et al. Chitosan/polyester-based scaffolds for cartilage tissue engineering: Assessment of extracellular matrix formation. Acta Biomaterialia. 2009;6: 1149–57.
29. Mankani M, Kuznetsov S, Wolfe R, Marshall G, Robey P. In Vivo Bone Formation by Human Bone Marrow Stromal Cells: Reconstruction of the Mouse Calvarium and Mandible. Stem Cells. 2006;24:2140-9.
30. Tuan HS, Hutmacher DW. Application of micro CT and computation modeling in bone tissue engineering. Computer-Aided Design. 2005;37(11):1151-61.
31. Cowan C, Shi Y, Aalami O, Chou Y, Mari C, Thomas R, et al. Adipose-derived adult stromal cells heal critical-size mouse calvarial defects. Nature Biotechnology. 2004;22(5):560-7.
32. Meinel L, Fajardo R, Hofmann S, Langer R, Chen J, Snyder B, et al. Silk implants for the healing of critical size bone defects. Bone. 2005 Nov;37(5):688-98.
33. Kim Y, Bae Y, Suh K, Jung J. Quercetin, a flavonoid, inhibits proliferation and increases osteogenic differentiation in human adipose stromal cells. Biochem Pharmacol 2006;72(10):1268-78.
34. Dégano I, Vilalta M, Bagó J, Matthies A, Hubbell J, Dimitriou H, et al. Bioluminescence imaging of calvarial bone repair using bone marrow and adipose tissue-derived mesenchymal stem cells. Biomaterials. 2008;29(4):427-37.

SECTION 6

CHAPTER VIII

GENERAL CONCLUSIONS AND FINAL REMARKS

CHAPTER IX

GENERAL CONCLUSIONS AND FINAL REMARKS

Bone is a complex and dynamic tissue composed of different cell types contributing to the maintenance of homeostasis throughout life. Fractures are one of the most common occurrences associated with the musculoskeletal system. They can result from trauma or they can be a side effect of bone related diseases, such as osteoporosis or bone cancer, which weakens the bone and compromises its integrity. One of the most promising therapies is bone tissue engineering. There are several strategies within this field such as delivery of isolated autologous cells, associate these autologous cells to an appropriate three-dimensional (3D) support - scaffold, and/or by incorporating bioactive molecules into scaffolds in order to promote bone regeneration.

The bone tissue engineering strategy followed under the scope of this thesis was based on the use of a biodegradable scaffold that will act as a support for cells to adhere, proliferate and differentiate into an osteogenic phenotype, creating a bone extracellular matrix (ECM). These *in vitro* structures (constructs) were ultimately implanted in a relevant animal model, validating the tissue engineering strategy.

The scaffold has a major importance in this strategy and several properties are required in order to be functional. It must have adequate mechanical properties to support the tissue growth at the bone defect. A highly porous and interconnected structure is required for cell ingrowth. Furthermore, it should be biodegradable in the human body at a similar rate to neo-tissue formation. The material used for scaffold production should be non-toxic, non-immunogenic and biocompatible. The natural occurring polymer chitosan has emerged as a suitable biomaterial to produce scaffolds for bone tissue engineering, since it presents the adequate characteristics.

In this thesis, the osteogenic potential of chitosan based scaffolds seeded and cultured with primary cultures of human bone marrow mesenchymal stem cells (hBMSCs) was evaluated. In chapter III, different scaffolds containing the same percentage of chitosan and different aliphatic polyesters poly(butylene succinate), poly(butylene terephtalate adipate) and poly(caprolactone) were studied, by means of cytotoxicity and direct contact tests using cell lines. It was demonstrated that all scaffolds produced by compression molding followed by salt leaching were cytocompatible and clearly non-toxic to the cells. The direct contact evaluation with a mesenchymal stem cell line, under osteogenic culture conditions, showed that chitosan-poly(butylene succinate) (Ch-PBS) formulation evidenced

superior results, when compared to all studied formulations. The previous results raised the following question: why Ch-PBS formulation promoted superior *in vitro* cellular response? In order to answer that question, the work described in chapter IV was designed to study the influence of different percentages of chitosan (0, 25 and 50%) and PBS (100, 75 and 50%) on cell behavior *in vitro*. The main aim of this study was to analyze the influence of chitosan content on cell viability and osteogenic differentiation of primary cultures of hBMSCs. Scaffolds containing a higher content of chitosan showed greater cell performance, by presenting major cell adhesion and enhanced cell viability. Furthermore, it evidenced higher levels of alkaline phosphatase (ALP) and upregulation of ostegenic genes. PBS scaffolds (100%) consistently showed the inferior results in terms of cell performance. Additionally, the *in vivo* tissue response was evaluated by implanting the higher chitosan containing formulation and PBS only, for one month, in different anatomic regions (cranial, auricular and submuscular) of rats. The selection of these regions was performed to verify about different inflammatory response, based on the degree of vascularization of each tissue. The resident inflammatory cells were macrophages, lymphocytes, plasma cells and foreign body giant cells. These types of cells are presented when chronic inflammatory reaction is developed, and is typical for implanted biomaterials, considered to be normal. The implanted scaffolds did not evidence fibrotic encapsulation. PBS scaffolds showed cell necrosis in all tissue locations, which is not a positive indication. These results demonstrated that chitosan showed a superior effect in terms of cell behavior, both *in vitro* as *in vivo*. After the initial screening of the proposed chitosan based materials for bone tissue engineering scaffolding it was possible to conclude that chitosan is, indeed, relevant to improve the biological performance of the scaffolds both *in vitro* as *in vivo* in terms of inflammatory response.

In chapter V, chitosan–poly(butylene succinate) scaffolds with a different morphology were produced to optimize cell ingrowth in the previous morphology. The scaffolds were prepared by a fiber bonding methodology, which allowed obtaining a fiber mesh porous structure, with an adequate porosity and interconnectivity. Several studies were conducted to conclude about cell adhesion, viability, proliferation and osteogenic differentiation onto these scaffolds structure. The developed scaffolds also evidenced cytocompatibility and no signs of cytotoxicity by showing excellent cell behavior, in terms of adhesion, proliferation and viability. Moreover, hBMSCs seeded and cultured onto the 3D structures in osteogenic culture conditions, evidenced successful osteogenic differentiation by expressing osteogenic related genes, as well as production of a mineralized ECM. This optimized scaffold morphology kept the excellent *in vitro* biological performance of the scaffolds. The next step

was to evaluate the degradation of those scaffolds, both *in vitro* and *in vivo*, as reported in chapter VI. It is known that biodegradation of the scaffold must be at a similar rate as new tissue is developed, which turns the study of the degradation of the scaffolds used in tissue engineering a key issue to be analyzed. To study chitosan-PBS degradation *in vitro*, enzymes responsible for the degradation of both scaffold components (lipase and lysozyme, respectively) were used, in concentrations similar to those in human serum. The weight loss and water uptake results showed that an enzymatic cocktail with lysozyme and lipase evidenced a greater effect on the scaffolds degradation *in vitro*. Moreover, in scanning electron microscopy (SEM) micrographs, it was possible to observe cracks in the fibers of the scaffold structure, being more pronounced for the condition with lipase and lysozyme together. The biodegradation of chitosan-PBS scaffolds was also evaluated *in vivo* by a period of three months. For that, a subcutaneous rat model was used. After 12 weeks all scaffolds maintained their structural integrity, denoting a slower degradation kinetics that the one observed *in vitro*. Host tissue response evidenced a normal chronic inflammatory response. The host tissue response was also assessed. After one week of implantation, it was visible an acute inflammatory reaction with the main cells being neutrophils. The evolution to a chronic inflammatory response was observed at the third week, when the presence of neutrophils was almost residual and the resident cells were macrophages, lymphocytes, plasma cells and foreign body giant cells. Alpha smooth muscle actin (α-SMA) immunostaining was visible throughout the implant, indicating that connective tissue was growing and the degreed of vascularization increased as a function of time. At the same time, collagen was being deposited by fibroblasts, confirmed by Masson´s thricrome staining that specifically stains mature collagen. After 12 weeks, the connective tissue became more organized, by marked presence of α-SMA and more giant cells were observed. Longer time periods of implantation are required to investigate about the biodegradation of these scaffolds, both *in vitro* as *in vivo*. However, the results obtained showed that the slower rate of degradation *in vivo*, as compared to the studied model *in vitro*, is positive, since the kinetics of biodegradation needs to match to the kinetics of the neotissue formation. Being the scaffolds a temporary support for tissue ingrowth, in the specific case of bone tissue, this time frame is not fast.

In the last chapter of this thesis, the tissue engineering strategy herein described was validated *in vivo*. For that, it was used a critical size defect in calvaria of nude mice, which allows to use human MSCs by excluding the immune response mediated by T cells. The cranial defects used were considered critical size defects with a diameter of 5 mm and two for each animal. The hBMSCs were pre-cultured in osteogenic conditions on chitosan-PBS

scaffolds obtained by compression molding followed by salt leaching. After assessing the *in vitro* biological performance of the hBMSCs seeded and cultured onto the scaffolds, in osteogenic culture conditions, these constructs were implanted into cranial defects in nude mice, demonstrating some bone regeneration with chitosan-PBS scaffolds *per se*, although the most prominent results were observed for *in vitro* matured constructs. These results confirm several reports described in the literature, where cell perform a key role in bone formation.

The work developed in this PhD thesis leads to the conclusion that chitosan-poly(butylene succinate) scaffolds in combination with autologous bone marrow MSCs have all the requisites *in vitro* as *in vivo* to design effective bone tissue engineering strategies.

It is, however, important to continue the research on these chitosan based scaffolds. One of the hypotheses is to assess the degree of bone regeneration in large animal models, combining the scaffolds with autologous cells pre-cultured in osteogenic culture conditions. Other hypothesis is to use other source of cells, different from bone marrow. Fetal stem cells are in the front line of regenerative medicine field, mostly due to its easy accessibility and associated non-immunogenicity, which turns these cells adequate to be used in an allogenic setting, avoiding issues of donor morbidity.